A sampled-data approach in control problems involving partial dynamics cancellation

Mohamed Elobaid

THESE DE DOCTORAT

NNT : 2022UPASG014

A sampled-data approach in control problems involving partial dynamics cancellation

Une approche échantillonnée de problèmes de contrôle impliquant une annulation partielle de la dynamique

Thèse de doctorat de l'université Paris-Saclay et de Sapienza Università di Roma

École doctorale n° 580 : Sciences et Technologies de l'information et de la Communication (STIC)
Spécialité de doctorat : Automatique
Graduate School : Informatique et sciences du numérique. Référent : Faculté des sciences d'Orsay
Thèse préparée dans les unités de recherche **Laboratoire des Signaux et Systèmes** (Université Paris-Saclay, CNRS, CentraleSupélec) et **Dipartimento di Ingegneria informatica automatica e gestionale** (Sapienza Università di Roma), sous la direction de **Dorothée NORMAND-CYROT**, Directrice de recherche, et la co-direction de **Salvatore MONACO**, Professeur

Thèse soutenue à Rome, le 24 février 2022, par

Mohamed ELOBAID

Composition du jury

Elena PANTELEY Directrice de recherche, L2S, CNRS - Université Paris-Saclay (France)	Présidente
Daniele PUCCI Directeur de recherche, Italian Institute of technology (Italy)	Rapporteur & Examinateur
Malek GHANES Professeur, Centrale Nantes (France)	Rapporteur & Examinateur
Paolo DI GIAMBERARDIMO Professeur associé, Sapienza Università di Roma (Italy)	Examinateur
Dorothée NORMAND-CYROT Directrice de recherche, L2S, CNRS - Université Paris-Saclay (France)	Directrice de thèse

université PARIS-SACLAY
ÉCOLE DOCTORALE
Sciences et technologies de l'information et de la communication (STIC)

Dipartimento di Ingegneria informatica automatica e gestionale Antonio Ruberti
Sapienza Università di Roma

Titre : Une approche échantillonnée de problèmes de contrôle impliquant une annulation partielle de la dynamique

Mots clés : Systèmes de données échantillonnées, contrôle prédictif de modèle, linéarisation à rétro-action transversale

Résumé : De nombreux problèmes de contrôle se ramènent à imposer que la sortie du système suive un signal donné, tout en rejetant les effets de perturbations. Dans ce vaste contexte de problématiques traitées principalement en temps continu, l'utilisation de techniques de contrôle reposant sur l'inversion est bien connue. Cependant, la présence incontournable de capteurs et d'actionneurs numériques nécessite une conception ad hoc en temps discret. Plus précisément, il s'agit de contrôler des systèmes dits échantillonnés, dont les mesures sont acquises à des instants échantillonnés dans le temps et pour lesquels les variables de commande sont maintenues constantes sur un intervalle de temps donné, la période d'échantillonnage. Dans ce domaine des systèmes échantillonnés, des systèmes supposés en temps continu à déphasage minimal, perdent cette propriété sous échantillonnage ; le système en temps discret équivalent n'est plus à déphasage minimal. L'objet de cette thèse est d'établir des résultats constructifs, procédures et algorithmes permettant de réduire les effets dus à l'inversion dans le contexte échantillonné.

Une première contribution propose une procédure d'inversion stable pour une classe de systèmes à déphasage non minimal multi-input multi-output (MIMO). L'approche repose sur le linéarisé tangent du système et une factorisation de la dynamique des zéros dont une partie seulement est a déphasage minimal. Les contributions suivantes concernent la commande prédictive (MPC) et la linéarisation transverse par bouclage (TFL), deux stratégies de commande concernées par la perte de la propriété de déphasage minimal sous échantillonnage.

Concernant la commande prédictive deux problématiques utilisant des techinques de discrétisation à échelles de temps multiques sont étudiées pour des objectifs de prédiction puis de planification de trajectoire. Les solutions développées sont validées sur plusieurs exemples allant de la conduite et poursuite de systèmes admettant des formes chainées jusqu'au maintien des quasi Halo orbites du système terre-lune.

Concernant la linéarisation transverse par bouclage, deux solutions préservant l'invariance des sous espaces caractérisant les objectifs de contrôle sont proposées. L'une repose sur des techniques d'échantillonnage simple et, quoique solution approchée, est très simple de calcul et présente des performances bien supérieures à une implantation classique par bloqueur d'orde zéro. La deuxième solution, proposée au sens exact, fait appel à des techniques d'échantillonnage multiple et propose aussi des solutions par blouclage statique dans des cas ou seul un bouclage dynamique résoud le problème en temps continu. Les deux approches sont validées sur des exemples académiques et appliquées à la résolution de problèmes de poursuite de trajectoires pour des robots mobiles ou de stabilisation d'orbites périodiques pour des systèmes mécaniques sous actionnés.

université PARIS-SACLAY
ÉCOLE DOCTORALE
Sciences et technologies de l'information et de la communication (STIC)

Dipartimento di Ingegneria informatica automatica e gestionale Antonio Ruberti
Sapienza Università di Roma

Title : A sampled-data approach in control problems involving partial dynamics cancellation
Keywords : sampled-data systems, model predictive control, transverse feedback linearization

Abstract : Several well studied control problems reduce to asking the output of a given process to track a desired signal while rejecting effects of undesired perturbations. In the rich body of knowledge dealing with problems of this type in continuous-time, the use of *partial inversion-based* controllers (i.e controllers that cancel part of the dynamics in the sense of rendering it unobservable) and their effectiveness is well established. Nowadays, however, sensing and actuation is done through digital devices so necessitating a suitable control design. In this setting, the control engineer works with systems referred to as sampled-data systems where measures of the output are available only at sporadic discrete-time instants while the control is piecewise constant over a fixed time interval. In this sampled-data context, systems that are originally minimum phase in continuous-time, and because of sampling and holding, may lose this property. The general argument of this thesis contributes to establishing constructive results, procedures and algorithms to the purpose of mitigating the issues caused by sampled-data design under partial inversion-based controllers.

Since partial inversion-based controllers typically cancel the zero dynamics, the central idea is to mitigate the loss of the minimum-phase property. A first contribution in this direction stands in proposing a procedure for stable partial inversion for a class of continuous-time non-minimum phase Multi-Input Multi-Output systems. The procedure proposed, generalizing a previous result, works over the linear tangent model of a system factorizing a sub-set of the zero dynamics known to be minimum-phase apriori. This preliminary result is at the basis of control strategies which are herein proposed for model predictive control and *digital* transverse feedback linearization. Both control strategies under sampling are affected by the above-mentioned pathology linked to the loss of the minimum-phase property.

In particular, for model predictive control, two solutions based on multi-rate sampling techniques, employed at the prediction, or the trajectory planning level are proposed and compared. Their validity is established through several case studies ranging from steering and tracking in systems admitting chained forms to quasi Halo orbits station-keeping for space-crafts in the Earth-Moon system.

Concerning transverse feedback linearization, two sampled-data solutions preserving the invariant subset specifying the control objectives are proposed. The former is based on single-rate sampling and, albeit approximate in nature, is computationally simple and outperforms zero-order holding of the continuous-time design. The later, an exact solution based on multi-rate sampling, improves upon the former solution and provides, in special cases, static state feedback solutions even when the problem is only solvable via dynamic feedback in continuous-time. Both solutions are validated over academic case studies as well as in solving path following for mobile robots and periodic orbits stabilization for underactucated mechanical systems.

université PARIS-SACLAY | ÉCOLE DOCTORALE Sciences et technologies de l'information et de la communication (STIC)

Dipartimento di Ingegneria informatica automatica e gestionale Antonio Ruberti

Sapienza Università di Roma

Titolo : Un approccio ai dati campionati nei problemi di controllo che coinvolgono la cancellazione parziale della dinamica.

Parole chiave : Sistemi di dati campionati, model Predictive control, transverse feedback linearization

Sommario : Numerosi problemi di controllo non lineare, tra questi quelli che richiedono di seguire prescritti comportamenti e/o compensare l'effetto di disturbi, si ispirano a procedure di inversione e richiedono una parziale cancellazione della dinamica. Tale cancellazione si realizza rendendo inosservabile, rispetto ad opportune funzioni, una parte della dinamica del sistema a ciclo chiuso. Tale procedura si confronta dunque con la massima inosservabilità che può essere ottenuta sotto controreazione rispetto a prefissate funzioni, quella corrispondente alla cosiddetta « dinamica zero » ; e con la sua stabilità, la proprietà di « fase minima ». In questo lavoro sono studiate alcune procedure di controllo che richiedono la cancellazione, eventualmente parziale, della dinamica zero e saranno riferiti come "basati su inversione, o cancellazione, parziale".

Oggi giorno i controllori vengono realizzati con componenti digitali ; si ottengono in tal modo sistemi di controllo « ibridi » caratterizzati da dinamiche a tempo continuo, misure ottenute mediante campionamento ad intervalli di tempo usualmente regolari, e ingressi al sistema controllato costanti a tratti durante i periodi di campionamento. Il progetto del controllo in questo contesto impiega il modello a tempo discreto equivalente del sottosistema controllato che non mantiene necessariamente le proprietà del modello a tempo continuo, prima tra tutte, la stabilita'della dinamica zero.

Come procedere nel progetto di un controllore digitale che risolva un problema di controllo basato su inversione dinamica parziale assicurando la stabilità del processo a tempo continuo ? La tesi contribuisce a rispondere a questa domanda per classi di problemi di controllo basati su inversione dinamica parziale fornendo metodologie costruttive che garantiscano il soddisfacimento della specifica di fase minima del modello a tempo discreto equivalente e la realizzabilitàdel sistema di controllo. Più nel dettaglio, nella prima parte viene proposta una nuova procedura di sintesi per inversione dinamica parziale di sistemi a fase non minima che garantisca la stabilità del sistema ad anello chiuso. La procedura è dapprima illustrata nel contesto di sistemi lineari e poi generalizzata per classi di sistemi non lineari. Questo primo risultato è alla basa dei contributi principali proposti nella tesi nel quadro dei metodi di "Model Predictive Control" (MPC) e "Transverse Feedback Linearization" (TFL) per sistemi a dati campionati. Nel primo caso, è ben noto che l'implementazione digitale di schemi di controllo basati su MPC non garantisce, in generale, la stabilità del

sistema ad anello chiuso. In generale, le soluzioni tipicamente utilizzate in letterature sono di natura empirica e valide caso per caso. Il primo contributo della tesi consiste quindi nella definizione di due nuove metodologie per l'implementazione di schemi di controllo MPC per sistemi a dati campionati mediante multi-rate a livello di controllo, in prima istanza, e pianificazione, in seconda. Sono proposti numerosi casi di studio tra cui l'applicazione a problemi di "station-keeping" per satelliti nel sistema Terra-Luna. Nella seconda parte sono invece illustrati i contributi sull'estensione delle metodologie di TFL al contesto di sistemi a dati campionati. In questo contesto, sono proposte due soluzioni. Nel primo caso viene proposto un controllore di tipo "single-rate" basato sulla ridefinizione dell'uscita associata alla superficie da stabilizzare. La soluzione, sebbene approssimata, garantisce prestazioni notevoli se confrontate a quelle del classico controllo per emulazione, tipicamente usato in letteratura. In seconda istanza viene proposta una soluzione esatta, basata su controllori di tipo multi-rate in cui l'ordine della frequenza di campionamento è fissato dal grado relativo del sistema a tempo continuo e, quindi, associato alla superficie da stabilizzare. Le soluzioni sono confrontate e applicate su diversi casi di studio tra cui la stabilizzazione orbiale di sistemi meccanici sotto attuati e il controllo di robot mobili.

La tristesse durera toujours

Acknowledgements

At the beginning there is family, who despite economic, health and emotional hardships, were nothing but supportive and with them lies the utmost gratitude.

The author is deeply indebted for the opportunity to his thesis Supervisors, Prof. Salvatore Monaco and Dr. Dorothée Normand-Cyrot whose wealth of knowledge and contributions was not only foundational in the field, but their personal understanding was instrumental for the author during some difficult times of his thesis period. On the same breath, it would be unfathomable to omit Dr. Mattia Mattioni who, while not officially a third supervisor, was very much so. Not least because he acted as the buffer and interpreter between the author and his supervisors when the author was lost and when he needed help with the technical side of things.

I thank both the DIAG and L2S for the opportunity of meeting and discussing with amazing people and researchers who have been filling my days through constructive chats and discussions as well as breaks from work. Among them, my special thanks goes to Roberto, Guilio, Spyros, Alessio and Mulham.

At the time of writing this document, and being the bad writer with focus issues that I am, my all-time friends Ahmed and Khalid were there to catch up my typos, grammatical and punctuation errors and just give me grief overall. Their help made this document possible.

Finally to Elham, I am forever in your favor for making the last year of my PhD possible by just being there.

Mohamed Elobaid, Rome, October 2021

Résumé détaillé

Cet mémoire rassemble les principales activités de recherche menées par l'auteur au cours de sa période de doctorat développées conjointement entre le *Dipartimento di ingegneria Informatica Automatica e Gestionale* (DIAG) à l'Università degli Studi di Roma La Sapienza et au *Laboratoire des Signaux et Systèmes* (L2S) de l'Université Paris-Saclay. La mobilité entre les deux institutions a été partiellement financée par *Université Franco-Italienne/Università Italo-Francese* UFI/UIF à travers la Bourse Vinci 2019.

Le cadre général de la recherche effectuée doit traiter des problèmes liés à la soi-disant *conception de données échantillonnées* des lois de contrôle par rétroaction. En termes plus simples, les problèmes concernant les lois de commande par rétroaction conçues pour fonctionner sur la dynamique résultant de l'échantillonnage d'un processus en temps continu.

Plus précisément, les problèmes traités sont limités à une classe spécifique de contrôleurs que nous appelons *contrôleurs basés sur l'inversion partielle*. Ce sont des contrôleurs qui annulent une partie de la dynamique, typiquement la dynamique zero, dans le sens de la rendre inobservable. À cet égard, ce document se concentre sur l'apport de solutions constructives ; lois de rétroaction, algorithmes et procédures préservant les propriétés requises d'un système de commande en temps continu malgré la perte de ces propriétés due à l'échantillonnage.

Plus en détail, les contributions apportées dans cette thèse peuvent être regroupées en trois domaines principaux ; stabilisation via annulation partielle de la dynamique en temps continu, annulation partielle stable en contrôle prédictif du modèle et annulation partielle stable en linéarisation par rétroaction transversale.

Stabilisation par annulation partielle de la dynamique en temps continu : la contribution apportée dans ce sens est principalement abordée au Chapitre 3 de ce document, en s'appuyant sur les notions introduites au Chapitre 1. En effet, le chapitre commence par raconter comment on peut atténuer l'obstruction posé par une dynamique zero instable lors de la conception de contrôleurs basés sur l'inversion en temps continu. Cela se fait en s'assurant que la dynamique annulée n'est qu'une sous-dynamique de la dynamique zero, connue pour être stable a priori. Cette procédure très intuitive consistant à assurer une stabilization via une factorisation à dynamique nulle a été formalisée pour une classe spéciale de systèmes non linéaires à entrée unique et sortie unique dans un travail récent du groupe de recherche. Il a en outre été utilisé pour résoudre certains problèmes de contrôle basés sur l'inversion, comme par exemple la stabilisation par équivalence de rétroaction linéaire et le découplage des perturbations avec stabilité à la fois en temps continu et sous échantillonnage.

En conséquence; une extension de la procédure par factorisation dynamique zero au cas des systèmes linéaires Multi-Input Multi-Output en temps continu. De plus, la même procédure s'est ensuite avérée rentable pour une classe spéciale de systèmes non linéaires à temps continu multi-entrées multi-sorties, au moins au sens local. Des applications à la résolution de problèmes de stabilisation et de découplage des perturbations sont également détaillées.

Annulation partielle stable en contrôle prédictif: Les contributions en ce sens couvrent la deuxième partie de ce document, à savoir les Chapitres 4,5,6. Dans le Chapitre 4, et en utilisant l'outil d'échantillonnage multi-taux discuté au Chapitre 2 au niveau de la conception de contrôle, il est montré que, sous certaines conditions, le problème MPC est grandement simplifié tout en four-

nissant également l'existence, des garanties d'unicité et de délimitation pour le retour d'expérience résolvant le problème. Le prix est cependant que, de par la nature du multi-taux, à certains sous-intervalles de la période d'échantillonnage, le système de contrôle fonctionne en boucle ouverte, avec des capteurs et des actionneurs nécessitant des fréquences d'échantillonnage asynchrones. Un autre problème réside dans la robustesse, ou son absence, associée au contrôle multi-taux.

Motivé par les lacunes ci-dessus, le Chapitre 5 améliore la solution proposée dans le chapitre précédent en reléguant l'utilisation d'un modèle équivalent échantillonné multi-taux en MPC au rôle d'un planificateur de trajectoire. Par conséquent, en modifiant les signaux de référence dans la formulation du problème MPC, on peut obtenir (presque) les mêmes avantages en termes d'existence et de délimitation tout en atténuant les deux problèmes soulevés.

Le Chapitre 6 valide plutôt les résultats méthodologiques obtenus sur une étude de cas complète concernant la stabilisation des orbites Halo autour du point L2 dans le système Terre-Lune.

Annulation partielle stable en linéarisation par rétroaction transversale: Les contributions dans cette direction couvrent la troisième partie de ce mémoire , à savoir les chapitres 7 et 8. Au chapitre 7, une conception à taux unique de données échantillonnées préservant la solution idéale en temps continu à la linéarisation par rétroaction transversale est présentée. Cette solution fonctionne en modifiant les sorties fictives spécifiant les objectifs de contrôle, de manière équivalente la sous-variété à stabiliser en temps continu. La solution s'avère simple du point de vue des calculs. Le prix à payer, cependant, est qu'il est approximatif de par sa conception.

Le chapitre 8, d'autre part, atteste de l'existence d'une solution exacte multi-taux de données échantillonnées chaque fois qu'une solution en temps continu existe. La mise en œuvre, cependant, est naturellement portée sur des approximations.

Étant une technique de stabilisation d'ensemble, les solutions obtenues ont un large éventail d'applications possibles. Le problème du suivi de path pour les robots mobiles à roues sous contrôle numérique est traité sous les deux angles, montrant les avantages supplémentaires de l'utilisation du multi-cadence. A savoir le fait qu'on n'exige pas d'extension dynamique préalable même lorsque c'est une exigence en temps continu. D'autres résultats sur la stabilisation des orbites et les contraintes holonomiques virtuelles pour les systèmes d'Euler-Lagrange sont discutés.

La thèse se termine par les principales questions ouvertes et les orientations futures possibles de l'intérêt de la recherche.

Sommario dettagliato

Questa tesi raccoglie le principali attività di ricerca svolte dall'autore durante il suo periodo di dottorato sviluppato congiuntamente dal *Dipartimento di ingegneria Informatica Automatica e Gestionale* (DIAG) presso l'Università degli Studi di Roma La Sapienza e presso il *Laboratorio di Segnali e Sistemi* (L2S) di Ateneo Parigi-Saclay. La mobilità tra le due istituzioni è stata parzialmente finanziata da *Université Franco-Italienne/Università Italo-Francese* UFI/UIF attraverso il Vinci Grant 2019.

Il quadro generale della ricerca svolta è quello di affrontare i problemi relativi al cosiddetto *sampled data design* delle leggi di controllo del feedback. In termini più semplici, problemi relativi a leggi di controllo di retroazione atte ad agire sulla dinamica risultante dal campionamento di un processo a tempo continuo.

Più precisamente, i problemi trattati sono limitati ad una specifica classe di controllori che chiamiamo *controllori basati su inversione parziale*. Si tratta di controllori che annullano parte dello slancio, tipicamente lo slancio zero, nel senso di renderlo non osservabile. A questo proposito, questo documento si concentra sulla fornitura di soluzioni costruttive; leggi di feedback, algoritmi e procedure che preservano le proprietà richieste di un sistema di controllo a tempo continuo nonostante la perdita di queste proprietà dovuta al campionamento.

Più in dettaglio, i contributi forniti in questa tesi possono essere raggruppati in tre aree principali; stabilizzazione tramite annullamento parziale della dinamica a tempo continuo, annullamento parziale stabile nel controllo predittivo del modello e annullamento parziale stabile nella linearizzazione mediante feedback trasversale.

Stabilizzazione per annullamento parziale della dinamica nel tempo continuo: il contributo dato in questa direzione è affrontato principalmente nel Capitolo 3 di questo documento, sulla base delle nozioni introdotte nel Capitolo 1. Il capitolo, infatti, inizia con raccontare come si può mitigare l'ostruzione posta da una dinamica zero instabile durante la progettazione di controller basati sull'inversione a tempo continuo. Ciò viene fatto assicurando che la dinamica annullata sia solo una sottodinamica della dinamica zero, nota per essere stabile a priori. Questa procedura molto intuitiva di fornire la stabilizzazione tramite la fattorizzazione dinamica zero è stata formalizzata per una classe speciale di sistemi non lineari a ingresso singolo e uscita singola in un recente lavoro del gruppo di ricerca. È stato inoltre utilizzato per risolvere alcuni problemi di controllo basati sull'inversione, come la stabilizzazione mediante equivalenza di feedback lineare e il disaccoppiamento dei disturbi con stabilità sia in tempo continuo che sotto campionamento.

Di conseguenza; un'estensione della procedura per fattorizzazione dinamica zero al caso di sistemi lineari Multi-Input Multi-Output in tempo continuo. Inoltre, la stessa procedura si è poi rivelata vantaggiosa per una classe speciale di sistemi non lineari a tempo continuo multi-ingresso e multi-uscita, almeno in senso locale. Vengono inoltre descritte in dettaglio le applicazioni per risolvere i problemi di stabilizzazione e disaccoppiamento dei disturbi.

Cancellazione parziale stabile nel controllo predittivo: I contributi in questa direzione coprono la seconda parte di questo documento, ovvero i capitoli 4,5,6. Nel Capitolo 4, e utilizzando lo strumento di campionamento multi-rate discusso nel Capitolo 2 a livello di progettazione del controllo, viene mostrato che, in determinate condizioni, il problema MPC è notevolmente semplificato fornendo anche l'esistenza, garanzie di unicità e delimitazione per il esperienza di feedback

risolvendo il problema. Il costo, tuttavia, è che, a causa della natura del multi-rate, a determinati sotto-intervalli del periodo di campionamento, il sistema di controllo opera in anello aperto, con sensori e attuatori che richiedono frequenze di campionamento asincrone. Un altro problema è la robustezza, o la sua mancanza, associata al controllo multi-rate.

Motivato dalle carenze di cui sopra, il Capitolo 5 migliora la soluzione proposta nel capitolo precedente relegando l'uso di un modello equivalente campionato multi-rate in MPC al ruolo di pianificatore di traiettoria. Pertanto, modificando i segnali di riferimento nella formulazione del problema MPC, si possono ottenere (quasi) gli stessi vantaggi in termini di esistenza e delimitazione, mitigando i due problemi sollevati.

Il capitolo 6 convalida piuttosto i risultati metodologici ottenuti su un caso di studio completo riguardante la stabilizzazione delle orbite di Halo attorno al punto L2 nel sistema Terra-Luna.

Stable Partial Cancellation in Linearization by Transverse Feedback: i contributi in questa direzione coprono la terza parte di questa tesi, vale a dire i capitoli 7 e 8. Nel capitolo 7, una progettazione a tasso singolo di dati campionati preservando la soluzione ideale in tempo continuo alla linearizzazione per retroazione trasversale. Questa soluzione funziona modificando gli output fittizi specificando gli obiettivi di controllo, equivalentemente la sottovarietà da stabilizzare in tempo continuo. La soluzione risulta essere computazionalmente semplice. Il prezzo da pagare, tuttavia, è che è disgustoso in base alla progettazione.

Il capitolo 8, d'altra parte, attesta l'esistenza di una soluzione esatta multi-rate dei dati campionati ogni volta che esiste una soluzione a tempo continuo. L'attuazione, tuttavia, è naturalmente vincolata ad approssimazioni.

Essendo una tecnica di stabilizzazione dell'insieme, le soluzioni ottenute hanno un'ampia gamma di possibili applicazioni. Il problema del path following per i robot mobili su ruote a controllo numerico viene affrontato da entrambe le angolazioni, mostrando gli ulteriori vantaggi dell'utilizzo del multi-rate. Vale a dire il fatto che non richiediamo un'estensione dinamica preventiva anche quando è un requisito a tempo continuo. Vengono discussi altri risultati sulla stabilizzazione dell'orbita e sui vincoli olonomi virtuali per i sistemi di Eulero-Lagrange.

La tesi si conclude con i principali quesiti aperti e le possibili future direzioni di interesse della ricerca.

Contents

List of Figures

List of publications

Journal articles

J2 Mohamed Elobaid, Mattia Mattioni, Salvatore Monaco and Dorothée Normand-Cyrot. *"Station-keeping of L_2 halo orbits under sampled-data model predictive control". Journal of Guidance, Control, and Dynamic*, 2022, articles in advance, DOI:10.2514/1.G006349

J1 Mohamed Elobaid, Salvatore Monaco and Dorothée Normand-Cyrot. *"Approximate transverse feedback linearization under digital control". IEEE Control System Letters (L-CSS)*, 2021, 6, 13 - 18. DOI: 10.1109/LCSYS.2020.3046539.

Conference proceedings

C5 Mohamed Elobaid, Mattia Mattioni, Salvatore Monaco and Dorothée Normand-Cyrot. *"Virtual Holonomic Constraints for Euler-Lagrange systems under sampling". European Control Conference* 2022, accepted (to appear).

C4 Mohamed Elobaid, Mattia Mattioni, Salvatore Monaco and Dorothée Normand-Cyrot. *"Digital path-following for a car-like robot". Control Conference Africa IFAC Papers On Line* 2021, 174-179. DOI: 10.1016/j.ifacol.2021.12.030.

C3 Mohamed Elobaid, Mattia Mattioni, Salvatore Monaco and Dorothée Normand-Cyrot. *"On stable right-inversion of non-minimum-phase systems". 59th IEEE Conference on Decision and Control IEEE CDC* 2020, 5153-5158. DOI: 10.1109/CDC42340.2020.9303851.

C2 Mohamed Elobaid, Mattia Mattioni, Salvatore Monaco and Dorothée Normand-Cyrot. *"Sampled-data tracking through MPC and multirate planning". 21st IFAC World Congress 2020*, 53(2), 3620-3625. DOI: 10.1016/j.ifacol.2020.12.2043.

C1 Mohamed Elobaid, Mattia Mattioni, Salvatore Monaco and Dorothée Normand-Cyrot. *"On unconstrained MPC through multirate sampling". IFAC-PapersOnLine*, 52(16), 388-393. DOI: 10.1016/j.ifacol.2019.11.811.

Basic definitions and notations

Table 1: Notations used throughout the thesis

Notation	Meaning
$\mathbb{Z}$	the set of integers
$\mathbb{R}$	the set of reals
$\mathbb{C}$	the set of complex numbers
$\mathbb{Z}_{\geq 0},\ \mathbb{R}_{\geq 0}$	non-negative integers and reals
$\mathbb{R}^n$	the Euclidean n-space
I, I_d	the identity operator and function
$0_{m\times n}$	the $n \times m$ matrix with all zero entries
$x^\top,\ A^\top$	the transpose of a vector x or a real valued matrix A
$\mathrm{col}(x, y)$	is the column of two vectors x, y i.e. $(x^\top,\ y^\top)^\top$
$\mathrm{blkdiag}(A, B)$	the block-diagonal matrix composed by the matrices A, B
$\|x\|^2$	the square of the Euclidean norm i.e $x^\top x$
$\|x\|^2_Q$	the weighted square of the Euclidean norm i.e $x^\top Qx$
$\nabla\lambda(x)$	the column vector derivative of $\lambda(x)$
L_f	the Lie derivative operator i.e $f : \mathbb{R}^n \to \mathbb{R}^n,\ L_f = \sum_{i=1}^n f_i(x)\frac{\partial}{\partial x_i}$
L_f^ℓ	the ℓ^{th} order Lie derivative operator i.e $L_f^\ell = L_f L_f^{\ell-1},\ L_f^0 = \mathrm{I}$
e^{L_f}	the exponential Lie operator along the vector field f i.e. $e^{L_f} = \mathrm{I} + \sum_{i\geq 1}\frac{L_f^i}{i!}$
$e^{L_f}x$	the exponential Lie operator evaluated at x i.e. $e^{L_f}\mathrm{I}_d\|_x$
$O(\delta^p)$	big O notation for approximation of series expansions via truncations
$\mathbb{C}^+$	right half of the complex plane, i.e. $\{p \in \mathbb{C} : \|\mathrm{Re}(p)\| > 0\}$
$\mathbb{C}^-$	left half of the complex plane, i.e. $\{p \in \mathbb{C} : \|\mathrm{Re}(p)\| < 0\}$
$\mathbb{S}^1$	the unit disk in the complex plane, i.e. $\mathbb{S}^1 = \{p \in \mathbb{C} : \|p\| < 1\}$

Additionally, the following notions, which are sometimes used, are defined in this way;

The symbols > 0 and < 0 (resp. $\succ$ and $\prec$) denote positive and negative definite functions (resp. matrices), respectively.

Given a manifold M and a closed connected set $N \subset M$, N is said to be invariant under the dynamics $\dot{x} = f(x) + g(x)u$ if $\forall x_0 \in N$ and any control $u(\cdot)$, $x(t) \in N$, $\forall t$.

N is *controlled* invariant if there exists a feedback $u^\star$ making N invariant for the closed loop system.

A continuous function $\beta(\cdot) : [0, \infty) \to [0, \infty)$, that is zero at zero and strictly increasing and unbounded is said to be of class κ_∞.

A continuous function $R(x, \delta)$ is of order $O(\delta^p)$ with $p \geq 1$ if, whenever it is defined, it can be written as $R(x, \delta) = \delta^{p-1}\tilde{R}(x, \delta)$ and there exists a function $\beta(\delta) \in \kappa_\infty$ and $\delta^\star > 0$ such that $\forall \delta \leq \delta^\star, |\tilde{R}(x, \delta)| \leq \beta(\delta)$.

Finally, some commonly used acronyms are listed herein;

Table 2: Acronyms

Acronym	**Meaning**
SISO	single-input single-output
MIMO	multi-input multi-output
SD	sampled-data
SR	single-rate
ASR	approximate single-rate
MR	multi-rate
MPC	model predictive control
TFL	transverse feedback linearization

Introduction

This work collects the main research activities carried out by the author during his PhD period developed jointly between the *Dipartimento di ingegneria Informatica Automatica e Gestionale* (DIAG) at Università degli Studi di Roma La Sapienza and the *Laboratoire des Signaux et Systèmes* (L2S) at Université Paris-Saclay. The mobility between the two institutions has been partially funded by *Université Franco-Italienne/Università Italo-Francese* UFI/UIF through the Vinci Grant 2019.

The overarching setting of the research carried out has to deal with issues arising due to the so-called *sampled-data design* of feedback control laws. In simpler terms, issues concerning feedback control laws designed working over dynamics resulting from sampling a continuous-time process.

Being a huge undertaking overall, the issues dealt with are limited to a specific class of controllers that are ubiquitous enough making this work both interesting and manageable. In this respect, this document focuses on providing constructive solutions; feedback laws, algorithms and procedures preserving required properties of a continuous-time control system despite the loss of those properties due to sampling when dealing with the class of control methodologies we call *partial inversion-based controllers*. These are controllers that cancel part of the dynamics, typically the zero dynamics, in the sense of rendering it unobservable. Maximal cancellation is gained under feedback through zero dynamics assignment and methods which employ this are denoted as inversion-based. Consequently, by generalizing this terminology we will refer to partial cancellation or partial inversion-based when a partial assignment of the zero dynamics is involved. These notions and choices of terminology will be made more apparent in Part I.

Before going into the details however, this chapter will provide a general historical and technical context for the topics addressed in this thesis as well as a sketch of the contributions and an outline of the thesis. Accordingly, we start by recalling the story of the developments relevant to our discussions. These developments will make clear the "source" of the addressed problems, namely the stability of the *zero dynamics* both in continuous-time and when modified by sampling. This sampling-induced "modification" of the zero dynamics structure of a continuous-time process is the main obstruction affecting performances of the class of control problems studied, and indeed a large part of this work is devoted to solutions to mitigate this issue.

The general context and motivation

Beginning in the seventies of the previous century, a huge body of work in the control and systems research community was devoted to generalizing concepts already well established in the linear setting to nonlinear control systems. A seminal work in this direction is that of Hermann and

Krener (1977) which generalized to the nonlinear control the geometric tools studying structural properties like observability and reachability.

This paper in turn had huge implications leading to the introduction of the *zero dynamics* by Byrnes and Isidori (1984); a dynamics characterizing the unobservable behavior of a system once initial conditions and control are chosen in such a way as to constrain the output to be zero.

It became rapidly clear that the properties of this dynamics, generalizing the concept of a transmission blocking zero of a transfer function, had similar impact on a huge array of feedback design methodologies and control problems. Naturally, the first place where such consequences are understood to arise is the disturbance decoupling problem for nonlinear systems discussed by Hirschorn (1981) where later it became clear that stability of the zero dynamics, rendered unobservable via the feedback solving this problem is paramount.

Additionally, stabilization and output tracking controllers that utilize linear feedback equivalence Krener (1973) are faced with the same limitation. They "*cancel*", in the sense of rendering unobservable, the dynamics coincident with the zero dynamics thus requiring stability of the zero dynamics (Isidori, 1995, Chapter 6). This is also clear in applications of such controllers relying on linear feedback equivalence. A major example of these applications stands in the problem of Input-Output non-interaction (see Isidori et al. (1981)). Examples of this are the results reported by Isidori and Grizzle (1988) concerning conditions for solvability of state feedback Input-Output non-interaction with stability. Similar results concerning the role of stability of the zero dynamics in solving the non-interaction problem with dynamic feedback were detailed by Battilotti (1990).

In the meantime, stabilizing feedback laws based on high-gain output were shown to require the zero dynamics to be (locally exponentially) stable by Sontag (1990). The same was shown to be the case when using dynamic feedback with a high gain robust observer in Teel and Praly (1995) (see also Ghanes et al. (2012) for a more recent note on observers design for nonlinear systems).

Perhaps even more surprisingly is the fact that this pathology is encountered when designing stabilizing and tracking state feedback laws in the optimal control setting. Particularly, the problem of *cheap optimal control*; a variation of the Linear Quadratic Regulator Kirk (2004) in which the penalty on the control is vanishingly small, exposes that a stabilizing feedback solution results in perfect regulation (or tracking) of the output only when the zero dynamics is stable Seron et al. (1999).

As the alert reader may have already gathered, the underlying common theme among all of the aforementioned control methodologies and problems is that feedback solutions impose (partial) cancellation of the dynamics effecting unobservability. Indeed, controllers like output tracking, disturbance decoupling, input-output non-interaction, local stabilization and even finite-horizon optimal controllers (e.g. tracking Model predictive control MPC) all require the cancellation of dynamics. State feedback controllers requiring (partial) cancellation of the (zero) dynamics are hence referred to, in this work, as the class of partial inversion-based controllers. The reason for this choice of nomenclature will be made apparent in Chapter 1.

It is important to stress that the brief recount on the developments concerning the zero dynamics is in no way comprehensive. The mentioned pioneering works are complemented by the contributions of many in the field which the author apologies for omitting in this document. All of the mentioned results concerning the zero dynamics and partial inversion-based controllers were developed in the continuous-time framework. Nowadays, however, computations, sensing and actuation are almost

always carried out using some digital device or a computer (in the general sense of the word). In fact, this is not a recent trend, and thus the study of *digital control* dates back to as early as the fifties of the last century as for instance in the work by Ragazzini and Franklin (1958). In the subsequent six decades, the investigations of digital control, and more specifically *sampled-data* systems (i.e. continuous-time systems whose information are available over discrete time instants and are fed by piecewise constant input signals switching at certain times) albeit not as exhaustive as their continuous-time counterpart were steadily progressing. This sampled-data nature necessitates the need for ad-hoc tools for both analysis and control design purposes.

From the analysis side, the study of basic properties was evolving throughout the seventies and eighties. Examples of this includes Sontag's realization of discrete time systems Sontag (1979), Normand-Cyrot's study of nonlinear discrete-time systems Normand-Cyrot (1983), controllability of discrete time nonlinear systems as studied by Fliess and Normand-Cyrot (1981), the proper introduction of the sampled-data equivalent model for nonlinear systems by Monaco and Normand-Cyrot (1985) and later a unified approach to the description of discrete and sampled-data systems in Monaco and Normand-Cyrot (1995).

On the control design front, the effects of sampling on the underlying continuous-time system properties came to the forefront of research. Indeed, having a mature body of knowledge on the continuous-time framework, control and systems researchers were concerned with the following question: "How to preserve the properties and structure of the continuous-time control system under sampling ?". In this respect, the seminal work by Åström et al. (1984) exposed the fundamental difficulty relevant to our current endeavor. Put in simple terms, the sampled equivalent model of a linear system of dimension n will always have $n-1$ zeros irrespective of the number of the zeros of the underlying continuous time process. This fact was shown to hold true even for the more general zero dynamics of nonlinear systems by Monaco and Normand-Cyrot (1988). This in turn implied that the relative degree, an important property of a control system used in the linear feedback equivalence design, is modified by sampling. At this point, one in principle could classify the research into the design paradigm of digital controllers into three distinct groups;

- **Design by emulation** the increasing performances of computers, sensors and actuators rendered the direct implementation of continuous-time controllers through emulation via a zero-order-holding device more attractive in recent times. In this respect the digital control research community focused on studying "bounds" on the sampling rate that preserves the continuous-time design when emulated. Examples of these studies in recent times are the work by Nesic et al. (2009), and the work addressing robustness to the sampling period by Mazenc et al. (2013) among others.

- **Discrete-time design** in which the feedback law is design working over typically approximate discrete-time model of the plant disregarding its underlying continuous-time nature. How close those approximate models evolution follow the continuous-time ones and conditions for a controller designed through this approach to stabilize the sampled nonlinear system are the main topics of research in this approach. Examples of recent works in this direction are those of Nešić et al. (1999).

- **Sampled-data design** where feedback laws are designed working over an exact or approximate discrete-time model of the plant obtained as a power series expansion in the sampling

period, but also taking the underlying continuous-time nature of the process. The appeal of this approach is the fact that controllers designed in this way almost always outperform emulation so cheap sensors and actuators can be utilized by the engineer. In this approach, Monaco and Normand-Cyrot have contributed significantly in enriching the available set of tools for controller synthesis, examples of their works can be found in Monaco and Normand-Cyrot (1983b), Monaco et al. (1986b), Monaco and Normand-Cyrot (1992), (Monaco and Normand-Cyrot, 1997, Chapter 5) among others.

With the preceding discussion in mind, this thesis is contextualized in the sampled-data design approach, and more specifically to designing sampled-data controllers preserving the properties of the ideal continuous-time solution in inversion-based control problems.

As it is not possible to cover all inversion-based controllers we will limit our focus to two examples of inversion-based controllers, Model predictive controllers, and Transverse feedback linearization set stabilizing controllers. The pathologies linked to the stability of the zero dynamics in continuous-time and the appearance of extra sampling zero dynamics that is typically unstable deteriorating the performances of those controllers will be discussed, and solutions provided.

The choice to study these two controllers is self-explanatory, however a small discussion is provided to further enforce this statement;

- **Model Predictive Control - MPC** originally developed by process engineers Clarke et al. (1987), is rapidly becoming the tool of choice for feedback design in almost all engineering applications due to its ability to handle constrained Multi-Input Multi-Output systems Camacho and Alba (2013), Boucher and Dumur (1996), Borrelli et al. (2017). When used to solve stabilization and tracking problems, MPC solves a constrained optimization problem working over a quadratic cost function penalizing the states or tracking error together with a penalty on the control. This optimization problem is subject to a so-called prediction model of the process, typically an approximate sampled-data model obtained via integration Bemporad et al. (2010). It is because of this, and the fact that tracking MPC when no state constraints are present and the penalty on the control is small enough falls under the inversion-based control problems class, that MPC is a very interesting candidate for our investigations.

- **Transverse Feedback Linearization - TFL** set stabilization (in the sense of Seibert (1969), see also Shiriaev (2000)) using transverse feedback linearization first introduced by Banaszuk and Hauser (1995) and later generalized by Nielsen and Maggiore (2008) relies on linear feedback equivalence, thus requiring the cancellation of the zero dynamics. This control technique, being a set stabilization as opposed to equilibria stabilization technique, finds a wide array of applications in current and pertinent control problems in a natural way. Examples include path fallowing for electro-mechanical systems Nielsen et al. (2010), Hladio et al. (2012), Akhtar et al. (2015) and synchronization and formation keeping Doosthoseini and Nielsen (2015a), to name a few.

This thesis hence contextualizes the effect of zero-dynamics cancellation on closed loop stability for the two mentioned inversion-based control problems. In the sequel, explicit reference to the contributions of this thesis, as well as the organization of the following chapters will be provided.

Of note is that, while perhaps not comprehensive, this document is written to be as self-contained and accessible as possible, and hence reference to tools and definitions will be made available when required. This is further supported with an attempt to unify the style, nomenclature and notations used throughout.

Outline and contributions of the thesis

In what follows, we describe the content of each part and chapter of this document. Details on contributions made by this work, together with a brief description of the relevant state of the art are made when appropriate.

Part I

Chapter 1 provides the basic notions and definitions needed concerning the zero dynamics and its link to inversion-based control in continuous-time for both Single-Input Single-Output and Multi-Input Multi-Ouput systems. Corresponding definitions for the discrete-time case are recalled briefly as well. The emphasis is put into how the stability properties of the zero dynamics defines obstructions when using inversion-based controllers.

Chapter 2 mirrors the discussion of the first chapter in the sampled-data context. Accordingly, the second main obstruction to the *direct digital design* of inversion based controllers, the appearance of extra unstable zero dynamics due to sampling is emphasized. An important tool mitigating this pathology, multi-rate sampling, is formally recalled and examples are given.

Chapter 3 starts by recounting how one can mitigate the obstruction posed by unstable zero dynamics when designing inversion based controllers in continuous-time. This is done by ensuring that the cancelled dynamics is only a subdynamics of the zero dynamics, known to be stable apriori. This very intuitive procedure of ensuring stable inversion via zero dynamics factorization was formalized for a special class of Single-Input Single-Output nonlinear systems in a recent work of Mattioni et al. (2017a). It was further used to solve some inversion-based control problems as for example stabilization through linear feedback equivalence and disturbance decoupling with stability by the same authors both in continuous-time and under sampling Mattioni et al. (2017a), Mattioni et al. (2019).
It is in this chapter that a **first contribution** is given; an extension of the procedure of stable inversion via zero dynamics factorization to the case of linear Multi-Input Multi-Output systems in continuous-time. Additionally, the same procedure was then demonstrated to be profitable for a special class of Multi-Input Multi-Output nonlinear continuous-time systems at least in a local sense. Application to solving stabilization problems and disturbance decoupling are also detailed in the results reported in Elobaid et al. (2020a). Similar technique were independently described in the work by Kavaja et al. (2018) for designing feed-forward control laws for continuous-time linear systems.

Part II

Chapter 4 stresses the fact that model predictive control implies cancellation of the zero dynamics under some conditions i.e. is an inversion-based control. This observation then allows the author to make the **second contribution** of this work. Namely, using the tool of multi-rate sampling discussed in Chapter 2 at the level of control design, it is shown that, under some conditions, the MPC problem is greatly simplified while also providing existence, uniqueness and boundedness guarantees for the feedback solving the problem.
This contribution stands in using a (possibly simplified) multi-rate sampled equivalent model of the plant as a prediction model in the MPC problem formulation. The payback is that for an originally minimum phase continuous-time plant in the cheap control setting of the problem, the MPC feedback preserves internal stability. The price however is that by the nature of multi-rate, at some sub-intervals of the sampling period, the control system works in open loop, with sensors and actuators requiring asynchronous sampling frequencies. Another issue stands in the robustness, or lack thereof, associated with multi-rate control. These particular downsides motivates the third contribution made in this work. The example of systems admitting chained form is treated in this chapter as a detailed case study so as to illustrate the benefits associated with this proposed solution.

Chapter 5 improves upon the solution proposed in the previous chapter by relegating the use of a multi-rate sampled equivalent model in MPC to the role of a trajectory planner. In this way a **third contribution** is proposed stressing that by modifying the reference signals in the MPC problem formulation, one can obtain (almost) the same benefits in terms of existence and boundedness while mitigating the two issues raised.
Namely, working as a trajectory planner, the references are known to be admissible apriori in the unconstrained case i.e. for which there exists bounded control achieving the control objective. Additionally, the need for asynchronous sampler is transferred to the planner, and the actuation and feedback sampling rates are left synchronous. Moreover, the feedback works over the smaller intervals defining the multi-rate, thus the loop is closed at all sampling instants. Lastly, and by exploiting some *nominal robustness* properties Allgöwer and Zheng (2012), working with this approach is shown, through a detailed case study on the Planar Vertical Take-Off and Landing - PVTOL aircraft to provide robustness to parameter uncertainties, additive perturbations and sampling period increase as compared to control design methods in the literature.
The comparison to the solution presented in Chapter 4 is made explicit by treating the same example of systems admitting chained forms in different situations. It is shown that the "enhancement" afforded by this approach greatly motivate its use. The contribution calumniates in a planning and control algorithm.

Chapter 6 presents a comprehensive case study for the use of multi-rate sampled equivalent models as a trajectory planner in performing station-keeping by space-crafts on quasi Halo orbits in the Earth-Moon system. The used multi-rate model is a simplified model obtained under an assumed nonlinear regulation feedback.
The associated optimization problem is further assumed to be a constrained one, thus incorporating the effect of the presence of box constraints on the controls (the thrusts in three directions) previously neglected in the proposed algorithm.

The contribution of this chapter is then twofold; on the one hand incorporating constraints and a more realistic simulation model incorporating eccentricity perturbations and solar radiation pressure allows to validate the algorithm proposed in Chapter 5 even in scenarios where no theoretical guarantees for existences and boundedness were provided. On the other hand, comparisons to several control techniques typically used in station keeping applications in terms of tracking performance and energy expenditure provides promising conclusions. How to mitigate high computation requirements are also briefly studied.
This chapter concludes by providing a summary of the contributions in Part II and a commentary on the open questions, chief among which is the effect of the presence of state constraints in the MPC problem on the guarantees obtained by the two solution methodologies.

Part III

Chapter 7 starts by recalling the well motivated and studied inversion-based control problem of sets stabilization through transverse feedback linearization. This problem is well studied in the continuous-time literature, but to the best of the author's knowledge, no work was dedicated to this problem by the digital control community.
Accordingly a **fifth contribution** is made in this chapter extending a previous result on the preservation of the relative degree under single-rate sampling due to Barbot et al. (1996) to this setting. The word "extending" is used loosely here, for the author means simply showing that the use of that previous result (after the necessary algebaraic manipulations associated with dealing with Multi-Input systems as compared to Single-Input systems) is fruitful in our context of set stabilization. The result provided is constructive, it provides a coordinate change and feedback under single-rate sampling preserving the zero-dynamics sub-manifold and the TFL structure, albeit in an approximate sense. The computations are simple and stand in modifying the continuous-time functions specifying the desired set to be stabilized and the control performances.
The chapter also further elaborates on the results reported in Elobaid et al. (2020c) by providing details on how to achieve higher orders of approximation in an iterative way. Additionally a further example than the ones treated in the cited paper is detailed to demonstrate the procedure and its effectiveness.
Chapter 8 improves upon the provided solution in the previous chapter by discussing the existence of an exact solution preserving TFL whenever a continuous-time one exits when using the tool of multi-rate sampling. The computation of the exact solution maybe impossible as is usual in the sampled-data design context and thus computations are carried over approximations obtained via truncation of the power series expansion describing the exact solution.
An additional and **final contribution** is also made in this chapter, namely showing that a state feedback solution may exist even when no continuous-time solution via TFL exists for some classes of set stabilization problems. This claim is demonstrated for the problem of path following with reference to the kinematic model of a car-like robot detailing and commenting on the results reported by Elobaid et al. (2021).
Additionally, the chapter compares this solution with that obtained in chapter 7 illustrating its superior performances. Note that both sampled-data solutions are shown to outperform emulation based design. The Chapter concludes with a small unpublished case-study on the use of this solution for periodic orbits stabilization of underactuated mechanical systems. The discussion not

only reports the detailed example, but the alert reader may gather the mechanics and more general statements that can be made. At the end, as is usual, some commentary summarizing the contributions made in this part and the still open questions most interesting of which is the application to nested-sets stabilization under sampling.

Comments on style and writing

Before delving into the technical details proper, an important note on the overall "style" and structure needs to be clarified. This is a thesis collecting the results on several articles. However, since the results are closely related treating an overarching single topic, this document is written with emphasis on having a cohesive structure and a "story".

Because of this, each chapter (apart from the first two) is written as a more accessible companion contextualizing the results given in a specific article as well as some self-criticism and discussion of open issues. By companion the author means providing additional commentary, examples and details of computations (e.g. Chapters 3 — 5), or even more technical details and unpublished examples and applications as is the case in Chapters 7 — 8. The article itself is then attached at the end of the corresponding chapter for the interested reader apart from that corresponding to Chapter 6 which is currently under review.

The reader is advised to read the chapters in a given Part in the order they appear, however it is not necessary to read Part II before part III. What is important is that Part I should always be tackled first. For those chapters corresponding to contributed articles, the reader may chose any order i.e. reading the full chapter first and then take a look at the attached article, read both at the same time moving from one to the other, read the article first, or omit reading the article altogether for a more informal and high-level treatment of the subject.

Important definitions, problem statements and results recalled from the literature or contributed by the author are all highlighted appropriately and color coded. In particular, every definition is marked with a blue box, every Problem statement is marked with red, every result recalled from the literature is marked in gray, and every result contributed by the author is marked in green. Some abuse of nomenclature is also present where sometimes inversion-based and partial inversion-based controllers are used interchangeably. The author thanks the reader for spending the time and hopes that this document is both accessible and easy to read.

On zero dynamics, sampling and inversion

Chapter 1

Background on zero dynamics in continuous-time

Contents

The purpose of this chapter is twofold. First; an overview of basic facts about the zeros of linear systems and the zero dynamics in a nonlinear setting will be provided for both Single-Input-Single-Output (SISO) systems and (square) Multi-Input-Multi-Output (MIMO) systems. In particular we utilize the relative degree and normal forms to define the zero dynamics (and their zeros counterpart in the linear context). Definitions of what it means for a system to be minimum phase, non-minimum phase and partially minimum phase will be provided. Second; some preliminary remarks on how cancellation of the zero dynamics, rendering it unobservable via feedback, faces limitations when the zero dynamics is non-minimum phase. These last aspects will constitute the motivations for the discussion in the following two chapters.

It is the hope of the author that this chapter provides a simple and concise starting point for the reader, thus it will be very synthetic and brief in nature. The notions appearing hereinafter are recalled from Isidori (1995), Isidori, Kailath (1980), Marro (1990), Mattioni et al. (2017a) and the references therein.

1.1 The Single-Input Single-Output case

Our point of departure is a nonlinear control affine system of the form

$$\dot{x} = f(x) + g(x)u \tag{1.1a}$$

$$y = h(x) \tag{1.1b}$$

with the states $x \in \mathbb{R}^n$, the control u is real analytic, and the output map $h(x) : \mathbb{R}^n \to \mathbb{R}$ and the vector fields $f(x), g(x)$ are smooth and real analytic. The following definition is instrumental;

Definition: the relative degree of a SISO nonlinear system

A SISO nonlinear system of the form (1.1a)-(1.1b) is said to have a well defined relative degree r at a point $x_0 \in \mathbb{R}^n$ if and only if

- $L_g L_f^{\ell} h(x) = 0$ on a neighbourhood of x_0 for $\ell = 1, \dots, r-2$
- $L_g L_f^{r-1} h(x_0) \neq 0$ at x_0.

Following (Isidori, 1995, Chapter 4) it results that if the above holds true, then there exists a coordinates change defined in a neighbourhood of x_0 of the form

$$\begin{aligned} z = \phi_1(x) &= \begin{pmatrix} h(x) & L_f h(x) & \dots & L_f^{r-1} h(x) \end{pmatrix}^\top && \in \mathbb{R}^r \\ \eta &= \phi_2(x) && \in \mathbb{R}^{n-r} \end{aligned} \tag{1.2}$$

with $\phi_2(x)$ such that $\phi(x)$ is a diffeomorphism (a differentiable bijection with a differentiable inverse). Moreover, in the SISO setting, it is always possible to find a special choice for the last $n-r$ coordinates $\eta_\star = \phi_2^\star(x)$ with $L_g \phi_2^\star(x) = 0$. If this choice is made then the system takes the following *normal form*

$$\begin{aligned} \dot{z}_1 &= z_2 \\ \dot{z}_2 &= z_3 \\ &\vdots \\ \dot{z}_{r-1} &= z_r \\ \dot{z}_r &= b(z, \eta_\star) + a(z, \eta_\star) u \\ \dot{\eta}_\star &= q_\star(z, \eta_\star) \\ y &= z_1 \end{aligned} \tag{1.3}$$

where $b(z,\eta) = L_f^r h(x)$, $a(z,\eta) = L_g L_f^{r-1} h(x)$, $q_\star(z,\eta_\star) = L_f \phi_2^\star(x)$ all computed at $x = \phi^{-1}(z,\eta)$. For the normal form (1.3), consider the following state feedback law;

$$u = \beta(z,\eta_\star) + \alpha(z,\eta_\star)\nu = \frac{-b(z,\eta_\star)}{a(z,\eta_\star)} + \frac{\nu}{a(z,\eta_\star)} \tag{1.4}$$

where $\nu \in \mathbb{R}$ an external control. The feedback system takes the form;

$$\begin{aligned} \dot{z}_1 &= z_2 \\ \dot{z}_2 &= z_3 \\ &\vdots \\ \dot{z}_{r-1} &= z_r \\ \dot{z}_r &= \nu \\ \dot{\eta}_\star &= q_\star(z, \eta_\star) \\ y &= z_1 \end{aligned}$$

This feedback makes the input-output link a chain of r integrators as depicted in the figure below and renders the $\eta_\star(t)$ sub-dynamics unobservable.

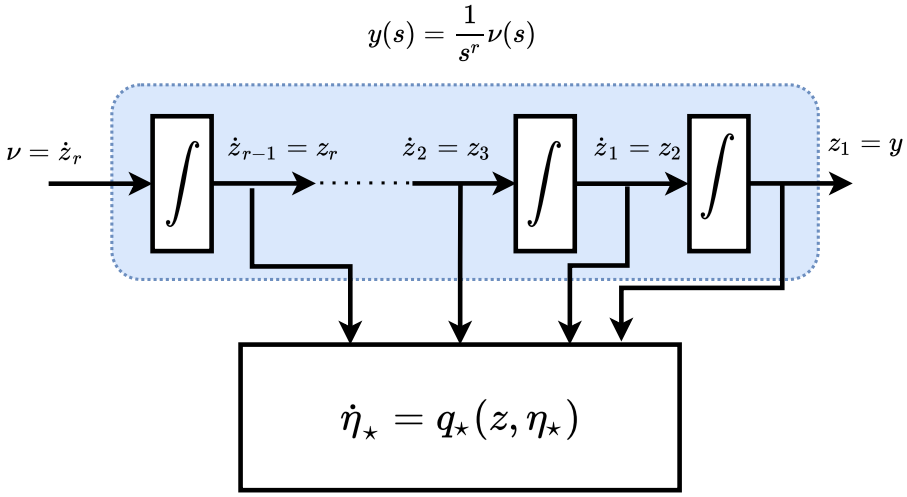

Figure 1.1: System structure under an inversion feedback and unobservability of the residual dynamics.

Roughly speaking an unobservable dynamics of dimension $n - r$ appears under the feedback (1.4). As a matter of fact such a feedback has the property of maximizing the unobservability reducing the input-output link to a linear transfer function $y(s) = \frac{1}{s^r}\nu(s)$ and a suitable further feedback actions can be used to get a closed loop;

$$G_F(s) = \frac{1}{(1+\tau s)^r} \qquad \tau \approx 0$$

so realizing an "almost inversion" of the given system. In this sense $q_\star(z, \eta_\star)$ represents the part which must be cancelled to allow the output to follow the input (thus the terminology inversion based controllers) Hirschorn (1979).

A related point of view stands in looking at the $q_\star(z, \eta_\star)$ dynamics when $\nu = 0$. It is readily verified that if the initial condition on the integrators is zero, then the output is identically zero. The following problem definition is instrumental: (Isidori, 1995, Chapter 4);

Problem: output zeroing

Consider a system of the form (1.1a)-(1.1b); ***Find*** *the set of initial conditions and controls* $(x(t_0), u(t)) \in \mathbb{R}^n \times \mathbb{R}$ *such that the output* $y(t)$ *is identically zero, for all* $t \geq t_0$.

In the $(z, \eta_\star)$ coordinates, and from the previous discussion it results that the set of initial conditions solving the output zeroing problem are necessarily such that

$$z_1(t_0) = z_2(t_0) = \ldots = z_r(t_0) = 0$$

and the feedback, starting from those initial conditions, is given by (1.4) when $\nu = 0, z = 0$ i.e;

$$u^\star = -\frac{b(0,\eta_\star)}{a(0,\eta_\star)} \tag{1.5}$$

where $\eta_\star$ is a solution to the differential equation defining the zero dynamics

$$\dot{\eta}_\star = q_\star(0,\eta_\star), \quad \eta_\star(t_0) = \eta_\star^\circ \tag{1.6}$$

This dynamic describes the motion on the zero dynamics submanifold;

$$\mathcal{Z}^\star = \{(z,\ \eta_\star) \in \mathbb{R}^n : z = 0\} \tag{1.7}$$

In the original x coordinates, the zero dynamics submanifold is characterized by;

$$\mathcal{Z}^\star = \{x \in \mathbb{R}^n : h(x) = L_f h(x) = \ldots = L_f^{r-1} h(x) = 0\} \tag{1.8}$$

on this surface, the feedback (1.5) reads

$$u^\star = -\frac{L_f^r h(x)}{L_g L_f^{r-1} h(x)} \tag{1.9}$$

with the zero dynamics describing the motion on $\mathcal{Z}^\star$ being;

$$\begin{aligned} \dot{x} &= f^\star(x)|_{\mathcal{Z}^\star} \\ &= \big[f(x) - g(x)\frac{L_f^r h(x(t))}{L_g L_f^{r-1} h(x(t))}\big]|_{\mathcal{Z}^\star} \end{aligned}$$

with this in place, we can recall the following solution to the output zeroing problem;

Zero dynamics in continuous-time

The solution to the output zeroing problem is given by the set of initial conditions characterized by (1.8) together with the feedback (1.9). Moreover, the restriction of the controlled dynamics under the feedback (1.9) to the submanifold $\mathcal{Z}^\star$ namely $f^\star(x)|_{\mathcal{Z}^\star}$ is called the *zero dynamics vector field* of the system, and $\mathcal{Z}^\star$ its corresponding *zero dynamics submanifold.*

In a linear setting, given a state space realization of the form;

$$\dot{x} = Ax + bu \tag{1.10a}$$

$$y = cx \tag{1.10b}$$

with the triplet $A \in \mathbb{R}^{n\times n}$ and $b, c^\top \in \mathbb{R}^n$, the relative degree is defined as the smallest integer r for which $cA^\ell b = 0$ for all $\ell = 0, \ldots, r-2$ and $cA^{r-1}b \neq 0$. If the relative degree is defined then a

suitable choice for the coordinates defining the normal form can be

$$z = \begin{pmatrix} cx & cAx & \dots & cA^{r-1}x \end{pmatrix}^\top$$
$$\eta_\star = \begin{pmatrix} x_1 & x_2 & \dots & x_{n-r} \end{pmatrix}^\top$$

one has that in these coordinates the system takes the form

$$\begin{aligned} \dot{z}_1 &= z_2 \\ \dot{z}_2 &= z_3 \\ &\vdots \\ \dot{z}_{r-1} &= z_r \\ \dot{z}_r &= Rz + S\eta_\star + au \\ \dot{\eta}_\star &= P_\star z + Q_\star \eta_\star \\ y &= z_1 \end{aligned} \tag{1.11}$$

with R, S row vectors of suitable dimension, $a = cA^{r-1}b \neq 0$ and $P_\star$, $Q_\star$ square matrices of dimension $n - r$. In this setting, the state feedback (1.4) reduces to

$$u = \frac{-Rz - S\eta_\star}{a} + \frac{\nu}{a} \tag{1.12}$$

Under this feedback the input-output link reduces again to a chain of r integrators, equivalently;

$$y(s) = \frac{1}{s^r}\nu(s) \tag{1.13}$$

and the $\eta_\star$ sub-dynamics is rendered unobservable. We turn our attention to the output zeroing problem now, and note that it is evident in the $(z, \eta_\star)$ coordinates, and from (1.11), the set of initial conditions solving the problem coincide with the set $z_1(t_0) = \dots = z_r(t_0) = 0$ characterizing the subspace

$$\mathcal{Z}^\star = \{(z, \eta_\star) : z = 0\}$$

on which the feedback solution coincides with (1.12) when $z = 0, \nu = 0$, namely;

$$u^\star = \frac{-S\eta_\star}{a} \tag{1.14}$$

In these coordinates the zero dynamics are characterized by the cancelled dynamics

$$\dot{\eta}_\star = Q_\star \eta_\star, \quad \eta_\star(t_0) = \eta_\star^\circ \tag{1.15}$$

and the zeros of the system are precisely the eigenvalues of the matrix $Q_\star$. In the original x coordinates of the system, the initial conditions solving the problem are the ones characterized by

the subspace;

$$\mathcal{Z}^\star = \ker \begin{pmatrix} c \\ cA \\ \vdots \\ cA^{r-1} \end{pmatrix}$$

on this subspace, the feedback (1.14) reads

$$u^\star = \frac{-cA^r x}{cA^{r-1}b}$$

and the zero dynamics, motion on $\mathcal{Z}^\star$, is

$$\dot{x} = (A + bu^\star)|_{\mathcal{Z}^\star} = \left[Ax - b\frac{cA^r}{cA^{r-1}b}x\right]|_{\mathcal{Z}^\star}$$

wherein the zeros are characterized by $\sigma((A + bu^\star)|_{\mathcal{Z}^\star}) = \sigma(Q_\star)$ ◀

If we now recall that regular state feedback does not modify reachability and that it modifies eigenvalues but not the zeros, we understand that the unobservability of the feedback system results from the assignment of eigenvalues to the zeros, i.e. pole-zero cancellations. Indeed, for a linear system with a transfer function $G(s) = \frac{n(s)}{d(s)}$, the feedback (1.12) corresponds to pole-zero cancellation of all the zeros of the transfer function i.e. this feedback is the one assigning the closed loop eigenvalues to roots of the polynomial $d_\star(s) = s^r n(s)$ so getting a closed loop;

$$G_F(s) = \frac{n(s)}{s^r n(s)} = \frac{1}{s^r}$$

This fact puts in light that the unobservability generated under (1.12) cancelling *all* the zeros is the *maximal* which can be obtained.

Remark 1.1 *note that the arguments presented concerning cancellation of the zeros via state feedback for a linear SISO system put in light also the possibility of partially cancelling the zeros; i.e. generating unobservability of smaller dimension. This is due to the possibility of factorization of the numerator of a transfer function. More in detail, let the numerator polynomial of a transfer function $G(s)$ admit a maximal factorization $n(s) = n_1(s)n_2(s)$. A feedback assigning a subset of the poles of the closed loop system to the roots of the polynomial $n_1(s)$ achieves cancellation of only the subset of the zeros coincident with roots of the polynomial $n_1(s)$. This later aspect does not appear to be as evident in the nonlinear context, and will be revisited again in Chapter 3.*

The same arguments discussed above can be precisely characterized making use of geometric objects; the so-called controlled and conditioned invariant subspaces introduced by Basile and Marro Basile and Marro (1969) and later used to solve tracking and disturbance decoupling problems by Wonham and Morse Wonham and Morse (1970). This geometric formalism, not herein recalled for brevity, is very attractive since it lends itself seamlessly to extending the notions of maximizing unobservability via state feedback to the nonlinear control affine setting making use of the corresponding so-called controlled invariant distributions, at least in a local sense (Isidori, 1995, Chapter 2).

As a result of these observations, inversion-based state feedback laws that cancel (in the sense of rendering unobservable) the zero dynamics (equivalently, perform pole-zero cancellations in the linear setting) in order to force the output to follow the input has to face with limitations pertaining to the stability properties of the cancelled dynamics.

Those limitations are at the core of this work in continuous-time and specially in a digital context as we will see in later chapters.

However before discussing possible methods for mitigating those limitations, we need to formally recall an important classification of control systems based on the stability properties of the zero dynamics. This classification exposes in a concise manner the main limitations in direct control design methods that utilize inversion. To this end, recall the following;

Definition: minimum and non-minimum phase systems

Let $f^\star(x)|_{\mathcal{Z}^\star}$ of dimension $n-r$ be the zero dynamics vector field associated with the system (1.1a),(1.1b) and let $x_\star = 0$ be a regular point for the zero dynamics algorithm and s.t. $f^\star(0) = 0$, then

- the system is minimum phase if $x_\star = 0$ is an asymptotically stable equilibrium of the zero dynamics; that is over $\mathcal{Z}^\star$
  - $\forall \epsilon > 0, \exists \delta_\epsilon > 0 : \|x(t_0) - x_\star\| \leq \delta_\epsilon \implies \|x(t) - x_\star\| \leq \epsilon \quad \forall t \geq t_0$
  - $\exists \mathcal{B}_r = \{x \in \mathbb{R}^n : \|x\| < r\} : \lim_{t\to\infty} \|x(t) - x_\star\| = 0 \implies \forall x(t_0) \in \mathcal{B}_r$
- the system is non-minimum phase if $x_\star = 0$ is an unstable equilibrium of the zero dynamics.

Remark 1.2 *as can be clearly seen, in the linear context, the above definition of minimum and non-minimum phase systems reduces to the property that the eigenvalues of the matrix $Q_\star$ in (1.15) lying in the open left half and right half of the complex plane respectively.*

1.2 The Multi-Input Multi-Output case

Similar arguments to the ones presented previously can be made for the *square* MIMO nonlinear system of the form

$$\dot{x} = f(x) + \sum_{i=1}^{m} g_i(x) u_i \tag{1.16a}$$

$$y_i = h_i(x), \quad i = 1, \dots m \tag{1.16b}$$

in which each output map $h_i(x) : \mathbb{R}^n \to \mathbb{R}$ smooth functions. The vector fields $f(x)$, $g_1(x)$, $\dots$, $g_m(x)$ are assumed smooth. To start, an equivalent definition of the relative degree in this setting is recalled (Isidori, 1995, Chapter 5);

Definition: the vector relative degree of MIMO nonlinear systems

System (1.16a),(1.16b) is said to have a well defined *vector relative degree* $r = (r_1 \ \dots \ r_m)$ at a point x_0 if and only if for $\ell = 1, \dots, r_i - 2$, $i, j = 1, \dots, m$;

- $L_{g_j} L_f^{\ell} h_i(x) = 0$ while $L_{g_j} L_f^{r_i - 1} h_i(x) \neq 0$ for some j at x_0.
- the $m \times m$ decoupling matrix

$$D(x) = \begin{bmatrix} L_{g_1} L_f^{r_1 - 1} h_1(x) & \dots & L_{g_m} L_f^{r_1 - 1} h_1(x) \\ & \ddots & \\ L_{g_1} L_f^{r_m - 1} h_m(x) & \dots & L_{g_m} L_f^{r_m - 1} h_m(x) \end{bmatrix} \tag{1.17}$$

  is full rank in a neighbourhood of x_0.

If the above definition holds, then necessarily $r_1 + r_2 + \ldots + r_m \leq n$ and there exists a coordinates change defined in a neighbourhood of x_0 mapping $x \mapsto (z_1 \ \dots \ z_m \ \eta)^\top$ of the form;

$$\begin{aligned} z_1 = \phi_1(x) &= \begin{pmatrix} h_1(x) & L_f h_1(x) & \dots & L_f^{r_1 - 1} h_1(x) \end{pmatrix}^\top && \in \mathbb{R}^{r_1} \\ &\vdots \\ z_m = \phi_m(x) &= \begin{pmatrix} h_m(x) & L_f h_m(x) & \dots & L_f^{r_m - 1} h_m(x) \end{pmatrix}^\top && \in \mathbb{R}^{r_m} \\ \eta = \phi_{m+1}(x) & && \in \mathbb{R}^{n-d} \end{aligned} \tag{1.18}$$

with $d = \sum_{i=1}^{m} r_i$. If the vector fields $g_1(x), \ \dots, g_m(x)$ are involutive[1], then it is possible to choose the last $n - d$ coordinates in a special way $\eta_\star = \phi_\star(x)$ such that $L_{g_i} \phi_\star = 0, \ i = 1, \dots, m$. If this is the case, and letting $z_{i,j}$ be the j^{th} component of the state vector $z_i \in \mathbb{R}^{r_i}$, the system in the new coordinates reads;

$$\begin{aligned} \dot{z}_{1,1} &= z_{1,2} \\ \dot{z}_{1,2} &= z_{1,3} \\ &\vdots \\ \dot{z}_{1,r_1 - 1} &= z_{1,r_1} \\ \dot{z}_{1,r_1} &= b_1(z, \eta_\star) + a_1(z, \eta_\star) u \\ &\vdots \\ \dot{z}_{m,1} &= z_{m,2} \\ \dot{z}_{m,2} &= z_{m,3} \\ &\vdots \end{aligned} \tag{1.19}$$

[1] meaning the Lie bracket of any pair in the set is not independent from the set (at a given point).

$$\vdots$$
$$\dot{z}_{m,r_m-1} = z_{m,r_m}$$
$$\dot{z}_{m,r_m} = b_m(z,\eta_\star) + a_m(z,\eta_\star)u$$
$$\dot{\eta}_\star = q_\star(z,\eta_\star)$$
$$y_1 = z_{1,1} \quad \dots \quad y_m = z_{m,1}$$

where for $i = 1,\dots,m$ we have $b_i(z,\eta_\star) = L_f^{r_i}h_i(x)$, $q_\star(z,\eta_\star) = L_f\phi_\star(x)$ and

$$a_i(z,\eta) = \begin{pmatrix} L_{g_1}L_f^{r_i-1}h_i(x) & \dots & L_{g_m}L_f^{r_i-1}h_i(x) \end{pmatrix} \tag{1.20}$$

all computed at $x = \phi^{-1}(z_1,\ \dots,\ z_m,\ \eta_\star)$. Consider now a state feedback of the form;

$$\begin{aligned} u &= \beta(z,\eta_\star) + \alpha(z,\eta_\star)\nu \\ &= -\begin{pmatrix} a_1(z,\eta_\star) \\ \dots \\ a_m(z,\eta_\star) \end{pmatrix}^{-1} \begin{pmatrix} b_1(z,\eta_\star) \\ \dots \\ b_m(z,\eta_\star) \end{pmatrix} + \begin{pmatrix} a_1(z,\eta_\star) \\ \dots \\ a_m(z,\eta_\star) \end{pmatrix}^{-1} \begin{pmatrix} \nu_1 \\ \dots \\ \nu_m \end{pmatrix} \end{aligned} \tag{1.21}$$

This feedback maximizes unobservability and renders the input-output behaviour of the closed loop to be linear with a transfer function representation;

$$\begin{pmatrix} y_1(s) \\ \dots \\ y_m(s) \end{pmatrix} = \begin{pmatrix} \frac{1}{s^{r_1}} & \dots & 0 \\ & \ddots & \\ 0 & \dots & \frac{1}{s^{r_m}} \end{pmatrix} \begin{pmatrix} \nu_1(s) \\ \dots \\ \nu_m(s) \end{pmatrix}$$

and the residual dynamics of dimension $n-d$ described by;

$$\dot{\eta}_\star = q_\star(z,\eta_\star)$$

As we would expect from the discussion in the previous section, and returning to the output zeroing problem in this setting we again note that the set of states solving the problem are essentially such that $z_{i,j}(t_0) = 0\ \forall i = 1,\dots,m, j = 1,\dots,r_i$. Moreover, the feedback solving the problem starting from those initial conditions is given by (1.21) when $\nu = 0, z_1 = \dots = z_m = 0$, i.e. ;

$$u^\star = -\begin{pmatrix} a_1(0,\eta_\star) \\ \dots \\ a_m(0,\eta_\star) \end{pmatrix}^{-1} \begin{pmatrix} b_1(0,\eta_\star) \\ \dots \\ b_m(0,\eta_\star) \end{pmatrix} \tag{1.22}$$

and the zero dynamics is described by

$$\dot{\eta}_\star = q(0,\eta_\star), \quad \eta_\star(t_0) = \eta_\star^\circ \tag{1.23}$$

coincident with the restriction of the feedback system to the zero dynamics submanifold defined as

$$\mathcal{Z}^\star = \{(z,\eta_\star) : z_{1,1} = z_{1,2} = \dots = z_{1,r_1} = \dots = z_{m,1} = z_{m,2} = \dots = z_{m,r_m} = 0\} \tag{1.24}$$

In the original x coordinates of the system, the zero dynamics submanifold reads;

$$\mathcal{Z}^\star = \{x \in \mathbb{R}^n : \\ h_1(x) = L_f h_1(x) = \ldots = L_f^{r_1-1} h_1(x) = \ldots = h_m(x) = L_f h_m(x) = \ldots = L_f^{r_m-1} h_m(x) = 0\}$$

over which the feedback solving the problem is;

$$u^\star = -D^{-1}(x) \begin{pmatrix} L_f^{r_1} h_1(x) \\ \ldots \\ L_f^{r_m} h_m(x) \end{pmatrix}$$

and the zero dynamics, motion on $\mathcal{Z}^\star$ takes the form;

$$\dot{x} = f^\star(x)|_{\mathcal{Z}^\star} = \big[f(x) + \sum_{i=1}^{m} g_i(x) u_i^\star(x)\big]|_{\mathcal{Z}^\star}$$

In the linear context, and for simplicity considering the case where $m = 2$ i.e. ;

$$\dot{x} = Ax + b_1 u_1 + b_2 u_2 \tag{1.25a}$$

$$y_1 = c_1 x, \quad y_2 = c_2 x \tag{1.25b}$$

we have that the integers r_i are the smallest integers such that $c_i A^\ell b_j = 0,\ j = 1, 2$ and $c_i A^{r_i - 1} b_j \neq 0$ for some j. Accordingly the decoupling matrix reads

$$D = \begin{pmatrix} c_1 A^{r_1-1} b_1 & c_1 A^{r_1-1} b_2 \\ c_2 A^{r_2-1} b_1 & c_2 A^{r_2-1} b_2 \end{pmatrix}$$

If the relative degree is defined then a suitable coordinates change $x \mapsto (z_1\ z_2\ \eta)^\top$ is

$$z_1 = T_1 x = \begin{pmatrix} c_1 x & c_1 A x & \ldots & c_1 A^{r_1-1} x \end{pmatrix}^\top$$

$$z_2 = T_2 x = \begin{pmatrix} c_2 x & c_2 A x & \ldots & c_2 A^{r_2-1} x \end{pmatrix}^\top$$

$$\eta = T_3 x$$

if in addition $T_3 : T_3 b_i = 0\ i = 1, 2$ one has for the last $n - d$ coordinates the choice $\eta_\star$ and the normal form is;

$$\dot{z}_{1,1} = z_{1,2}$$

$$\dot{z}_{1,2} = z_{1,3}$$

$$\vdots$$

$$\dot{z}_{1,r_1-1} = z_{1,r_1}$$

$$\dot{z}_{1,r_1} = R_1 z + S_1 \eta_\star + a_{1,1} u_1 + a_{1,2} u_2$$

$$\vdots$$

$$
\begin{aligned}
\dot{z}_{2,1} &= z_{2,2} \\
\dot{z}_{2,2} &= z_{2,3} \\
&\vdots \\
\dot{z}_{2,r_2-1} &= z_{2,r_2} \\
\dot{z}_{2,r_2} &= R_2 z + S_2 \eta_\star + a_{2,1} u_1 + a_{2,2} u_2 \\
\dot{\eta}_\star &= P z + Q_\star \eta_\star \\
y_1 = z_{1,1}, &\quad y_2 = z_{2,1}
\end{aligned}
$$

where for $i, j = 1, 2$ $a_{i,j}$ being the $[i, j]$ element of the decoupling matrix, R_i, S_i row vectors of suitable dimension and P, $Q_\star$ square matrices of dimension $n - r_1 - r_2$. In this setting, the state feedback (1.21) that maximizes unobservability reduces to

$$
u = D^{-1}\nu - D^{-1} \begin{pmatrix} R_1 z + S_1 \eta_\star \\ R_2 z + S_2 \eta_\star \end{pmatrix} \tag{1.26}
$$

under which the input-output link becomes

$$
y_i(s) = \frac{1}{s^{r_i}} \nu_i(s), \quad i = 1, 2
$$

Finally, and mirroring the previous section, when the output is constrained to remain identically zero setting $\nu = 0, z_1 = z_2 = 0$, the unobservable dynamics reduce to the zero dynamics;

$$
\dot{\eta}_\star = Q_\star \eta_\star, \quad \eta_\star(t_0) = \eta_\star^\circ \tag{1.27}
$$

and the zeros of the system coincide with the eigenvalues of the matrix $Q_\star$. Moreover, the feedback (1.26) with $\nu = 0, z = 0$ is the one cancelling all the zeros.

Remark 1.3 *the matrix transfer function corresponding to (1.25a),(1.25b) takes the form*

$$
G(s) = C(sI - A)^{-1}B = \frac{det \begin{pmatrix} sI - A & -B \\ C & \mathbf{0} \end{pmatrix}}{det(sI - A)}
$$

for $C = (c_1^\top \; c_2^\top)^\top$, $B = (b_1 \; b_2)$ because of the definition of the determinant of a partitioned matrix. The matrix in the numerator is commonly referred to as the (Rosenbrock) system matrix Rosenbrock (1967), and the roots of it's determinant polynomial coincide with the zeros of the system. If the linear system is minimal and square, those modes not only coincide with $\sigma(Q_\star)$ in (1.27), but also with the Smith McMillan zeros of the matrix transfer function associated with the system Skogestad and Postlethwaite (2007). The Smith McMillan form and other corresponding aspects will be revisited again in detail in Chapter 3.

Remark 1.4 *for a non-square control system with more inputs than outputs the same definition for the relative degree applies with the non-square decoupling matrix required to be full row rank. However, in this case the arguments concerning the geometric characterization of the zero dynamics sub-manifold (the zero dynamics subspace and the Smith McMillan zeros in the linear setting),*

do not carry over and more sophisticated machinery are needed; at that point one speaks of right invertibility as the discussion in Chapter 3 highlights. See also for example Silverman (1969); Hirschorn (1979); Basile and Marro (1992).

Remark 1.5 *if the system lacks vector relative degree, one can still define the zero dynamics utilizing the so-called generalized normal forms obtained via Singh's structure algorithm Singh (1981) (see also (Isidori, Chapter 9)). These aspects will be revisited in a linear setting when we discuss stable inversion in continuous-time at a later point in this work.*

1.3 Inversion based control and the zero dynamics

As already hinted at, inversion based control is ubiquitous and not only used to force the output to track a given input arbitrarily fast, but in other applications as well, e.g. disturbance decoupling.

Clearly under inversion based feedback laws the stability properties of the residual dynamics is paramount. In this sense, a non-minimum phase zero dynamics presents an obstruction, in continuous-time, to the utilization of such direct inversion based control methods.

A possible workaround in continuous-time is to design the feedback law in such a way as to render unobservable only a sub-dynamics of the zero dynamics known to be minimum phase apriori. This is typically done via *partial cancellation through output redefinition*; finding a new dummy output function with respect to which the system has only the minimum phase component as the zero dynamics and designing the control laws based on this new dummy output under some technical assumptions (Isidori, 1995, Chapter 4).

As maybe clear to the reader, for a SISO linear system with a transfer function $G(s) = \frac{n_1(s)n_2(s)}{d(s)}$ and let $r_1 = \deg(n_1(s))$, a feedback assigning the poles of the closed loop to the roots of the polynomial $p_\star(s) = s^{r_1} n_1(s)$ achieves cancellation of only the subset of the zeros coincident with roots of the polynomial $n_1(s)$. This methodology can be directly translated to the linear state space context and, in a local sense using the Linear Tangent Model LTM at a given point x_0, to a special class of nonlinear control affine SISO systems Mattioni et al. (2017a, 2019). In fact, if the minimum phase component of the zeros polynomial of the transfer function is of the form $n_1(s) = b_0^1 + b_1^1 s + \ldots + b_{m_1}^1 s^{m_1}$ then the system (at least locally under a suitable coordinates change) will have the zero dynamics coinciding with $n_1(s)$ with respect to the output $\tilde{y} = \tilde{c}\, x$ with $\tilde{c} = \begin{pmatrix} b_0^1 & \ldots b_{m_1}^1 & 0 & \ldots & 0 \end{pmatrix}$.

A more elegant and easier to generalize method for partial cancellation utilizing directly the normal form of linear SISO systems (equivalently the normal form of the LTM of a nonlinear SISO system at a point) can be hypothesized;

Claim 1.1 *let $T_Q : \mathbb{R}^{n-r} \to \mathbb{R}^{n-r}$ be the transformation putting the matrix $Q_\star$ in (1.15) in Jordan form such that $Q_\star = diag(Q_\star^1,\ Q_\star^2)$. Assume that one is interested in finding a dummy output with respect to which the zero dynamics is described by $\eta_\star^2 = Q_\star^2 \eta_\star^2$. Defining $r_2 = n - dim(Q_\star^2)$, an iterative procedure can then be applied in the new coordinates obtaining an output $\tilde{y} = \tilde{c}\eta_\star^2$; linear combination of the states $\eta_\star^2$ and the original output, having a relative degree r_2 and with respect to which Q_2 characterize the zeros of the system. If $\sigma(Q_\star^2) \subset \mathbb{C}^-$ then the system is minimum phase with respect to $\tilde{y}$.* ◀

Following from the discussion presented in Section 1.1 and the above remarks for SISO systems, the obstruction caused by the zero dynamics (equivalently the zeros) of a square MIMO system for direct controller synthesis via inversion could be mitigated utilizing partial cancellation techniques. In a linear square LTI MIMO setting this could be done in the matrix transfer function context directly extending the previous comments. In fact, the Smith McMillan form of a given matrix transfer function being diagonal lends itself to a so called partial matrix fraction description (Kailath, 1980, Chapter 6). As a result, one can write the transfer function matrix as $G(s) = N_1(s)\tilde{G}(s)$ in which $N_1(s)$ contains only a subset of the zeros and $\tilde{G}(s)$ proper (possibly after introducing a so-called right divisor Kailath (1980)) containing the remaining zeros and all the poles of the system. As a byproduct, if $\tilde{G}(s)$ is minimum phase, one has obtained a dummy output with respect to which direct controller synthesis design via inversion preserves stability. In state space setting, and let $\tilde{y}(s) = \tilde{C}x$ be the output associated with the minimal state space realization of $\tilde{G}(s)$, then the original system, after suitable coordinates transformations, will be minimum phase with respect to this dummy output $\tilde{y}$.

These techniques, as the reader may surmise, will carry over seamlessly to nonlinear square MIMO systems with a linear output map locally using the LTM. Additionally, direct output redefinition for partial zero dynamics cancellation via the normal form (as stated in Claim 1.1) will be shown, via an example, to work on a nonlinear square MIMO system in a local sense.

1.4 Concluding remarks

A few final comments to close this chapter are in order;

- When the zeros and zero dynamics are non minimum phase (more precisely when the residual dynamics under feedback is unstable) they pose limitations to inversion based control design.
- A possible way to mitigate those limitations is partial zero dynamics cancellation and output redefinition.
- In a digital context, this workaround is not enough on it's own as will be seen in the sequel and additional sampled-data methodologies are needed detailed in the next chapter.

It is important to note that this chapter, while introducing most of the necessary definitions needed for our work, is *not* a complete treatment of the structure of zero dynamics in continuous-time.

In fact, in the linear context, arguments pertaining to the frequency domain analysis of the zeros Bode et al. (1945), Monaco (2020), the zeros of non-square LTI MIMO systems Marro (1990), and the zeros at infinity (Kailath, 1980, Chapter 4) were not covered and the interested reader is referred to those references for more comprehensive study.

Concerning the non-linear setting, treatment of non-square MIMO systems Hirschorn (1979), the zero dynamics algorithm for systems lacking vector relative degree (Isidori, Chapter 9), MIMO systems in discrete time Califano et al. (1999), Aranda-Bricaire et al. (1996), Monaco and Normand-Cyrot (1983b) are omitted for brevity and the interested reader is advised to refer to the cited references.

Chapter 2

Background on zero dynamics under sampling

Contents

In this chapter, we will mirror the discussion in the previous chapter in the sampled-data context i.e when the control and sensing of a continuous-time system are implemented at discrete time instants. More in detail, this chapter will attempt to:

- give an overview of basic facts about Single-Rate sampling (SR) of a continuous-time system both in SISO and MIMO contexts. The effects of sampling on the structure of the resulting *sampled-data equivalent* system will be discussed in details. Focus will be on aspects related to the so-called sampling zero dynamics and loss of relative degree with some examples.

- recall a powerful tool that mitigates the issues pertaining to the loss of the relative degree and the appearance of sampling zero dynamics, namely multi-rate sampling. In this sense, multi-rate sampling allows one to overcome the limitations imposed on inversion based control in a digital context. This fact is at the basis of the results obtained in later chapters of this work.

This chapter will define the notation, nomenclature and the mechanics of the discussions related to sampling in the rest of the thesis. It is also intended as a motivating chapter for some of the problems addressed in this work. The notions appearing hereinafter are recalled from Monaco (2020), Franklin et al. (1998), Monaco and Normand-Cyrot (1985), Åström et al. (1984), Monaco et al. (1986b), Monaco and Normand-Cyrot (1992), Monaco and Normand-Cyrot (1997), and Yuz and Goodwin (2005a).

Before proceeding to present formal definitions and comments on sampled-data equivalent models and the loss of control properties under sampling, we start with an example.

Example 2.1 consider a simple triple integrator in continuous-time

$$G(s) = \frac{1}{s^3}$$

which has relative degree $r = 3$ and *no* zeros. Given a desired reference y_r, one can find a state feedback such that the output-reference transfer function $y(t) - y_r(t)$ is almost unity. This is done in the following manner, looking at the triple integrator;

$$\begin{aligned}\dot{z}_1 &= z_2\\ \dot{z}_2 &= z_3\\ \dot{z}_3 &= u\\ y &= z_1\end{aligned}$$

and using the feedback

$$u = \frac{\nu}{cA^2b} - \frac{\cancel{cA^3z}}{\cancel{cA^2b}} = \nu = F(z - z_r)$$

with $z_r = (y_r \ \dot{y}_r \ \ddot{y}_r)^\top$, (A, b, c) are the Brunovsky's triplet of dimension 3 Brunovskỳ (1970). Choosing F placing the poles of the closed loop at $\{-\frac{1}{\tau}, -\frac{1}{\tau}, -\frac{1}{\tau}\}$, $\tau \approx 0$, small enough, one can get a sort of inversion via feedback because $\frac{y(s)}{y_r(s)} = \frac{1}{(1+\tau s)^3} \approx 1$.

However if we want to implement a digital control of the same type designed working over the sampled model we face a limitation. In fact the triple integrator zero-order-holding pulse transfer function (Franklin et al., 1998, Chapter 4) reads;

$$H(z) = \frac{\delta^3(z^2 + 4z + 1)}{6(z - 1)^3}$$

with $\delta > 0$ sampling period. This pulse transfer function has two *new* zeros, the so-called sampling zeros being $z_d^\star = \{-\sqrt{3} - 2, \ \sqrt{3} - 2\}$ the former of which is non-minimum phase (outside the unit disk), and thus the excess of poles over zeros under sampling falls to $r_d = 1$. Consequently, following the same logic as in continuous-time of designing a feedback that renders the $y(k) - y_r(k)$ link (almost) unity which requires zeros cancellation results in placing the closed loop poles in $\{-\sqrt{3} - 2, \ \sqrt{3} - 2, \ \star\}$ leading to closed-loop instability.

This examples emphasizes that under sampling extra zeros appear that are typically non-minimum phase. This fact poses an obstruction to inversion-based control design working over the sampled model irrespective of minimum phaseness of the underlying continuous-time system. These aspects and methods to mitigate these issues are the subject of this chapter.

2.1 The discrete-time case

In the purely discrete-time context the definitions and arguments presented for the relative degree, normal forms and zero dynamics in continuous-time, can be developed along the same lines in the linear case. Difficulties arise in nonlinear context not only from a computations point of view

Monaco and Normand-Cyrot (1997). Let us recall the definition of relative degree in discrete time Monaco and Normand-Cyrot (1983a);

Definition: relative degree in DT

Consider the discrete-time (DT) SISO system described by the difference equation

$$\begin{aligned} x(k+1) &= F(x(k), u(k)) \\ y(k) &= h(x(k)) \end{aligned}$$

with $x \in \mathbb{R}^n$, $u, y \in \mathbb{R}$. Denote by $F_0^j(x) = F_0(\cdot) \circ F_0(\cdot) \circ \ldots \circ F_0(x)$ the $j-$times composition with $F_0(x) = F(x, 0)$. The *discrete relative degree* r_d is the smallest integer satisfying

$$\begin{aligned} \frac{\partial h \circ F_0^\ell \circ F(x,u)}{\partial u} &= 0, \quad \ell = 0 \ldots r_d - 2 \\ \frac{\partial h \circ F_0^\ell \circ F(x,u)}{\partial u} &\neq 0, \quad \ell = r_d - 1. \end{aligned}$$

In words, the discrete relative degree is the number of delays in time-steps for the input to influence the output. If this is the case it results that a coordinates change of the form

$$\begin{aligned} z = \phi_1(x) = \begin{pmatrix} h(x) & h \circ F(x,u) & \ldots & h \circ F_0^{r_d-1} \circ F(x,u) \end{pmatrix}^\top & \quad \in \mathbb{R}^{r_d} \\ \eta = \phi_2(x) & \quad \in \mathbb{R}^{n-r_d} \end{aligned} \tag{2.1}$$

with $\phi_2(x)$ completing the coordinates change allow the system to take the *discrete normal form*

$$\begin{aligned} z_1(k+1) &= z_2(k) \\ z_2(k+1) &= z_3(k) \\ &\vdots \\ z_{r_d-1}(k+1) &= z_{r_d}(k) \\ z_{r_d}(k+1) &= F_z(z(k), \eta(k), u(k)) \\ \eta(k+1) &= q(z(k), \eta(k), u(k)) \\ y(k) &= z_1(k) \end{aligned} \tag{2.2}$$

where $F_z(z, \eta, u) = h \circ F(x,u) \circ \ldots \circ F(x,u)$ for r_d times and $q(z, \eta, u) = \phi_2 \circ F(x,u)$ all computed at $x = \phi^{-1}(z, \eta)$. This normal form highlights two difficulties;

- the nonlinear dependence of the map $q(z, \eta, u)$ on the states and control. It is not obvious if one can always find coordinates $\eta_\star$ such that the η dynamics is independent of the control
- more importantly, the map $F_z(z, \eta, u)$ highlights the difficulty of designing an output zeroing feedback and defining the zero dynamics as done in the continuous-time case.

Remark 2.1 *for a linear system described by*

$$\begin{aligned} x(k+1) &= A_d x(k) + b_d u(k) \\ y(k) &= c_d x(k) \end{aligned}$$

with $x(k) \in \mathbb{R}^n$ and $u(k), y(k) \in \mathbb{R}$, it can be easily verified that one recovers for the discrete relative degree the usual identities

$$c_d A_d^{\ell} b_d = 0, \quad \ell = 1, \dots, r_d - 1, \qquad c_d A_d^{r_d - 1} b_d \neq 0$$

and the same arguments for the normal form apply. Additionally, notions of minimum phase and non-minimum phase zeros are well defined with reference to stability in discrete time Monaco (2020).

On linear equivalence and partial inversion in discrete-time

Following Monaco and Normand-Cyrot (1987), if the discrete-time relative degree is well defined, (2.2) rewrites;

$$\begin{aligned} z_1(k+1) &= z_2(k) \\ z_2(k+1) &= z_3(k) \\ &\vdots \\ z_{r_d-1}(k+1) &= z_{r_d}(k) \\ z_{r_d}(k+1) &= h \circ F_0^{r_d} \circ F(x,u) = h \circ F_0^{r_d}(x(k)) + S(x(k), u(k)) \\ \eta(k+1) &= q(z(k), \eta(k), u(k)) \\ y(k) &= z_1(k) \end{aligned}$$

where

$$S(\cdot, 0) = 0, \quad \frac{\partial S(\cdot, u)}{\partial u} \neq 0$$

Consequently, one can find a control $u = \gamma_d(x, \nu)$ of the form

$$\gamma_d(x(k), \nu(k)) = S^{-1}(x(k), \nu(k)) - h \circ F_0^{r_d}(x(k)) \tag{2.3}$$

under which the discrete-time normal form reads;

$$\begin{aligned} z_1(k+1) &= z_2(k) \\ z_2(k+1) &= z_3(k) \\ &\vdots \\ z_{r_d-1}(k+1) &= z_{r_d}(k) \\ z_{r_d}(k+1) &= \nu(k) \\ \eta(k+1) &= q(z(k), \eta(k), \gamma_d(x(k), \nu(k))) \\ y(k) &= z_1(k) \end{aligned}$$

It is clear that this control mirrors the "partial inversion" control in continuous-time treated in Section 1.1 and under which the $\eta(k+1)$ dynamics is unobservable. If in addition one restricts the output and its prediction for r_d steps to be precisely zero by suitably choosing $\nu(k)$ and the initial conditions $z(0)$, one mirrors the definition of zero dynamics in continuous-time in this setting.

The Multi-Input Multi-Output discrete-time case

In the square MIMO setting, things become much more involved Monaco and Normand-Cyrot (1983b), Califano et al. (1999), and so we will limit our discussion to defining the discrete vector relative degree. Detailed aspects pertaining to normal forms and zero dynamics properties in this case will be ommitted since they are not needed for the developments in this work. To this purpose, consider a discrete-time square MIMO system of the form;

$$\begin{aligned} x(k+1) &= F(x(k), u_1(k), \dots, u_m(k)) \\ y(k) &= \begin{pmatrix} h_1(x(k)) & \dots & h_m(x(k)) \end{pmatrix}^\top \end{aligned}$$

with $x \in \mathbb{R}^n$, $u_i, y_i \in \mathbb{R}$ for $i = 1, \dots, m$. Recall the following definition Califano et al. (1999);

Definition: vector relative degree in DT

The DT square MIMO system has a well defined *discrete vector relative degree* $r_d = (r_{d,1} \ \dots \ r_{d,m})$ at a point x_0 if and only if

- For each $r_{d_i}, i = 1, \dots, m$;

$$\frac{\partial h_i \circ F_0^{\ell} \circ F(x,u)}{\partial u} = 0, \quad \ell = 0 \dots r_{d_i} - 2, \quad \frac{\partial h_i \circ F_0^{r_{d_i}-1} \circ F(x,u)}{\partial u} \neq 0$$

- the following matrix is full rank at x_0;

$$D = \begin{pmatrix} \frac{\partial h_1 \circ F_0^{r_{d,1}-1} \circ F(x,u)}{\partial u_1} & \dots & \frac{\partial h_1 \circ F_0^{r_{d,1}-1} \circ F(x,u)}{\partial u_m} \\ & \ddots & \\ \frac{\partial h_m \circ F_0^{r_{d,m}-1} \circ F(x,u)}{\partial u_1} & \dots & \frac{\partial h_m \circ F_0^{r_{d,m}-1} \circ F(x,u)}{\partial u_m} \end{pmatrix} |_{u=0} \tag{2.4}$$

The same arguments concerning a linearizing and "inverting feedback" can be carried in this case as well and the interested reader is referred to Califano et al. (1999).

2.2 The sampled-data Single-Input Single-Output case

Motivated by the above fact, we now turn to a more general and formal discussion of sampling and its effects on the structure of the control system. How sampling induces further obstructions on inversion based control in addition to the ones in continuous-time will be discussed as well, and a multi-rate sampling scheme to mitigate this issue is highlighted. To this end, let the continuous-time SISO system of the form (1.1a)-(1.1b) assumed having a well defined continuous-time relative

degree r (see Section 1.1). By Single-Rate (SR) sampling, typically resulting from the use of a holding device and a sampler, we mean the following;

- the control is piecewise constant over time intervals of length $\delta > 0 \in \mathbb{R}$ called the *sampling period*, namely for $k \in \mathbb{Z}_+$; $\quad u(t) = u(k), \qquad \forall t \in [k\delta, (k+1)\delta[$
- measures of the states (outputs) are available only at the sampling instants, i.e. $x(t) = x(k\delta), \quad y(t) = y(k\delta)$ at the sampling instant.

Accordingly, the SR sampled-data system equivalent to (1.1a)-(1.1b) at the sampling instants is

$$x(k+1) = F^\delta(x(k), u(k)) \tag{2.5a}$$
$$y(k) = h(x(k)) \tag{2.5b}$$

The map $F^\delta(x,u)$ is obtained by integrating the continuous time dynamics (1.1a) under the piecewise constant control at $t = k\delta$ over the period $t \in [k\delta, (k+1)\delta[$, which admits a formal Taylor expansion parametrized by δ, i.e.

$$\begin{aligned} F^\delta(x(k), u(k)) &= x(k) + \int_{k\delta}^{(k+1)\delta} \Big(f(x(\tau)) + g(x(\tau))u(k) \Big) d\tau \\ &= e^{\delta(\mathrm{L}_f + u(k)\mathrm{L}_g)} x(k) = x(k) + \sum_{i>0} \frac{\delta^i}{i!} (\mathrm{L}_f + u(k)\mathrm{L}_g)^i x(k) \end{aligned} \tag{2.6}$$

with this in mind, we have the following definition;

Definition: SR sampled equivalent model

Consider the continuous-time input affine SISO system (1.1a)-(1.1b), then there exists $T^\star > 0$ small enough such that $\forall \delta \in [0, T^\star[$ the exponential (2.6) converges. If this is the case then (2.5a)-(2.5b) is called the SR sampled-data equivalent model.

Remark 2.2 *in the case of LTI systems of the form (1.10a),(1.10b), the SR equivalent model (2.5a),(2.5b) reduces to*

$$\begin{aligned} x(k+1) &= A^\delta x(k) + b^\delta u(k) \\ y(k) &= cx(k) \end{aligned} \tag{2.7}$$

where

$$A^\delta = e^{\delta A}, \qquad b^\delta = \int_0^\delta e^{\tau A} b \; d\tau \tag{2.8}$$

Noting that (2.6) is an infinite series expansion in powers of δ; the question of existence of a closed form solution and other practical limitations requires one to consider approximations. In this sense, consider truncations of (2.6) up to a given power $p \geq 1$ in δ, namely (dropping the time

argument for simplicity)

$$F^{\delta}(x(k),u(k)) = x(k) + \sum_{i=1}^{p} \frac{\delta^i}{i!}(\mathrm{L}_f + u(k)\mathrm{L}_g)^i x + O(\delta^{p+1}) = F^{\delta[p]}(x(k),u(k)) + O(\delta^{p+1}) \tag{2.9}$$

this approximation then defines the following property;

Definition: ASR sampled equivalent model

Consider the continuous-time input affine SISO system (1.1a)-(1.1b), then there exists $T^\star > 0$ small enough such that $\forall \delta \in [0, T^\star[$ the exponential (2.6) converges. Accordingly, for any $p \geq 1$

$$\|F^{\delta}(x(k),u(k)) - F^{\delta[p]}(x(k),u(k))\| \leq O(\delta^{p+1})$$

for all k where $F^{\delta[p]}(x,u)$ as in (2.9) is called the Approximate SR (ASR) sampled-data equivalent dynamics at the order p.

Remark 2.3 *it is clear from (2.7) that in the linear context, the SR sampled equivalent model is exactly computable.*

Applying the definition of the discrete-time relative degree in Section 2.1 to the SR sampled equivalent system (2.5a)-(2.5b), using the expansion (2.6), we recall the following Lemma Monaco and Normand-Cyrot (1997);

Lemma: zero dynamics under sampling

Consider a continuous-time SISO system with a well defined relative degree r, and let (2.5a)-(2.5b) be it's SR sampled equivalent model, then the discrete relative degree of the SR sampled equivalent model always falls to $r_d = 1$; namely for all $x(k)$,

$$\frac{\partial y(k+1)}{\partial u(k)} = \frac{\delta^r}{r!}\mathrm{L}_g\mathrm{L}_f^r h(x)\big|_{x(k)} + O(\delta^{r+1}) \neq 0.$$

As a consequence, whenever in continuous-time $r > 1$, the sampling process induces a further (possibly) unstable so-called *sampling zero dynamics* of dimension $r-1$.

A more precise characterization of this fact can be drawn in the LTI setting using the example

of a chain of n integratos described by the triplet (A_n, b_n, c_n);

$$A_n \in \mathbb{R}^{n\times n} = \begin{pmatrix} 0 & 1 & 0 & \dots & 0 \\ 0 & 0 & 1 & \dots & 0 \\ & & \vdots & & \\ 0 & 0 & 0 & \dots & 1 \\ 0 & 0 & 0 & \dots & 0 \end{pmatrix}, \quad b_n \in \mathbb{R}^{n\times 1} = \begin{pmatrix} 0 \\ 0 \\ \vdots \\ 0 \\ 1 \end{pmatrix}$$
$$c_n \in \mathbb{R}^{1\times n} = \begin{pmatrix} 1 & 0 & \dots & 0 & 0 \end{pmatrix} \tag{2.10}$$

The SR sampled equivalent model, applying the definition (2.7), takes the form

$$\begin{aligned} x(k+1) &= A_n^\delta x(k) + b_n^\delta u(k) \\ y(k) &= c_n x(k) \end{aligned} \tag{2.11}$$

with

$$A_n^\delta = \begin{pmatrix} 1 & \delta & \dots & \frac{\delta^{n-1}}{(n-1)!} \\ 0 & 1 & \dots & \frac{\delta^{n-2}}{(n-2)!} \\ & & \ddots & \\ 0 & 0 & \dots & 1 \end{pmatrix}, \quad b_n^\delta = \begin{pmatrix} \frac{\delta^n}{n!} \\ \frac{\delta^{n-1}}{(n-1)!} \\ \vdots \\ \delta \end{pmatrix} \tag{2.12}$$

consequently, it is clear that $c_n b_n^\delta = \frac{\delta^n}{n!} \neq 0$ for all $\delta > 0$ and so $r_d = 1$.

With this in mind, we can now recall, with slight rewording, the following statement due to Åström et al. (1984);

Theorem: LTI sampling zeros

Let (2.7) be the SR sampled equivalent model to a SISO LTI continuous-time system with a continuous-time relative degree $r > 1$, then the discrete-time relative degree will always fall to $r_d = 1$ and unstable zeros appear under sampling. Moreover, as $\delta \to 0$, the $r-1$ sampling zeros are the roots to the Euler-Frobenius polynomial given by

$$E_r(z) = b_1^r z^{r-1} + b_2^r z^{r-2} + \dots + b_r^r$$
$$b_k^j = \sum_{\ell=1}^{k} (-1)^{k-\ell} \ell^j \binom{j+1}{k-\ell}$$

The above result states that, given a continuous-time transfer function $G(s) = \frac{n(s)}{d(s)}$ having m zeros $z_i^\star$, then the sampled-data equivalent transfer function $G(z) = \frac{n(z)}{d(z)}$ will have $n-1$ zeros. Those $n-1$ zeros, while not always easy to characterize explicitly, can be divided into two groups asymptotically as $\delta \to 0$;

$$\text{Zeros of } G(z): \begin{cases} \text{m zeros corresponding to the continuous-time zeros under sampling being} & e^{z_i^\star \delta} \\ \text{n-m-1 sampling zeros roots of the polynomials} & E_j(z) = 0, \quad j = n-m \end{cases}$$

and for the first terms one has the polynomials $E_i(z)$ being;

$$\begin{aligned} E_1(z) &= 1 \\ E_2(z) &= z + 1, \\ E_3(z) &= z^2 + 4z + 1 \\ &\vdots \end{aligned}$$

Example 2.2 For the case of the triple integrator in continuous-time and looking at the SR sampled equivalent model (2.11) it is clear that the determinant polynomial of the corresponding Rosenbrock system matrix coincide with

$$\det \begin{pmatrix} z-1 & -\delta & -\frac{\delta^2}{2} & -\frac{\delta^3}{6} \\ 0 & z-1 & -\delta & -\frac{\delta^2}{2} \\ 0 & 0 & z-1 & -\delta \\ 1 & 0 & 0 & 0 \end{pmatrix} = \frac{\delta^3}{6}(z^2 + 4z + 1) = \frac{\delta^3}{6} E_3(z)$$

and it's roots, for all $\delta > 0$ are precisely those of $E_3(z)$, namely the sampling zeros are $z_d^\star = \{-\sqrt{3} - 2,\ \sqrt{3} - 2\} \approx \{-3.732,\ -0.268\}$.

An important consequence of the comments made above is the fact that, even when starting with a continuous-time minimum phase system where direct controller synthesis via inversion applies with stability, sampling introduces an additional obstruction. This obstruction is caused by the appearance of extra $r - 1$ sampling zeros which are typically non-minimum phase.

2.3 Preserving the relative degree under single-rate sampling

As already explained, the fall of the relative degree under sampling is emblematic of the appearance of extra sampling zero-dynamics responsible for serious limitations in feedback design. In the sequel, and for Single-Input Single-Output systems we recall a result due to Barbot et al. (1996) where a δ-dependent change to the output function defining the normal form in continuous-time is shown to preserve the relative degree of the system in a predefined order of approximation. We will illustrate this procedure for a SISO system assuming $r = 3$ thus explaining the intuition behind the result in Barbot et al. (1996). This procedure is then generalized in Chapter 7 to the setting of MIMO systems. In this simple case of $r = 3$, the normal form in continuous-time reads;

$$\begin{aligned} \dot{z}_1 &= z_2 \\ \dot{z}_2 &= z_3 \\ \dot{z}_3 &= b(z, \eta_\star) + a(z, \eta_\star) u \\ \dot{\eta}_\star &= q_\star(z, \eta_\star) \\ y &= z_1 \end{aligned}$$

and under single-rate sampling with rate δ this form reads;

$$\begin{aligned}
z_1(k+1) &= z_1(k) + \delta z_2(k) + \frac{\delta^2}{2!} z_3(k) + \frac{\delta^3}{3!}\left(b(z(k),\eta_\star(k)) + a(z(k),\eta_\star(k))u(k)\right) + O(\delta^4)\\
z_2(k+1) &= z_2(k) + \delta z_3(k) + \frac{\delta^2}{2!}\left(b(z(k),\eta_\star(k)) + a(z(k),\eta_\star(k))u(k)\right) + O(\delta^3)\\
z_3(k+1) &= z_3(k) + \delta\left(b(z(k),\eta_\star(k)) + a(z(k),\eta_\star(k))u(k)\right) + O(\delta^2)\\
\eta_\star(k+1) &= \eta_\star(k) + \delta q_\star(z(k),\eta_\star(k)) + O(\delta^2)\\
y(k) &= z_1(k)
\end{aligned}$$

Define the "modified" dummy output

$$y^\delta = y - \delta\dot{y} + \frac{\delta^2}{3}\ddot{y} = z_1 - \delta z_2 + \frac{\delta^2}{3} z_3$$

and note that the prediction of this output can be written as;

$$\begin{aligned}
y^\delta(k+1) &= z_1(k+1) - \delta z_2(k+1) + \frac{\delta^2}{3} z_3(k+1)\\
&= z_1(k) - \frac{\delta^2}{3!} z_3(k) + O(\delta^4)\\
y^\delta(k+2) &= z_1(k+2) - \delta z_2(k+2) + \frac{\delta^2}{3} z_3(k+2)\\
&= z_2(k) + \frac{\delta}{2} z_3(k) + O(\delta^3)\\
y^\delta(k+3) &= z_1(k+3) - \delta z_2(k+3) + \frac{\delta^2}{3} z_3(k+3)\\
&= z_3(k) + \delta\left(b(z(k),\eta_\star(k)) + a(z(k),\eta_\star(k))u(k)\right) + O(\delta^2)
\end{aligned}$$

In this way, the effect of the control on the output y^δ is relegated to terms in $O(\delta^4)$. Consequently, defining the new coordinates ;

$$z_1^\delta(k) = y^\delta(k), \quad z_2^\delta(k) = z_2(k) - \frac{\delta}{2} z_3(k), \quad z_3^\delta(k) = z_3(k)$$

one has

$$\begin{aligned}
z_1^\delta(k+1) &= z_1^\delta(k) + \delta z_2^\delta(k) + O(\delta^4)\\
z_2^\delta(k+1) &= z_2^\delta(k) + \delta z_3^\delta(k) + O(\delta^3)\\
z_3^\delta(k+1) &= z_3^\delta(k) + \delta\left(b(\cdot,\eta_\star(k)) + a(\cdot,\eta_\star(k))u(k)\right) + O(\delta^2)\\
\eta_\star(k+1) &= \eta_\star(k) + \delta q_\star(\cdot,\eta_\star(k)) + O(\delta^2)\\
y^\delta(k) &= z_1^\delta(k)
\end{aligned}$$

truncating the z^δ dynamics at the vector of *non-homogeneous orders* (for $p=1,\ r=3$)

$$O(\Delta^{p+1}) = \begin{pmatrix} O(\delta^{r+p}) \\ \vdots \\ O(\delta^{p+1}) \end{pmatrix} = \begin{pmatrix} O(\delta^4) \\ O(\delta^3) \\ O(\delta^2) \end{pmatrix}$$

and applying the definition of the relative degree in discrete-time, we can say that, different from Euler's truncation, the relative degree of the sampled system with respect to y^δ is preserved up to approximations in order of $O(\delta^{r+1})$ when considering the dynamics in approximations of order $O(\Delta^{p+1}), p=1$. A generalization of this procedure for any $r \geq 1$ and in any order $p \geq 1$ can be found in Barbot et al. (1996) for SISO systems. This procedure will be adapted in Chapter 7 to the case of MIMO systems allowing us to treat a special type of partial inversion-based controllers under single rate sampling.

2.4 Multi-rate sampling of continuous-time systems

An interesting method for handling the issues arising due to SR sampling in terms of loss of relative degree and zero dynamics structure is multi-rate sampling Monaco and Normand-Cyrot (1992). As the name suggests, and compared to SR sampling, by multi-rate sampling of order m we mean the following;

- the control is piecewise constant over *sub intervals* of the sampling period of length $\bar{\delta} = \frac{\delta}{m}$, namely for $k \in \mathbb{Z}_+, i = 1, \ldots, m$; $\quad u(t) \coloneqq u^i(k) = u(k\delta + i\bar{\delta}), \qquad \forall t \in [k\delta + (i-1)\bar{\delta}, k\delta + i\bar{\delta}[$
- measures of the states (or outputs) are available only at the sampling instants i.e. $x(t) = x(k\delta), \quad y(t) = y(k\delta)$ at the sampling instants.

Given a continuous-time SISO dynamics of the form (1.1a), the multi-rate sampled-data dynamics of order m equivalent at the sampling instant reads

$$x(k+1) = F_m^\delta(x(k), \underline{u}(k)) \tag{2.13}$$

where $\underline{u}(k) = \begin{pmatrix} u^1(k) & u^2(k) & \ldots & u^m(k) \end{pmatrix}^\top$. The map $F_m^\delta(x, \underline{u})$ is obtained by integrating the continuous time dynamics (1.1a) under the piecewise constant multi-rate controls and admitting a formal Taylor expansion, parametrized by $\bar{\delta}$, i.e.

$$\begin{aligned} F_m^\delta(x(k), \underline{u}(k)) &= e^{\bar{\delta}(\mathrm{L}_f + u^1(k)\mathrm{L}_g)} \ldots e^{\bar{\delta}(\mathrm{L}_f + u^m(k)\mathrm{L}_g)} x \big|_{x(k)} \\ &= F^{\bar{\delta}}(\cdot, u^m(k)) \circ \cdots \circ F^{\bar{\delta}}(x(k), u^1(k)) \end{aligned} \tag{2.14}$$

and we have the following definition;

Definition: multi-rate sampled equivalent dynamics

Consider the continuous-time input affine SISO system (1.1a)-(1.1b), then there exists $T^\star > 0$ small enough such that the expansion (2.14) converges. If this is the case then (2.13) is called the multi-rate sampled-data equivalent dynamics.

Preserving the zero dynamics under multi-rate sampling

In what follows, let the SISO continuous-time system (1.1a),(1.1b) have a well defined relative degree r, and consider it's multi-rate sampled equivalent dynamics of order r, i.e. setting in (2.13) $m = r$. Additionally, consider the dummy output vector defined by

$$H(x) = \begin{pmatrix} h(x) & L_f h(x) & \dots & L_f^{r-1} h(x) \end{pmatrix}^\top \tag{2.15}$$

namely a vector containing the original continuous-time output and it's higher $r-1$ derivatives. Applying the DT vector relative degree definition, it is possible to verify that the multi-rate sampled-data dynamics (2.13) has a well defined MIMO vector relative degree $r_d = (1\ 1\ \dots\ 1)$ with respect to the dummy output (2.15). Consequently, the zero dynamics submanifold of the multi-rate sampled equivalent model is the $n-r$ dimensional submanifold

$$\mathcal{Z}^\star = \{x \in \mathbb{R}^n : H(x) = 0\} \tag{2.16}$$

which recovers the same properties as that of the continuous-time zero dynamics submanifold (1.8). Similar discussion can be carried out about the zero dynamics and its stability properties. Accordingly, whenever the continuous-time system is minimum-phase; so is the corresponding multi-rate sampled model (2.13),(2.15) and partial inversion-based techniques can be designed working over the multi-rate sampled-data model with the confidence that the residual dynamics under feedback is stable.

Remark 2.4 *if the continuous-time dynamics is LTI with relative degree r then the multi-rate sampled equivalent dynamics of order r with $\delta = r\bar{\delta}$ reads;*

$$x(k+1) = (A^{\bar{\delta}})^r x(k) + (A^{\bar{\delta}})^{r-1} b^{\bar{\delta}} u^1(k) + \ \dots\ + A^{\bar{\delta}} b^{\bar{\delta}} u^{r-1}(k) + \ b^{\bar{\delta}} u^r(k) \tag{2.17}$$

where the pair $(A^{\bar{\delta}}, b^{\bar{\delta}})$ as in (2.7).

Returning to the same example of the triple integrator, we discuss how varying the input in sub-intervals of the sampling period in this manner mitigates the sampling zeros.

Example 2.3 consider again the triple integrator. This system has no zeros in continuous-time and relative degree $r = 3$ while it's SR sampled equivalent model applying (2.7) has two zeros roots of the Euler-Frobenius polynomial $E_3(z) = z^2 + 4z + 1 = 0$.

- *Multi-rate of order 3:* Let us augment the sampling rate even more. The multi-rate sampled

equivalent dynamics of order $r = 3$ for the triple integrator takes the form (2.17) with

$$z(k+1) = A_m z(k) + B_m \underline{u}(k)$$
$$A_{m=3} = \begin{pmatrix} 1 & 3\bar{\delta} & \frac{9\bar{\delta}^2}{2!} \\ 0 & 1 & 3\bar{\delta} \\ 0 & 0 & 1 \end{pmatrix}, \quad B_{m=3} = \begin{pmatrix} \frac{19\bar{\delta}^3}{6} & \frac{7\bar{\delta}^3}{6} & \frac{\bar{\delta}^3}{6} \\ \frac{5\bar{\delta}^2}{2} & \frac{3\bar{\delta}^2}{2} & \frac{\bar{\delta}^2}{2} \\ \bar{\delta} & \bar{\delta} & \bar{\delta} \end{pmatrix}$$

where $\underline{u}(k) = \begin{pmatrix} u^1(k) & u^2(k) & u^3(k) \end{pmatrix}^\top$. Consider the augmented output vector $y(k) = C_{m=3} z(k)$ with $C_m = \text{col}(c_3 \;\; c_3 A \;\; c_3 A^2)$ as the original output and it's higher $r-1$ derivatives. This multi-rate sampled equivalent system has vector relative degree $r_d = (1\ 1\ 1)$. Indeed this system is a MIMO square system that has no zeros recovering the properties of the continuous-time original system. An interesting fact is that each muli-rate order reduces the sampling zeros by one as seen below.

- *Multi-rate of order* 2*:* apply a multi-rate of order 2, increasing the degrees of freedom by 1, and notice that the multi-rate sampled model reads;

$$z_1(k+1) = z_1(k) + 2\bar{\delta} z_2(k) + 2\bar{\delta}^2 z_3(k) + \frac{7\bar{\delta}^3}{6} u^1(k) + \frac{\bar{\delta}^3}{6} u^2(k)$$
$$z_2(k+1) = z_2(k) + 2\bar{\delta} z_3(k) + \frac{3\bar{\delta}^2}{2} u^1(k) + \frac{\bar{\delta}^2}{2} u^2(k)$$
$$z_3(k+1) = z_3(k) + \bar{\delta} u^1(k) + \bar{\delta} u^2(k)$$

  Now consider the augmented output vector

$$y(k) = H(x(k)) = \begin{pmatrix} z_1(k) \\ z_2(k) \end{pmatrix}$$

  which is the the original output and it's first derivative. The determinant of the Rosenbrock system matrix in this case reads;

$$\det \begin{pmatrix} z-1 & -2\,\bar{\delta} & -2\,\bar{\delta}^2 & -\frac{7\bar{\delta}^3}{6} & -\frac{\bar{\delta}^3}{6} \\ 0 & z-1 & -2\,\bar{\delta} & -\frac{3\bar{\delta}^2}{2} & -\frac{\bar{\delta}^2}{2} \\ 0 & 0 & z-1 & -\bar{\delta} & -\bar{\delta} \\ 1 & 0 & 0 & 0 & 0 \\ 1 & \bar{\delta} & \frac{\bar{\delta}^2}{2} & 0 & 0 \end{pmatrix} = \frac{\bar{\delta}^6 (5z+1)}{6}$$

  which has a single root. Thus this multi-rate sampled model of the continuous-time triple interator, by increasing the multi-rate order, decreased the number of sampling zeros by (1).

This example highlights how multi-rate sampling can be used to recover the relative degree and the zeros (zero dynamics) properties of the continuous-time system under sampling by properly choosing the multi-rate order. It also emphasizes the interesting fact that, while the limiting sampling zeros of a SISO system are well understood, the same can not be said about MIMO systems, which brings us to the following section.

2.5 The sampled-data Multi-Input Multi-Output case

Consider the continuous-time square MIMO system (1.16a)-(1.16b), the associated SR sampled-data equivalent model will take the form

$$x(k+1) = F^{\delta}(x(k), u_1(k), \ldots, u_m(k)) \tag{2.18a}$$

$$y_i(k) = h_i(x(k)), \quad i = 1, \ldots, m \tag{2.18b}$$

and the map $F^{\delta}(x, u_1, \ldots, u_m)$ is of the form

$$\begin{aligned} F^{\delta}(x(k), u(k)) &= e^{\delta(\mathrm{L}_f + u_1(k)\mathrm{L}_{g_1} + \ldots + u_m(k)\mathrm{L}_{g_m})} x(k) \\ &= x(k) + \sum_{i>0} \frac{\delta^i}{i!} (\mathrm{L}_f + u_1(k)\mathrm{L}_{g_1} + \ldots + u_m(k)\mathrm{L}_{g_m})^i x(k) \end{aligned} \tag{2.19}$$

The following definition of ASR sampled equivalent model generalizes the one in the SISO case;

Definition: ASR sampled equivalent model

Consider the continuous-time input affine SISO system (1.16a)-(1.16b) with a well defined vector relative degree $(r_1 \ \ldots \ r_m)$, then there exists $T^{\star} > 0$ small enough such that $\forall \delta \in [0, T^{\star}[$ the exponential (2.19) converges. If that is the case, then for $p \geq \max(r_j)$, $j = 1 \ldots m$

$$\|F^{\delta}(x(k), u_1(k), \ldots, u_m(k)) - F^{\delta[p]}(x(k), u_1(k), \ldots, u_m(k))\| \leq O(\delta^{p+1}).$$

for all k and $F^{\delta[p]}(x, u_1, \ldots, u_m)$ is called the ASR sampled equivalent model of order p.

Remark 2.5 *a similar way to define ASR sampled equivalent models is used interchangeably in the sequel. Namely; when truncating each row of the expansion (2.19) at any fixed order $col(p_1, \ldots, p_n)$ in δ, so neglecting row-wise the remaining terms in $(O(\delta^{p_1+1}), \ldots, O(\delta^{p_n+1}))$ in the infinite series expansion, the resulting SR sampled equivalent model is said to be approximated at the order $col(p_1, \ldots, p_n)$. This notion of vector heterogeneous approximation in powers of δ will be used in Chapter 7.*

Applying the DT vector relative degree definition to the sampled-data system (2.18a),(2.18b) one has that the integers $r_{d,i} = 1$, $\forall i = 1, \ldots, m$ and the decoupling matrix loses rank, when taking the sampled-data equivalent model (2.18a)-(2.18b), or an ASR of order $col(p_1, \ldots, p_n)$ such that $\forall i = 1, \ldots, n, p_i \geq \max(r_j), j = 1, \ldots m$. A consequence of the above is that the zero dynamics as well as the structure of the continuous-time system is not preserved, and additional possibly unstable sampling zero dynamics appear.

In a linear setting, and unlike in the SISO case, the limiting zeros (i.e. zeros of the SR sampled equivalent model as $\delta \to 0$) of an LTI MIMO system are not only dependent on the relative degree and the original continuous-time invariant zeros but also on the system parameters Hayakawa et al. (1983). However, in some simple cases, the results on the limiting zeros of SISO systems carry over.

This fact explains the limiting zero obtained when we took a multi-rate of order 2 of the triple integrator. The following example further enforces this difficulty associated with the asymptotic characterization of the sampling zeros of a MIMO LTI system;

Example 2.4 Let a continuous-time LTI MIMO system be described by the following triplet;

$$A = \begin{pmatrix} 0 & 1 & 0 & 0 & 0 \\ 0 & 0 & 1 & 0 & 0 \\ -1 & -3 & -3 & 0 & 1 \\ 4 & 0 & 0 & -1 & 1 \\ 0 & 0 & 0 & 0 & 0 \end{pmatrix}, \quad B = \begin{pmatrix} 0 & 0 \\ 0 & 0 \\ 1 & 0 \\ 0 & 0 \\ 0 & 1 \end{pmatrix}$$
$$C = \begin{pmatrix} -2 & -2 & 0 & 1 & 0 \\ 0 & 0 & 0 & -2 & 0 \end{pmatrix}$$

and note that the continuous-time vector relative degree is $r = (2 \;\; 2)$ and $CB = 0, CAB \neq 0$ and full rank. As a consequence, the continuous-time system has a single zero because $n - r_1 - r_2 = 1$, this zero being $z^\star = -1$. Let $\delta = 0.1$ and using the expressions in (2.7) we have

$$A^\delta = \begin{pmatrix} 0.9998 & 0.0995 & 0.0045 & 0 & 0.0002 \\ -0.0045 & 0.9863 & 0.0860 & 0 & 0.0045 \\ -0.0860 & -0.2624 & 0.7284 & 0 & 0.0860 \\ 0.3806 & 0.0193 & 0.0006 & 0.9048 & 0.0952 \\ 0 & 0 & 0 & 0 & 1 \end{pmatrix}, \quad B^\delta = \begin{pmatrix} 0.0002 & 0 \\ 0.0045 & 0.0002 \\ 0.0860 & 0.0045 \\ 0.00001 & 0.0048 \\ 0 & 0.1 \end{pmatrix}$$

and $r_d = (1 \;\; 1)$ while $CB^\delta \neq 0$ and full rank. Clearly, the SR sampled equivalent model has $n - r_{d,1} - r_{d,2} = 3$ zeros being $z_d^\star = \{0.9048, -0.9354, -0.9674\}$. The first zero corresponds to the limiting zero of the continuous-time one i.e. $e^{z^\star \delta} \approx e^{-0.1} \approx 0.9048$ while the other 2 are extra sampling zeros. Those sampling zeros as can be seen do not relate to the solution of a corresponding Euler-Frobenius polynomial, even as δ decreases further.

2.6 Concluding remarks

A few comments to summarize this chapter are in order;

- when designing control laws, it is beneficial to remember that both sensing and actuation are implemented through digital devices and sensors acting over discrete time instants in a synchronous or asynchronous manner.
- in this *sampled-data* context, properties of the continuous-time system are not preserved. Examples of such lost properties are the relative degree and zero dynamics structure and stability.
- the loss of such properties, particularly the loss of minimum phaseness of the zero dynamics, imposes limitation on control design that utilizes partial inversion techniques.
- to avoid such limitations, single-rate and multi-rate sampled data mythologies are available that prove beneficial.

The effects of sampling, and the rise of sampling zero dynamics is a rich subject and this chapter is in no way a complete overview of sampled-data systems and the loss of control properties under sampling.

Different approaches are available in the literature for defining the sampled-data equivalent model to a nonlinear system. In Yuz and Goodwin (2005b), the equivalent models of sampled systems were derived using the so-called $\delta-$operator. Alternatively, in Hetel et al. (2017) sampling effect was viewed as a time-delay, specifically when dealing with aperiodic and generalized sample and hold strategies Kabamba (1987). A more recent viewpoint is modelling the sampled-data systems using the tools of hybrid systems Goedel et al. (2012).

The representation of nonlinear discrete and sampled systems in a unified manner was treated in Monaco and Normand-Cyrot (1995), while a different representation, being the so-called Differential-Difference Representation DDR was properly formalized in Monaco and Normand-Cyrot (2005). Additionally, aspects pertaining to finite descritzability Di Giamberardino et al. (1996b) and the structure of the sampled equivalent models Arapostathis et al. (1989) are contained on those cited references for the interested reader (see also Mattioni (2018) for a more recent recount).

Chapter 3

On stabilization via partial cancellation of the zero dynamics

Contents

With this chapter, concepts pertaining to stabilization through partial inversion-based controllers as well as obstructions to the design of stabilizing inversion-based controllers in continuous-time are elaborated. In this sense, the chapter will start by discussing the current literature on stabilization via partial zero dynamics cancellation for continuous-time SISO nonlinear systems. This method recalled for the SISO case based on the results reported in Mattioni et al. (2017a), constitute the basis for a preliminary contribution in the continuous-time LTI MIMO case. Finally, a discussion on the possible extension, at least in a local sense, of the proposed result to a special class of nonlinear MIMO systems will be provided. In this sense, this chapter serves as a more accessible companion to the formal statements, proofs and results reported in;

> Mohamed Elobaid, Mattia Mattioni, Salvatore Monaco and Dorothée Normand-Cyrot. *"On stable right-inversion of non-minimum-phase systems". 59th IEEE Conference on Decision and Control IEEE CDC 2020, 5153-5158. DOI: 10.1109/CDC42340.2020.9303851.*

The notions and formal definitions provided in this chapter are based on Basile and Marro (1992), Mattioni et al. (2017a), Mattioni et al. (2019) and the references therein.

Before proceeding further, and as done in the previous chapter, we present a simple example to motivate the discussion that follows;

Example 3.1 Consider the following transfer function

$$G(s) = \frac{(s-1)(s+1)}{(s+2)(s+3)(s+4)}$$

and assume we want to stabilize this system and render the input-output link almost unity (inversion). Notice that $r = 1$ and the transfer function has two zeros at $s = \pm 1$ the former of which is

non-minimum phase. This system admits the following state space canonical realization

$$\begin{aligned}\dot{x}_1 &= x_2\\ \dot{x}_2 &= x_3\\ \dot{x}_3 &= -24x_1 - 26x_2 - 9x_3 + u\\ y &= x_3 - x_1\end{aligned}$$

Define a coordinate change using y as in Section 1.1 putting the system in the normal form;

$$\begin{aligned}\dot{z} &= -9z - 33\eta_{\star,1} - 27\eta_{\star,2} + u\\ \dot{\eta}_{\star,1} &= -\eta_{\star,2}\\ \dot{\eta}_{\star,2} &= -z - \eta_{\star,1}\\ y &= z\end{aligned}$$

from which it is clear that a feedback of the form

$$u^\star = 9z + 33\eta_{\star,1} + 27\eta_{\star,2} + \nu$$

with $\nu = Fz$ cancels both the zeros, rendering the input-output link almost unity, but the closed loop unstable. Now, looking at the transfer function isolating the non-minimum phase zero;

$$G(s) = (s-1)\frac{(s+1)}{(s+2)(s+3)(s+4)} = (s-1)G_s(s)$$

this corresponds to defining a dummy output $Y^s(s)$ corresponding to $G_s(s)$ and related to the original output of the system by;

$$Y(s) = (s-1)Y^s(s)$$

Note that $G_s(s)$ defines a transfer function with $r = 2$ and only the minimum phase zero. In the original state space coordinates, $G_s(s)$ can be realized with the same dynamics by modifying the output to be;

$$y^s = x_1 + x_2$$

this new dummy output can then be used to define the following normal form;

$$\begin{aligned}\dot{z}_1^s &= z_2^s\\ \dot{z}_2^s &= -18z_1^s - 8z_2^s - 6\eta_\star^s + u\\ \dot{\eta}_\star^s &= z_1^s - \eta_\star^s\\ y^s &= z_1^s\end{aligned}$$

It results that over this y^s defined normal form, the feedback cancelling all the zeros

$$u^\star = 18z_1^s + 8z_2^s + 6\eta_\star^s + \nu$$

transforms the system into;

$$\begin{aligned}\dot{z}_1^s &= z_2^s\\ \dot{z}_2^s &= \nu\\ \dot{\eta}_\star^s &= z_1^s - \eta_\star^s\\ y^s &= z_1^s\end{aligned}$$

so a suitable ν can be designed to stabilize the z sub-dynamics rendering the zero dynamics

$$\dot{\eta}_\star^s = -\eta_\star^s$$

Additionally, from the fact that $y = \dot{y}^s - y^s$ we have in this normal form, the original output reads;

$$y = z_2^s - z_1^s$$

thus stabilization via inversion with respect to y could be attained.

The above example shows that; even when starting from a non-minimum phase LTI system, an inversion based feedback maybe obtained via partial cancellation of only the minimum phase zeros ensuring stability. Can we utilize this procedure, at least in a local sense, in the nonlinear setting is the question addressed in the next section.

3.1 The case of continuous-time Single-Input Single-Output systems

Consider the nonlinear SISO system of the form (1.1a),(1.1b), assumed to have a linear output map;

$$\begin{aligned}\dot{x} &= f(x) + g(x)u\\ y &= cx\end{aligned} \tag{3.1}$$

With $c^\top \in \mathbb{R}^n$ and let $f(0) = 0$, equivalently the origin $x^\circ = 0 \in \mathbb{R}^n$ is an equilibrium point. we further assume that the system has a well defined relative degree r at x°. Consequently the system admits the following normal form recalled in a compact manner;

$$\dot{z} = A_r z + b_r(b(z,\eta_\star) + a(z,\eta_\star)u) \tag{3.2a}$$

$$\dot{\eta}_\star = q_\star(z,\eta_\star) \tag{3.2b}$$

$$y = c_r z \tag{3.2c}$$

with $b(z,\eta_\star),\ a(z,\eta_\star),\ q_\star(z,\eta_\star)$ are as in (1.3) and A_r, b_r, c_r as in (2.10). Now recall the following;

Problem: stable inversion

For system (3.1), let $y_r(t)$ be a desired output reference with bounded higher derivatives $y_r(t), \dot{y}_r(t), \dots, y_r^{(r-1)}(t)$. ***Find*** *$(u(t),\ x(0))$ such that;*

- *the pair $u(t), x(0)$ satisfy the dynamics of the system (3.1) for $0 \leq t \leq \infty$.*
- *under $u(t)$, the output of the system exactly tracks the desired reference i.e. $y(t) = y_r(t), \quad \forall 0 \leq t \leq \infty$.*
- *the pair $u(t), x(t)$ are bounded.*

Problem 3.1 above is equivalent to ask; given a desired bounded, in the sense of L_2-norm, output signal $y_r(t)$ with bounded derivatives, one is interested in an *inverse* of the system in which the internal dynamics is stable. As we have seen from the discussion in Chapter 1, a possible solution to this problem resulting from the normal form (3.2a)-(3.2c) is obtained by noting that $y_r^{(i)}(t) = z_i(t),\ i = 0, \dots, r-1$, and so setting in (3.2a)

$$z_r = \begin{pmatrix} y_r & \dot{y}_r & \dots & y_r^{(r-1)} \end{pmatrix}^\top$$

for which $u(t)$ solving Problem 3.1 above, starting from initial conditions $z(t_0) = z_r$, takes the form;

$$u = \frac{y_r^{(r)} - b(z_r, \eta_\star)}{a(z_r, \eta_\star)} \tag{3.3}$$

and $\eta_\star(t)$ is the solution to

$$\dot{\eta}_\star = q(z_r, \eta_\star), \quad \eta_\star(t_0) = \eta_\star^\circ \tag{3.4}$$

which characterizes the residual dynamics of the system, and thus Problem 3.1 admits a bounded solution whenever the equilibrium of (3.4) is stable. In the special case that $y_r(t) = 0$ and all it's higher derivatives, the dynamics (3.4) and the feedback (3.3) reduce to the zero dynamics and the output zeroing feedback respectively.

Consequently, stability of the cancelled zero dynamics is a main obstruction to solving the stable inversion problem in this setting. This fact explains the common convention that minimum phase systems are easier to deal with, in terms of controller design. How to handle this obstruction in continuous-time when the system is non-minimum phase is the question addressed in this chapter. For those systems, it is well known that one of the most common approaches to stable inversion is inversion with respect to a suitably redefined dummy output. The state-of-the-art on stable inversion via partial zero dynamics cancellation for SISO systems is discussed next.

Following Mattioni et al. (2017a), let the linear tangent model LTM corresponding to system (3.1) at the origin be

$$\dot{x} = Ax + bu \tag{3.5a}$$
$$y = cx \tag{3.5b}$$

assumed controllable, that is;

$$A = \frac{\partial f(x)}{\partial x}|_{x=x^\circ} = \begin{pmatrix} 0 & 1 & 0 & \dots & 0 \\ & & & \ddots & \\ 0 & 0 & \dots & 0 & 1 \\ -a_0 & -a_1 & \dots & -a_{n-2} & -a_{n-1} \end{pmatrix} \quad b = g(x)|_{x=x^\circ} = \begin{pmatrix} 0 \\ \vdots \\ 0 \\ 1 \end{pmatrix}$$
$$c = \begin{pmatrix} b_0 & \dots & b_{n-r} & 0 \dots & 0 \end{pmatrix}$$

possibly after a suitable coordinates change. The coefficients $a_i, b_i \in \mathbb{R}$ are those characterizing the numerator and denominator polynomials of the transfer function of (3.5a),(3.5b) i.e.

$$G(s) = c(sI - A)^{-1}b = \frac{n(s)}{d(s)} = \frac{b_0 + b_1 s + \ldots + b_{n-r}s^{n-r}}{a_0 + a_1 s + \ldots + a_{n-1}s^{n-1} + s^n} \tag{3.6}$$

with r being the relative degree. It is possible to find a non-trivial maximal factorization of the numerator polynomial such that;

$$\begin{aligned} n(s) &= n_1(s)n_2(s) \\ &= (b_0^1 + b_1^1 s + \ldots + b_{m_1}^1 s^{m_1})(b_0^2 + b_1^2 s + \ldots + b_{m_2}^2 s^{m_2}) \end{aligned}$$

Let $r_1 = n - m_1,\ r_2 = n - m_2$ such that;

$$\begin{aligned} n(s) &= n_1(s)n_2(s) \\ \text{root}(n_1(s)) \cap \text{root}(n_2(s)) &= \emptyset \\ \text{root}(n_i(s)) &= \{s \in \mathbb{C} : n_i(s) = 0\} \neq \emptyset, \quad i = 1, 2 \end{aligned} \tag{3.7}$$

Now, assume that system (3.1) is partially minimum phase in the sense of $n(s)$ being hyperbolic, then a nontrivial factorization of the form (3.7) can be chosen denoting $n_1(s) = n_s(s),\ n_2(s) = n_u(s)$ where

$$\text{root}(n_s(s)) \in \mathbb{C}^- \qquad \text{root}(n_u(s)) \in \mathbb{C}^+ \tag{3.8}$$

equivalently $n_s(s)$ being Hurwitz having all roots with negative real part, while $n_u(s)$ is non Hurwitz. Accordingly, define the dummy output

$$\begin{aligned} y^s(t) &= c^s x(t) \\ c^s &= \begin{pmatrix} b_0^1 & \dots & b_{n-r_1}^1 & 0 \dots & 0 \end{pmatrix} \end{aligned} \tag{3.9}$$

corresponding to the coefficients of the Hurwitz polynomial $n_s(s)$. It is then possible to verify that the original output is related to this dummy output, near x°, via the differential relation (noting

that $n - r_2 = r_1 - r$)

$$\begin{aligned} y(t) &= n_u(\frac{d}{dt})y^s(t) \\ &= b_0^2 y^s(t) + b_1^2 \frac{d}{dt} y^s(t) + \ldots + b_{n-r_2}^2 \frac{d^{n-r_2}}{dt^{n-r_2}} y^s(t) \\ &= b_0^2 y^s(t) + b_1^2 \dot{y}^s(t) + b_2^2 \ddot{y}^s(t) + \ldots + b_{n-r_2}^2 y^{s^{(r_1-r)}}(t) \end{aligned} \tag{3.10}$$

and let

$$c_2 = \begin{pmatrix} b_0^2 & b_1^2 & \ldots & b_{n-r_2}^2 & 0 \ldots & 0 \end{pmatrix} \tag{3.11}$$

With this relationship, the following statement holds true Mattioni et al. (2017a);

Lemma: stable zero dynamics factorization

The partially non-minimum phase system 3.1 is locally minimum phase with respect to the dummy output $y^s(t)$ given in (3.9).

The interested reader can follow the original statement of this result and its proof in Mattioni et al. (2017a). It is then clear that a direct consequence of the above statement is the following statement reported in Mattioni et al. (2017a);

Theorem: stable inversion for SISO systems

If the system is invertible with respect to the dummy output (3.9), then the system is invertibile with stability with respect to the original output.

Proof: Let $y^s(t)$ be the dummy output defined in (3.9) having a relative degree r_1, and define the coordinates change

$$\begin{aligned} \begin{pmatrix} z^s \\ \eta_\star^s \end{pmatrix} &= \begin{pmatrix} \phi_1^s(x) \\ \phi_2^s(x) \end{pmatrix} \\ \phi_1^s(x) &= \begin{pmatrix} c^s x & L_f c^s x & \ldots & L_f^{r_1-1} c^s x \end{pmatrix}^\top \end{aligned}$$

where $\phi_2^s(x) : L_g \phi_2^s(x) = 0$. Under this coordinates change the system takes the strict normal form

$$\begin{aligned} \dot{z}^s &= A_{r_1} z + b_{r_1}(b^s(z^s, \eta_\star^s) + a^s(z^s, \eta_\star^s)u) \\ \dot{\eta}_\star^s &= q_\star^s(z^s, \eta_\star^s) \\ y &= n_u(\frac{d}{dt})y^s = c_2 z^s \end{aligned}$$

where $n_2(\cdot), c_2$ are as in the stable factorization (3.10),(3.11). Let y_r be a desired bounded output signal as in Problem 3.1 and define the inversion feedback w.r.t $y^s(t)$ as in (3.3). Under this feedback

the closed loop system has internal dynamics described by

$$\dot{\eta}_\star^s = q_\star^s(z_r^s, \eta_\star^s)$$

which has an LTM with a Hurwitz polynomial by construction which verifies boundedness of the closed loop trajectories under the inversion feedback, thus solving Problem 3.1. ■

The statement of Theorem 3.1 gives a sufficient condition for solving the problem i.e. it is enough that there exists an inversion feedback with respect to the dummy output y^s to get stable inversion with respect to the original output. However, This is not necessary, because other types of feedback (and initial conditions) solution to the stable inversion problem may exist, even if the system is not partially minimum phase e.g. stable inversion via dynamic feedback Descusse and Moog (1985).

This intuitive statement proved very useful in solving control problems that require cancellation of the zero dynamics for SISO linear and nonlinear systems with a linear output map such as input-output feedback linearization, tracking and disturbance decoupling with stability Mattioni et al. (2017a), Mattioni et al. (2019). In the following section we give an extension of this method to the linear MIMO setting as discussed in Elobaid et al. (2020a) together with some comments about local applicability to the nonlinear MIMO case.

3.2 The case of continuous-time Multi-Input Multi-Output systems

In what follows, an extension to the previous statements concerning stable inversion of partially minimum phase SISO systems is developed for the special LTI MIMO case. The main difficulty of extending the result is the fact that the zeros of a matrix transfer function in the LTI MIMO setting is not as straightforward to tackle. Formally we ask the following;

Problem: stable inversion of LTI MIMO systems

Given a minimal LTI MIMO system with p inputs and q outputs respectively. Let $y = Cx$ be the output of the system, ***Find*** *if possible an output $y^s = C^s x$ associated with the stable component of the zero dynamics such that solving the stable inversion problem for this dummy output y^s implies solving inversion-based problems with stability for the original output y.*

For the sake of simplicity, we constrain ourselves to the case $p = q = 2$, namely we consider;

$$\dot{x} = Ax + Bu \tag{3.12a}$$

$$y = Cx \tag{3.12b}$$

with $u, y \in \mathbb{R}^2$, $x \in \mathbb{R}^n$ and $B = \begin{pmatrix} b_1 & b_2 \end{pmatrix}$, $C^\top = \begin{pmatrix} c_1^\top & c_2^\top \end{pmatrix}$ and transfer function

$$G(s) = C(sI - A)^{-1}B = \frac{1}{d(s)}N(s) \tag{3.13}$$

where $d(s)$ is the characteristic polynomial and $N(s)$ is a sqaure polynomial matrix. In this case, right and left invertibility coincide Marro (1990) and thus we will speak only of invertibility. Before proceeding further, the following standing assumptions are set;

Assumption 3.1 *System (3.12a),(3.12b) is assumed to be such that;*

A1. *The system is minimal, i.e.* (A, B) *and* (C, A) *are, respectively, controllable and observable.*

A2. *The system is invertible in the sense of Marro (1990).*

A3. *The system is partially minimum-phase; i.e., the zero polyonmial defined as*

$$z(s) = \det \begin{pmatrix} sI - A & B \\ -C & \mathbf{0} \end{pmatrix} = z_u(s)z_s(s), \quad s \in \mathbb{C}$$

is non-Hurwitz with $z_s(s)$ *denoting the corresponding Hurwitz component with roots in the left hand side of the complex plane.*

For the matrix transfer function (3.13) consider the polynomial matrix $N(s)$ and following (Kailath, 1980, Chapter 6) we can always find elementary row and column operations i.e. unimodular matrices $\{L^{-1}(s), R^{-1}(s)\}$ such that

$$N(s) = L(s)N_{sm}(s)R(s) \tag{3.14}$$

with

$$N_{sm}(s) = \begin{pmatrix} \epsilon_1(s) & 0 \\ 0 & \epsilon_2(s) \end{pmatrix} \tag{3.15}$$

where $\{\epsilon_i(s)\}$ are unique monic polynomials verifying $\epsilon_1(s)$ is a factor of $\epsilon_2(s)$. Moreover, by denoting as $\Delta_i(s)$ the greatest common divisor of all $i \times i$ minors of $N(s)$ for $i = 1, 2$ one gets that $\epsilon_i(s) = \frac{\Delta_i(s)}{\Delta_{i-1}(s)}$ with $\Delta_0(s) = 1$. Note that, although $N_{sm}(s)$ is unique, $\{L^{-1}(s), R^{-1}(s)\}$ are not. Accordingly, one gets that the (rational) matrix transfer function (3.13) always admits a unique Smith McMillan form;

$$G(s) = L(s)N_{sm}(s)D^{-1}(s)R(s) \tag{3.16}$$

with

$$M(s) = N_{sm}(s)D^{-1}(s) = \begin{pmatrix} \frac{z_1(s)}{d_1(s)} & 0 \\ 0 & \frac{z_2(s)}{d_2(s)} \end{pmatrix} = \begin{pmatrix} \frac{\epsilon_{1,1}(s)\epsilon_{1,2}(s)}{d_1(s)} & 0 \\ 0 & \frac{\epsilon_{2,1}(s)\epsilon_{2,2}(s)}{d_2(s)} \end{pmatrix}$$

where, $d(s) = d_1(s)d_2(s)$ is the pole-polynomial with the property that $d_2(s)$ is a factor of $d_1(s)$.

From **A3.** one has

$$\begin{aligned} z(s) &= \epsilon_1(s)\epsilon_2(s) = \epsilon_{1,1}(s)\epsilon_{1,2}(s)\epsilon_{2,1}(s)\epsilon_{2,2}(s) \\ &= \underbrace{\epsilon_{1,1}(s)\epsilon_{2,1}(s)}_{=:z_u(s)}\underbrace{\epsilon_{1,2}(s)\epsilon_{2,2}(s)}_{=:z_s(s)} = z_u(s)z_s(s) \end{aligned}$$

corresponds to a maximal factorization of the zero-polynomial.

Example 3.2 To illustrate the computations associated with the factorization presented, consider an LTI MIMO system with the following canonical form

$$A = \begin{pmatrix} 0 & 1 & 0 & 0 \\ -20 & -21 & 0 & 0 \\ 0 & 0 & 0 & 1 \\ 0 & 0 & -20 & -21 \end{pmatrix}, \quad B = \begin{pmatrix} 0 & 0 \\ 1 & 0 \\ 0 & 0 \\ 0 & 1 \end{pmatrix}, \quad C = \begin{pmatrix} -\frac{4}{5} & \frac{4}{5} & 0 & \frac{4}{5} \\ -\frac{168}{5} & 0 & 16 & \frac{4}{5} \end{pmatrix}$$

corresponding to which one can has the transfer function

$$G(s) = \frac{1}{s^2 + 21s + 20} \begin{pmatrix} \frac{4\,s}{5} - \frac{4}{5} & \frac{4\,s}{5} \\ -\frac{168}{5} & \frac{4\,s}{5} + 16 \end{pmatrix} = \frac{N(s)}{d(s)}$$

To obtain the Smith-McMillan form, one can compute;

$$L = \begin{pmatrix} \frac{1}{42} - \frac{s}{42} & 1 \\ 1 & 0 \end{pmatrix}, \qquad R = \begin{pmatrix} -42 & s + 20 \\ 0 & \frac{1}{42} \end{pmatrix}$$

corresponding to which we have

$$N_{sm}(s) = \begin{pmatrix} 1 & 0 \\ 0 & s^2 + 61\,s - 20 \end{pmatrix}$$

As a result, and continuing from (3.12a),(3.12b), we identify a new dummy output

$$y^s(t) = C^s x(t)$$

corresponding to the stable component of the zero dynamics associated to the system output and related to (3.12b) through a differential equation of the form

$$y(t) = Z_u(\mathrm{d})y^s(t) \tag{3.17}$$

with $\mathrm{d} = \frac{\mathrm{d}}{\mathrm{d}t}$ and a suitably defined two dimensional square differential matrix $Z_u(d)$ such that $\det(\mathcal{L}(Z_u(d))) = z_u(s)$. This new dummy output corresponds to factorizing the matrix transfer

function (3.13) in the following way;

$$\begin{aligned} G(s) &= \frac{1}{d(s)} L(s) M(s) R(s) \\ &= \frac{1}{d(s)} L(s) \begin{pmatrix} \epsilon_{1,1}(s) & 0 \\ 0 & \epsilon_{2,1}(s) \end{pmatrix} \begin{pmatrix} \epsilon_{1,2}(s) d_2(s) & 0 \\ 0 & \epsilon_{2,2}(s) d_1(s) \end{pmatrix} R(s) \\ &= L(s) N_u(s) \frac{1}{d(s)} N_s(s) R(s) = Z_u(s) G_s(s) \end{aligned}$$

thus obtaining a transfer function matrix $G_s(s)$ with zeros polynomial $z_s(s)$. Accordingly, in a compact form the transfer function (3.16) rewrites as

$$G(s) = Z_u(s) G_s(s) \tag{3.18}$$

and in particular, $Z_u(s)$ is a polynomial matrix in s whereas $G_s(s)$ is transfer function matrix.

Example 3.3 [example continued] Having obtained

$$N_{sm}(s) = \begin{pmatrix} 1 & 0 \\ 0 & s^2 + 61\, s - 20 \end{pmatrix}$$

it is straight to see that the factorization (3.18) corresponds to writing

$$\begin{aligned} N_{sm}(s) &= N_s(s) N_u(s) \\ &= \begin{pmatrix} 1 & 0 \\ 0 & s + \frac{\sqrt{3801}}{2} + \frac{61}{2} \end{pmatrix} \begin{pmatrix} 1 & 0 \\ 0 & s - \frac{\sqrt{3801}}{2} + \frac{61}{2} \end{pmatrix} \end{aligned}$$

with the minimum and non-minimum phase zeros provided by $\{-\frac{\sqrt{3801}}{2} - \frac{61}{2},\ \frac{\sqrt{3801}}{2} - \frac{61}{2}\}$ respectively. From which one obtains directly;

$$Z_u(s) = \begin{pmatrix} \frac{1}{42} - \frac{s}{42} & s - \frac{\sqrt{3801}}{2} + \frac{61}{2} \\ 1 & 0 \end{pmatrix}, \quad G_s = \frac{1}{s^2 + 21s + 20} \begin{pmatrix} -42 & s + 20 \\ 0 & \frac{s}{42} + \frac{\sqrt{3801}}{84} + \frac{61}{84} \end{pmatrix}$$

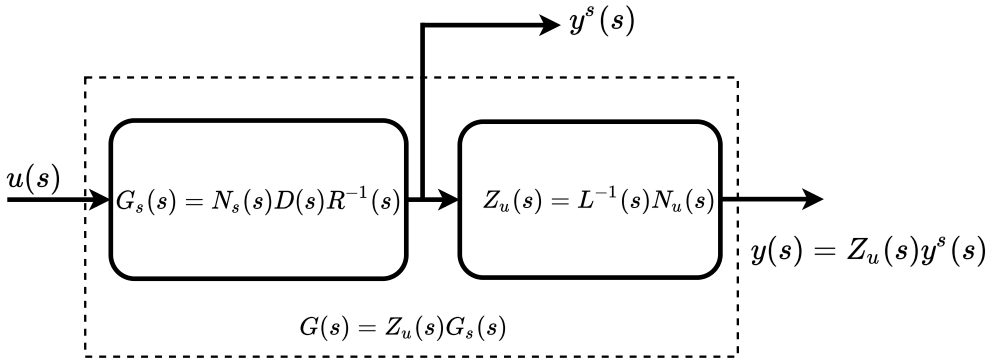

Figure 3.1: Stable factorization of the zeros of LTI MIMO systems.

When system (3.12a),(3.12b) possesses distinct poles with unitary algebraic multiplicity the

term $N_s(s)D^{-1}(s)R(s)$ is improper as $(L(s), R(s))$ introduce poles at $s = \infty$ Kailath (1980). To handle this issue, one can compute a matrix $K(s)$ (the so-called *right divisor*) such that:

$$\tilde{G}_s(s) = K(s)N_s(s)D^{-1}(s)R(s)$$

is proper and with the same poles as (3.13) and

$$\tilde{Z}_u(s) = L(s)N_u(s)K^{-1}(s)$$

is a polynomial matrix in $s \in \mathbb{C}$. Accordingly, (3.18) rewrites as

$$G(s) = \tilde{Z}_u(s)\tilde{G}_s(s) \tag{3.19}$$

such that $G_s(s)$ is strictly proper and verifying

$$\tilde{G}_s(s) = C^s(sI - A)^{-1}B. \tag{3.20}$$

From now on, for the sake of clarity, we shall assume $K(s) = \mathrm{I}$ although all the statements to follow hold true in general whenever such $K(s)$ exists.

The new output (3.23b) in the original state space coordinates of the system can be computed as follows. Let $(\hat{A}, \hat{B}, \hat{C})$ with $\hat{A} \in \mathbb{R}^{\hat{n}\times\hat{n}}$ with $\hat{n} \geq n$ be a realization of (3.20) and $(\hat{A}_\star, \hat{B}_\star, \hat{C}_\star)$ with $\hat{A}_\star \in \mathbb{R}^{n\times n}$ the corresponding restriction onto the observable and controllable subspaces. Denote by T and $T_\star$ the non-singular transformations putting, respectively, (A, B) and $(\hat{A}_\star, \hat{B}_\star)$ into the *eigenvalues assigmenent* canonical form Marro (1990). Then, because $TAT^{-1} = T_\star\hat{A}T_\star^{-1}$ and $TB = T_\star\hat{B}_\star$ one gets $C^s = \hat{C}_\star T_\star^{-1}T$.

With the previous discussion, we are now in position to make the following statement, corresponding to (Elobaid et al., 2020a, Proposition 3.1) attached at the end of this chapter;

Result: stable zeros factorization for LTI MIMO systems

Consider the system (3.12a),(3.12b) under Assumptions 3.1 **A1-A3** and let $z(s) = z_u(s)z_s(s)$ be the zero-polynomial where $z_s(s)$ denotes the Hurwitz component. Let the transfer function matrix $G(s)$ be of the form (3.19) with $G_s(s)$ as in (3.20) and $y^s = C^s x$ solution to (3.17). Then, the system

$$\dot{x} = Ax + Bu \tag{3.21a}$$
$$y^s = C^s x \tag{3.21b}$$

identifies the minimum-phase component of (3.12a) with zero polynomial given by $z_s(s)$.

Remark 3.1 *Two matrices $sI - A$ and $sI - \hat{A}$ possess the same Smith form if and only if, A and $\hat{A}$ are similar. This easily extends to the case of two realizations (A, B, C) and $(\hat{A}, \hat{B}, \hat{C})$ (with the same dimension) sharing the same transfer function $G(s)$.*

Remark 3.2 *Starting from a system with a well defined vector relative degree, one may obtain an output with respect to which the system is invertible but lacks a well defined vector relative degree. This observation shows that non interaction (and input/output decoupling) for an invertible system may not be achieved with stability through static state-feedback while the same does not stand for disturbance decoupling. A more rigorous treatment of these aspects are carried out utilizing generalized normal forms and reported in Elobaid et al. (2020a).*

3.3 Extensions to the continuous-time nonlinear Multi-Input Multi-Output case

The alert reader can see that the results presented in the previous section apply, in a local sense, to the class of nonlinear control affine square MIMO systems with linear output mapping. In fact, consider a system of the form;

$$\begin{aligned} \dot{x} &= f(x) + \sum_{i=1}^{m} g_i(x)u_i \\ y_i &= c_i x, \quad i = 1, \dots, m \end{aligned} \tag{3.22}$$

having a well defined vector relative degree. Let the origin be an equilibrium point for (3.22), and assume the LTM at the origin be of the form (3.12a),(3.12b). If the LTM satisfies Assumption 3.1, then the following statement (which is also reported in the attached paper) can be made generalizing that of (Elobaid et al., 2020a, Proposition 3.1);

Result: stable inversion via partial zero dynamics cancellation

Consider the system (3.22) with the origin being an equilibrium point. Let (3.12a),(3.12b) be its LTM at the origin satisfying Assumption 3.1 and $z(s) = z_u(s)z_s(s)$ be the zero-polynomial of the LTM model where $z_s(s)$ denotes the Hurwitz component. Let the LTM transfer function matrix $G(s)$ be of the form (3.19) with $G_s(s)$ as in (3.20) and $y^s = C^s x$ solution to (3.17). Then;

- the system

$$\dot{x} = f(x) + \sum_{i=1}^{m} g_i(x)u_i \tag{3.23a}$$

$$y^s = C^s x \tag{3.23b}$$

  is locally minimum-phase near the origin.

- the system is (locally) invertible with stability.

The above fact is demonstrated via the following benchmarking example;

Example 3.4 Consider the case of a 4-tanks system Johansson and Nunes (1998) given by

$$\dot{h} = f(h) + Bu \tag{3.24a}$$
$$y = Ch \tag{3.24b}$$

with $h = \text{col}\{h_1, h_2, h_3, h_4\}$, $f(h) = 2F(h)h$

$$F(h) = \begin{pmatrix} -p_1(h_1) & 0 & \frac{A_3}{A_1}p_3(h_3) & 0 \\ 0 & -p_2(h_2) & 0 & \frac{A_4}{A_2}p_4(h_4) \\ 0 & 0 & -p_3(h_3) & 0 \\ 0 & 0 & 0 & -p_4(h_4) \end{pmatrix}$$

$$B = \begin{pmatrix} \frac{\gamma_1 k_1}{A_1} & 0 \\ 0 & \frac{\gamma_2 k_2}{A_2} \\ 0 & \frac{(1-\gamma_2)k_2}{A_3} \\ \frac{(1-\gamma_1)k_1}{A_4} & 0 \end{pmatrix}, \quad C = \kappa_t \begin{pmatrix} 1 & 0 \\ 0 & 1 \\ 0 & 0 \\ 0 & 0 \end{pmatrix}^\top$$

$p_i(h_i) = \frac{c_i\sqrt{2gh_i}}{2A_ih_i}$. For the sake of compactness, let b_{ij} correspond to the element in position (i, j) of the input-state matrix B. In particular, h_i, A_i and c_i are, respectively, the level of water in the i^{th}-tank, its cross-section area and the cross-section of the outlet hole for $i = 1, 2, 3, 4$. The control signals u_j with $j = 1, 2$ correspond to the voltage applied to j^{th}-pump with k_ju_j being the corresponding flow. We consider the problem of locally asymptotically tracking the output of (3.24) to a desired $y_\star = (h_1^\star,\ h_2^\star)$ corresponding to make $h^\star = (h_1^\star, h_2^\star, h_3^\star, h_4^\star)^\top$ with

$$h_3^\star = \frac{(c_1\gamma_2\sqrt{h_1^\star} - c_2(1-\gamma_2)\sqrt{h_2^\star})^2}{c_3^2a_3^2\gamma_2^2}$$
$$h_4^\star = \frac{(c_2\gamma_1\sqrt{h_2^\star} - c_1(1-\gamma_1)\sqrt{h_1^\star})^2}{c_4^2a_4^2\gamma_1^2}$$

for $a_3 = \frac{\gamma_2}{1-\gamma_2} - \frac{1-\gamma_1}{\gamma_1}$ and $a_4 = \frac{\gamma_1}{1-\gamma_1} - \frac{1-\gamma_2}{\gamma_2}$ a locally asymptotically stable equilibrium for the closed-loop system under nonlinear feedback.

Analysis of the zero-dynamics

The vector relative degree of (3.24) is well defined and given by $r = (1\ 1)$ so that it exhibits a two-dimensional zero-dynamics. Accordingly, for investigating minimum-phaseness of (3.24), one computes the linear tangent model (LTM) at $h^\star$ of the form (3.12a) with $x = h - h^\star$ and $A = 2F(h^\star)$ with corresponding transfer function matrix

$$G(s) = \kappa_t \begin{pmatrix} \frac{b_{11}}{s+p_1} & \frac{b_{32}\,p_3}{(s+p_1)\,(s+p_3)} \\ \frac{b_{41}\,p_4}{(s+p_2)\,(s+p_4)} & \frac{b_{22}}{s+p_2} \end{pmatrix} \tag{3.25}$$

$p_i = p_i(h_i^\star) > 0$ for $i = 1, 2, 3, 4$, Smith form as $M(s) = \text{diag}\{\frac{1}{d(s)}, z(s)\}$, with pole-polynomial $d(s) = (s+p_1)(s+p_2)(s+p_3)(s+p_4)$ and zero-polynomial $z(s) = s^2+(p_3+p_4)s+\frac{p_3p_4}{b_{11}b_{22}}(b_{11}b_{22}-b_{32}b_{41})$. Thus, (3.24) is nonminimum-phase if $b_{11}b_{22}-b_{32}b_{41} < 0$ so that one can factorize $z(s) = (s-z_u)(s-z_s)$ for $z_u \in \mathbb{R}^+$ and $z_s \in \mathbb{R}^-$. As a consequence, if $b_{11}b_{22} - b_{32}b_{41} < 0$, output regulation to $y_\star$

cannot be achieved through classical right-inversion even if the relative degree is well-defined.

In the following we show how the factorization procedure detailed in the previous section allows to deduce a new output $y_s = C_s h$ and a nonlinear feedback locally solving the regulation problem with stability for (3.24).

The new dummy output using matrix transfer function factorization

Because (A, B, C) possesses three distinct poles in general, one gets that the matrix $G_s(s) = \mathrm{diag}\{1, s - z_s\}\mathrm{diag}\{d(s), 1\}R(s)$ is improper for all choices of $(L(s), R(s))$. However, for the pair

$$L(s) = \begin{pmatrix} -\frac{\psi_1(s)}{b_{32}\, {b_{41}}^2\, p_3\, {p_4}^2\, (p_2-p_3)\, (p_3-p_4)} & -\frac{p_2-p_1+p_4+s}{(p_1-p_2)\, (p_1-p_4)} \\ -\frac{\psi_2(s)}{b_{32}\, b_{41}\, p_3\, p_4\, (p_2-p_3)\, (p_3-p_4)} & -\frac{b_{41}\, p_4}{b_{11}\, (p_1-p_2)\, (p_1-p_4)} \end{pmatrix}$$

$$R(s) = \begin{pmatrix} b_{41}\, p_4\, (p_3+s) & -\frac{\psi_3(s)}{b_{11}\, (p_1-p_2)\, (p_1-p_4)} \\ -\frac{{b_{11}}^2\, b_{22}\, (p_1-p_2)\, (p_1-p_4)}{b_{32}\, b_{41}\, p_3\, p_4\, (p_2-p_3)\, (p_3-p_4)} & \frac{\psi_4(s)}{b_{32}\, {b_{41}}^2\, p_3\, {p_4}^2\, (p_2-p_3)\, (p_3-p_4)} \end{pmatrix}$$

where

$$\begin{aligned}
\psi_1(s) = {} & b_{11}\, (p_2+s)\, (p_4+s) \Big(b_{11}\, b_{22}\, s^4 + b_{32}\, b_{41}\, {p_3}^3\, p_4 + b_{11}\, b_{22}\, p_2\, s^3 + b_{11}\, b_{22}\, p_3\, s^3 + 2\, b_{11}\, b_{22}\, p_4\, s^3 \\
& - b_{32}\, b_{41}\, {p_3}^2\, {p_4}^2 - b_{11}\, b_{22}\, {p_1}^2\, s^2 + b_{11}\, b_{22}\, {p_4}^2\, s^2 + b_{11}\, b_{22}\, p_1\, p_3\, {p_4}^2 - b_{11}\, b_{22}\, {p_1}^2\, p_3\, p_4 - b_{32}\, b_{41}\, p_1\, p_3\, {p_4}^2 \\
& + b_{32}\, b_{41}\, {p_1}^2\, p_3\, p_4 + b_{32}\, b_{41}\, p_2\, p_3\, {p_4}^2 - b_{32}\, b_{41}\, p_2\, {p_3}^2\, p_4 + b_{11}\, b_{22}\, p_1\, p_2\, s^2 - b_{11}\, b_{22}\, {p_1}^2\, p_3\, s + b_{11}\, b_{22}\, p_1\, p_4\, s^2 \\
& + b_{11}\, b_{22}\, p_1\, {p_4}^2\, s + b_{11}\, b_{22}\, p_2\, p_3\, s^2 - b_{11}\, b_{22}\, {p_1}^2\, p_4\, s + b_{11}\, b_{22}\, p_2\, p_4\, s^2 + 2\, b_{11}\, b_{22}\, p_3\, p_4\, s^2 + b_{11}\, b_{22}\, p_3\, {p_4}^2\, s \\
& - b_{32}\, b_{41}\, p_3\, p_4\, s^2 - b_{32}\, b_{41}\, p_3\, {p_4}^2\, s + b_{11}\, b_{22}\, p_1\, p_2\, p_3\, p_4 - b_{32}\, b_{41}\, p_1\, p_2\, p_3\, p_4 + b_{11}\, b_{22}\, p_1\, p_2\, p_3\, s \\
& + b_{11}\, b_{22}\, p_1\, p_2\, p_4\, s + b_{11}\, b_{22}\, p_1\, p_3\, p_4\, s + b_{11}\, b_{22}\, p_2\, p_3\, p_4\, s - b_{32}\, b_{41}\, p_2\, p_3\, p_4\, s \Big)
\end{aligned}$$

$$\begin{aligned}
\psi_2(s) = {} & (p_1+s)\, (p_3+s) \Big(b_{32}\, b_{41}\, {p_3}^2\, p_4 - b_{32}\, b_{41}\, p_3\, {p_4}^2 - b_{32}\, b_{41}\, p_3\, p_4\, s - b_{32}\, b_{41}\, p_2\, p_3\, p_4 + b_{11}\, b_{22}\, {p_4}^2\, s \\
& + b_{11}\, b_{22}\, p_2\, {p_4}^2 + 2\, b_{11}\, b_{22}\, p_4\, s^2 + 2\, b_{11}\, b_{22}\, p_2\, p_4\, s + b_{11}\, b_{22}\, s^3 + b_{11}\, b_{22}\, p_2\, s^2 \Big)
\end{aligned}$$

$$\begin{aligned}
\psi_3(s) = {} & (p_4+s) \Big(b_{11}\, b_{22}\, s^3 - b_{11}\, b_{22}\, {p_1}^2\, p_3 - b_{11}\, b_{22}\, {p_1}^2\, s + b_{11}\, b_{22}\, p_2\, s^2 + b_{11}\, b_{22}\, p_3\, s^2 + b_{11}\, b_{22}\, p_4\, s^2 \\
& + b_{11}\, b_{22}\, p_1\, p_2\, p_3 + b_{11}\, b_{22}\, p_1\, p_3\, p_4 - b_{32}\, b_{41}\, p_2\, p_3\, p_4 \\
& + b_{11}\, b_{22}\, p_1\, p_2\, s + b_{11}\, b_{22}\, p_1\, p_4\, s + b_{11}\, b_{22}\, p_2\, p_3\, s + b_{11}\, b_{22}\, p_3\, p_4\, s - b_{32}\, b_{41}\, p_3\, p_4\, s \Big)
\end{aligned}$$

$$\begin{aligned}
\psi_4(s) = {} & b_{11}\, b_{22} \Big(- b_{11}\, b_{22}\, {p_1}^2\, p_4 - b_{11}\, b_{22}\, {p_1}^2\, s + b_{11}\, b_{22}\, p_1\, {p_4}^2 + b_{11}\, b_{22}\, p_1\, p_4\, s + b_{11}\, b_{22}\, p_2\, p_1\, p_4 + b_{11}\, b_{22}\, p_2\, p_1\, s \\
& + b_{32}\, b_{41}\, {p_3}^2\, p_4 - b_{32}\, b_{41}\, p_3\, {p_4}^2 - b_{32}\, b_{41}\, p_3\, p_4\, s - b_{32}\, b_{41}\, p_2\, p_3\, p_4 + b_{11}\, b_{22}\, {p_4}^2\, s + 2\, b_{11}\, b_{22}\, p_4\, s^2 \\
& + b_{11}\, b_{22}\, p_2\, p_4\, s + b_{11}\, b_{22}\, s^3 + b_{11}\, b_{22}\, p_2\, s^2 \Big)
\end{aligned}$$

One can obtain a matrix $K(s)$ so getting in the proper factorization (3.19) the minimum phase proper component;

$$\tilde{G}_s(s) = \begin{pmatrix} \frac{b_{11}}{p_1+s} & \frac{b_{32}\, p_3}{(p_1+s)\, (p_3+s)} \\ \psi_5(s) & \psi_6(s) \end{pmatrix}$$

where

$$\psi_5(s) = \frac{b_{32}\, b_{41}\, p_4\ (\beta + 2\, b_{11}\, b_{22}\, p_2 - b_{11}\, b_{22}\, p_3 + b_{11}\, b_{22}\, p_4 + 2\, b_{11}\, b_{22}\, s)}{2\,\beta\ (p_2 + s)\ (p_4 + s)} - \frac{b_{11}\, b_{22}\, b_{32}\, b_{41}\, p_4}{\beta\ (p_1 + s)}$$

$$\psi_6(s) = \frac{b_{22}\, b_{32}\ (\beta - b_{11}\, b_{22}\, p_3 + b_{11}\, b_{22}\, p_4)}{2\,\beta\ (p_2 + s)} - \left(\frac{b_{32}\beta(p_1 + s) b_{22}\ (\beta - b_{11}\, b_{22}\, p_3 + b_{11}\, b_{22}\, p_4) - 2 b_{32} b_{22}\, b_{32}\, b_{41}\, p_3\, p_4}{2\,\beta\,(p_1 + s)\,(p_3 + s)} \right)$$

In the original state space coordinates, a suitable realization of $G_s(s)$ yeids;

$$y_s = \begin{pmatrix} 1 & 0 & 0 & 0 \\ -\frac{b_{32} b_{41} p_4}{2 b_{11} \beta} & \frac{b_{32}}{2} - \frac{b_{32}(p_3+p_4)}{2\beta} & -\frac{b_{22}}{2} - \frac{b_{22}(p_3+p_4)}{2\beta} & \frac{b_{32}\, p_4}{2\beta} \end{pmatrix} h \tag{3.26}$$

with $\beta = \sqrt{(p_3 + p_4)^2 - 4\frac{p_3 p_4}{b_{11} b_{22}}(b_{11} b_{22} - b_{32} b_{41})}$ making the LTM model of (3.24a) minimum-phase.

The new dummy output using the normal form

At this point, it is interesting to verify the claim stated in Section 1.3, namely to try, through the iterative procedure described to arrive the the dummy output (3.26) directly utilizing a normal form for the LTM of the 4-tanks system. To this end, note that the coordinates change

$$T = \begin{pmatrix} 1 & 0 & 0 & 0 \\ 0 & 1 & 0 & 0 \\ b_{41} & 0 & 0 & -b_{11} \\ 0 & b_{32} & -b_{22} & 0 \end{pmatrix}$$

puts LTM at $h^\star$ of the 4-tanks system into the normal form;

$$\begin{aligned} \dot{z}_1 &= R_1 z + S_1 \eta_\star + a_{1,1} u_1 + a_{1,2} u_2 \\ \dot{z}_2 &= R_2 z + S_2 \eta_\star + a_{2,1} u_1 + a_{2,2} u_2 \\ \dot{\eta}_\star &= P z + Q_\star \eta_\star \\ y_1 &= z_1, \qquad y_2 = z_2 \end{aligned}$$

where $a_{1,1} = b_{11},\ a_{2,2} = b_{22},\ a_{1,2} = a_{2,1} = 0$ and

$$R_1 = \begin{pmatrix} -p_1 & \frac{b_{32}\, p_3}{b_{22}} \end{pmatrix}, \quad R_2 = \begin{pmatrix} \frac{b_{41}\, p_4}{b_{11}} & -p_2 \end{pmatrix}, \quad S_1 = \begin{pmatrix} 0 & -\frac{p_3}{b_{22}} \end{pmatrix}, \quad S_2 = \begin{pmatrix} -\frac{p_4}{b_{11}} & 0 \end{pmatrix}$$

$$P = \begin{pmatrix} -b_{41}\ (p_1 - p_4) & \frac{b_{32}\, b_{41}\, p_3}{b_{22}} \\ \frac{b_{32}\, b_{41}\, p_4}{b_{11}} & -b_{32}\ (p_2 - p_3) \end{pmatrix}, \quad Q_\star = \begin{pmatrix} -p_4 & -\frac{b_{41}\, p_3}{b_{22}} \\ -\frac{b_{32}\, p_4}{b_{11}} & -p_3 \end{pmatrix}$$

The transformation V putting $Q_\star$ in Jordan canonical form is;

$$V = \begin{pmatrix} \frac{\beta - b_{11}\, b_{22}\, p_3 + b_{11}\, b_{22}\, p_4}{2\, b_{22}\, b_{32}\, p_4} & -\frac{\beta + b_{11}\, b_{22}\, p_3 - b_{11}\, b_{22}\, p_4}{2\, b_{22}\, b_{32}\, p_4} \\ 1 & 1 \end{pmatrix} \implies \tilde{Q} = V Q V^{-1} = \begin{pmatrix} z_s & 0 \\ 0 & z_u \end{pmatrix}$$

Step 1: Fix the first output as $\tilde{y}_1^s = h_1$ and for the second output the $\tilde{y}_2^s = \eta_\star^2$ corresponding to z_u in original h coordinates. Namely, let

$$\begin{aligned}\tilde{y}_2^s &= \tilde{C}_2^s h\\ \tilde{C}_2^s &= \begin{pmatrix} 0 & 0 & -\frac{b_{22}\, b_{32}\, p_4}{\beta} & \frac{\beta - b_{11}\, b_{22}\, p_3 + b_{11}\, b_{22}\, p_4}{2\,\beta}\end{pmatrix} T^{-1}\\ &= \begin{pmatrix} -\frac{b_{32} b_{41} p_4}{2 b_{11}\beta} & \frac{b_{32}}{2} & -\frac{b_{32}(p_3+p_4)}{2\beta} & -\frac{b_{22}}{2} & -\frac{b_{22}(p_3+p_4)}{2\beta} & \frac{b_{32}\, p_4}{2\beta}\end{pmatrix}\end{aligned}$$

and testing this output, it has relative degree $r = (1 \;\; 2)$ and with respect to which only z_s is the corresponding zero. In fact this output $\tilde{y}^s = (\tilde{y}_1^s \;\; \tilde{y}_2^s)^\top$ is precisely that found in (3.26). Consequently, no need to reiterate and the procedure terminates.

Asymptotic tracking with stability

It is easily checked that, the nonlinear dynamics (3.24a) with output as in (3.26) possesses a well-defined relative degree $r_s = (1,\; 2)$ at $h^\star$. Also, it is a matter of computations to verify that (3.24a) with output (3.26) is locally minimum-phase with zero-dynamics $\dot{\eta}^s = q_s(0, \eta^s)$ verifying $\frac{\partial q_s}{\partial \eta_s}(0, \eta_\star^s) = z_s < 0$. At this point, along the lines the previous section and by exploiting the results in (Isidori, 1995, Chapter 5), one gets that output tracking of (3.24) can be solved over the dummy output (3.26) by setting the constant $y_\star^s = (y_{1,\star}^s, y_{2,\star}^s)^\top \in \mathbb{R}^2$ as solution to $y_\star = Z_u(\mathrm{d}) y_s^\star$ which is given by construction as $y_\star^s = C_s h^\star$. Accordingly, for all $k_0, k_1 > 0$ the feedback

$$u = -M_s^{-1}(h)\begin{pmatrix} c_1^s f(h) + y_1^s - y_{1,\star}^s \\ \mathrm{L}_f c_2^s f(h) + k_1 c_2^s f(h) + k_0(y_2^s - y_{2,\star}^s)\end{pmatrix} \tag{3.27}$$

with decoupling matrix

$$M_s^{-1}(h) = \begin{pmatrix} c_1^s B \\ \mathrm{L}_f^2 c_2^s f(h) B)\end{pmatrix}$$

ensures local asymptotic regulation of y to the desired $y^\star$ while preserving internal stability.

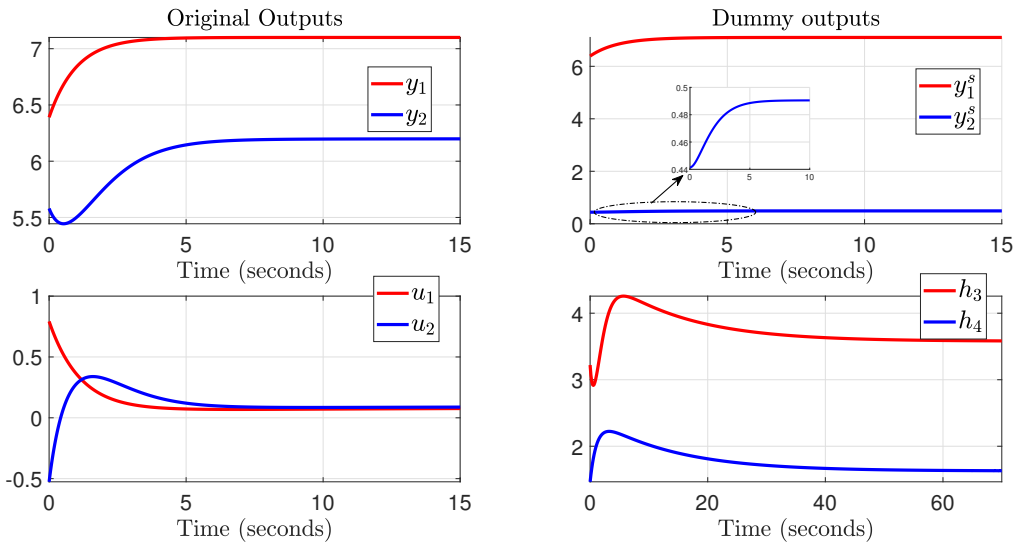

Figure 3.2: The four tank model under stable dynamic inversion.

Simulations

For completeness, simulations are reported in Figure 3.2 for the closed-loop system under the stabilizing feedback designed over the new dummy output highlighting the locally minimum-phase components of (3.24). Simulations are performed for the parameters fixed as in the Table below.

$A_1\ [cm^2]$	28	$A_3\ [cm^2]$	28
$A_2\ [cm^2]$	32	$A_4\ [cm^2]$	32
$c_1\ [cm^2]$	0.071	$c_3\ [cm^2]$	0.071
$c_2\ [cm^2]$	0.057	$c_4\ [cm^2]$	0.057
$k_t\ [V/cm]$	1	$g\ [cm/s^2]$	981
γ_1	0.43	γ_2	0.34
k_1	65.12	k_2	94.12

In addition, we fixed $y_\star = (7.1,\ 6.2)^\top$ corresponding to $h^\star = (7.1,\ 6.2,\ 3.58, 1.632)^\top$. In particular, with this choice of parameters, the plant is nonminum-phase with the zeros of LTM model at the desired equilibrium provided by $z_u = 0.018$ and $z_s = -0.0789$. The gains of the controller (3.27) are fixed as $(k_0, k_1) = (1, 2)$. Simulations report the story of the original and dummy outputs plus the real residual internal-dynamics of the feedback plant (that is the water levels of the third and fourth tank with respect to the real output) while proving the effectiveness of the proposed design approach.

3.4 Concluding remarks

A few comments to summarize this chapter and conclude the first part of the thesis are in order;

- the stability of the zero dynamics in continuous-time presents an obstruction to inversion based control design which is ubiquitous in different applications.
- an established workaround in the SISO case, is the partial cancellation of only the minimum phase component of the zero dynamics via output redefinition. This method was extended to the MIMO case in continuous-time for LTI systems.
- the method of partial cancellation of the zero dynamics is also valid, for a class of nonlinear MIMO systems in a local sense, utilizing the design techniques introduced in the linear context on the LTM model of the nonlinear system.
- the sampled-data context, inherently introduces additional limitations being the non-minimum phase sampled zero dynamics have not been addressed in this chapter. In the sequel, and similar to the reasoning presented for the continuous-time case, sampled-data methodologies are discussed addressing stable inversion in two classes of control problems; nonlinear Model Predictive Control MPC, and Transverse Feedback Linearization TFL.

It is important to note that this chapter, while introducing most of the necessary state of the art and some contributions in the MIMO setting, is still not a comprehensive treatise on the topic of stable inversion via partial zero dynamics cancellation. The interested reader is advised to refer to Isidori and Byrnes (1990), Sepulchre et al. (2012), Astolfi et al. (2008).

2020 59th IEEE Conference on Decision and Control (CDC)
Jeju Island, Republic of Korea, December 14-18, 2020

On stable right-inversion of non-minimum-phase systems

Mohamed Elobaid[1,2], Mattia Mattioni[1], Salvatore Monaco[1] and Dorothée Normand-Cyrot[2]

***Abstract*— The paper deals with the characterization of a dummy 'output function' associated with the stable component of the zero-dynamics of a linear square multi-input multi-output system. With reference to the 4-Tank dynamics, it is shown how such a procedure, applied to the linear tangent model of a nonlinear plant, may be profitably applied to assure local stability in closed loop.**

***Index Terms*— Algebraic/geometric methods; Linear systems; Stability of nonlinear systems**

I. Introduction

As well known, most control problems are concerned with partial cancellation of the dynamics which is achieved by forcing unobservability [1]–[8]. In the linear case, this is achieved by designing a feedback assigning part of the eigenvalues coincident with the zeros of the system so making the corresponding dynamics unobservable. Such an approach is at the basis of feedback linearization which is achieved, in general, by cancelling the so-called zero-dynamics whose stability is thus necessary for guaranteeing feasibility of the control system [9].

The idea of employing *factorization*, properly introduced in [10] for studying the zero-dynamics of sampled-data systems, and consequently partial dynamic cancellation has been formalized and developed in [11] to deal with feedback linearization of nonlinear single-input single-output (SISO) non-minimum phase systems (i.e., whose zero-dynamics are unstable). The design approach represents a first generalization to the nonlinear context of the idea of assigning part of the eigenvalues over part of the zeros of the transfer function of a linear system (partial zero-pole cancelation). When considering dynamical systems, stability of the feedback system can be achieved when only a stable component of the zero-dynamics is cancelled. Such a stable component can be identified, in the SISO case, by considering the output associated with the minimum-phase factorization of the transfer function of the linear tangent model at the origin. However, when dealing with MIMO systems identifying such a stable component and hence the corresponding dummy output is still challenging.

Supported by *Université Franco-Italienne/Università Italo-Francese* (Vinci Grant 2019) and by *Sapienza Università di Roma* (*Progetti di Ateneo 2018*-Piccoli progetti *RP11816436325B63*).

[1]Dipartimento di Ingegneria Informatica, Automatica e Gestionale *A. Ruberti* (Sapienza University of Rome); Via Ariosto 25, 00185 Rome, Italy {mohamed.elobaid, mattia.mattioni,salvatore.monaco}@uniroma1.it.

[2]Laboratoire de Signaux et Systèmes (L2S, CNRS); 3, Rue Joliot Curie, 91192, Gif-sur-Yvette, France {mohamed.elobaid,dorothee.normand-cyrot }@centralesupelec.fr

In this paper, the results in [11] are extended to the multi-input multi-output context by providing a systematic procedure for extracting, via factorization, a dummy output identifying the minumum-phase component of a dynamical system. In particular, focusing on linear time-invariant and right-invertible dynamics, we show how the Smith form can be suitably exploited for factorizing the matrix transfer function and extract, in the state-space representation, the output identifying the minimum-phase component of the original system. Then, the geometric relations among the original system and the one with the dummy output are investigated in terms of invariant subspaces and making reference to MIMO normal forms [12]. In particular, it is shown that the new output identifies the largest control-invariant subspace contained in the kernel of the original one maximizing unobservability while, at the same time, preserving stability of the closed loop. This allows the definition of systematic solutions with stability of a large variety of control problems dealing with right-inversion (e.g., disturbance decoupling, tracking). The case of nonlinear systems is sketched through the simulated example of a four tanks dynamics dealt with at an academic level. The case of square systems is dealt with as the extension to larger number of inputs and outputs follows the same lines.

The paper is organized as follows. In Section II, recalls on MIMO systems are given and the problem is formulated. In III, the procedure for constructing an output associated to the minimum-phase component is presented and applied to several control problems in Section IV. In Section V, the example of a four tank dynamics serves, at an academic level, for sketching the extension to nonlinear dynamics with linear output while conclusions and perspectives are in Section VI.

Notations: $\mathbb{R}$ and $\mathbb{N}$ denote the set of real and natural numbers including 0, respectively. $\mathbb{C}^+$ (resp. $\mathbb{C}^-$) denote the left-hand (resp. right-hand) side of the complex plane. $\mathrm{Mat}_{\mathbb{R}}(n,m)$ defines the group of real matrices of dimension $n\times m$ with, for short, $\mathrm{Mat}_{\mathbb{R}}(n) = \mathrm{Mat}_{\mathbb{R}}(n,n)$. Given a matrix $A \in \mathrm{Mat}_{\mathbb{R}}(n)$, $\sigma\{A\}$ defines its spectrum. For a sorted set of $a_i \in \mathbb{R}$ with $i = 1,\dots,n$, $\mathrm{diag}\{a_1,\dots,a_n\}$ defines a diagonal matrix with a_i being the diagonal elements. For a smooth vector field f, L_f denotes the Lie derivative operator, $\mathrm{L}_f = \sum_{i=1}^{n} f_i(\cdot)\frac{\partial}{\partial x_i}$.

II. Preliminaries and problem statement

Consider a linear time invariant (LTI) system of the form

$$\dot{x} = Ax + Bu \tag{1a}$$

$$y = Cx \tag{1b}$$

with $u,\, y \in \mathbb{R}^2$, $x \in \mathbb{R}^n$, $B = \begin{pmatrix} b_1 & b_2 \end{pmatrix}$, $C^\top = \begin{pmatrix} c_1^\top & c_2^\top \end{pmatrix}^\top$ and transfer function

$$P(s) = C(sI - A)^{-1}B. \tag{2}$$

The following standing assumptions are set.

- **A1.** The pairs (A, B) and (C, A) are, respectively, controllable and observable.
- **A2.** The system (1) is right-invertible [12], [13].
- **A3.** The system (1) is partially minimum-phase; i.e., the zero polyonmial defined as

$$z(s) = \det \begin{pmatrix} sI - A & B \\ -C & \mathbf{0} \end{pmatrix} = z_u(s) z_s(s), \quad s \in \mathbb{C}$$

is non-Hurwitz with $z_s(s)$ denoting the corresponding Hurwitz component with roots in the left hand side of the complex plane.

In the following, general recalls for MIMO linear systems are given as instrumental for the problem we address.

A. The Smith McMillan form

Consider any $p \times p$ polynomial matrix $N(s)$, then there exist elementrary row and column operations, or corresponding unimodular matrices $\{L^{-1}(s), R^{-1}(s)\}$ such that

$$N(s) = L(s) N_{sm}(s) R(s) \tag{3}$$

with

$$N_{sm}(s) = \text{diag}\{\epsilon_1(s), \dots, \epsilon_p(s)\} \tag{4}$$

where $\{\epsilon_i(s)\}$ are unique monic polynomials verifying $\epsilon_i(s)$ is a factor of $\epsilon_{i+1}(s)$ for all $i = 1, \dots, p-1$. Moreover, by denoting as $\Delta_i(s)$ the greatest common divisor of all $i \times i$ minors of $N(s)$ for $i = 1, \dots, p$ one gets that $\epsilon_i(s) = \frac{\Delta_i(s)}{\Delta_{i-1}(s)}$ with $\Delta_0(s) = 1$ [14]. Note that, although $N_{sm}(s)$ is unique, $\{L(s), R(s)\}$ are not. Accordingly, one gets that the (rational) matrix transfer function (2) always admits a unique Smith form, that is

$$P(s) = L(s) N_{sm}(s) D^{-1}(s) R(s) \tag{5}$$

with $M(s) = N_{sm}(s) D^{-1}(s) = \text{diag}\{\frac{z_1(s)}{d_1(s)}, \dots, \frac{z_p(s)}{d_p(s)}\}$ where from **A1.**: $z(s) = z_1(s) \dots z_p(s) = z_u(s) z_s(s)$ corresponds to the zero-polynomial defined in **A3.**; $d(s) = d_1(s) \dots d_p(s)$ is the pole-polynomial with the property that $d_{i+1}(s)$ is a factor of $d_i(s)$. For the sake of notational simplicity, and without loss of generality, we will assume in the sequel that $p = 2$.

Remark 2.1: [14] Two matrices $sI - A$ and $sI - A_r$ possess the same Smith form if, and only if, A and A_r are similar. This easily extends to the case of two realizations (A, B, C) and (A_r, B_r, C_r) (with the same dimension) sharing the same transfer function $P(s)$.

B. Generalized normal forms and the zero-dynamics

As (1) is invertible [12, Chapter 9], one can pick constant $r_2 \geq r_1 > 0$ such that

$$c_i A^\ell B = 0, \quad \ell = 0, \dots r_i - 2, \quad c_i A^{r_i - 1} B \neq 0$$

and $\nu \geq 0$ such that there exist constant $\alpha_{r_2}, \dots, \alpha_{r_2+\nu-1} \in \mathbb{R}$ verifying for $j = 0, \dots, \nu - 1$

$$c_2 A^{r_2+j-1} B + c_1 A^{r_1} (\alpha_{r_2+j} I + \dots + \alpha_{r_2} A^{j-1}) B = 0.$$

and

$$M = \begin{pmatrix} c_1 A^{r_1 - 1} B \\ c_2 A^{r_2+\nu-1} B + c_1 A^{r_1} (\alpha_{r_2+\nu-1} I + \dots + \alpha_{r_2} A^{\nu-1}) B \end{pmatrix}$$
$$\det\{M\} \neq 0.$$

In this setting, one can define a coordinate transformation

$$\begin{pmatrix} z_1 \\ z_2 \\ z_3 \\ \vdots \\ z_{\nu+2} \\ \eta \end{pmatrix} = \begin{pmatrix} T_1 \\ T_2 \\ T_3 \\ \vdots \\ T_{\nu+2} \\ T_\eta \end{pmatrix} x, \quad z_i = \begin{pmatrix} z_{i,1} \\ \dots \\ z_{i,r_i} \end{pmatrix} \tag{6}$$

for $i = 1, 2$ and , for $j = 0, \dots, \nu - 1$ with

$$T_i = \begin{pmatrix} c_i^\top & \dots & (c_i A^{r_i - 1})^\top \end{pmatrix}^\top, \quad T_\eta B = 0$$
$$T_{j+3} = c_2 A^{r_2+j} + c_1 A^{r_1} (\alpha_{r_2+j} I + \dots + \alpha_{r_2} A^j)$$

such that

$$\begin{aligned}
\dot{z}_{i,\ell} &= z_{i,\ell+1}, \quad i = 1, 2, \ \ell = 1, \dots, r_i - 1 \\
\dot{z}_{1,r_1} &= c_1 A^{r_1} x + c_1 A^{r_1 - 1} B u \\
\dot{z}_{2,r_2} &= c_2 A^{r_2} x + c_2 A^{r_2 - 1} B u \\
&= z_3 - \alpha_{r_2} \big(c_1 A^{r_1} x + c_1 A^{r_1 - 1} B u \big) \\
\dot{z}_{j+3} &= c_2 A^{r_2+j+1} x + c_1 A^{r_1+1} (\alpha_{r_2+j} I + \dots + \alpha_{r_2} A^j) x \\
&= z_{j+4} - \alpha_{r_2+j+1} \big(c_1 A^{r_1} x + c_1 A^{r_1 - 1} B u \big) \\
\dot{z}_{\nu+2} &= c_2 A^{r_2+\nu} x + c_1 A^{r_1+1} (\alpha_{r_2+\nu-1} I + \dots + \alpha_{r_2} A^{\nu-1}) x \\
&\quad + \big(c_2 A^{r_2+\nu-1} + c_1 A^{r_1} (\alpha_{r_2+\nu-1} I + \dots + \alpha_{r_2} A^{\nu-1}) B \big) u
\end{aligned}$$

Accordingly, defining

$$\begin{aligned}
R_1 z + S_1 \eta + \hat{b}_1 u &:= c_1 A^{r_1} T^{-1} \begin{pmatrix} z \\ \eta \end{pmatrix} + c_1 A^{r_1 - 1} B u \\
R_2 z + S_2 \eta &:= \big(c_2 A^{r_2+\nu} \\
&\quad + c_1 A^{r_1+1} (\alpha_{r_2+\nu-1} I + \dots + \alpha_{r_2} A^{\nu-1}) \big) T^{-1} \begin{pmatrix} z \\ \eta \end{pmatrix} \\
\hat{b}_2 &:= \big(c_2 A^{r_2+\nu-1} + c_1 A^{r_1} (\alpha_{r_2+\nu-1} + \dots + \alpha_{r_2} A^{\nu-1}) B \big) u
\end{aligned}$$

one gets for $i = 1, 2$, $\ell_i = 1, \dots, r_i - 1$ and $j = 0, \dots, \nu - 2$

$$\begin{aligned}
\dot{z}_{1,\ell_1} &= z_{1,\ell_1+1}, \quad \dot{z}_{1,r_1} = R_1 z + S_1 \eta + \hat{b}_1 u \\
\dot{z}_{2,\ell_2} &= z_{2,\ell_2+1} \\
\dot{z}_{2,r_2} &= z_3 - \alpha_{r_2} \big(R_1 z + S_1 \eta + \hat{b}_1 u \big) \\
\dot{z}_{j+3} &= z_{j+4} - \alpha_{r_2+j+1} \big(R_1 z + S_1 \eta + \hat{b}_1 u \big) \\
z_{\nu+2} &= R_2 z + S_2 \eta + \hat{b}_2 u \\
\dot{\eta} &= P z + Q \eta \\
y_1 &= z_{1,1}, \quad y_2 = z_{2,1}
\end{aligned} \tag{7}$$

that is the MIMO normal form associated to (1).

As a straightforward consequence of (7), one gets that the zero-dynamics of (1) is $\dot{\eta} = Q\eta$ with $\eta \in \mathbb{R}^{n-r_1-r_2-\nu}$ with $n-r_1-r_2-\nu$ being the excess poles-zeros and $\sigma\{Q\} = \{s \in \mathbb{C} \text{ s.t. } z(s) = 0\}$ that is, the eigenvalues of Q correspond to the transmission zeros of (1).

From the properties described above it is hence immediate to state that the control

$$\begin{aligned} u =& M^{-1}(v - Lx) \\ \overset{(6)}{=}& M^{-1}v - M^{-1}\begin{pmatrix} R_1 z + S_1\eta \\ R_2 z + S_2 z \end{pmatrix} \end{aligned} \tag{8}$$

with $v = \text{col}(v_1, v_2)$ and

$$L = \begin{pmatrix} c_1 A^{r_1} \\ c_2 A^{r_2+\nu} + c_1 A^{r_1+1}(\alpha_{r_2+\nu-1} I + \cdots + \alpha_{r_2} A^{\nu-1}) \end{pmatrix}$$

achieves right-invertibility of (1); namely, one gets

$$\begin{aligned} \dot{z}_{1,\ell} =& z_{1,\ell+1}, \quad \dot{z}_{1,r_1} = v_1 \\ \dot{z}_{2,\ell} =& z_{2,\ell+1}, \quad \dot{z}_{2,r_2} = z_3 - \alpha_{r_2} v_1 \\ \dot{z}_{j+3} =& z_{j+4} - \alpha_{r_2+j+1} v_1 \\ z_{\nu+2} =& v_2 \\ \dot{\eta} =& Pz + Q\eta \\ y_1 =& z_{1,1}, \quad y_2 = z_{2,1}. \end{aligned} \tag{9}$$

Remark 2.2: In this setting, the largest control-invariant subspace contained in $\ker C$ is given by

$$\mathcal{V}^\star = \ker \begin{pmatrix} c_1 \\ \vdots \\ c_1 A^{r_1-1} \end{pmatrix} \cap \ker \begin{pmatrix} c_2 \\ \vdots \\ c_2 A^{r_2-1} \end{pmatrix}$$
$$\cap_{j=0}^{\nu-1} \ker \begin{pmatrix} c_2 A^{r_2} + \alpha_{r_2} c_1 A^{r_1} \\ \vdots \\ c_2 A^{r_2+\nu-1} + c_1 A^{r_1}(\alpha_{r_2+\nu-1} I + \ldots + \alpha_{r_2} A^{\nu-1}) \end{pmatrix}.$$

Accordingly, the feedback law (8) represents the friend of $\mathcal{V}^\star \subset \ker C$ and thus the one achieving maximum unobservability via zeros cancellation. In general, we refer to $\mathcal{V}^\star$ as the zero-dynamics subspace.

Remark 2.3: We note that if $\nu = 0$ one recovers the standard normal form issued when (1) possesses a well-defined relative degree with non-singular decoupling (and right-invertibility) matrix provided by

$$M = \begin{pmatrix} c_1 A^{r_1-1} B \\ c_2 A^{r_2-1} B \end{pmatrix}.$$

In general, as $\nu > 0$ the above form shows that non interaction (and input/output decoupling) cannot be achieved through static state-feedback. However, the same does not stand for disturbance decoupling.

III. Stable zero factorization of MIMO systems

In this section, we extend the approach proposed in [11] for extracting the minimum-phase component of a general non-minimum phase systems (1). The approach is based on *output factorization*; namely, starting from (1), we identify a new dummy output $y^s(t) = C_s x(t)$ corresponding to the stable component of the zero-dynamics associated to (1) and related to (1b) through the differential equation

$$y(t) = Z_u(\mathrm{d}) y^s(t) \tag{10}$$

with $\mathrm{d} = \frac{\mathrm{d}}{\mathrm{d}t}$ and a suitably defined two dimensional square differential matrix

$$Z_u(\mathrm{d}) = \begin{pmatrix} z_{1,1}(\mathrm{d}) & z_{1,2}(\mathrm{d}) \\ z_{2,1}(\mathrm{d}) & z_{2,2}(\mathrm{d}) \end{pmatrix}. \tag{11}$$

More in details, starting from (5), one can split the zero-matrix as $N_{sm}(s) = N_u(s)N_s(s)$ with $N_u(s) = \text{diag}\{z_{u,1}(s), z_{u,2}(s)\}$ and $N_s(s) = \text{diag}\{z_{s,1}(s), z_{s,2}(s)\}$ such that $z_u(s) = z_{u,1}(s)z_{u,2}(s), z_s(s) = z_{s,1}(s)z_{s,2}(s)$ containing, respectively, the zeros on the right and left hand side of the complex plane; that is $\det(N_s(s)) = z_s(s)$ and $\det(N_u(s)) = z_u(s)$. Accordingly, the (5) rewrites as

$$\begin{aligned} P(s) =& L(s)N_u(s)N_s(s)D^{-1}(s)R(s) \\ =& Z_u(s)P_s(s) \end{aligned} \tag{12}$$

with $Z_u(s) = L(s)N_u(s)$ and $P_s(s) = N_s(s)D^{-1}(s)R(s)$.

In particular, $Z_u(s)$ is a polynomial matrix in s whereas $P_s(s)$ is transfer function matrix.

Remark 3.1: When (1) possesses distinct poles with unitary algebraic multiplicity the term $N_s(s)D^{-1}(s)R(s)$ is improper as $(L(s), R(s))$ introduce poles at $s = \infty$ [14]. To handle this issue [14], one can compute a matrix $K(s)$ (the so-called *right divisor*) such that: $\tilde{P}_s(s) = K(s)N_s(s)D^{-1}(s)R(s)$ is proper and with the same poles as (2) and z_s as zeros polynomial; $\tilde{Z}_u(s) = L(s)N_u(s)K^{-1}(s)$ is a polynomial matrix in $s \in \mathbb{C}$. Accordingly, (12) reads

$$P(s) = \tilde{Z}_u(s)\tilde{P}_s(s) \tag{13}$$

such that $\tilde{P}_s(s)$ is strictly proper and verifying (Remark 2.1)

$$\tilde{P}_s(s) = C_s(sI - A)^{-1}B. \tag{14}$$

The computation of such $K(s)$ might not be an easy task and needs to be performed through a vis-a-vis study. From now on, for the sake of clarity, we shall assume $K(s) = \text{I}$ although all the results to come hold true in general as illustrated through the case study.

Proposition 3.1: Consider the system (1) under Assumptions **A1** to **A3** and let $z(s) = z_u(s)z_s(s)$ be the zero-polynomial where $z_s(s)$ denotes the Hurwitz component. Let the transfer function $P(s)$ be of the form (13) with $P_s(s)$ as in (14) and $y^s = C_s x$ solution to (10). Then, the system

$$\dot{x} = Ax + Bu \tag{15a}$$
$$y^s = C_s x \tag{15b}$$

identifies the minimum-phase component of (1) with zero polynomial given by $z_s(s)$.

Proof: The proof is a straightforward consequence of the Smith McMillan form associated to (2) and (12). ■

Remark 3.2: The new output (15b) can be computed as follows. Let $(\hat{A}, \hat{B}, \hat{C})$ with $\hat{A} \in \text{Mat}_{\mathbb{R}}(\hat{n})$ with $\hat{n} \geq n$ be a realization of (14) and $(\hat{A}_\star, \hat{B}_\star, \hat{C}_\star)$ with $\hat{A}_\star \in \text{Mat}_{\mathbb{R}}(n)$

the corresponding restriction onto the observable and controllable subspaces. Denote by T and $T_\star$ the non-singular transformations putting, respectively, (A, B) and $(\hat{A}_\star, \hat{B}_\star)$ into the *eigenvalues assignment* canonical form [13](Ch.5). Then, because $TAT^{-1} = T_\star \hat{A} T_\star^{-1}$ and $TB = T_\star \hat{B}_\star$ one gets $C_s = \hat{C}_\star T_\star^{-1} T$.

IV. Applications

A. Right-invertibility with stability

As a consequence of the factorization in Section III, because of Assumption **A2**, one gets the following result.

Lemma 4.1: Consider the system (1) under Assumptions **A1** to **A3** and let (15) identify its minimum-phase component with transfer function (14). Then, (15) is right-invertible with indexes (r_1^s, r_2^s, ν^s) verifying $r_1^s + r_2^s + \nu^s = n - deg(z_s(s))$.

Proof: The proof is a straightforward consequence of the factorization (12). Indeed, as $R(s)$ is unimodular, the result follows from [15]. ∎

Remark 4.1: From the result above it is always possible to choose $L(s)$ such that the components of the matrix $Z_u(s)$ in (11) are such that $\deg\{z_{1,1}(s)\} = r_1^s - r_1$, $\deg\{z_{1,2}(s)\} = r_2^s + \nu^s - r_1$, $\deg\{z_{2,1}(s)\} = r_2^s + \nu^s - r_1$, $\deg\{z_{2,2}(s)\} = r_2^s + \nu^s - r_2 - \nu$ with $\deg\{\cdot\}$ denoting the degree of the corresponding polynomial and (r_1, r_2, ν) being the invertibility indices associated to (1).

By virtue of the result above and Section II-B, right-invertibility of the stable component of (1) can be achieved through right-invertibility of the same system with dummy output (15b).

Proposition 4.1: Consider the system (1) under Assumptions **A1** to **A3**. Let (15) identify the minimum phase component of (1) with invertibility indices (r_1^s, r_2^s, ν^s). Then, there exist $\alpha_{r_2^s+j} \in \mathbb{R}$ with $j = 0, \dots, \nu^s - 1$ such that

$$c_2^s A^{r_2^s+j-1} B + c_1^s A^{r_1^s} \sum_{\ell=0}^{j-1} \alpha_{r_2^s+\ell} A^{j-\ell-1} B = 0 \qquad (16)$$

and

$$M_s = \begin{pmatrix} c_1^s A^{r_1^s-1} B \\ c_2^s A^{r_2^s+\nu^s-1} B + c_1^s A^{r_1^s} \sum_{i=0}^{\nu^s-1} \alpha_{r_2^s+i} A^{\nu^s-i-1} B \end{pmatrix}$$

with $\det\{M_s\} \neq 0$. Accordingly, the feedback

$$u = M_s^{-1}(v - L_s x) \qquad (17)$$

with

$$L_s = \begin{pmatrix} c_1^s A^{r_1^s-1} \\ c_2^s A^{r_2+\nu} + c_1^s A^{r_1^s+1}(\alpha_{r_2^s+\nu^s-1} I + \dots + \alpha_{r_2^s} A^{\nu^s-1}) \end{pmatrix}$$

performs right-invertibility of the minimum-phase component of (1).

Proof: Along the lines of Section II-B, we introduce the coordinate transformation

$$\begin{pmatrix} z_1^s \\ z_2^s \\ z_3^s \\ \vdots \\ z_{\nu^s+2} \\ \eta \end{pmatrix} = \begin{pmatrix} T_1^s \\ T_2^s \\ T_3^s \\ \vdots \\ T_{\nu^s+2}^s \\ T_{\eta^s} \end{pmatrix} x, \quad z_i^s = \begin{pmatrix} z_{i,1}^s \\ \dots \\ z_{i,r_i^s}^s \end{pmatrix} \qquad (18)$$

for $i = 1, 2$ and with, for $j = 3, \dots, \nu^s + 2$ so that, under the control (17), (15) gets the form

$$\begin{aligned} \dot{z}_{1,\ell}^s &= z_{1,\ell+1}^s, \quad \dot{z}_{1,r_1}^s = v_1 \\ \dot{z}_{2,\ell}^s &= z_{2,\ell+1}^s, \quad \dot{z}_{2,r_2^s}^s = z_3^s - \alpha_{r_2^s} v_1 \\ \dot{z}_{j+3}^s &= z_{j+4}^s - \alpha_{r_2^s+j+1} v_1 \\ z_{\nu^s+2}^s &= v_2 \\ \dot{\eta}^s &= P^s z^s + Q^s \eta^s \\ y_1^s &= z_{1,1}^s, \quad y_2^s = z_{2,1}^s \end{aligned}$$

with $\dot{\eta}^s = Q^s \eta^s$ being the asymptotically stable zero-dynamics with $\sigma\{Q^s\} = \{s \in \mathbb{C} \text{ s.t. } z_s(s) = 0\} \subseteq \{s \in \mathbb{C} \text{ s.t. } z(s) = 0\}$. From (10), one gets in the new coordinates

$$y = Z_u(\mathrm{d}) y^s = Z_u(\mathrm{d}) \begin{pmatrix} z_{1,1}^s \\ z_{2,1}^s \end{pmatrix} = \hat{C} z^s$$

and thus the result. ∎

As a consequence, one gets the following result.

Proposition 4.2: Consider the systems (1) and (15) and let $\mathcal{V}^\star$ and $\mathcal{V}_s^\star$ be, respectively, the largest controlled (A,B)-invariant subspaces contained in $\ker\{C\}$ and $\ker\{C_s\}$. Then, $\mathcal{V}_s^\star \subset \mathcal{V}^\star$.

Proof: For the ease of the proof, assume that for (1) $\nu = 0$. By virtue of (10) one has, for $i = 1, 2$ and $j = 0, \dots, r_i - 1$

$$\begin{aligned} \mathrm{d}^j y_i(t) = c_i A^j x &= \mathrm{d}^j z_{i,1}(\mathrm{d}) y_2^s + \mathrm{d}^j z_{i,2}(\mathrm{d}) y_2^s \\ &= z_{i,1}(\mathrm{d}) c_1^s A^j x + \mathrm{d}^j z_{i,2}(\mathrm{d}) c_s^s A^j x \end{aligned}$$

with, by definition of r_1, r_2, $\nabla_u(Z_u(\mathrm{d}))\mathrm{d}^j y^s) = 0$. By exploiting (16), it is a matter of computations to deduce that

$$\underbrace{\begin{pmatrix} T_1 \\ T_2 \end{pmatrix}}_{V} = N \underbrace{\begin{pmatrix} T_1^s \\ \vdots \\ T_{\nu^s+2}^s \end{pmatrix}}_{V_s}.$$

with T_i and T_j^s as in (6) and (18) for $i = 1, 2$ and $j = 1, \dots, \nu^s + 2$ and N being an upper triangular full rank matrix. From the equality above one gets that $\mathcal{V}_s^\star = \ker\{V_s\} \subset \ker\{V\} = \mathcal{V}^\star$ and thus the result. ∎

The feedback (17) is the one generating in closed loop the maximal unobservability constrained to stability; namely, (17) is the one canceling only the Hurwitz component of the zero dynamics of the original system (1). In other words, (17) is rendering only the stable component of $\mathcal{V}^\star$ feedback-invariant (that is $\mathcal{V}_s^\star$).

Remark 4.2: It must be noted that, albeit (1) possesses a well-defined relative degree (that is $\nu = 0$), when introducing the new dummy output issued from Proposition 3.1 through the Smith form, one might get $\nu_s \geq 0$. However, ν^s defines the order of the dynamic extension that is necessary (over the control input u_1) for recovering a well-defined relative degree $(\hat{r}_1^s, r_2^s)$.

Remark 4.3: By virtue of Assumption **A2** and Remark 2.3, one gets that the asymptotic tracking problem of a smooth reference $y_r(t) \in \mathbb{R}^2$, corresponding to $z_r^s(t)$ in

the new coordinates, admits a solution with stability (under dynamical feedback if $\nu^s > 0$) by solving the equivalent problem over the partially minimum-phase system (15) and with respect to the dummy output reference $y_r^s(t) \in \mathbb{R}^2$.

B. DDP of non minimum-phase systems with stability

Let (1) be affected by a disturbance $w \in \mathbb{R}^2$ that is

$$\dot{x} = Ax + Bu + Pw \tag{19a}$$
$$y = Cx \tag{19b}$$

with $P \in \mathrm{Mat}_{\mathbb{R}}(n, 2)$. In this section, it is shown how disturbance decoupling (DDP) can be solved with stability by making use of the new output deduced in Section III. It is worth recalling that, in general and regardless stability, disturbance decoupling is solvable if and only if $\mathrm{Im}\{P\} \subset \mathcal{V}^\star \subset \ker\{C\}$. However, the corresponding solution guarantees stability of the closed loop if and only if the zero-dynamics associated to (19) is asymptotically stable. The next statement provides a new result ensuring the existence of a disturbance decoupling controller preserving stability of the internal dynamics.

Theorem 4.1: Consider (19) under assumptions **A1.** to **A3.** and the dummy output (15b) defined by Proposition 3.1. Then, output disturbance decoupling with stability for (19) is solvable for all P verifying $\mathrm{Im}\{P\} \subset \mathcal{V}_s^\star \subset \ker\{C\}$ where $\mathcal{V}_s^\star$ is the largest (A, B)-invariant subspace contained in $\ker\{C_s\}$. In addition, the corresponding feedback is (17).

Proof: The proof is a straightforward consequence of Proposition 4.2 ensuring $\mathcal{V}_s^\star \subset \mathcal{V}^\star \subset \ker\{C\}$. ∎

Remark 4.4: By virtue of Remark 4.2, one gets that dynamical feedback extension is unnecessary for solving DDP whenever the system is right-invertible even if (15) do not possess a well-defined relative degree.

V. The 4-Tanks as an example

Consider the case of a 4-tanks system [16] given by

$$\dot{h} = f(h) + Bu \tag{20a}$$
$$y = Ch \tag{20b}$$

with $h = \mathrm{col}\{h_1, h_2, h_3, h_4\}$, $f(h) = 2F(h)h$

$$F(h) = \begin{pmatrix} -p_1(h_1) & 0 & \frac{A_3}{A_1}p_3(h_3) & 0 \\ 0 & -p_2(h_2) & 0 & \frac{A_4}{A_2}p_4(h_4) \\ 0 & 0 & -p_3(h_3) & 0 \\ 0 & 0 & 0 & -p_4(h_4) \end{pmatrix}$$

$$B = \begin{pmatrix} \frac{\gamma_1 k_1}{A_1} & 0 \\ 0 & \frac{\gamma_2 k_2}{A_2} \\ 0 & \frac{(1-\gamma_2)k_2}{A_3} \\ \frac{(1-\gamma_1)k_1}{A_4} & 0 \end{pmatrix}, \quad C = \kappa_t \begin{pmatrix} 1 & 0 \\ 0 & 1 \\ 0 & 0 \\ 0 & 0 \end{pmatrix}^\top$$

$p_i(h_i) = \frac{c_i\sqrt{2gh_i}}{2A_ih_i}$. For the sake of compactness, let b_{ij} correspond to the element in position (i, j) of the input-state matrix B. In particular, h_i, A_i and c_i are, respectively, the level of water in the i^{th}-tank, its cross-section area and the cross-section of the outlet hole for $i = 1, 2, 3, 4$. The control signals u_j with $j = 1, 2$ correspond to the voltage applied to j^{th}-pump with k_ju_j being the corresponding flow. We consider the problem of locally asymptotically tracking the output of (20) to a desired $y_\star = (h_1^\star,\ h_2^\star)$ corresponding to make $h^\star = (h_1^\star, h_2^\star, h_3^\star, h_4^\star)^\top$ with

$$h_3^\star = \frac{(c_1\gamma_2\sqrt{h_1^\star} - c_2(1-\gamma_2)\sqrt{h_2^\star})^2}{c_3^2a_3^2\gamma_2^2}$$
$$h_4^\star = \frac{(c_2\gamma_1\sqrt{h_2^\star} - c_1(1-\gamma_1)\sqrt{h_1^\star})^2}{c_4^2a_4^2\gamma_1^2}$$

for $a_3 = \frac{\gamma_2}{1-\gamma_2} - \frac{1-\gamma_1}{\gamma_1}$ and $a_4 = \frac{\gamma_1}{1-\gamma_1} - \frac{1-\gamma_2}{\gamma_2}$ a locally asymptotically stable equilibrium for the closed-loop system under nonlinear feedback.

1) Analysis of the zero-dynamics: The vector relative degree of (20) is well defined and given by $r = (1\ 1)$ so that it exhibits a two-dimensional zero-dynamics. Accordingly, for investigating minimum-phaseness of (20), one computes the linear tangent model (LTM) at $h^\star$ of the form (1) with $x = h - h^\star$ and $A = 2F(h^\star)$ with corresponding transfer function matrix

$$P(s) = \kappa_t \begin{pmatrix} \frac{b_{11}}{s+p_1} & \frac{b_{32}\,p_3}{(s+p_1)\,(s+p_3)} \\ \frac{b_{41}\,p_4}{(s+p_2)\,(s+p_4)} & \frac{b_{22}}{s+p_2} \end{pmatrix} \tag{21}$$

$p_i = p_i(h_i^\star) > 0$ for $i = 1, 2, 3, 4$, Smith form as $M(s) = \mathrm{diag}\{\frac{1}{d(s)}, z(s)\}$, with pole-polynomial $d(s) = (s + p_1)(s + p_2)(s + p_3)(s + p_4)$ and zero-polynomial $z(s) = s^2 + (p_3 + p_4)s + \frac{p_3p_4}{b_{11}b_{22}}(b_{11}b_{22} - b_{32}b_{41})$. Thus, (20) is nonminimum-phase if $b_{11}b_{22} - b_{32}b_{41} < 0$ so that one can factorize $z(s) = (s - z_u)(s - z_s)$ for $z_u \in \mathbb{R}^+$ and $z_s \in \mathbb{R}^-$. As a consequence, if $b_{11}b_{22} - b_{32}b_{41} < 0$, output regulation to $y_\star$ cannot be achieved through classical right-inversion even if the relative degree is well-defined.

In the following we show how the procedure detailed in Section III allows to deduce a new output $y_s = C_sh$ and a nonlinear feedback locally solving the regulation problem with stability for (20).

2) The new dummy output: By virtue of Remark 3.1, because (A, B, C) possesses three distinct poles in general, one gets that the matrix $P_s(s) = \mathrm{diag}\{1, s - z_s\}\mathrm{diag}\{d(s), 1\}R(s)$ is improper for all choices of $(L(s), R(s))$. However, by suitably setting $K(s)$[1] so to make $\tilde{P}_s(s) = K(s)P_s(s)$ rational one gets the dummy output

$$y_s = \begin{pmatrix} 1 & 0 & 0 & 0 \\ -\frac{b_{32}b_{41}p_4}{2b_{11}\beta} & \frac{b_{32}}{2} - \frac{b_{32}(p_3+p_4)}{2\beta} & -\frac{b_{22}}{2} - \frac{b_{22}(p_3+p_4)}{2\beta} & \frac{b_{32}\,p_4}{2\beta} \end{pmatrix} h \tag{22}$$

with $\beta = \sqrt{(p_3 + p_4)^2 - 4\frac{p_3p_4}{b_{11}b_{22}}(b_{11}b_{22} - b_{32}b_{41})}$ making the LTM model of (20a) minimum-phase.

3) Asymptotic tracking with stability: It is easily checked that, the nonlinear dynamics (20a) with output as in (22) possesses a well-defined relative degree $r_s = (1,\ 2)$ at $h^\star$. Also, it is a matter of computations to verify that (20a) with output (22) is locally minimum-phase with zero-dynamics $\dot{\eta}^s = q_s(0, \eta^s)$ verifying $\frac{\partial q_s}{\partial \eta_s}(0, \eta_\star^s) = z_s < 0$. At this point,

[1]For the sake of space, $(L(s), R(s), K(s))$ are reported at `https://hal.archives-ouvertes.fr/hal-02526676`.

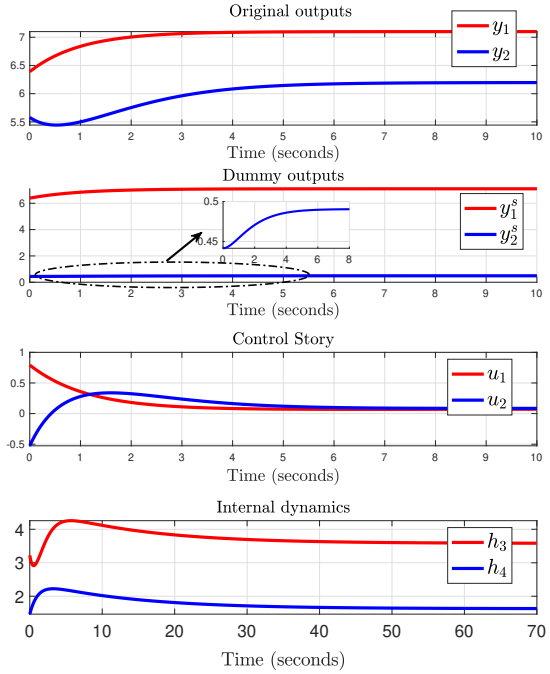

Fig. 1. The four tank model under stable dynamic inversion.

along the lines of Remark 4.3 and by exploiting the results in [9, Chapter 5], one gets that output tracking of (20) can be solved over the dummy output (22) by setting the constant $y_\star^s = (y_{1,\star}^s, y_{2,\star}^s)^\top \in \mathbb{R}^2$ as solution to $y_\star = Z_u(\mathrm{d})y_s^\star$ which is given by construction as $y_\star^s = C_s h^\star$. Accordingly, for all $k_0, k_1 > 0$ the feedback

$$u = -M_s^{-1}(h)\begin{pmatrix} c_1^s f(h) + y_1^s - y_{1,\star}^s \\ \mathrm{L}_f c_2^s f(h) + k_1 c_2^s f(h) + k_0(y_2^s - y_{2,\star}^s) \end{pmatrix} \quad (23)$$

with decoupling matrix

$$M_s^{-1}(h) = \begin{pmatrix} c_1^s B \\ \mathrm{L}_f^2 c_2^s f(h) B) \end{pmatrix}$$

ensures local asymptotic regulation of y to the desired $y^\star$ while preserving internal stability.

4) Simulations: For completeness, simulations are reported in Figure 1 for the closed-loop system under the stabilizing feedback designed over the new dummy output highlighting the locally minimum-phase components of (20). Simulations are performed for the parameters fixed as in the Table below.

$A_1\ [cm^2]$	28	$A_3\ [cm^2]$	28
$A_2\ [cm^2]$	32	$A_4\ [cm^2]$	32
$c_1\ [cm^2]$	0.071	$c_3\ [cm^2]$	0.071
$c_2\ [cm^2]$	0.057	$c_4\ [cm^2]$	0.057
$k_t\ [V/cm]$	1	$g\ [cm/s^2]$	981
γ_1	0.43	γ_2	0.34
k_1	65.12	k_2	94.12

In addition, we fixed $y_\star = (7.1,\ 6.2)^\top$ corresponding to $h^\star = (7.1,\ 6.2,\ 3.58, 1.632)^\top$. In particular, with this choice of parameters, the plant is nonminum-phase with the zeros of LTM model at the desired equilibrium provided by $z_u = 0.018$ and $z_s = -0.0789$. The gains of the controller (23) are fixed as $(k_0, k_1) = (1, 2)$. Simulations report the story of the original and dummy outputs plus the real residual internal-dynamics of the feedback plant (that is the water levels of the third and fourth tank with respect to the real output) while proving the effectiveness of the proposed design approach.

VI. Conclusions

In this paper, a systematic procedure for controlling MIMO non-minimum phase systems has been proposed based on output factorization. In particular, recurring to the Smith-MacMillan form, a dummy output associated with the stable component of the zero-dynamics is exhibited to perform inversion of the minimum-phase component. The results locally apply to the case of nonlinear dynamics with linear outputs. Perspectives concern the extension of this methodology to the case of nonlinear output mappings.

References

[1] A. Isidori, A. Krener, C. Gori-Giorgi, and S. Monaco, "Nonlinear decoupling via feedback: a differential geometric approach," *IEEE Transactions on Automatic Control*, vol. 26, no. 2, pp. 331–345, 1981.

[2] A. Isidori and C. I. Byrnes, "Output regulation of nonlinear systems," *IEEE Transactions on Automatic Control*, vol. 35, no. 2, pp. 131–140, Feb 1990.

[3] A. De Luca, *Zero Dynamics in Robotic Systems*. Boston, MA: Birkhäuser Boston, 1991, pp. 68–87.

[4] C. D. Persis and A. Isidori, "A geometric approach to nonlinear fault detection and isolation," *IEEE Transactions on Automatic Control*, vol. 46, no. 6, pp. 853–865, Jun 2001.

[5] R. Ortega, A. Van Der Schaft, F. Castanos, and A. Astolfi, "Control by interconnection and standard passivity-based control of port-hamiltonian systems," *IEEE Transactions on Automatic Control*, vol. 53, no. 11, pp. 2527–2542, 2008.

[6] A. Giuseppi, A. Pietrabissa, S. Cilione, and L. Galvagni, "Feedback linearization-based satellite attitude control with a life-support device without communications," *Control Engineering Practice*, vol. 90, pp. 221–230, 2019.

[7] A. Astolfi, D. Karagiannis, and R. Ortega, *Nonlinear and adaptive control with applications*. Springer Publishing Company, 2008.

[8] A. Di Giorgio, A. Pietrabissa, F. D. Priscoli, and A. Isidori, "Robust output regulation for a class of linear differential-algebraic systems," *IEEE Control Systems Letters*, vol. 2, no. 3, pp. 477–482, 2018.

[9] A. Isidori, *Nonlinear Control Systems*. Springer-Verlag, 1995.

[10] S. Monaco and D. Normand-Cyrot, "Multirate sampling and zero dynamics: from linear to nonlinear," in *Nonlinear Synthesis*. C. Byrnes, A. Isidori Eds., Birkauser, 1991, pp. 200–213.

[11] M. Mattioni, M. Hassan, S. Monaco, and D. Normand-Cyrot, "On partially minimum-phase systems and disturbance decoupling with stability," *Nonlinear Dynamics*, vol. 97, no. 1, pp. 583–598, 2019.

[12] A. Isidori, *Lectures in feedback design for multivariable systems*. Springer, vol. 3.

[13] G. Marro, *Teoria dei sistemi e del controllo*. Zanichelli, 1990.

[14] T. Kailath, *Linear systems*. Prentice-Hall Englewood Cliffs, NJ, 1980, vol. 156.

[15] M. Sain and J. Massey, "Invertibility of linear time-invariant dynamical systems," *IEEE Transactions on automatic control*, vol. 14, no. 2, pp. 141–149, 1969.

[16] K. H. Johansson and J. L. R. Nunes, "A multivariable laboratory process with an adjustable zero," in *Proceedings of the 1998 American Control Conference. ACC (IEEE Cat. No. 98CH36207)*, vol. 4. IEEE, 1998, pp. 2045–2049.

Sampled-data model predictive control

Chapter 4

Stable partial inversion via sampled-data multi-rate model predictive control

Contents

STARTING from the major points which have been raised in Chapter 2 that brought us to understand that direct digital control strategies may induce instability also due to the loss of minimum phase property of the sampled-data model of the process, we will address in the sequel MPC control which is strongly affected by this pathology.

Accordingly, the chapter starts by providing an overview of the fact that the so-called tracking nonlinear MP at the limit, i.e. when the problem is unconstrained and the control penalty is small enough implies inversion. This fact clearly puts in light possible instability of the closed loop system under MPC when using the sampled-data model for prediction is a consequence of the unstable zero dynamics which characterize the sampled-data equivalent model.

This fact, and taking into account the discussion in Section 2.4, lead one naturally to understand that the use of multi-rate sampled-data equivalent models for prediction in the MPC formulation can be a way to mitigate the obstructions linked to the cancellation of unstable zero dynamics and guaranteeing closed loop stability. These aspects are discussed and settled in;

> Mohamed Elobaid, Mattia Mattioni, Salvatore Monaco and Dorothée Normand-Cyrot. *"On unconstrained MPC through multirate sampling". IFAC-PapersOnLine, 52(16), 388-393. DOI: 10.1016/j.ifacol.2019.11.811.*

The proposed solution will be called sampled-data multi-rate MPC. It is characterized by the use, at the control and prediction level of an MPC formulation, a multi-rate discrete time model over which the optimization problem is worked out. Some concluding remarks on the costs and benefits related to the proposed solution are also provided. It results that robustness, also linked to multi-rate control remains a major point, which leads us to ask for a "better" solution detailed in

Chapter 5. The notions appearing hereinafter are recalled from Camacho and Alba (2013), Grüne et al. (2008), Allgöwer and Zheng (2012), Mayne et al. (2000a), Seron et al. (1999) and the references therein.

4.1 Cheap unconstrained model predictive control implies partial inversion

We start by considering a nonlinear SISO input affine system herein recalled for completeness

$$\dot{x} = f(x) + g(x)u \tag{4.1a}$$
$$y = h(x) \tag{4.1b}$$

assumed minimum phase having a well defined continuous-time relative degree r. We recall the finite time optimal control problem Grüne and Pannek (2017);

$$\begin{aligned} V = \min_u & \int_{t_0}^{t_f} \ell(y(t), y_r(t), u(t))dt \\ s.t.\ \dot{x}(t) &= f(x(t)) + g(x(t))u(t),\ \ y(t) = h(x(t)) \\ & x(t) \in \mathcal{X}, t \in [t_0, t_f], \\ & u(t) \in \mathcal{U}, t \in [t_0, t_f] \end{aligned} \tag{4.2}$$

where V is the so-called optimal value function, t_0, t_f are initial and final time respectively, the term $\ell(y(t), y_r(t), u(t))$ is the stage cost function to be penalized and $y_r(t)$ a desired reference signal. The sets $\mathcal{X}$,$\mathcal{U}$, being the state and control constraints sets are assumed compact, convex and containing the origin (equivalently the trajectory $y(t) = y_r(t)$) in their interior.

In the limit when: (1) the sets $\mathcal{X}$,$\mathcal{U}$ are the whole state and input space respectively (unconstrained problem), (2) the penalty on the control is very small, and (3) the stage cost is quadratic in the tracking error the resulting optimal control problem is known in the literature as the *cheap optimal control problem* Seron et al. (1999). In this cheap control setting, the optimal value of the cost index is known as the *ideal performance*. It is then natural to ask; when the ideal performance, typically proportional to the tracking error, is exactly zero? and to this end recall;

Problem: cheap optimal control

Given a nonlinear control affine system and $\epsilon \in \mathbb{R}$ small, the cheap optimal control problem asks for a feedback that minimizes the cost function

$$V = min_u \int_{t_0}^{\infty} \|y(t) - y_r(t)\|_Q^2 + \epsilon \|u(t)\|_R^2 dt \tag{4.3}$$

subject to the system dynamics. Moreover, at the limit when $\epsilon = 0$, the problem asks for conditions under which this feedback results in zero ideal performance for the system.

In Seron et al. (1999) (equivalently in Qiu and Davison (1993) for the linear case), it was shown

that, the ideal performance of a control system, that is the lowest attainable norm of its output tracking error, is the least amount of energy required to stabilize the zero dynamics and that unstable zero dynamics represent a structural obstacle to attaining zero ideal performance. The following statement is herein recalled to emphasize this fact;

Lemma: zero ideal performance

For a (locally observable and controllable) nonlinear control affine systems having a continuous-time relative degree r, the feedback solving the cheap optimal control problem achieves zero ideal performance if and only if the system is minimum phase.

The continuous-time optimal control problem is an infinite dimensional Nonlinear Program NLP hindering the ability to provide numerical/implementable solutions. A workaround this issue is the transformation of this infinite dimensional non-convex NLP into a finite dimensional nonlinear MPC problem through transcription methods (also called shooting) and integration. In this sense, and following Camacho and Alba (2013), one obtains the following equivalent nonlinear MPC problem;

$$V = \min_U V_{n_p}(x(k+n_p)) + \sum_{i=1}^{n_p-1} \ell(y(k+i), y_r(k+i), u(k+i-1)) \tag{4.4a}$$

$$st. \quad x(k+1) = F^{\delta}(x(k), u(k)), \;\; y(k) = h(x(k)) \tag{4.4b}$$

$$x(k+i) \in \mathcal{X}, i = 1 \ldots, n_p - 1 \tag{4.4c}$$

$$u(k+j) \in \mathcal{U}, \;\; j = 0, \ldots, n_c - 1 \tag{4.4d}$$

$$u(k+j) = u_{n_p}, \;\; j = n_c, \ldots, n_p - 1 \tag{4.4e}$$

$$x(k+n_p) \in \mathcal{X}_{n_p} \tag{4.4f}$$

where U is the control decision variable over n_c steps, n_p, n_c are the so-called prediction and control horizons respectively such that $t_0 = k\delta, t_f = (k+n_p)\delta$. Note that, through integration (and possibly truncation as in (2.9)), one obtains an equivalent ASR sampled-data model of the continuous-time system as a so-called prediction model (4.4b). Typically the stage cost function in tracking MPC is quadratic in the error Camacho and Alba (2013), namely;

$$\ell(y(k+i), y_r(k+i), u(k+i-1)) = \|y(k+i) - y_r(k+i)\|_Q^2 + \|u(k+i-1)\|_R^2 \tag{4.5}$$

with Q, R positive definite and positive semi-definite penalizing matrices respectively. The terminal penalty $V_{n_p}(\cdot)$, terminal control $u_{n_p}(\cdot)$ and terminal constraints set $\mathcal{X}_{n_p}(\cdot)$ are added to the optimization problem to the purpose of ensuring closed loop stability. In fact, the following conditions on the terminal ingredients are imposed as detailed in the important survey Mayne et al. (2000a);

- terminal penalty $V_{n_p}(x(k+n_p))$: this is "typically" designed as a quadratic form $x(k+n_p)^\top P x(k+n_p)$, where P is the solution to the discrete algebraic Riccati equation associated with the Linear Quadratic Regulator LQR problem Anderson and Moore (2007) of the LTM model of the system. The terminal penalty serves as a local Lyabonuv function over the

terminal constraints set.

- terminal control $u(k+j) = u_{n_p}(x)$ after n_c time steps, being the LQR feedback deriving the LTM model of the system to the reference. This feedback should ensure that the terminal constraints set is positively forward invariant.

- terminal constraints set $x(k+n_p) \in \mathcal{X}_{n_p}$ ensuring that the trajectories of the closed loop converge to a predefined (typically a closed subset of the maximal output admissible set Gilbert and Tan (1991)) region.

Those terminal ingredients are specifically designed to ensure, absent other horizon length and technical controllability assumptions, closed loop stability under MPC. These ingredients are done in conjunction with the usual practical recommendation of setting bounds on the minimum length of n_p and selecting $n_c << n_p$.

All of this discussion suggests that indeed when the output is required to track the input via MPC, some cancellation of the zero dynamics occur provided the penalty on the control small enough and the problem is unconstrained. And while the above intuition is discussed in the continuous-time literature, it is not difficult to see that also holds in the digital context Qiu and Davison (1993).

In the following simple example, we illustrate this fact, that MPC requires the cancellation of zeros in the linear case at the cheap control limit;

Example 4.1 recall the triple integrator;

$$G(s) = \frac{1}{s^3}$$

which has a pulse transfer function;

$$H(z) = \frac{\delta^3(z^2+4z+1)}{z^3-3z^2+3z-1}$$

where δ is the sampling period. As already discussed in Section 2.2, the sampled-data model has an additional $r-1=2$ sampling zeros one of which lies outside the unit disk. The sampled-data state-space model matrices, recalled again for completeness, read

$$A_d = \begin{pmatrix} 1 & \delta & \frac{\delta^2}{2} \\ 0 & 1 & \delta \\ 0 & 0 & 1 \end{pmatrix}, \quad B_d = \begin{pmatrix} \frac{\delta^3}{3!} \\ \frac{\delta^2}{2!} \\ \delta \end{pmatrix}, \quad C_d = \begin{pmatrix} 1 & 0 & 0 \end{pmatrix}$$

Consider now a tracking unconstrained MPC problem with a quadratic cost function, namely let the decision variable over the prediction horizon be $U = (u(k)\ u(k+1)\ \dots u(k+n_p-1))^\top$ and define

$$V = \min_U \sum_{i=1}^{n_p} \left(\|y(k+i) - y_r(k+i])\|_Q + \|u(k+i-1])\|_R \right)$$

$$\text{s.t } x(k+i) = A_d x(k+i-1) + B_d u(k+i-1), \quad y(k+i) = C_d x(k+i)$$

Applying the first order necessary optimality conditions we have and taking only the first optimal

control;

$$\frac{\partial V}{\partial U} = \frac{\partial}{\partial U}\sum_{i=1}^{n_p}\left(\|y(k+i) - y_r(k+i])\|_Q + \|u(k+i-1])\|_R\right)|_{U^\star} = 0$$
$$\implies u^\star = \begin{pmatrix}1 & 0 & \dots & 0\end{pmatrix}(B_e^\top Q_e B_e + R_e)^{-1}B_e^\top Q_e(y_{r_e} - A_e x)$$

where $Q_e = Q \otimes I_{n_p}, R_e = R \otimes I_{n_p}$, $y_{r_e} = \begin{pmatrix} y_r(k+1) & y_r(k+2) & \dots & y_r(k+n_p)\end{pmatrix}^\top$ and

$$A_e = \begin{pmatrix} C_dA_d \\ C_dA_d^2 \\ \vdots \\ C_dA_d^{n_p}\end{pmatrix}, \quad B_e = \begin{pmatrix} C_dB_d & 0 & \dots & 0 \\ C_dA_dB_d & C_dB_d & \dots & 0 \\ \vdots & \vdots & \ddots & \vdots \\ C_dA_d^{n_p-1}B_d & C_dA_d^{n_p-2}B_d & \dots & C_dA_d^{n_p-n_c}B_d\end{pmatrix}$$

As the figure below illustrates, fixing the prediction horizon at $n_p = 5$ and changing the control horizon n_c one can see the closed loop poles and zeros under the feedback $u^\star$ and note that as $n_c \to n_p, R \to 0$ zero-poles cancellation occurs. Consequently we have unstable inversion in MPC.

The example above demonstrates how unconstrained tracking MPC reduces to inversion and zero dynamics cancellation when the prediction and control horizon coincide. This fact also explains a suggested practice among engineers of setting $n_p >> n_c$ (see for example the guidelines of MATLAB (2020)), as well as gives a hint on how unstable inversion with a sampled-data prediction model is a key factor motivating the use of technical terminal ingredients to guarantee stability in MPC formulations Camacho and Alba (2013).

This last aspect, tracking MPC under sampling being an inversion based control at the limit, compounded with the additional knowledge of the rise of non minimum phase zero dynamics under sampling, is the reason we study some possible solutions so that, at the limit, MPC provides (an almost) zero ideal performance while maintaining stability.

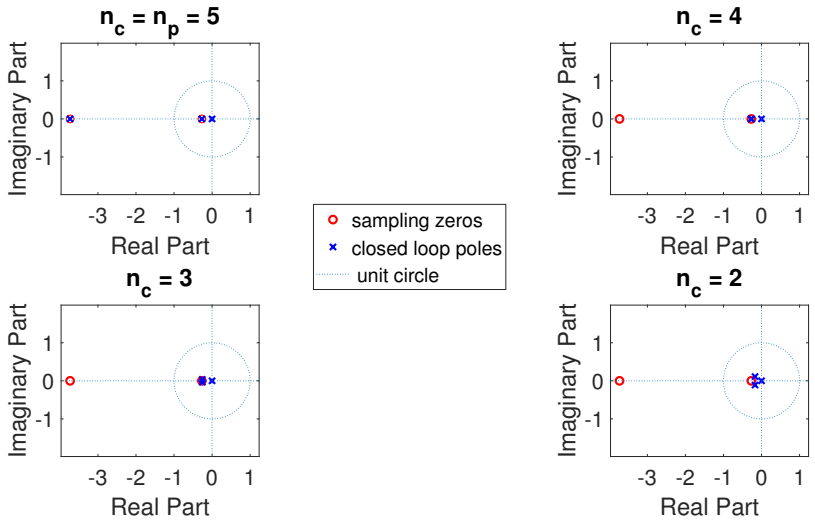

Figure 4.1: Poles and zeros map of the triple integrator under unconstrained MPC $n_p = 5, R = 0.1\mathrm{I}, Q = \mathrm{I}$

4.2 Stable partial inversion in model predictive control via multi-rate sampling

Building upon the discussion in the previous section, and the reality of digital implementation we restrict the problem to ask for finding a solution at all instants of time $t = k\delta,\ k \in \mathbb{Z}_{\geq 0}$ with δ a suitable sampling period, namely;

Problem: unconstrained cheap MPC under sampling

Find a bounded digital feedback ensuring that at the sampling instants that: $y(k) = y_r(k)$, $k \geq k^\star$ *with* $y_r(k) = y_r(k\delta)$ *by minimizing:*

$$J = \sum_{i=1}^{n_p} \left(\|y_r(k+i) - y(k+i)\|_Q^2 + \epsilon \|u(k+i-1)\|_R^2 \right) \tag{4.6}$$

with $Q, R > 0$ *being appropriate penalizing weights and* $\epsilon \in \mathbb{R}$ *small.*

Note that this is a cheap optimal finite-time control problem and thus we will address it using a multi-rate sampled-data equivalent model for prediction in a nonlinear MPC design. This is motivated by: (1) cheap optimal control implies cancellation of the zero dynamics and (2) multi-rate sampling preserves the structure of the zero dynamics.

In this sense, the proposed nonlinear MPC problem is an optimization problem, subject to the system dynamics described by a multi-rate sampled-data equivalent model of order r, repeated herein for completeness of the form;

$$x(k+1) = F_m^\delta(x(k), \underline{u}(k)) \tag{4.7a}$$

$$Y(k) = H(x(k)) \tag{4.7b}$$

where the output map $H(x)$ is as in (2.15). The dynamics constraint above is joined by possibly additional requirements and bounds. In essence, we are replacing (4.4b) with (4.7a) in the nonlinear MPC problem, and removing the terminal ingredients. Additionally the following assumption is needed;

Assumption 4.1 *The following assumptions are assumed to hold;*

- *Measures of the desired output reference* y_r *and it's higher* $r-1$ *derivatives* $y_r^{(i)},\ i = 1 \ldots r-1$ *are available at the sampling instants.*
- *The sets* $\mathcal{X}$,$\mathcal{U}$ *in (4.4c), (4.4d) are the whole state and input space respectively.*
- *The control and prediction horizons coincide* $n_c = n_p$

The above assumption is not restrictive and can be weakened via an exogenous system generator of the reference, which allows us to predict the future values of $y_r^{(i)},\ i = 0\ \ldots\ r-1$.

To solve the problem we adopt the so called *direct single shooting* (Hicks and Ray (1971)) in which one rewrites the cost function (4.6) as;

$$J = \sum_{i=1}^{n_p} L(., y_\star(k+i), \underline{u}(k+i-1)) \circ (F_m^\delta(., \underline{u}(k+i-1)) \circ \ldots \circ (F_m^\delta(x(k), \underline{u}(k)))$$

essentially plugging (4.7a),(4.7b) into (4.6). At this point, an optimum is found applying the first order necessary conditions solving

$$\frac{\partial J}{\partial u_e} = 0$$

where

$$u_e(k) = \begin{pmatrix} \underline{u}(k) & \ldots & \underline{u}(k+n_p-1) \end{pmatrix}^\top$$

For our purposes it is interesting to repeat that in its usual implementation MPC makes use of a sampled data model of the plant for prediction. This induces the loss of the minimum-phaseness, so indeed, forcing the designer to choose $n_c << n_p$ to guarantee internal stability while also defining a dynamical controller to ensure off-set free tracking. In the approach we are proposing, the use of multirate sampled data model will provide a static feedback overcoming both issues.

For the sake of compactness, define the extended output vector dynamics for n_p future steps;

$$Y_e(k+1) = A_e Y(k) + B_e(x(k))u_e(k) + \Theta(x(k), u_e(k)) \tag{4.8}$$

with

$$Y_e(k+1) = \begin{pmatrix} Y(k+1) & Y(k+2) & \ldots & Y(k+n_p) \end{pmatrix}^\top$$

and

$$B_e(.) = \mathrm{L}_g \mathrm{L}_f^{r-1} h(.) \begin{bmatrix} B & 0 & \ldots & 0 \\ AB & B & \ldots & 0 \\ \vdots & & & \\ A^{n_p-1}B & A^{n_p-2}B & \ldots & B \end{bmatrix}, \quad B = D\Delta(r) \quad D = diag(\bar{\delta}^r/r!, \ldots, \bar{\delta})$$

$$\Delta(r+j) = \begin{bmatrix} (r+j)^{r+j} - (r+j-1)^{r+j} & \ldots & (j+1)^{r+j} - (j)^{r+j} \\ & \ddots & \\ (r+j)^{j} - (r+j-1)^{j} & \ldots & (j+1)^{j} - (j)^{j} \end{bmatrix}, \quad A_e = \begin{bmatrix} A \\ A^2 \\ \vdots \\ A^{n_p} \end{bmatrix}$$

$$A = \begin{bmatrix} 1 & \delta & \ldots & \delta^{r-1}/(r-1)! \\ & \ddots & & \\ 0 & 0 & \ldots & 1 \end{bmatrix}$$

with $j \geq 0$ and $\Theta(.)$ containing all other terms in $\bar{\delta}^i$, $i > r$ Mattioni et al. (2017a). Let the extended reference over n_p steps be denoted by;

$$Y_{r_e}(k+1) = \begin{pmatrix} Y_r(k+1) & Y_r(k+2) & \ldots & Y_r(k+n_p) \end{pmatrix}^\top$$
$$Y_r(k) = \begin{pmatrix} y_r(k) & \dot{y}_r(k) & \ldots & y_r^{(r-1)}(k) \end{pmatrix}^\top$$

The next result from (Elobaid et al., 2019, Theorem 2) shows that the problem stated in the previous section is always solvable with $n_p = n_c > 1$ under multirate feedback, provided the relative degree is well defined.

Result: unconstrained MPC through multi-rate sampling

Given a continuous-time nonlinear SISO control affine system that possesses a relative degree $r \leq n$, and let (4.7a),(4.7b) be its multi-rate sampled-data equivalent model of order r. Consider the sampled-data optimal cheap control problem with internal stability and cost functional (4.6) and let $e(k) = \|Y(k) - Y_r(k)\|^2$. Then the sampled-data optimal cheap control problem (4.2) is solvable for all $n_p = n_c \geq 1$. Moreover, the feedback solving the problem is defined as the unique solution to:

$$K(x, u_e)Q_e(B_e(x) + R_e)u_e = B_e(.)(Y_{r_e} - A_eY - \Theta(x, u_e)) \tag{4.9}$$

with $Q_e = I \otimes Q$, $R_e = \epsilon I \otimes R$ and

$$K(x, u_e) = (B_e^\top(x) + \frac{\partial}{\partial u_e}\Theta(x, u_e))$$

Remark 4.1 *the solution obtained in the Theorem above is implicitly defined by the above equality and is a formal series in powers of $\bar{\delta}$. Such a solution cannot be exactly computed in practice although several procedures are available for deducing approximation up to any desired order so to guarantee the required performances (see Monaco and Normand-Cyrot (1997)) for further details).*

Remark 4.2 *as $\epsilon \to 0$, the feedback defined by (4.9) coincides with the deadbeat inverting control that steers the output to the desired y_r in one step; such a feedback comes with an effort that is in general, inversely proportional to δ, thus by suitably setting ϵ, R one can reduce the effort while still guaranteeing off-set free tracking in finite time.*

It is rather straightforward to show that when the system (3.1) is linear (i.e. $f(x) = Fx, g(x) = G$ and $h(x) = Cx$) one recovers the known prediction matrices of the output trajectory of the discrete time equivalent model and the explicit MPC solution as in (Camacho and Alba, 2013, Chapter 2). To see this in detail, one can refer to the paper (Elobaid et al., 2019, Remark 5).

4.3 Optimality of multi-rate control

As discussed in the beginning of this chapter, we will limit our attention to the limit case, i.e. the cheap optimal control problem in which the penalty on the control is vanishingly small. Thus, in this section we attempt to show the interesting fact that a multi-rate sampled-data control deriving the states to a desired point in one step is equivalent to the feedback solving a minimum time cheap optimal control problem at the sampling instants when the system is minimum phase. This observation will highlight the interesting fact that the solution proposed to the MPC problem via multi-rate prediction recovers, at the limit, this multi-rate control.

This aspect can be more readily seen through the special class of systems that admits the so-called chained form, as discussed in the sequel.

Cheap control and steering of systems in chained form

A nonholonomic driftless mechanical system Sastry (1999) with configuration $x \in \mathbb{R}^n$ is a mechanical control affine dynamics of the form

$$\begin{aligned} \dot{x} &= g_1(x)u_1 + g_2(x)u_2 \\ g_1(x) &= \frac{\partial}{\partial x_1} + \sum_{i=2}^{n} g_1^i(x)\frac{\partial}{\partial x_i} \\ g_2(x) &= \sum_{i=2}^{n} g_2^i(x)\frac{\partial}{\partial x_i} \end{aligned}$$

subject to k kinematic constraints of the form

$$\alpha_i(x)\dot{x} = 0, \quad i = 1, \ldots, k \tag{4.10}$$

where $\alpha_i(\cdot)$ are smooth and linearly independent, and such that any point in the configuration space is reachable. Define the distributions;

$$\begin{aligned} \Delta_0(x) &= \text{span}\{g_1,\ g_2,\ ad_{g_1}g_2,\ \ldots,\ ad_{g_1}^{n-2}g_2\} \\ \Delta_1(x) &= \text{span}\{g_2,\ ad_{g_1}g_2,\ \ldots,\ ad_{g_1}^{n-3}g_2\} \end{aligned}$$

and define the function $h(x)$ satisfying $dh(x)\ \Delta_1 = 0$ and $dh(x)\ \text{ad}_{g_1}^{n-2}g_2 \neq 0$. If $\Delta_0(x) = \mathbb{R}^n$ and $\Delta_1(x)$ is involutive, then there exists a coordinates change;

$$\begin{aligned} z &= \phi(x) \\ \phi(x) &= \begin{pmatrix} x_1 & L_{g_1}^{n-2}h(x) & \ldots & L_{g_1}h(x) & h(x) \end{pmatrix}^\top \end{aligned}$$

and feedback;

$$\begin{aligned} \nu_1 &= u_1 \\ \nu_2 &= L_{g_1}^{n-1}h(x)u_1 + L_{g_2}L_{g_1}^{n-2}h(x)u_2 \end{aligned}$$

such that the system takes the so-called single chained form Murray and Sastry (1991);

$$\begin{aligned} \dot{z}_1 &= \nu_1 \\ \dot{z}_2 &= \nu_2 \\ \dot{z}_i &= z_{i-1}\nu_1 \quad i = 3, \ldots, n \end{aligned} \tag{4.11}$$

It is possible to verify that systems of the form (4.11) admit a finitely computable sampled-data

equivalent model, applying (2.6), of the form

$$z_1(k+1) = z_1(k) + \delta\nu_1(k) \tag{4.12a}$$
$$\underline{z}(k+1) = A(\delta,\nu)\underline{z}(k) + b(\delta,\nu_1(k))\nu_2(k) \tag{4.12b}$$

where $\underline{z}(k) = (z_2(k)\ z_3(k)\ \dots\ z_n(k))^\top$, and

$$A(\delta,\nu) = \begin{pmatrix} 1 & 0 & 0 & \dots & 0 \\ \delta\nu_1(k) & 1 & 0 & \dots & 0 \\ \vdots & \ddots & \ddots & & \\ \frac{\delta^{n-2}}{(n-2)!}\nu_1(k) & \frac{\delta^{n-3}}{(n-3)!}\nu_1 & \dots & \delta\nu_1 & 1 \end{pmatrix}, \quad b(\delta,\nu_1) = \begin{pmatrix} \delta \\ \frac{\delta^2}{2!}\nu_1 \\ \vdots \\ \frac{\delta^{n-1}}{(n-1)!}\nu_1 \end{pmatrix} \tag{4.13}$$

Writing the sampled-data equivalent dynamics to a system in chained form in the compact form (4.12a), (4.12b) highlights that not only are they finitely computable, but also is still affine in the second control $\nu_2(k)$. At this point we recall that our cheap optimal control problem asks us to minimize the cost function (4.3) at the sampling instants $t = k\delta$. Let $y = z,\ y_r = z_\star$ in (4.3), then at the sampling instants, the problem asks for a digital control that steers the system (4.11) from an initial configuration $z(t_0)$ to a final configuration z_r.

Being affine in the second control input $\nu_2(k)$, and the fact that $\nu_1(k)$ can be used to steer $z_1(t_0)$ to it's desired configuration in one step of length δ, one can set a multi-rate of order $n-1$ on $\nu_2(k)$. Namely, let $\nu_1(k)$ be constant over the sampling interval of length δ and let $\bar{\delta} = \frac{\delta}{n-1}$. Define

$$\nu_2^i(k) = \nu_2(k),\ t \in [k\delta + (i-1)\bar{\delta}, k\delta + i\bar{\delta}[\quad i = 1,\dots,n-1 \tag{4.14}$$

and denote $\underline{\nu_2}(k) = \begin{pmatrix}\nu_2^1(k) & \nu_2^2(k) & \dots & \nu_2^{n-1}(k)\end{pmatrix}^\top$. With this in mind, it is possible to verify that the multi-rate sampled equivalent model to (4.11) of order $n-1$ on ν_2 takes the form

$$z_1(k+1) = z_1(k) + \delta\nu_1(k) \tag{4.15a}$$
$$\underline{z}(k+1) = A^{n-1}(\bar{\delta},\nu_1(K))\underline{z}(k) + R(\bar{\delta},\nu_1(k))\underline{\nu_2}(k) \tag{4.15b}$$

where

$$R(\bar{\delta},\nu_1) = \begin{pmatrix} b(\bar{\delta},\nu_1) & A(\bar{\delta},\nu_1)b(\bar{\delta},\nu_1) & \dots & A^{n-2}(\bar{\delta},\nu_1)b(\bar{\delta},\nu_1) \end{pmatrix} \tag{4.16}$$

is a full rank matrix. With this discussion, the following statements can be made Di Giamberardino et al. (1996a);

Lemma: zero ideal performance and multi-rate digital steering

Given the chained form (4.11), together with the cheap optimal control cost function (4.3) where the output is the configuration vector $y(t) = z(t)$. Let (4.15a),(4.15b) be the multi-rate equivalent model of order $n-1$ on the second control. Furthermore let $z_{1,r}, \underline{z_r}$ be the first component of z_r and the vector of remaining desired configurations respectively. Then the feedback

$$\nu_1(k) = \frac{z_{1,r}(k) - z_1(k)}{\delta} \tag{4.17a}$$

$$\nu_2(k) = R^{\#}(\bar{\delta}, \nu_1)\big(\underline{z_r}(k) - A^{n-1}(\bar{\delta}, \nu_1)\underline{z}(k)\big) \tag{4.17b}$$

exactly steers the system in one step of length δ from $z(k)$ to $z_r(k)$ and coincides with the solution to the cheap optimal control problem in finite time with zero ideal performance.

Taking into account of the preliminary feedback, steering is achieved under piece-wise continuous control designed on the basis of the multirate sampled model.

Having established the fact that multi-rate sampled feedback, in some cases, is an optimal feedback, and recalling that MPC induces cancellation of the zero dynamics, it is natural to utilize multi-rate sampling whenever designing MPC control laws as done in Section 4.2. In the sequel we utilize the proposed multi-rate MPC to solve steering and tracking problems for finitely descritizable systems. To this end we use the example of systems admitting chained forms. It is also highlighted how, in the limit, the feedback defined by the MPC scheme and the feedback obtained from (4.17a),(4.17b) coincide.

4.4 Application to the control of systems in chained form

For simplicity, the following discussion will consider a chained form in $\mathbb{R}^3$ albeit the arguments extend to the general case.

Suppose one wants the state of the system to converge to a desired trajectory $y_r = (y_{r,1}\ y_{r,2}\ y_{r,3})^\top \in \mathbb{R}^3$. Considering $\nu_2(t) = \nu_2^i(k) = \nu_2(k\delta + (i-1)\bar{\delta})$ for $t \in [k\delta + (i-1)\bar{\delta}, k\delta + i\bar{\delta}[$, $i = 1, 2$, one can write the output prediction $y(k) = z(k)$ over n_p steps as

$$\begin{aligned} z_1(k+n_p) &= z_1(k) + \delta \sum_{i=0}^{n_p-1} \nu_1(k+i) \\ \underline{z}(k+n_p) &= \phi(k+n_p, k)z(k) + \sum_{i=0}^{n_p-1} \phi(k+n_p-1, k+i+1)R(\cdot, \nu_1(k+i))\underline{\nu_2}(k+i) \end{aligned} \tag{4.18}$$

where $\underline{z}(k) = (z_2(k)\ z_3(k))^\top$, $\underline{\nu_2}(k) = (\nu_2^1(k\ \nu_2^2(k))^\top$ and

$$\phi(k+n_p, k) = \prod_{i=0}^{n_p-1} A_m(\bar{\delta}, \nu_1(k+n_p-i-1)) \tag{4.19}$$

with $A_m(\cdot) = A^2(\bar{\delta}, \nu_1)$ and

$$A(\bar{\delta}, \nu) = \begin{pmatrix} 1 & 0 \\ \bar{\delta}\nu_1(k) & 1 \end{pmatrix}, \quad b(\bar{\delta}, \nu_1) = \begin{pmatrix} \bar{\delta} \\ \frac{\bar{\delta}^2}{2!}\nu_1(k) \end{pmatrix}, \quad R(\bar{\delta}, \nu_1) = \begin{pmatrix} A(\bar{\delta}, \nu_1)b(\bar{\delta}, \nu_1) & b(\bar{\delta}, \nu_1) \end{pmatrix} \tag{4.20}$$

Over this prediction, and proceeding in a similar fashion to the previous section, using the cost index (4.6) we have the following result corresponding to (Elobaid et al., 2019, Theorem 8)

Result: stable inversion in chained forms via multi-rate and MPC

Consider a nonholonomic system admitting a chained form and let the associated multirate equivalent model be of the form (4.15a),(4.15b). Then, the multirate plant-inverting feedback (4.17a),(4.17b) solves the MPC problem associated with (4.6) under the multi-rate sampled-data model as a prediction model with perfect steering and zero ideal performance, whenever $n_p = n_c$, $Q = I, \epsilon = 0$ *for any* $n_p \geq 1$.

The proof of the above result is omitted and the interested reader is referred to (Elobaid et al., 2019, Section 4) for the corresponding formal statements and related proofs. However, through the following example of a differential drive we will highlight two aspects;

- The correspondence between multi-rate deadbeat control and multi-rate prediction in MPC.
- How using multi-rate prediction in MPC problems not only simplifies the problem (by discarding the terminal ingredients) but preserves boundedness of the closed loop at the limit. This is in contrast with the standard implementation of MPC without terminal ingredients.

The differential drive example

Given a unicycle kinematics;

$$\begin{aligned} \dot{x} &= v\cos\theta \\ \dot{y} &= v\sin\theta \\ \dot{\theta} &= \omega \end{aligned} \tag{4.21}$$

and following Section 4.3, first we convert the system to the standard nonholonomic form by defining the scaling $u_1 = \cos\theta v$, $u_2 = \omega$ so getting;

$$\begin{aligned} \dot{x} &= u_1 \\ \dot{y} &= \tan\theta u_1 \\ \dot{\theta} &= u_2 \end{aligned}$$

It is then possible to define a coordinates change;

$$\begin{aligned} z_1 &= x \\ z_2 &= \tan\theta \\ z_3 &= y \end{aligned}$$

and feedback

$$u_1 = \nu_1$$
$$u_2 = \frac{\nu_2}{\cos^2\theta}$$

putting the system in the chained form;

$$\dot{z}_1 = \nu_1$$
$$\dot{z}_2 = \nu_2$$
$$\dot{z}_3 = z_2\nu_1$$

This system, applying the identities (4.15a), (4.15b) admits the following multi-rate equivalent model;

$$z_1(k+1) = z_1(k) + \delta\nu_1(k)$$
$$\underline{z}(k+1) = A^2(\bar{\delta}, \nu_1(K))\underline{z}(k) + R(\bar{\delta}, \nu_1(k))\underline{\nu_2}(k)$$

with $\underline{z} = (z_2 \;\; z_3)^\top$ and

$$A^2(\bar{\delta}, \nu_1(k)) = \begin{pmatrix} 1 & 0 \\ 2\bar{\delta}\nu_1(k) & 1 \end{pmatrix}, \quad R(\bar{\delta}, \nu_1) = \begin{pmatrix} \bar{\delta} & \bar{\delta} \\ \frac{3\bar{\delta}^2}{2}\nu_1(k) & \frac{\bar{\delta}^2}{2}\nu_1(k) \end{pmatrix}$$

Simulations are performed to first to establish how, in the limit, the proposed control scheme (hereinafter denoted MPC-MR) reduces to to the classical multi-rate deadbeat control (Figs 4.4). More interestingly, we compare the use of multi-rate models for prediction in MPC against the standard MPC implementation that uses a single-rate sampled model for prediction (Figs 4.5,4.6) respectively. In all the cases the sampling period is set to $\delta = 1$.

Two cases of simulations have been carried out. In the first case, the overall simulations scheme is depicted in the figure below, where the feedback controlling the plant is a piecewise continuous feedback resulting from the digital MPC feedback under the feedback transformation bringing the system to a finitely descritizable one (the chained form). Notice how the sampling and hold rates are asynchronous.

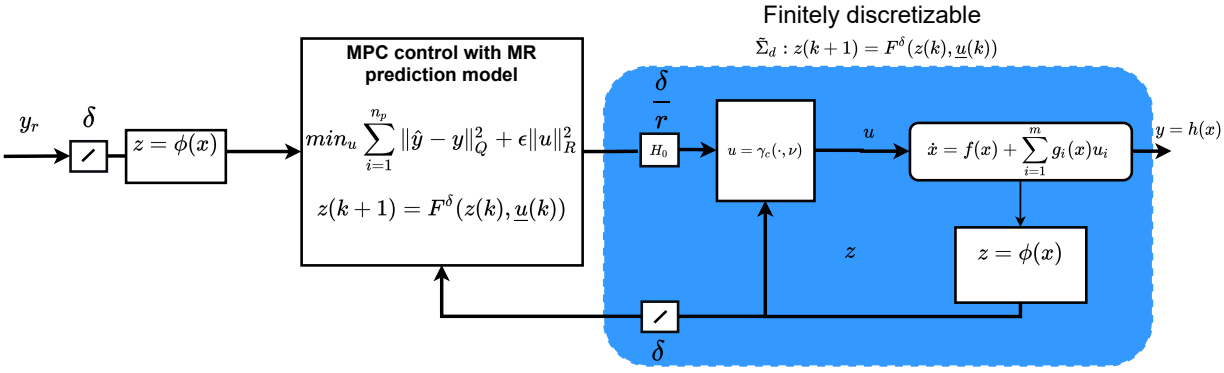

Figure 4.2: The simulation scheme for a finitely descritizable chained form in the first test scenario

In the second scenario, the feedback transformation putting the system into the finitely descritizable form is removed. Nevertheless, in the MPC controller we use the multi-rate sampled model of the finitely desctizable dynamics in chained form. In this sense, we are relying on the inherent robutsness, discussed more formally in the next chapter, of the MPC controller to handle the unmodeled dynamics. Additionally, this results in a purely piecewise constant feedback that is more suitable for digital implementation.

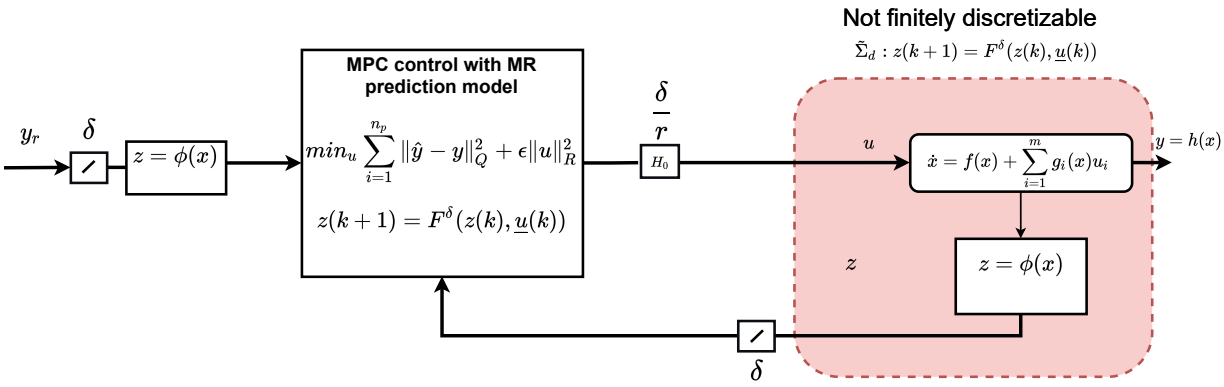

Figure 4.3: The simulation scheme for a finitely descritizable chained form in the second test scenario

As done in the original attached manuscript (Elobaid et al., 2019, Figure 1), which is not repeated here, we can see the pathology motivating this work; the MPC may fail when $n_p = n_c$ and no stability constraints are incorporated, when considering the cheap control specifications at the limit. However, in Figure 4.4 under the same conditions, we show that the multi-rate MPC reduces exactly the multi-rate steering deadbeat control at the limit thus emphasizing the motivation for utilizing multi-rate sampled prediction models.

In this situation depicted in Figure 4.4, we are starting from an initial pose of $(0 \quad 0 \quad 0)^\top$ to a desired pose of $(1 \quad 1 \quad 0)^\top$. The prediction horizon is set to $n_p = n_c = 4$ in the proposed MPC-MR depicted on the left column, as compared to the multi-rate deadbeat control depicted on the right column. In the upper plot, we show the movement of the differential drive from it's initial pose to the desired pose on the plane. On the middle plots we show the trajectories of the states, namely the $x-$displacement depicted in blue, the $y-$displacement depicted in red and the angle θ depicted in green. The bottom figure depicts the linear velocity v in red and the angular velocity ω in blue. The proposed MPC-MR is always depicted using solid lines while the other control scheme being compared to is depicted with dashed lines.

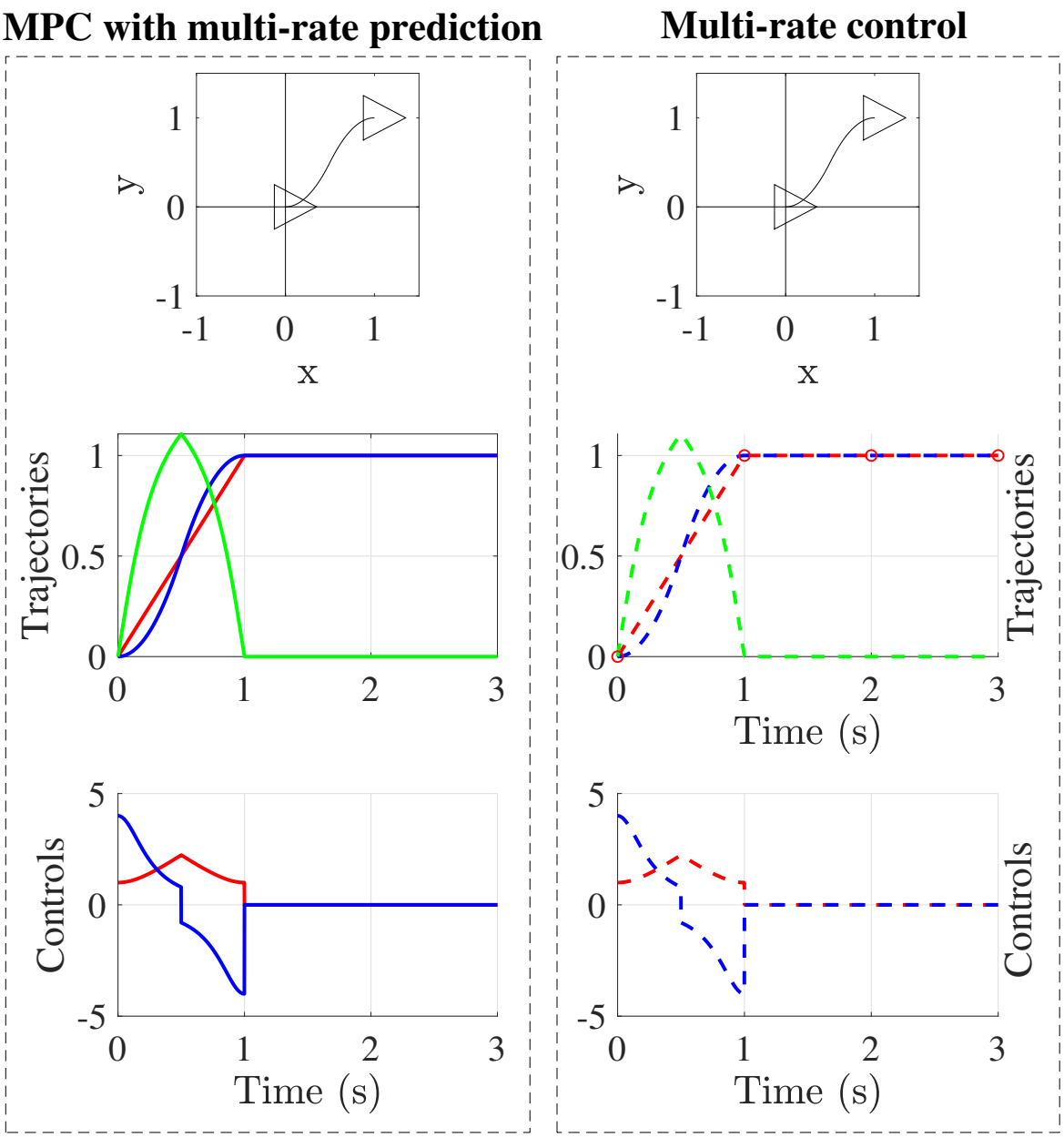

Figure 4.4: MPC-MR vs multi-rate steering with $\epsilon = 0, Q = I$.

In the second case, depicted in Figure 4.5, we simulate the situation where the differential drive is required to track a line with slope 0.5. The standard MPC works with $n_p = 4 > n_c = 2$ as well as a penalty on the control $\epsilon = 0.2,\ R = \mathrm{I}$. This is done to avoid the cheap control limit that is shown to result in instability. The same parameters are also set for the proposed MR MPC. It is clear that better performances, both in terms of tracking error, and control effort are achieved thanks to the proposed MPC-MR even when not working in the cheap control limit.

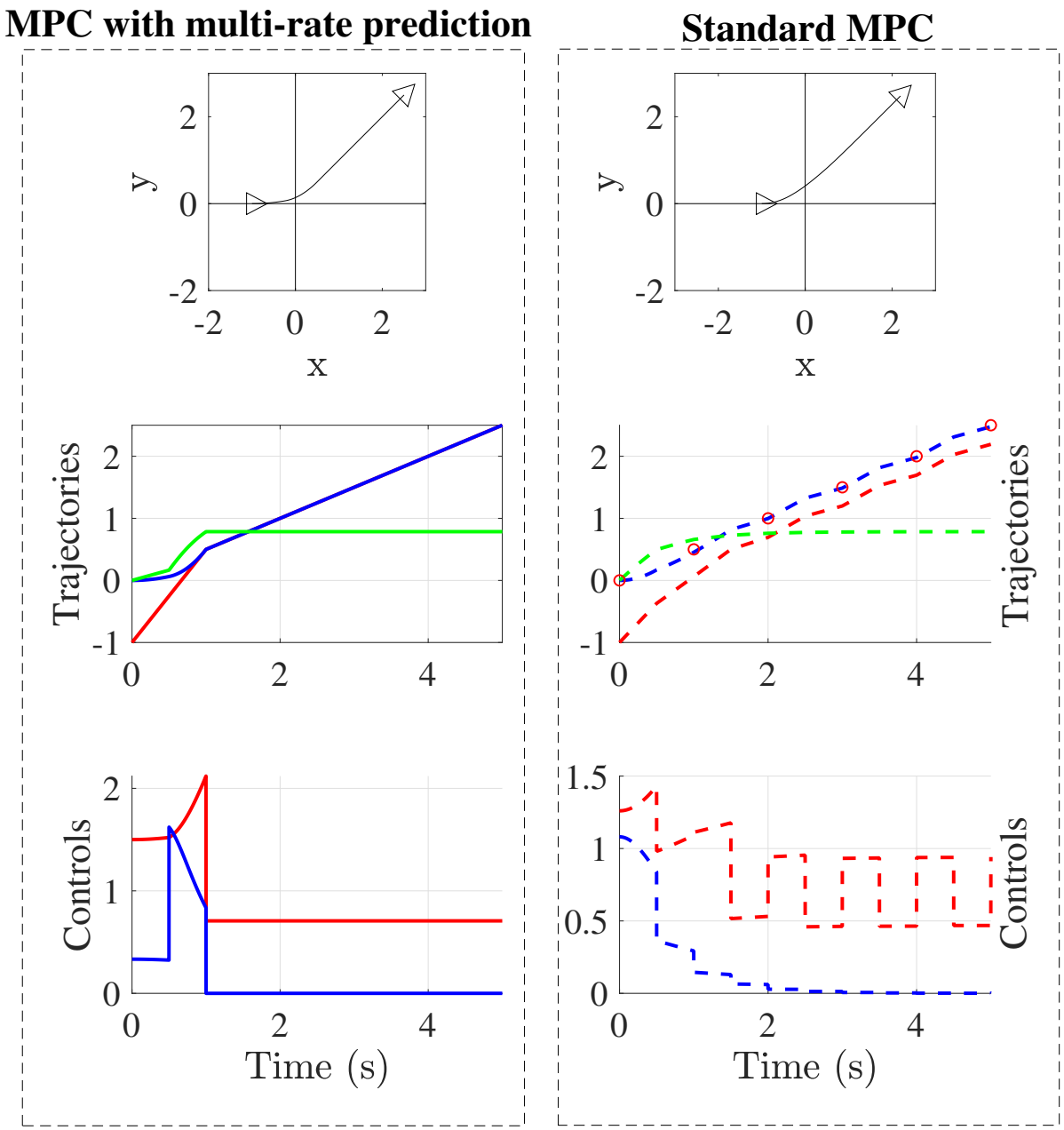

Figure 4.5: MPC-MR vs Standard MPC tracking scenario 1 $\epsilon = 0.2,\ R = I,\ Q = 2I$.

A more interesting comparison is shown in Figure 4.6 where the input transformation putting the system in chained form is unmodelled as suggested in Figure (4.3). We require both controllers, working away from the cheap control limit with $\epsilon = 0.2,\ R = \mathrm{I},\ Q = 3\mathrm{I}$ to perform the same steering action as in the first simulation. Because of nominal robustness, both MPC based schemes are able to handle the unmodelled dynamics, however, it is again clear that the proposed MPC-MR scheme outperforms standard MPC both in terms of tracking and control effort.

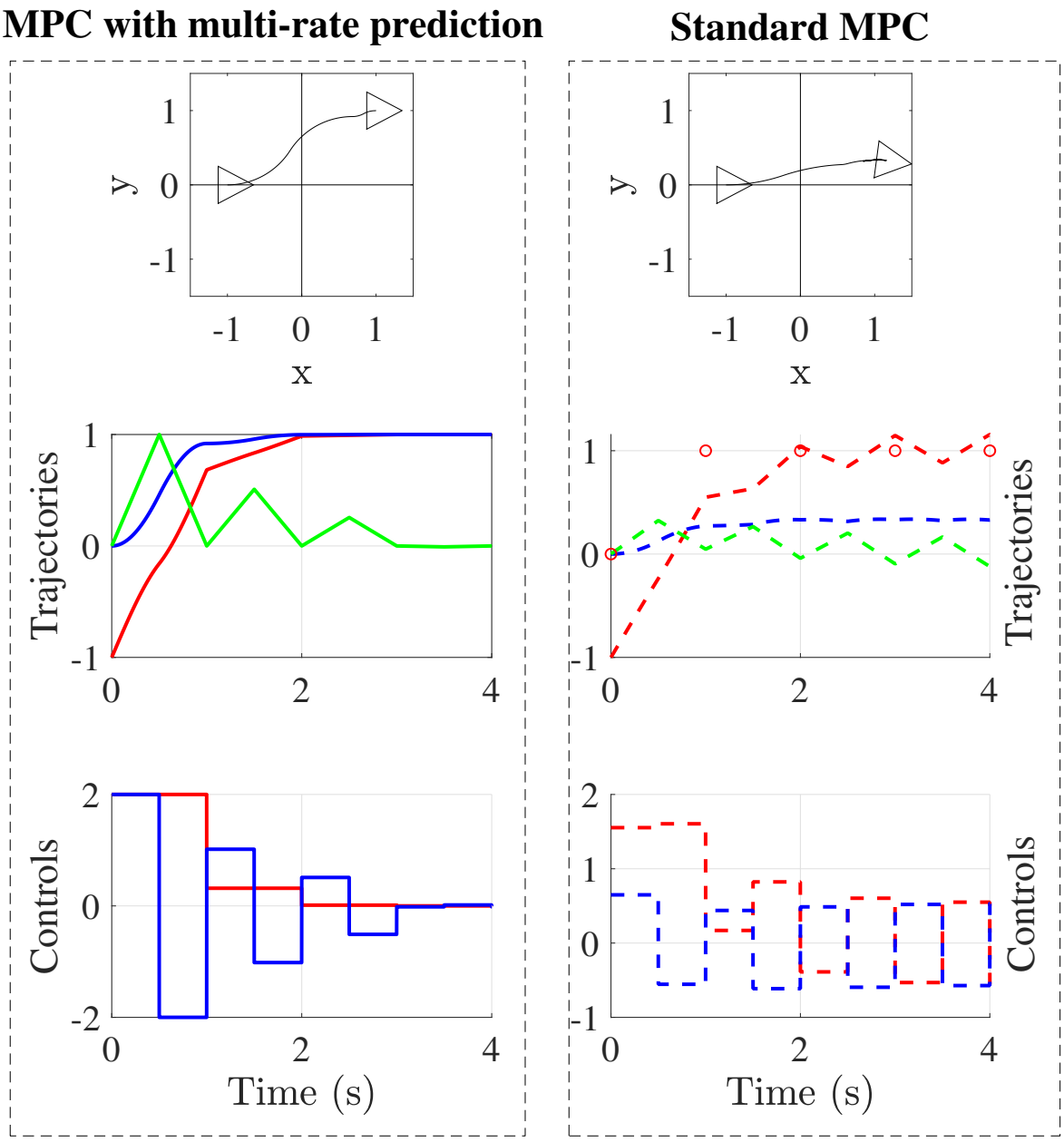

Figure 4.6: MPC-MR vs Standard MPC steering scenario 2 $\epsilon = 0.2,\ R = I,\ Q = 3I$.

4.5 Concluding remarks

A few comments to summarize this chapter are in order;

- Unconstrained (nonlinear) tracking MPC problem in the cheap optimal control formulation under sampling reduces to cancellation of the internal dynamics when $n_p = n_c$.
- Systems that are non-minimum phase represents an obstruction to achieving zero ideal performance when solving this problem. This is further complicated by the unstable zero dynamics induced by the sampling process Qiu and Davison (1993).

- To mitigate those issues, terminal ingredients are typically used in the literature to provide stability guarantees of the closed loop system with no guarantee of zero ideal performance.
- A preliminary workaround is proposed utilizing multi-rate sampled-data models for prediction in the MPC problem. This not only allows for zero ideal performance when $\epsilon, R \to 0$, but also simplifies the optimization problem by removing the need for terminal ingredients when the system is minimum phase and $n_p = n_c$.

While the solution proposed in this chapter is attractive, it has some disadvantages, namely;

- The proposed scheme necessities the use of asynchronous sampling and actuation devices in the control loop with different frequencies.
- The feedback is computed only at the big sampling intervals and work in open loop during the smaller sub-intervals.
- All the obtained results hold only at the limit when treating unconstrained MPC problems with cheap control.
- While MPC by itself is inherently robust, the obtained results lack in terms of bounds on the possible handled additive perturbations and unmodelled dynamics.

With these observation we ask if multi-rate sampling can be combined with MPC in a better way to handle stable inversion at the limit. In the following chapter, one possible improvement is proposed and validated through case studies.

On unconstrained MPC through multirate sampling ⋆

Mohamed Elobaid [*,**] **Mattia Mattioni** [*] **Salvatore Monaco** [*]
Dorothée Normand-Cyrot [**]

[*] *Dipartimento di Ingegneria Informatica, Automatica e Gestionale* A. Ruberti *(La Sapienza University of Rome); Via Ariosto 25, 00185 Rome, Italy (e-mail: {mohamed.elobaid,mattia.mattioni,salvatore.monaco}@uniroma1.it).*
[**] *Laboratoire de Signaux et Systèmes (L2S, CNRS-CentraleSupelèc); 3, Rue Joliot Curie, 91192, Gif-sur-Yvette, France (e-mail: {elobaid, cyrot}@l2s.centralesupelec.fr).*

Abstract: This paper formally highlights how the multirate sampled data equivalent model can be exploited for prediction in an MPC formulation in order to mitigate the possible instability arising from an MPC design while ensuring prefixed boundedness of the control amplitude. This last aspect is in particular addressed and solved with reference to the class of systems which admit, under feedback, a computable sampled model.

Keywords: Control of Sampled-Data Systems; Model-Predictive; Optimal Control.

1. INTRODUCTION

Model Predictive Control (MPC) has become a widely investigated research area in linear and nonlinear control and their applications (e.g., Boucher and Dumur (1996); Camacho and Alba (2013); Borrelli et al. (2017); Kwon et al. (1982)). Roughly speaking the control action is designed by solving a constrained optimization problem subject to the system dynamics and possibly additional requirements and bounds.
The simplest way to design and implement the resulting control law makes use of a sampled data model of the plant for prediction that is exploited for solving the optimization problem over a finite prediction horizon of length n_p. In this context, one implicitly assumes the dependence of the predicted future values of the output over n_c future controls actions, generally referred to as the control horizon.
Driving the output trajectory to a desired reference at the sampling instants via discrete time model predictive control while preserving stability in closed loop may induce difficulties especially when the plant (and the model used for prediction) is not minimum phase. In that case, the choice of the prediction and control horizons plays a key role. In fact, typically, one sets n_c much smaller than n_p to address this fact as well as minimizing the computations required (Clarke et al. (1987)).
As proven in Monaco and Normand-Cyrot (1988), single-rate (or standard) sampling generally induces unstable and extra zero-dynamics so that minimum-phaseness is lost independently of the continuous-time plant properties; to overcome such a pathology, a multirate sampling procedure has been properly introduced to preserve the continuous-time internal properties. With this in mind, it is proposed and shown in the sequel that the use of a multirate (MR) sampled equivalent model at the prediction and implementation level overcomes the aforementioned problems in an MPC control scheme.
Recalling moreover the peculiar properties of MR sampling when applied to nonholonomic systems (Monaco and Normand-Cyrot (1992)), it is shown that a MR based MPC control scheme can be fruitfully employed to limit the amplitude and increase the robustness of MR solution to the steering problem. This result relies on the fact that MPC restitutes the MR steering solution.
The work is organised as follows. In Section 2 recalls on single and multi-rate sampling are given and the problem under investigation is stated. Section 3 is devoted to the proposed MR-MPC control scheme and prove its effectiveness. Section 4 investigates the relation between MPC and MR controllers in the sampled data context with reference to the steering control of nonholonomic dynamics; the example of the unicycle dynamics is used to verify the effectiveness of the proposed control scheme. Concluding remarks end the paper.

2. RECALLS AND STATEMENT OF THE PROBLEM

2.1 Notation and definitions

All functions and vector fields defining the dynamics are assumed smooth and complete over the respective definition spaces. M_U (resp. M_U^I) denotes the space of measurable and locally bounded functions $u : \mathbb{R} \to U$ ($u : I \to U$, $I \subset \mathbb{R}$) with $U \subseteq \mathbb{R}$. $\mathcal{U}_\delta \subseteq M_U$ denotes the set of piecewise constant functions over time intervals of fixed length $\delta \in]0, T^*[$; i.e. $\mathcal{U}_\delta = \{u \in M_U \text{ s.t. } u(t) = u_k, \forall t \in [k\delta, (k+1)\delta[; k \geq 0\}$. When $u(t) \in \mathbb{R}^m$ then $u_k^j, (u_k)^j, u_k^{(j)}$ are the jth component of u for $t \in [k\delta, (k+1)\delta[; k \geq 0\}$, u_k raised to the power j and the jth derivative respectively. Given a vector field f, L_f denotes the Lie

⋆ Partially funded by *Université Franco-Italienne/Università Italo-Francese* (UFI/UIF) through the Vinci Program.

derivative operator, $\mathrm{L}_f = \sum_{i=1}^{n} f_i(\cdot)\nabla_{x_i}$ with $\nabla_{x_i} := \frac{\partial}{\partial x_i}$ while $\nabla = (\nabla_{x_1}, \ldots, \nabla_{x_n})$. The Lie exponential operator is denoted as e^{L_f} and defined as $e^{\mathrm{L}_f} := \mathrm{I} + \sum_{i\geq 1} \frac{\mathrm{L}_f^i}{i!}$. A function $R(x,\delta) = O(\delta^p)$ is said to be of order δ^p ($p \geq 1$) if whenever it is defined can be written as $R(x,\delta) = \delta^{p-1}\tilde{R}(x,\delta)$ and there exist function $\theta \in \mathcal{K}_\infty$ and $\delta^* > 0$ such that $\forall \delta \leq \delta^*$, $|\tilde{R}(x,\delta)| \leq \theta(\delta^*)$.

2.2 Sampled data systems and multirate sampling

The following recalls on sampled-data systems are given (see Monaco and Normand-Cyrot (2001) and the references therein). Given a SISO system

$$\dot{x} = f(x) + g(x)u, \quad y = h(x) \tag{1}$$

and considering $u(t) \in \mathcal{U}_\delta$ and $y(t) = y(k\delta)$ for $t \in [k\delta, (k+1)\delta[$ (δ the sampling period), the dynamics of (1) at the sampling instants is described by the single-rate sampled-data equivalent model

$$x_{k+1} = F^\delta(x_k, u_k), \quad y_k = h(x_k) \tag{2}$$

with $x_k := x(k\delta)$, $y_k := y(k\delta)$, $u_k := u(k\delta)$. The mapping $F^\delta(\cdot, u) : \mathbb{R}^n \times \mathbb{R} \to \mathbb{R}^n$ gets the form of formal series expansion in powers of δ that is (dropping the time subscript for clarity)

$$F^\delta(x,u) = e^{\delta(\mathrm{L}_f + u\mathrm{L}_g)}x = x + \sum_{i>0} \frac{\delta^i}{i!}(\mathrm{L}_f + u\mathrm{L}_g)^i x. \tag{3}$$

It is a matter of computations to verify that if (1) has well defined relative degree $r \leq n$, the relative degree of the sampled-data equivalent (2) always falls to $r_d = 1$; namely, one has

$$y_{k+1} = \sum_{i=0}^{r} \frac{\delta^i}{i!}\mathrm{L}_f^i h(x)\big|_{x_k} + \frac{\delta^r}{r!}u_k \mathrm{L}_g \mathrm{L}_f^r h(x)\big|_{x_k} + O(\delta^{r+1})$$

so that $\nabla_{u_k} y_{k+1} = \frac{\delta^r}{r!}\mathrm{L}_g\mathrm{L}_f^r h(x)\big|_{x_k} + O(\delta^{r+1}) \neq 0$. As a consequence, whenever $r > 1$, the sampling process induces a further zero-dynamics of dimension $r-1$ (the so-called *sampling zero-dynamics*) that is in general unstable for small values of δ when $r > 1$. As a consequence, dynamics-inverting controllers via single-rate sampling do not guarantee internal stability.

Multirate sampling has been developed in a nonlinear context to overcome those issues. Namely, by setting $u(t) = u_k^i$ for $t \in [(k+i-1)\bar{\delta}, (k+i)\bar{\delta}[$ for $i = 1, \ldots, r$ and $y(t) = y_k$ for $t \in [k\delta, (k+1)\delta[$, the multirate equivalent model of order r of (1) gets the form

$$x_{k+1} = F_m^{\bar{\delta}}(x_k, \underline{u}_k), \quad Y_k = H(x_k) \tag{4}$$

with $\bar{\delta} = \frac{\delta}{r}$, $\underline{u} \in \mathbb{R}^r = \begin{pmatrix} u^1 & \ldots & u^r \end{pmatrix}^\top$, a dummy output vector $H(x) = \begin{pmatrix} h(x) & \mathrm{L}_f h(x) & \ldots & \mathrm{L}_f^{r-1}h(x) \end{pmatrix}^\top$ and

$$F_m^{\bar{\delta}}(x_k, \underline{u}_k) = e^{\bar{\delta}(\mathrm{L}_f + u_k^1 \mathrm{L}_g)} \ldots e^{\bar{\delta}(\mathrm{L}_f + u_k^r \mathrm{L}_g)}x\big|_{x_k} = F_m^{\bar{\delta}}(\cdot, u_k^r) \circ \cdots \circ F^{\bar{\delta}}(x_k, u_k^1).$$

One gets so far a MIMO system possessing vector relative degree $r^\delta = (1, \ldots, 1)$ and zero dynamics which inherits the zero-dynamics stability properties of (1).

It must be recalled that exact computation of the sampled data equivalent model cannot in general be achieved, so that approximated models are usually computed by truncation in different ways of the expansion (3). Related to the properties of (3), the notion of exact and finite computability of the sampled data model, possibly under preliminary feedback, has also been introduced in Monaco and Normand-Cyrot (1992).

2.3 Multirate digital steering of chained forms

Multirate sampling has been shown to be of interest in the digital design of nonholonomic and under actuated mechanical systems (see Monaco and Normand-Cyrot (1992)). Under preliminary continuous-time feedback, a nonholonomic mechanical system admits the so-called single chained dynamics

$$\dot{\xi}_1 = u_1, \quad \dot{\xi}_2 = u_2, \quad \dot{\xi}_i = \xi_{i-1}u_1 \quad i = 3, \ldots, n \tag{5}$$

admitting a finitely computable sampled dynamics; moreover, the one-step ahead dynamics can be easily inverted with respect to the control input to deduce a multirate feedback ensuring exact deadbeat steering. For, consider (5) and $(\underline{\xi}_0, \underline{\xi}_f)$ then there exists a multirate control of order $(n-1)$ on u_2 and 1 on u_1 (i.e. $\bar{\delta} = \frac{\delta}{n-1}$) such that system (5) is *exactly steered* in one step δ from $\underline{\xi}_0$ to $\underline{\xi}_f$. The feedback ensuring exact steering for (5) can be easily deduced by inverting the multirate sampled data equivalent model of (5) provided by

$$\begin{aligned}
\xi_{1,k+1} &= \xi_{1,k} + \delta u_{1,k}, \quad \xi_{2,k+1} = \xi_{2,k} + \bar{\delta}\sum_i u_{2,k}^i \\
\xi_{3,k+1} &= \xi_{3,k} + \delta u_{1,k}\xi_{2,k} + \eta_1(\bar{\delta}^2, u_{1,k})\underline{u}_{2,k} \\
&\vdots \\
\xi_{n,k+1} &= \xi_{n,k} + G(\delta, \xi_k, u_{1,k}) + \eta_{n-2}(\bar{\delta}^{n-1}, u_{1,k})\underline{u}_{2,k}
\end{aligned} \tag{6}$$

with $\eta_1(\cdot), G(\cdot)$ and $\eta_n(\cdot)$ being

$$\begin{aligned}
\eta_1(u_{1,k}) &= \frac{1}{2!}\begin{bmatrix} c_1^1 u_{1,k} & c_1^2 u_{1,k} & \ldots & c_1^{n-1}u_{1,k} \end{bmatrix} \\
G(\delta, \xi_{i,k}, u_{1,k}) &= \xi_{n,k} + \delta u_{1,k}\xi_{n-1,k} + \frac{\delta^2}{2!}(u_{1,k})^2\xi_{n-2,k} \\
&\quad + \ldots + \frac{\delta^{n-2}}{(n-2)!}(u_{1,k})^{n-2}\xi_{2,k} \\
\eta_{n-2}(u_{1,k}) &= \frac{1}{(n-1)!}\begin{bmatrix} c_{n-2}^1 u_{1,k} & c_{n-2}^2 u_{1,k} & \ldots & c_{n-2}^{n-1}u_{1,k} \end{bmatrix}
\end{aligned}$$

with some suitable constants c_i^j.

For all fixed $\xi_0 = \xi[k\delta], \xi_f = \xi[k\delta + \delta]$, directly solving the above system in the unknowns $(u_{1,k}, \underline{u}_{2,k})$, one gets

$$\begin{aligned}
u_{1,k} &= \frac{1}{\delta}(\xi_{1,k+1}) - \xi_{1,k}) \\
\underline{u}_{2,k} &= \underline{\eta}^{-1}(\underline{\xi}_{k+1} - \underline{G}(\cdot))
\end{aligned} \tag{7}$$

with $\underline{\eta}(\cdot), \underline{G}(\cdot)$ and $\underline{\xi}(\cdot)$ being the compact forms of the corresponding elements in (6). Taking into account the preliminary feedback, steering is achieved under piecewise continuous control designed on the basis of the multirate sampled model. Roughly speaking, the multirate sampling is used as a *trajectory planner*.

A key thing to note on the control solution above is that, while it does steer the system to the desired final state, it is indeed an inverting controller and the control effort might grow unboundedly so making the feedback not implementable in practice. To overcome this issue, we shall improve such a feedback via MPC.

2.4 Problem statement

Consider the continuous-time system (1) under sampling, with relative degree $r \leq n$ being minimum phase . Hereinafter we shall address the problem of driving the output trajectory, to a desired reference $\nu(t)$ at the sampling instants $t = k\delta$, $k \geq 0$ via discrete time MPC (Camacho and Alba (2013)) while preserving stability in closed loop; that is $y_k = \nu_k$, $k \geq k^*$ with $\nu_k = \nu(k\delta)$ by minimizing the cost functional

$$\begin{aligned} J &= \sum_{i=1}^{n_p} \left(\|e_{k+i}\|_Q^2 + \|\underline{u}_{k+i-1}\|_R^2 \right) \\ &= \sum_{i=1}^{n_p} L(x_{k+i}, \nu_{k+i}, \underline{u}_{k+i-1}) \end{aligned} \tag{8}$$

with $Q > 0, R \geq 0$ being appropriate penalizing weights on the tracking error and input magnitude and n_p being the prediction horizon; moreover, e is a suitably defined error map, such that $e_k = 0$ *iff* $y_k = \nu_k$.
MPC induces a constrained optimization problem subject to the dynamics (4) and possibly additional requirements and bounds. To solve this problem several methods are available, the simplest to implement of which is the so called *direct single shooting* (Hicks and Ray (1971)) by plugging (4) into (8) so getting

$$J = \sum_{i=1}^{n_p} L(\cdot, \underline{u}_{k+i-1}) \circ (F_m^{\bar{\delta}}(\cdot, \underline{u}_{k+i-1}) \circ \ldots \circ (F_m^{\bar{\delta}}(x_k, \underline{u}_k)).$$

Hence, an optimal solution $u_e = \left(\underline{u}_k \ \ldots \ \underline{u}_{k+n_c-1}\right)^\top$ is computed by solving $\nabla_{u_e} J = 0$ with n_c being the so-called *control horizon*.
For our purposes it is interesting to note that in its usual implementation MPC makes use of a single-rate sampled data model of the plant of the form (2) for prediction. This induces the loss of the minimum-phaseness, so forcing the designer to set $n_c < n_p$ to recover internal stability (or using terminal penalties and/or constraints sets) while also defining a dynamical controller (in the sense of using feedback on the states and also on the previous controls) to ensure off-set free tracking. In the approach we are proposing, the use of multirate sampled data model will provide a static feedback overcoming both issues.

3. PREDICTIVE MULTIRATE DIGITAL CONTROL OF NONLINEAR SYSTEMS

With reference to the problem statement in the previous section, and the augmented output vector, we set out to state our main result, however to do so one needs the following assumption;

Assumption 1. Measures of ν and its derivatives $\nu^{(i)}$ for $i = 1 \ldots r-1$ are available at all $t = k\delta$, $k \geq 0$.

For the sake of compactness, we shall define the extended output vector dynamics for $n_p = n_c$ future values as

$$Y_{e_{k+1}} = A_e Y_k + B_e(x_k)\underline{u}_{e_k} + \Theta(x_k, \underline{u}_{e_k})$$

with $Y_{e_{k+1}} = \left(Y_{k+1} \ Y_{k+2} \ \ldots \ Y_{k+n_p}\right)^\top$ and $\underline{u}_{e_k} = \left(\underline{u}_k \ \underline{u}_{k+1} \ \cdots \ \underline{u}_{k+n_c-1}\right)^\top$

$$B_e(\cdot) = \mathrm{L}_g \mathrm{L}_f^{r-1} h(\cdot) \begin{bmatrix} B & 0 & \ldots & 0 \\ AB & B & \ldots & 0 \\ \vdots & & & \\ A^{n_p-1}B & A^{n_p-2}B & \ldots & B \end{bmatrix},$$

$$B = D\Delta(r) \quad D = diag(\bar{\delta}^r/r!, \ldots, \bar{\delta})$$

$$\Delta(r+j) = \begin{bmatrix} (r+j)^{r+j} - (r+j-1)^{r+j} & \ldots & (j+1)^{r+j} - (j)^{r+j} \\ & \ddots & \\ (r+j)^j - (r+j-1)^j & \ldots & (j+1)^j - (j)^j \end{bmatrix}$$

$$A = \begin{bmatrix} 1 & \delta & \ldots & \delta^{r-1}/(r-1)! \\ & \ddots & & \\ 0 & 0 & \ldots & 1 \end{bmatrix} \quad A_e = \begin{bmatrix} A \\ A^2 \\ \vdots \\ A^{n_p} \end{bmatrix}$$

with $j \geq 0$ and $\Theta(\cdot)$ containing all higher order terms in $O(\bar{\delta}^{r+1})$. The next result shows that the problem in Section 2.4 is always solvable with $n_p = n_c > 1$ under multirate feedback, provided the relative degree is well defined.

Theorem 2. Let (1) possess relative degree $r \leq n$, and (4) be its multirate equivalent model of order r. Consider the MPC problem with cost functional (8) and $e_k = Y_k - \underline{\nu}_k$ with $\underline{\nu}_k = \left(\nu_k \ \ldots \ \nu_k^{(r-1)}\right)^\top$. Then, there exists $\delta^* > 0$ such that for all $\delta \in [0, \delta^*[$, the MPC problem is solvable with internal stability for all $n_p = n_c \geq 1$. The feedback is defined as the unique solution to the equality

$$\begin{aligned} &(K(x, \underline{u}_e)Q_e B_e(x) + R_e)\underline{u}_e = \\ &B_e(\cdot)(\underline{\nu}_e - A_e Y - \Theta(x, \underline{u}_e)) \end{aligned} \tag{9}$$

with $Q_e = I \otimes Q$, $R_e = I \otimes R$

$$K(x, \underline{u}_e) = (B_e^\top(x) + \nabla_{u_e}\Theta(x, \underline{u}_e))$$

$$\underline{\nu}_{e_k} = \left(\underline{\nu}_{k+1} \ \cdots \ \underline{\nu}_{k+n_p}\right).$$

Sketch of proof. To prove that (9) is optimal, we first rewrite (8) as $J = \|Y_{e_{k+1}} - \nu_{e_k}\|_{Q_e} + \|u_{e_k}\|_{R_e}$ whose jacobian is clearly annihilated by the solution to (9). Existence of a feedback solution can be deduced by rewriting (9) a formal series expansion in powers of δ and applying the *implicit function theorem*. Indeed, the term $(D^{-1}K(x, \underline{u}_e)Q_e B_e(x) + R_e)$ is invertible as $\delta \to 0$ (Monaco and Normand-Cyrot (2001); Mattioni et al. (2017)). Internal stability is ensured by the minimum phaseness of the continuous-time plant which is consequently preserved under multirate sampling (Monaco and Normand-Cyrot (1988)).

Remark 3. The solution obtained in Theorem 2 is implicitly defined by the above equality and is a formal series in powers of $\bar{\delta}$. Such a solution cannot be generally exactly computed in practice although several procedures are available for deducing approximation up to any desired order so to guarantee the required performances (see Monaco and Normand-Cyrot (2001) for further details).

Remark 4. As $R \to 0$, the feedback defined by (9) coincides with the deadbeat inverting control that steers the output to the desired ν in one step of length δ. Such a feedback comes with an effort that is in general, inversely proportional to δ, thus by suitably setting R one can reduce the effort while still guaranteeing off-set free tracking in finite time.

Remark 5. It is rather straightforward to show that when (1) is linear (i.e. $f(x) = Fx, g(x) = G$ and $h(x) =$

Cx) one recovers the known output trajectory prediction of the discrete time model with $A_d = e^{F\delta}, B_d = [\bar{A}^{\bar{\delta}(r-1)}\bar{B}\dots\bar{B}], \bar{A} = e^{F\bar{\delta}}, \bar{B} = \int_0^{\bar{\delta}} e^{Fs}\mathrm{d}sG$ and $C_d = C$; i.e,

$$\underline{Y}_{e_{k+1}} = \begin{bmatrix} C_dA_d \\ C_dA_d^2 \\ \vdots \\ C_dA_d^{n_p} \end{bmatrix} x_k + \begin{bmatrix} C_dB_d & 0 & \dots & 0 \\ C_dA_dB_d & C_dB_d & \dots & 0 \\ \vdots & & & \\ C_dA_d^{n_p-1}B_d & C_dA_d^{n_p-2}B_d & \dots & C_dA_d^{n_p-n_c}B_d \end{bmatrix} \underline{u}_{e_k}$$

which in compact form can be written as $Y_{e_{k+1}} = A_e x_k + B_e u_{e_k}$. Along the lines of Borrelli et al. (2017), the optimal control is $u_e^* = (B_e^\top Q_e B_e + R_e)^{-1}B_e^\top Q_e(\nu_e - A_e x)$. When implementing the above optimal control trajectory a receding horizon algorithm (i.e. selecting the first m components of $u_e[k]$ and discarding the rest and repeating at each sampling instant) one has

$$u_k^\star = (I_m \ 0 \ \dots \ 0)\,(B_e^\top Q_e B_e + R_e)^{-1}B_e^\top Q_e(\nu_e - A_e x).$$

Thus, when $n_p = n_c, Q_e = I$ and $R_e = 0$ the MR-MPC feedback reduces to $u_k^\star = (C_dB_d)^{-1}(\nu - C_dA_dx)$, which is the classical dynamics inverting feedback.

Roughly speaking, with reference to a minimum-phase plant, Theorem 2 suggests the use of MR-MPC control law of order equal to the relative degree. In what follows, we explicitly define this solution for nonholonomic systems that are feedback-equivalent to chained forms (Brockett et al. (1983)). In doing so, we formally show that as $R \to 0$ one recovers the standard deadbeat control. As a byproduct, we also provide an extension of Theorem 2 to the case of MIMO systems for which the relative degree might not be defined.

4. PREDICTIVE MULTIRATE STEERING FOR CHAINED FORMS

For illustrative purposes, the following discussion will consider the chained form (5) with $n = 3$ albeit the arguments extend to the general case as highlighted. For, suppose one wants the state of the system to converge to a desired trajectory $\nu \in \mathbb{R}^n$. Considering $u_2(t) = u_{2,k}^i = u_2(k\delta + (i-1)\bar{\delta})$ for $i = 1, 2$, one can write the output prediction over $n_p = 1$ as

$$\begin{bmatrix} x_{1,k+1} \\ x_{k+1} \end{bmatrix} = \begin{bmatrix} 1 & \mathbf{0} \\ \mathbf{0} & A_m^2(\cdot) \end{bmatrix} \begin{bmatrix} x_{1,k} \\ x_k \end{bmatrix} + \begin{bmatrix} 1 & \mathbf{0} \\ \mathbf{0} & R_m(\cdot) \end{bmatrix} \begin{bmatrix} u_{1,k} \\ \underline{u}_{2,k} \end{bmatrix} \tag{10}$$

with $\underline{u}_2 = (u_2^1 \ u_2^2)^\top$ and

$$A_m(\cdot) = \begin{bmatrix} 1 & 0 \\ \bar{\delta}u_{1,k} & 1 \end{bmatrix}, b = \begin{bmatrix} \bar{\delta} \\ \frac{\bar{\delta}^2}{2!}u_{1,k} \end{bmatrix}, R_m(\cdot) = [A_m(\cdot)b \ b]$$

which compactly rewrites as $Y = F(\delta, u_1)X + G(\delta, u_1, \underline{u}_2)\underline{u}_2$. One can then proceed in a similar fashion to the previous section, using the cost index (8) with $e = \mathrm{col}(e_1, e_2, e_3) = \left(x_1 \ x^\top\right)^\top - \nu$ and setting $\nabla_u J = 0$, so getting (when $Q = I$) that the optimal control $u = u^\star$ is solution to (dropping time subscript for clarity)

$$\begin{aligned} u_1 &= \frac{-2\delta e_1 - e_3(3\bar{\delta}^2u_2^1 + \bar{\delta}^2u_2^2 + 4\bar{\delta}x_2)}{2\delta^2 + (3\bar{\delta}^2u_2^1 + \bar{\delta}^2u_2^2 + 4\bar{\delta}x_2)} \\ u_2^1 &= -\frac{2\bar{\delta}(e_2 + \bar{\delta}u_2^2) - 3\bar{\delta}^2u_1(e_3 + 2\bar{\delta}u_1x_2 - 0.5\bar{\delta}^2u_1u_2^2)}{2\bar{\delta}^2 + 4.5\bar{\delta}^4u_1^2} \\ u_2^2 &= -\frac{2\bar{\delta}(e_2 + \bar{\delta}u_2^1) - \bar{\delta}^2u_1(e_3 - 2\bar{\delta}u_1x_2 - 1.5\bar{\delta}^2u_1u_2^1)}{2\bar{\delta}^2 - 0.5\bar{\delta}^4u_1^2} \end{aligned} \tag{11}$$

with u_2^i $(i = 1, 2)$ being the two controls resulting from multirate of order 2 over u_2 and $\nu_i, i = 1, 2, 3$ being the reference values over the single step prediction horizon. To show that the solution to this system of equations coincides with that of the multirate inverting controller, it is sufficient to show that the multirate inverting solution, is indeed a solution of this system of equations.

Proposition 6. The multirate inverting controller (7) is a solution of the optimal control problem with the cost function (8) and $n_p = n_c = 1, Q = I, R = 0$.

Proof: Starting from (7), one has that

$$\begin{aligned} u_1 &= \frac{\nu_1 - x_1}{\delta}, \quad u_2^1 = -\frac{\nu_2 - x_2}{2\,\bar{\delta}} - \frac{x_3 - \nu_3 + 2\,\bar{\delta}\,u_1\,x_2}{\bar{\delta}^2\,u_1} \\ u_2^2 &= \frac{3\,(\nu_2 - x_2)}{2\,\bar{\delta}} + \frac{x_3 - \nu_3 + 2\,\bar{\delta}\,u_1\,x_2}{\bar{\delta}^2\,u_1} \end{aligned}$$

solves (11). As a matter of fact, (11) admit two solutions for (u_1, u_2^1, u_2^2), one of which corresponds to the solution $u_1 = 0$ which is discarded [1] whereas the other one is $u_1 = \frac{e_1}{\delta}$ and

$$\begin{aligned} u_2^1 &= \frac{-2\,\delta\,e_3 - \bar{\delta}\,\nu_1\,\nu_2 - 3\,\bar{\delta}\,\nu_1\,x_2 + \bar{\delta}\,\nu_2\,x_1 + 3\,\bar{\delta}\,x_1\,x_2}{2\,\bar{\delta}^2\,(\nu_1 - x_1)} \\ u_2^2 &= -\frac{-2\,\delta\,e_3 - 3\,\bar{\delta}\,\nu_1\,\nu_2 - \bar{\delta}\,\nu_1\,x_2 + 3\,\bar{\delta}\,\nu_2\,x_1 + \bar{\delta}\,x_1\,x_2}{2\,\bar{\delta}^2\,(\nu_1 - x_1)} \end{aligned}$$

clearly coinciding with the expression above from (7). ◁

4.1 The case of $n_p = n_c > 1$

We write the prediction model for the two components of the states vector as follows

$$\begin{aligned} x_{1,k+n_p} &= x_{1,k} + \delta \sum_{i=0}^{n_p-1} u_{1,k+i} \\ x_{k+n_p} &= \phi(k+n_p, k)x_k + \\ &\sum_{i=0}^{n_p-1} \phi(k+n_p-1, k+i+1)R(\cdot, u_{1,k+i})u_{2,k+i} \end{aligned} \tag{12}$$

where

$$\phi(k+n_p, k) = \prod_{i=0}^{n_p-1} A(\bar{\delta}, u_{1,k+n_p-i-1}) \tag{13}$$

and $A(\cdot) = A_m^2(\cdot)$.

We can then substitute this expression of prediction in our cost function and take the partial derivatives with respect to each u_i and, then prove that whenever $n_p = n_c$ the multirate inversion control is an optimum control with respect to our cost function. The following statement highlights this fact.

[1] Since, this solution doesn't bring the error on the state x_1 to zero.

Proposition 7. As $R \to 0$, the control minimizing (8) computed over the prediction model (12) reduces to the multirate plant inversion solution (7) if $n_p = n_c$ and $Q = I$.

Proof: The proof follows from induction starting with Proposition 6 which proves $n_p = n_c = 1$. By assuming that the statement holds for some $n_p = N$, we show it holds for $n_p = N + 1$. Let us split the cost functional (8) along the prediction model (12) as follows

$$J = \underbrace{J_1}_{\text{first } N \text{ steps terms}} + \underbrace{J_2}_{\text{last step terms}}$$

$$J_1 = \sum_{j=1}^{N} \Bigg((\nu_{1,k+j} - x_{1,k} - \delta \sum_{i=0}^{j-1} u_{1,k+i})^2 + (r(k+j) - \phi(k+j-1,k)x_k - \sum_{i=0}^{j-1} \phi(k+j-1,k+i) R(\cdot, u_{1,k+i}) u_{2,k+i})^2 \Bigg)$$

$$J_2 = (\nu_{1,k+N+1} - x_{1,k} - \delta \sum_{i=0}^{N} u_{1,k+i})^2 + (r(k+N+1) - \phi(k+N+1,k)x_k - \sum_{i=0}^{N} \phi(k+N+1,k+i) R(\cdot, u_{1,k+i}) u_{2,k+i})^2.$$

Denoting by u^*_{mr} the multirate inverse controller which satisfies by assumption $\nabla_u J_1(u^*_{mr}) = 0$, it remains to prove that that $\nabla_u J_2(u^*_{mr}) = 0$. For, notice that

$$\phi(k+N+1,k) = \begin{bmatrix} 1 & 0 \\ 2\bar{\delta} \sum_{s=0}^{N} u_{1,k+s} & 1 \end{bmatrix}$$

and recalling that u^*_{mr} is of the form (7), the proof proceeds as follows; one gets that as $\nabla_{u_2} J_2 = 0$ (for compactness we omit the time variable k and we write i for $k+i$)

$$-2n\phi(N,i+1)R(\cdot,u_{1,i}) \Bigg(r(N+1) - \phi(N+1,.)x - \sum_{i=0}^{N-1} \phi(N,i+1) R(\cdot, u_1[i]) u_{2,i} \Bigg)^{\top} = 0$$

Inspecting the second equation above, namely $\nabla_{u_2} J_2 = 0$ gives two possibilities, either the term $-2n\phi(N,i+1)R(\cdot,u_{1,i}) = 0$ or the term between the large brackets is 0, which upon inspection is 0 exactly when we set for $i = 1 \dots N-1$

$$\begin{aligned} u_{2,i} &= \Xi(\bar{\delta}, u_1)^{-1} (r(i+1) - \phi(N+1,\cdot)x_k) \\ u_{2,N} &= R(\cdot, u_{1,N})^{-1} (r(N+1) - \phi(N+1,\cdot)x_k) \end{aligned} \tag{14}$$

with $\Xi(\bar{\delta}, u_1)$ collecting the product terms of $\phi(N,i+1)R(\cdot,u_{1,i})$ which coincides with the solution obtained from (7). We then write only $\nabla_{u_{1,N}} J_2$, since by assumption and from the expression above for u_2, $\nabla_{u_{1,i}} J_2 = 0, \nabla_{u_{2,j}} J_2 = 0 \ \forall i = 1 \dots N-1, j = 1 \dots N$ so getting

$$\begin{aligned} &2\,\delta\,(x_{1,N} - \nu_{1,N+1} + \delta\, u_{1,N}) + \\ &\bar{\delta}\,\left(4\, x_{2,N} + 3\,\bar{\delta}\, u^1_{2,N} + \bar{\delta}\, u^2_{2,N}\right) \\ &(x_{3,N} - \nu_{3,N+1} + \frac{3\,\bar{\delta}^2\, u_{1,N}\, u^1_{2,N}}{2} + \frac{\bar{\delta}^2\, u_{1,N}\, u^2_{2,N}}{2} + \\ &\qquad 2\,\bar{\delta}\, u_{1,N}\, x_{2,N}) = 0. \end{aligned}$$

By substituting $u^1_{2,N}, u^2_{2,N}$ as in (14) one recovers

$$u_{1,N} = \frac{\nu_{1,N+1} - x_{1,N}}{\delta}$$

which possesses the same form as in Proposition 6. ◁

It is rather intuitive to see that the discussion above holds for general chained forms, and the statements can be extended along the same lines, albeit the notations and algebraic manipulations will get rather long and cumbersome, the following statement summarizes this.

Theorem 8. Consider the dynamics of the form (5) admitting multirate equivalent model (6). Then, the multirate plant-inverting feedback (7) solves the MPC problem with (8) under prediction model (6) with perfect steering, whenever $n_p = n_c \geq 1, Q = I, R = 0$.

5. SIMULATION RESULTS AND COMMENTS

Simulations are performed to compare the proposed control scheme (MPC-MR) with respect to the standard MPC implementation (Figs 1,2) and the classical MR control (Figs 3,4). In all the cases MPC-MR is implemented with $n_p = n_c, \delta = 1$. Figure 1 clearly emphasises the pathology motivating this work; the MPC may fail when $n_p = n_c$ and no stability constraints are incorporated, even with no penalty on the control. To prevent this, as suggested in the literature, in Fig 2 MPC works with $n_p > n_c$; the comparison with the proposed MPC-MR with $R > 0$ in this case shows the better performance of our solution. A deeper comparison is proposed in Figs 3 and 4 where the proposed MPC-MR and the standard MR solutions are shown for steering and tracking maneuvers under the penalty $R > 0$. The proposed MPC-MR scheme appears to be the *natural* context to be adopted to account for the control amplitude in standard MR.

6. CONCLUSION

We establish an intuitive interpretation of MR inverting controllers, by highlighting the roles of the prediction and control horizons, and their relations to the relative degree. We then motivate the use of MPC with a MR prediction model through penalizing the controls, and obtaining comparable performance to the plant inversion controller, while maintaining low control effort. Future works concern the application of this improved MPC scheme to several case studies as in power systems or automotive control Giuseppi et al. (2018); Gionfra et al. (2016). Ongoing work is addressing the extension to other classes of systems, possibly non-minimum phase Mattioni et al. (2019).

REFERENCES

Borrelli, F., Bemporad, A., and Morari, M. (2017). *Predictive control for linear and hybrid systems.* Cambridge University Press.

Boucher, P. and Dumur, D. (1996). *La commande prédictive*, volume 8. Editions Technip.

Brockett, R.W., Millman, R.S., and Sussmann, H.J. (1983). *Differential geometric control theory: proceedings of the conference held at Michigan Technological University, June 28-July 2, 1982*, volume 27. Birkhauser.

Camacho, E.F. and Alba, C.B. (2013). *Model predictive control.* Springer Science & Business Media.

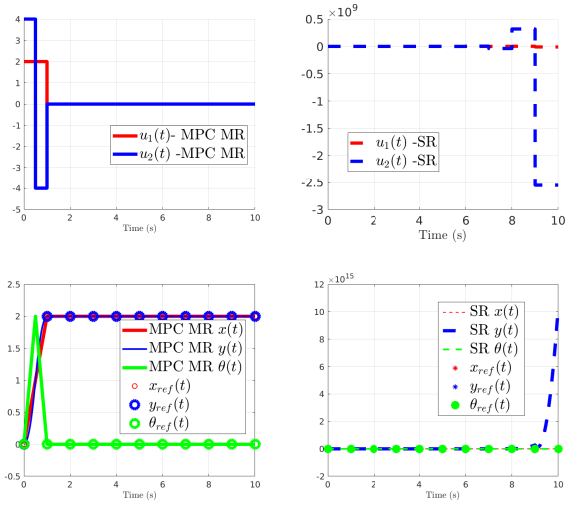

Fig. 1. MPC-MR vs MPC SR steering with $R = 0, Q = I$.

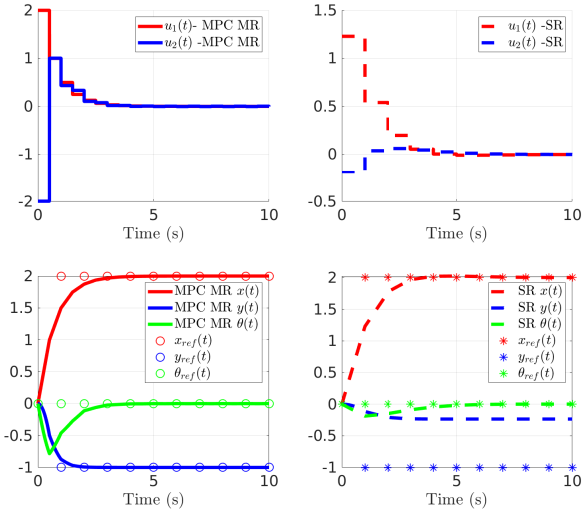

Fig. 2. MPC-MR vs MR steering with $R = 0.2I, Q = 2I$.

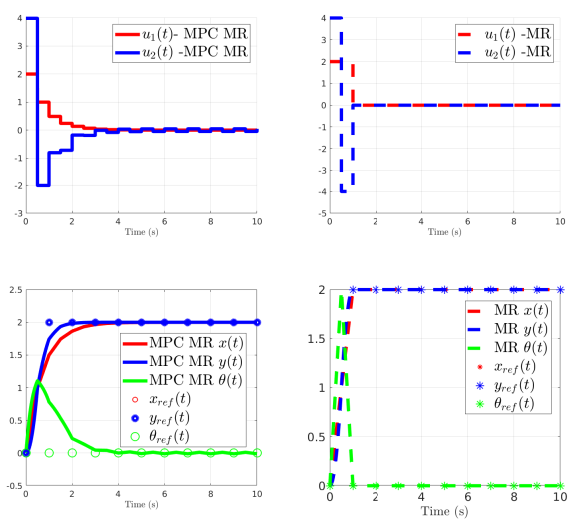

Fig. 3. MPC-MR vs MR steering with $R = 0.2I, Q = 10I$

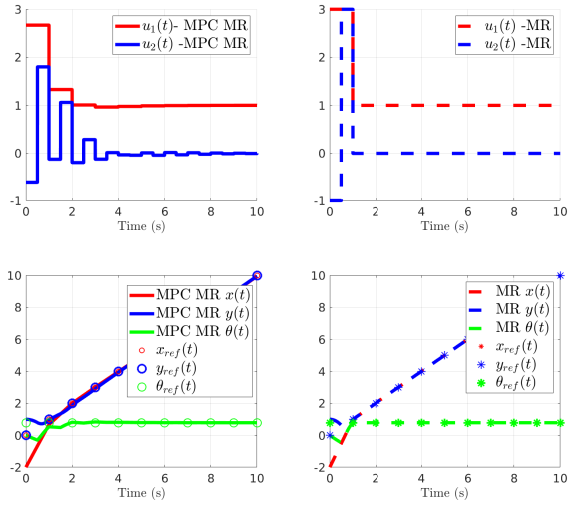

Fig. 4. MR-MPC Vs MR tracking with $R = 0.5I, Q = 2I, \theta_d = \frac{\pi}{4}, x_0 = (-2 \ -1 \ 0)^\top$.

Clarke, D.W., Mohtadi, C., and Tuffs, P. (1987). Generalized predictive control—part i. the basic algorithm. *Automatica*, 23(2), 137–148.

Gionfra, N., Siguerdidjane, H., Sandou, G., Faille, D., and Loevenbruck, P. (2016). Combined feedback linearization and mpc for wind turbine power tracking. In *Control Applications (CCA), 2016 IEEE Conference on*, 52–57. IEEE.

Giuseppi, A., Germana, R., and Di Giorgio, A. (2018). Risk adverse virtual power plant control in unsecure power systems. In *2018 26th Mediterranean Conference on Control and Automation (MED)*, 1–9. IEEE.

Hicks, G. and Ray, W. (1971). Approximation methods for optimal control synthesis. *The Canadian Journal of Chemical Engineering*, 49(4), 522–528.

Kwon, W.H., Bruckstein, A.M., and Kailath, T. (1982). Stabilizing state-feedback design via the moving horizon method. In *1982 21st IEEE Conference on Decision and Control*, 234–239. doi:10.1109/CDC.1982.268433.

Mattioni, M., Hassan, M., Monaco, S., and Normand-Cyrot, D. (2019). On partially minimum-phase systems and disturbance decoupling with stability. *Nonlinear Dynamics*, 1–16.

Mattioni, M., Monaco, S., and Normand-Cyrot, D. (2017). Immersion and invariance stabilization of strict-feedback dynamics under sampling. *Automatica*, 76, 78 – 86.

Monaco, S. and Normand-Cyrot, D. (1988). Zero dynamics of sampled nonlinear systems. *Systems & Control Letters*, 11(3), 229 – 234.

Monaco, S. and Normand-Cyrot, D. (1992). An introduction to motion planning under multirate digital control. In *Decision and Control, 1992., Proceedings of the 31st IEEE Conference on*, 1780–1785. IEEE.

Monaco, S. and Normand-Cyrot, D. (2001). Issues on nonlinear digital control. *European Journal of Control*, 7(2-3), 160–177.

Chapter 5

Stable partial inversion in model predictive control via multi-rate planning

Contents

In this chapter a different solution approach to the one detailed in Chapter 4 is proposed. It is shown that a sampled-data planned trajectory computed making use of a multi-rate sampled-data model provides references for the MPC which overcomes stability issues linked to the loss of the minimum phase property under sampling.

The difference with respect to the solution previously proposed stands in the fact that now multi-rate is employed to plan the reference trajectory so that to circumvent the problems of unstable zero dynamics at the planning level. As a consequence, one also relaxes the demand on asynchronous actuation and sampling frequencies. Indeed, existing control loops employing MPC with synchronous sampling and actuation frequencies are left intact and the designer only works on the trajectory planner.

The striking aspect which highlights the benefit of the proposed solution is the fact that when setting the prediction horizon very large compared to the control horizon, as done typically to overcome stability issues, no significant benefits are obtained when using the proposed control scheme.

As specified in the sequel, in the proposed control scheme, MPC is used to robustify multi-rate design and mutli-rate planning is used to imporve MPC. Some examples and applications will be developed to compare the performances in the two proposed approaches and to highlight these aspects. This chapter is written to serve as a companion to the results formalized in;

> Mohamed Elobaid, Mattia Mattioni, Salvatore Monaco and Dorothée Normand-Cyrot. *"Sampled-data tracking through MPC and multirate planning". 21st IFAC World Congress 2020, 53(2), 3620-3625. DOI: 10.1016/j.ifacol.2020.12.2043.*

The notions appearing hereinafter are recalled from Elobaid et al. (2020b), Camacho and Alba (2013), Grüne et al. (2008), Allgöwer and Zheng (2012), Allgöwer and Zheng (2012), Isidori (1995) and the references therein.

Again as done in the previous chapter, we motivate our discussion in the sequel by the simple example of the triple integrator.

Example 5.1 Given a tracking MPC problem over the triple integrator;

$$V = \min_{u(k)} \sum_{i=1}^{n_p} \left(\|y(k+i) - y_r(k+i])\|_Q^2 + \|u(k+i-1])\|_R^2 \right)$$
$$\text{s.t } x(k+i) = A_d x(k+i-1) + B_d u(k+i-1), \quad y(k+i) = C_d x(k+i)$$

with A_d, B_d, C_d as in Section 4.1. As we have seen, using the explicit solution to MPC computed from the sampled-data equivalent model, an unstable closed loop is obtained. The multi-rate sampled equivalent model of the triple integrator of order $m = r = 3$;

$$x(k+1) = A_m x(k) + B_m \underline{u}(k)$$

with $A_m, B_m, \underline{u}$ as in Section 2.4. As we discussed in Chapter 2, this multi-rate sampled model has no zeros with respect to the output

$$y_e = H(x) = x$$

and with respect to which there exists an inversion feedback

$$\underline{u}(k) = B_m^{-1}(y_{r_e}(k) - A_m x(k))$$

with $y_{r_e} = (y_r \ \dot{y}_r \ \ddot{y}_r)^\top$ maintaining stability while rendering the $y(k)$—$y_r(k)$ link almost unity. Let $\hat{y}_e(k)$ be the evolution of the output of the multi-rate model under the above feedback. This output is *admissible* in the sense that it defines the evolution, over sub-intervals of the sampling period, of the states to reach the reference while maintaining stability under the multi-rate inversion feedback. Let us now replace the reference in the tracking MPC problem with $\hat{y}_e(k)$, i.e

$$\hat{V} = \min_{u} \sum_{i=1}^{n_p} \left(\|y(k+i) - \hat{y_e}(k+i])\|_Q^2 + \|u(k+i-1])\|_R^2 \right)$$
$$\text{s.t } x(k+i) = A_d x(k+i-1) + B_d u(k+i-1), \quad y(k+i) = C_d x(k+i)$$

As discussed, in the cheap control limit when $R \to 0$, we know apriori that a solution to the above problem is (almost) the control $\underline{u}(k)$. Using the Matlab© MPC solver, and setting $Q = \mathrm{I}$, $R = 0.1$, $\delta = 1$ we get the closed loop evolution depicted in Figure 5.1.

This simple example suggests that, given a standard tracking MPC problem over a non-minimum phase system, one can avoid exciting the unstable sampling zero dynamics through modifying the reference. A multi-rate sampled equivalent model, for which there exists inversion feedback rendering the output-reference link almost unity can be used to plan reference trajectories over the sampling instants. Those planned references allows for obtaining a solution, which at the limit (almost) replicates the multi-rate deadbeat feedback. "Can we say something more" is the question

discussed in this chapter.

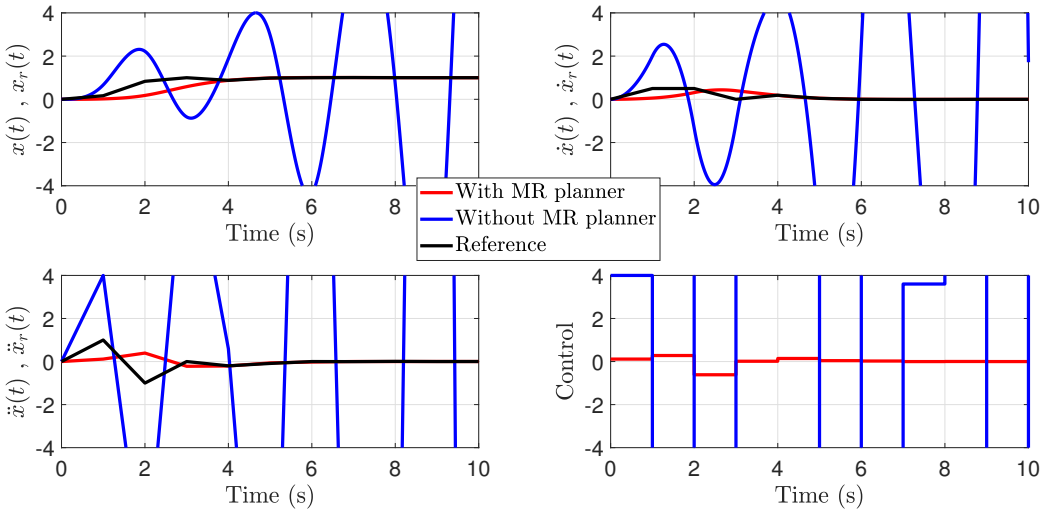

Figure 5.1: Modified MPC problem VS standard MPC problem for the triple integrator.

5.1 Background material

We turn our attention to formalize the idea of modifying the reference signal via multi-rate sampling. We start with a sampled equivalent model of the form;

$$x(k+1) = F^{\delta}(x(k), u(k)) \tag{5.1a}$$
$$y(k) = h(x(k)) \tag{5.1b}$$

with δ the sampling period, and $F^{\delta}(x,u)$ as in (2.6). The multi-rate equivalent model of order $m = r$ is

$$x(k+1) = F_r^{\delta}(x(k), \underline{u}(k)) \tag{5.2a}$$
$$Y(k) = H(x(k)) \tag{5.2b}$$

where $F_r^{\delta}(x,\underline{u})$ is as in (2.14), $\underline{u} = \begin{pmatrix} u^1 & \dots u^r \end{pmatrix}^{\top}$, $r \in \mathbb{N}$, with $u^i(k) = u(t)$, $t \in [k\delta + (i-1)\bar{\delta}, k\delta + i\bar{\delta}$. Moreover, $H(x)$ is as in (2.15).

Problem: sampled-data tracking through multi-rate sampling and MPC

Design a single-rate piecewise constant state feedback (with sampling period $\bar{\delta}$) that tracks samples of suitable reference $y_r(t)$ at prefixed sampling instants by minimizing the cost:

$$J = \sum_{i=1}^{n_p} \left(\|y(k+i) - y_r(k+i)\|_Q^2 + \epsilon \|u(k+i-1)\|_R^2 \right) \tag{5.3}$$

at all $t = k\delta$, $k \geq 0$ and ensuring boundedness of the closed loop trajectories for small ϵ.

With reference to the Problem statement, and in the cheap control limit when $\epsilon = 0$ and $Q = \mathrm{I}$, a zero ideal performance can be achieved, as discussed in the previous chapter, by solving in $\underline{u}(k)$ the following system of nonlinear algebraic equations

$$H(F_m^{\delta}(x(k), u^1(k), \ldots, u^m(k)) = Y_r(k+1) \tag{5.4}$$

and setting $m = r$ where the vector Y_r is an augmented reference vector of y_r and it's higher $r-1$ derivatives, so as to guarantee that, by invoking the implicit function theorem, a solution exists Monaco and Normand-Cyrot (1992). While the possibility of varying the control several times in the sampling interval confers more degrees of freedom to the control action Monaco and Normand-Cyrot (2001), however, a major limitation in the use of multi-rate control stands in its intrinsic dependence on the model so implying lack of robustness. Moreover, since the input signal changes over sub-intervals of the sampling period, the control works in open loop at all those sub-intervals since the corresponding measures of the states are not available. In this sense, nonlinear MPC can be used coupled with multi-rate, as discussed in the example, to improve multi-rate control robustness. This is due to the fact that MPC is known to possess inherent robustness properties as the following discussion highlights.

Inherent robustness in model predictive control

By inherent robustness, we refer to the fact that a sampled-data nonlinear MPC controller based on a *nominal* model of the plant possess certain robustness properties with respect to small model uncertainties and additive disturbances. To this end, consider the perturbed system associated with the dynamics (1.1a) in a sampled-data equivalent form

$$x(k+1) = F^{\delta}(x(k), u(k), d(k)) \tag{5.5}$$

where $d \in \mathcal{W} \subset \mathbb{R}^p$ for some $p < n \in \mathbb{Z}_+$ is a *disturbance*. Then the sampled-data unperturbed dynamics of the form (5.1a) is called the *nominal* dynamics, and by the *nominal MPC* controller, we refer to the solution of the unconstrained cheap MPC problem utilizing the nominal dynamics for prediction. To this end, we recall the following definition **?**;

Definition 5.1 The system (5.5) is said to be input-to-states stable (ISS) under feedback $u(k) = \alpha(x(k))$, if there exists class $\mathcal{KL}$ function β and class $\mathcal{K}$ function γ such that, for any initial state, and any bounded disturbances, a solution exists for all $k \geq 0$ and is bounded; i.e. it satisfies

$$\|x(k)\| \leq \beta(\|x(0)\|, k) + \gamma\big(\sup \|d(k)\|\big).$$

By *robust input to state stability* we mean input to state stability on a robustly positive invariant set denoted Γ for system (5.5) under a given bounded disturbance $d(k)$.

To prove nominal robustness of MPC, the following body of assumptions are recalled.

Assumption 5.1 (Grimm et al. (2004)) *the minimization problem associated to the sampled-data dynamics (5.1a) with cost function 5.3 is feasible for the given initial state $x(k)$; Moreover, the presence of uncertainties and disturbances does not cause loss of feasibility.*

Remark 5.1 *For a general cost function, it has been proved in (Picasso et al. (2010); Limon et al. (2009)) that for ISS of the closed-loop of the perturbed dynamics (5.5) under an optimal feedback, the stage cost needs to be continuous, zero at zero and bounded from below by some $\mathcal{K}_\infty$ function $\alpha_l(x)$. However, our stage cost is quadratic as (5.3), and thus this assumption is trivially verified.*

Assumption 5.2 *Following similar arguments as in the previous chapter (see also Limon et al. (2009) and others), assume that the unconstrained MPC problem is enriched with terminal stability ingredients satisfying the conditions in Section 4.1.*

The theorem below due to Picasso et al. (2010) (and separately to Grimm et al. (2007)) addresses *inherent robustness* of the closed loop system under a nonlinear MPC control feedback solution to a problem of the form (4.4a)-(4.4f);

Lemma: inherent robustness of sampled-data MPC

Consider a continuous-time system with a sampled data equivalent dynamics (5.1a) with feedback $u^\star(x(k))$ being the optimal with respect to the cost function (5.3) and under Assumptions 5.1-5.2. Assume that there exists a compact set Γ in whose interior the cost function is continuous. Then the closed loop perturbed system (5.5) under $u(k) = u^\star(x(k))$ is robustly ISS.

5.2 Stable partial inversion in model predictive control via multi-rate reference planning

In this section we present a solution to Problem 5.1 making use of multi-rate sampling to modify the reference signal. Consequently, given a nonlinear system of the form (1.1a),(1.1b), and it's sampled equivalent model (5.1a),(5.1b). it is required to design a single rate piecewise constant state feedback (with sampling period $\bar{\delta}$) that tracks samples of suitable reference y_r at prefixed sampling instants (that is $y_r(k) = y_r(k\delta)$, $\delta = m\bar{\delta}$ for some $m \in \mathbb{N}$) by minimizing the cost functional (5.3) at all $t = k\bar{\delta}$, $k \geq 0$ and ensuring boundedness of the closed loop trajectories.

Remark 5.2 *notice that the relaxation of the problem by requiring tracking only at the big sampling instants $\delta = m\bar{\delta}$ is not restrictive for $\bar{\delta}$ can be chosen very small.*

To achieve the above, it is proposed to design a sampled-data single-rate control law, acting at all $t = k\bar{\delta}$ and based on the corresponding sampled measures of the state, through a sampled-data MPC procedure that makes use of the intermediate reference output values denoted $\hat{y}_r^i(k)$ resulting from the application of the nominal control sequence computed from (5.4) to the multi-rate sampled-data model (5.2a),(5.2b). This reference is said to be admissible in the sense of the definition below;

Definition: admissible reference sequence

A sampled-data reference sequence $\{y_r(k), k \geq 0\}$ is said to be admissible for the continuous-time system of the form (1.1a),(1.1b) from an initial state $x_0 \in \mathbb{R}^n$ if, for a suitable integer $m \leq n$, equality (5.4) has a solution $\{u^i(k), i = 1, \ldots, m\}$ which remains bounded. It will be said single-rate or multi-rate admissible if $m = 1$ or $m > 1$, respectively.

Note that, from the definition above, a multi-rate admissible sequence can be suitably enriched to be single-rate admissible. This in turn allows us to state the following result elaborating on that in (Elobaid et al., 2020b, Theorem 3.1);

Result: sampled-data tracking through MPC and multi-rate planning

Consider a system of the form (1.1a),(1.1b) and let $y_r(t)$ be a reference signal to be tracked at $t = k\delta$ for $k \to \infty$ and $\delta = m\bar{\delta}$. Denote by $\{y_r(k) = y_r(k\delta), k \geq 0\}$ the sequence of multi-rate admissible samples of the reference under the input sequence $\{\hat{u}^i(k), \quad k \geq 0, i = 1, \ldots, m\}$ solution for all $k \geq 0$ to

$$\begin{pmatrix} y_r(k+1) \\ y_r(k+2) \end{pmatrix} = \begin{pmatrix} H \circ F_m^\delta(x(k), \hat{u}^1(k), \ldots, \hat{u}^m(k)) \\ H \circ F_m^\delta(\cdot, \hat{u}^1(k+1), \ldots, \hat{u}^m(k+1)) \circ F_r^\delta(x(k), \hat{u}^1(k), \ldots, \hat{u}^m(k)) \end{pmatrix} \tag{5.6}$$

Let $\{\hat{y}^i(k), \quad k \geq 0, i = 1, \ldots, m\}$ be the augmented reference generated by $\hat{y}^1(k) = y_r(k)$, and for, $i = 2, \ldots, m$, $\hat{y}^i(k) = h(\hat{x}^i(k))$ with

$$\begin{aligned} \hat{x}^1(k) &= x(k\delta) \\ \hat{x}^i(k) &= F^\delta(\hat{x}^{i-1}(k), \hat{u}^{i-1}(k)) \end{aligned}$$

Then, the MPC problem defined via the cost function (5.3) together with a single-rate sampled-data prediction model of the form (5.1a),(5.1b) admits a solution which is bounded for $n_p = n_c \geq m$ at the cheap limit when $\epsilon \to 0$ small enough.

Note that the statement above does not assume that the reference can be tracked in continuous time, but merely that it is multi-rate admissible. Given a reference $y_r(t)$ that the continuous-time system can exactly track (in the sense of Isidori (1995)[Chapter 4]), then a sufficiently fast sampling of this reference $y_r(k)$ is multi-rate admissible, namely one can define $H(x) = (h(x), \ldots, L_f^{r-1}h(x))^\top$ and $Y_r = (y_r, \dot{y_r}, \ldots, y_r^{(r-1)})^\top$ as in (Monaco and Normand-Cyrot, 1997) corresponding to which (5.4), and by extension (5.6) admits a solution. The following consequence can be hence given;

Corollary: existence of solution for minimum phase systems

Given a nonlinear control affine SISO system of the form (1.1a),(1.1b) assumed minimum-phase and has a well defined relative degree $r \leq n$, then equality (5.4) always admits a solution with a multi-rate of order $m \geq r$.

5.3 Planning and Control algorithm

In this section, and referring to the discussion above, we present in a detailed manner the control scheme for designing a sampled-data feedback ensuring tracking of a given output profile at the sampling instants $t = k\delta$ for all $k \geq 0$ by exploiting a planned *admissible* trajectory generated via the multi-rate model (5.2a),(5.2b) at the sub-intervals of length $\bar{\delta} = \frac{\delta}{m}$.

We assume that the continuous-time dynamics is finitely descritizable with the map $F_m^{\delta}(x, \underline{u})$ denoting the corresponding multi-rate finite model of order m (possibily computed under coordinate change and preliminary feedback).

The following algorithm is proposed by using the admissible sequence $\{\hat{y}^i(k), \quad i = 1, \ldots, m, \ k \geq 0\}$ defined in Theorem 5.2 as a reference trajectory for the MPC fixing the prediction horizon at $n_p = m$. Such a trajectory is computed and updated at all $t = k\delta$ based on the nominal multi-rate solution defined through (5.6). Thus, for all $t \in \{k\delta, k\delta + i\bar{\delta}, \ldots, k\delta + (m-1)\delta\}$ the planned reference sequence is fed to the MPC for computing the optimizing controller which is guaranteed to exist for $\epsilon \geq 0$ small enough by virtue of Theorem 5.2.

Specifically, the algorithm works over the steps below depicted in Algorithm 1 below.

Remark 5.3 *With reference to the algorithm below and the previous discussion, we only exploit the samples of the reference over two big steps (that is $y_r(k+1), y_r(k+2)$ and correspondingly setting in the MR planner (5.4) an augmented output vector $H_e(x) = (y(k), y(k+1))^{\top}$). This is due to the fact that in the implementation of a receding horizon algorithm, we will need explicitly the values of the desired reference sequence over $n_p = m$ steps, and writing the second iteration of the MPC (i.e., at time $t = k\delta + \bar{\delta}$), one notes the explicit dependence of the (optimal) control on values of the desired output trajectories at $\hat{y}^{m+1}(k) = \hat{y}^1(k+1)$.*

Algorithm 1 Planning and control algorithm

Initialization:

$$Y_r \leftarrow (y_r(k+1) \quad y_r(k+2))^\top$$
$$x(k) \leftarrow x(k\delta), Q \leftarrow Q, R \leftarrow R, m \leftarrow r, n_p \leftarrow m$$

while $t \geq 0$ **do**
  if $t = (k+j)\delta, j \in \mathbb{Z}_{\geq 0}$ **then**
    $k \leftarrow k + j$
    $(\hat{y}(k+1), \hat{y}(k)) = \text{Planning}(x(k), Y_r)$
    $u(k) = \text{Control}(m, Q, R, \hat{y}(k), \hat{y}(k+1))$
  else
    for $t = k\delta + i\bar{\delta}, i = 1, \ldots, m-1$ **do**
      $u^i(k) = \text{Control}(m, Q, R, \hat{y}(k), \hat{y}(k+1))$

procedure $\hat{y}(k+1), \hat{y}(k) = \textsc{Planning}(x(k), Y_r)$

$$\begin{pmatrix} y_r(k+1) \\ y_r(k+2) \end{pmatrix} = \begin{pmatrix} H \circ F_m^\delta(x(k), \hat{u}^1(k), \ldots, \hat{u}^m(k)) \\ H \circ F_m^\delta(\cdot, \hat{u}^1(k+1), \ldots, \hat{u}^m(k+1)) \circ F_r^\delta(x(k), \hat{u}^1(k), \ldots, \hat{u}^m(k)) \end{pmatrix}$$

  for $j = 0:1$ **do**
    for $i = 2:m$ **do**

$$\hat{x}^i(k+j) = F^\delta(\hat{x}^{i-1}(k+j), \hat{u}^{i-1}(k+j))$$
$$\hat{y}^i(k+j) = h(\hat{x}^i(k+j)).$$

procedure $u^\star(k) = \textsc{Control}(m, Q, R, \hat{y}^1(k), \ldots, \hat{y}^{n_p}(k))$

$$u(k) = \min_u \quad \sum_{i=1}^{n_p} \left(\|\hat{y}^i(k) - y^i(k)\|_Q^2 + \|u^{i-1}(k)\|_R^2 \right)$$

  $u^\star(k) = u^1(k)$

Remark 5.4 *The design of the planner can be worked out on a simplified sampled-data model so to reduce the computational burden related to solve equality (5.6). When the conditions of the corollary are met, the computations associated with the planner are simply the inversion of a matrix B_m^δ which is full rank by construction. Consequently, as will be shown in the next chapter, one in principle uses a simplified finite model for the planner, while a more exhaustive one is employed by MPC for prediction.*

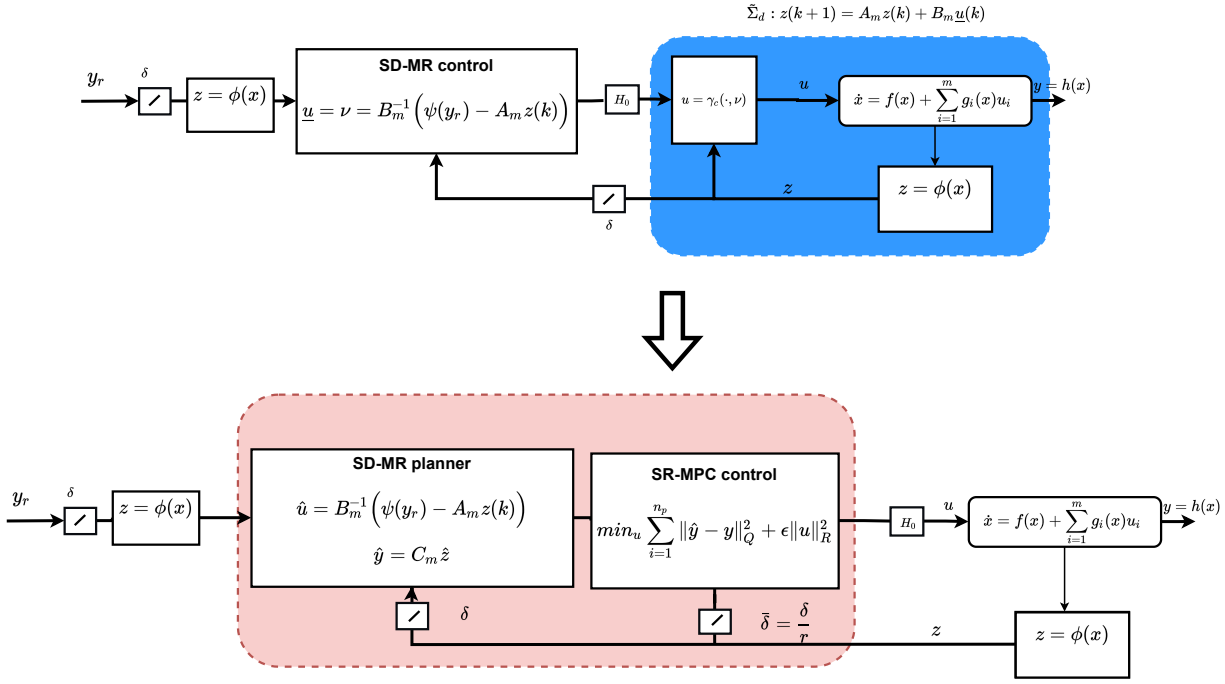

Figure 5.2: Multi-rate planning and MPC control based on a simplified model

From the figure, in the standard multi-rate control, one designs the feedback based on a simplified model obtained via coordinates change and feedback. This feedback works over time steps of length δ, while over the sub-interval the system is running in open loop. The resulting feedback is piecewise continuous. On the other hand, in the proposed scheme one can replicate the zero ideal performance obtained in nominal conditions via multi-rate control using MPC and multi-rate planning instead. The MPC still uses an "assumed" simplified model of the plant but discarding the continuous-time feedback and relying on the nominal robustness of MPC. The result is a simplified MPC problem with no terminal ingredients replicating zero ideal performance at the limit of cheap control. Moreover the feedback is piecewise constant (completely digital design).

Remark 5.5 *The proposed control scheme inherits the nominal robustness properties of the (nonlinear) MPC; see for example Grimm et al. (2007); Picasso et al. (2010); Grimm et al. (2004). This will be further demonstrated in Chapter 6.*

5.4 Comparison between the two multi-rate strategies for the differential drive

In this section, and recalling again the example of the differential drive kinematics in Section 4.4, we compare the two solution approaches to the problem of stable inversion in MPC via multi-rate sampling. We will mirror the situations depicted there, however this time comparing the use of multi-rate at the prediction level and at the planning level.

In all of the simulations we set $n_p = n_c$ and $\delta = 1$ and the MPC solver is the standard Matlab© one. Figure 5.3 emphasizes that at the cheap control limit, when no penalty is applied on the control inputs, when using multi-rate at the prediction level we recover the multi-rate deadbeat control as a solution to the optimization problem. On the other hand, when multi-rate is applied at the planning level we almost get inversion with the notable difference being the control effort (in terms of magnitude is noticeably lower). This later observation also explains the smooth movement towards the reference point $(y_r = (2\ 2\ \frac{\pi}{4})^\top$.

In Figure 5.4 similar observations can be made as in the case of steering when both methodologies are applied at the cheap control limit, when no penalty is applied on the control inputs. When using multi-rate at the prediction level, and as expected and depicted in Chapter 4, we recover the multi-rate deadbeat control as a solution to the optimization problem. On the other hand, when multi-rate is applied at the planning level we almost get an inversion-like control with lower control effort and smoother movement towards the reference trajectory being a line on the $(x,\ y)$ plane unity slope.

Finally in Figure 5.5 we have a more interesting situation in which both multi-rate solutions to the inversion problem in MPC are compared when $\epsilon - 0.5$ i.e. when the problem is not that of a cheap control. Similarly to Section 4.4, the differential drive is required to track a line on the plane with unity slope. Both solutions are able to achieve perfect tracking with the sampled-data solution employing a multi-rate planner perfroming better in terms of required control effort.

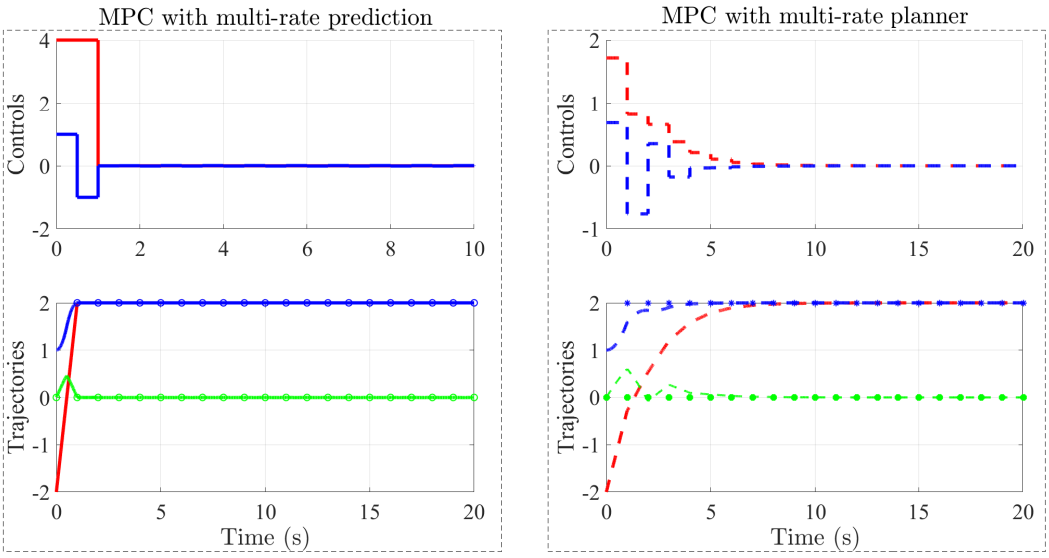

Figure 5.3: MPC with MR prediction and MPC with MR planning steering $\epsilon = 0,\ Q = \mathrm{I}$.

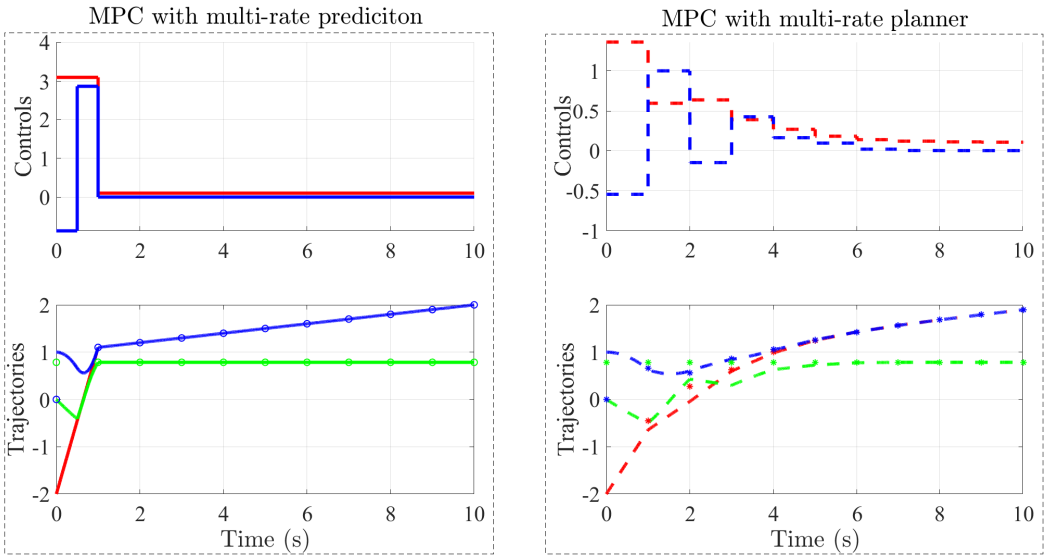

Figure 5.4: MPC with MR prediction and MPC with MR planning tracking $\epsilon = 0,\ Q = \mathrm{I}$.

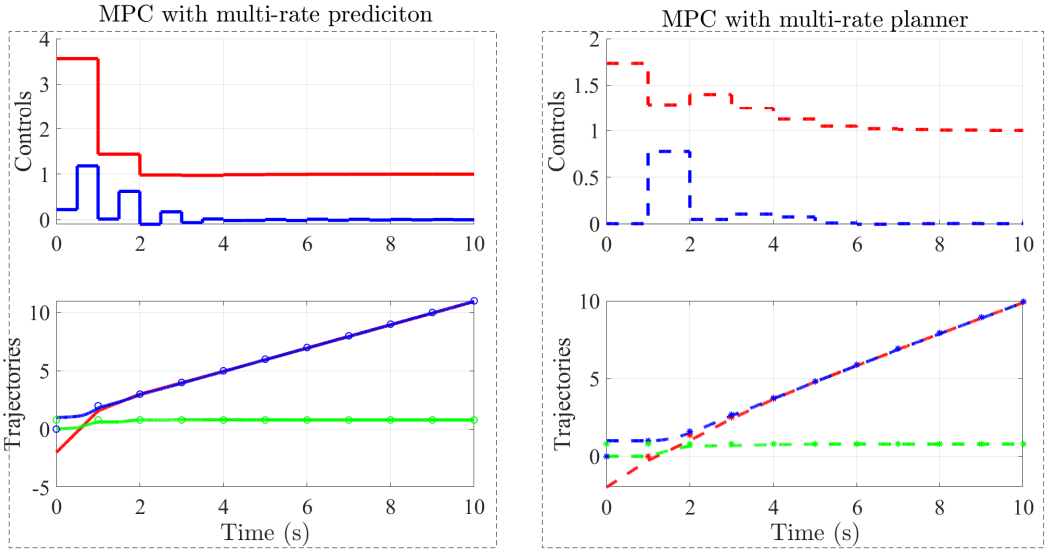

Figure 5.5: MPC with MR prediction and MPC with MR planning tracking $\epsilon = 0.5,\ Q = 2\mathrm{I}$.

5.5 Steering and tracking for the PVTOL aircraft

In this section we introduce a more comprehensive case study that highlight the validity of the proposed approach in terms of following a given trajectory. This case study reports simulations and detailed comparisons not published in Elobaid et al. (2020b). This scheme is compared to the stand-alone multi-rate control (see for example Di Giamberardino et al. (1994), Pucci et al. (2011) and the references therein), thus specifying the results to this particular example, as well as a typical implementation of single-rate nonlinear MPC (denoted SR MPC) with a given trajectory planner. Let the model of the dynamics of a Planar Vertical Take-Off and Landing PVTOL in the $x-z$ (Figure 5.6) plane of $\mathbb{R}^3$ take the form:

Figure 5.6: PVTOL in the plane.

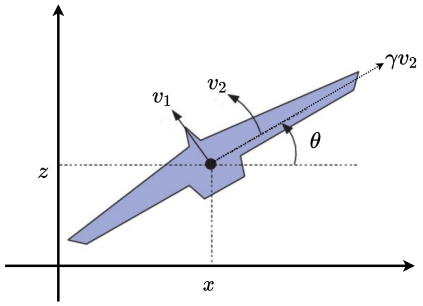

$$\begin{aligned}\ddot{x} &= -\sin(\theta)v_1 + \gamma\cos(\theta)v_2\\ \ddot{z} &= \cos(\theta)v_1 - 1 + \gamma\sin(\theta)v_2\\ \ddot{\theta} &= v_2\end{aligned} \tag{5.7}$$

for which the position is $p = h(x, \dot{x}, z, \dot{z}, \theta, \dot{\theta}) = (x, z)^\top$.

Construction of the MR planner model

To use our control scheme, we first define the multi-rate sampled data model of the PVTOL. To this end, it is known that (5.7) is feedback equivalent to a finitely discretizable system, by setting

$$v = \begin{pmatrix} \frac{1}{\cos\theta} + \gamma\dot{\theta}^2 \\ -2\dot{\theta}^2\tan\theta \end{pmatrix} + \begin{pmatrix} \frac{1}{\cos\theta} & 0 \\ 0 & \cos^2\theta \end{pmatrix} u$$

together with the coordinates change

$$\zeta = \varphi(x, \dot{x}, z, \dot{z}, \theta, \dot{\theta}) = \gamma \begin{pmatrix} \cos\theta \\ -\dot{\theta}\sin\theta \\ 0 \\ -\sin\theta \\ 0 \\ -\dot{\theta}\cos\theta \end{pmatrix} + \begin{pmatrix} z \\ \dot{z} \\ \tan\theta \\ x \\ \frac{\dot{\theta}}{\cos^2\theta} \\ \dot{x} \end{pmatrix}.$$

Thus obtaining

$$\begin{aligned}\dot{\zeta} &= \tilde{f}(\zeta) + \tilde{g}_1(\zeta)u_1 + \tilde{g}_2(\zeta)u_2\\ \tilde{f}(\zeta) &= \begin{pmatrix}\zeta_2 & 0 & \zeta_5 & \zeta_6 & 0 & -\zeta_3\end{pmatrix}^\top, \tilde{g}_1(\zeta) = \begin{pmatrix}0 & 1 & 0 & 0 & 0 & -\zeta_3\end{pmatrix}^\top\\ \tilde{g}_2(\zeta) &= \begin{pmatrix}0 & 0 & 0 & 0 & 1 & 0\end{pmatrix}^\top\end{aligned} \tag{5.8}$$

The above model (5.8) admits the closed-form sampled-data equivalent model of the form (5.1a),(5.1b) that can be computed. We then select our multi-rate order $m = 4$ and, in particular

$$u_1(t) = u_1^j(k),\ t \in [(k + \frac{j-1}{2})\delta, (k + \frac{j}{2})\delta[,\ j = 1, 2$$
$$u_2(t) = u_2^j(k),\ t \in [(k + \frac{j-1}{4})\delta, (k + \frac{j}{4})\delta[,\ j = 1, \ldots, 4.$$

so getting the multi-rate planner dynamics (dropping the subscript k for the control):

$$\begin{aligned}\zeta(k+1) = {} & (A^{\bar\delta} + B_1^{\bar\delta}(u_1^2))^2(A^{\bar\delta} + B_1^{\bar\delta}(u_1^1))^2\zeta(k) \\ & + (A^{\bar\delta} + B_1^{\bar\delta}(u_1^2))^2(I + B_1^{\bar\delta}(u_1^1))B_0^{\bar\delta}(u_1^1, u_2^1) \\ & + (A^{\bar\delta} + B_1^{\bar\delta}(u_1^2))^2 B_0^{\bar\delta}(u_1^1, u_2^2) \\ & + (I + B_1^{\bar\delta}(u_1^1))B_0^{\bar\delta}(u_1^2, u_2^3) + B_0^{\bar\delta}(u_1^2, u_2^4)\end{aligned} \tag{5.9}$$

with $\zeta(k) = \varphi(x(k), \dot x(k), z(k), \dot z(k), \theta(k), \dot\theta(k))$ for all $k \geq 0$ with

$$A^{\bar\delta} = \begin{pmatrix} 1 & \bar\delta & 0 & 0 & 0 & 0 \\ 0 & 1 & 0 & 0 & 0 & 0 \\ 0 & 0 & 1 & 0 & \bar\delta & 0 \\ 0 & 0 & -\frac{\bar\delta^2}{2} & 1 & -\frac{\bar\delta^3}{6} & \bar\delta \\ 0 & 0 & 0 & 0 & 1 & 0 \\ 0 & 0 & -\bar\delta & 0 & -\frac{\bar\delta^2}{2} & 1 \end{pmatrix}, B_1^{\bar\delta}(u_1) = \begin{pmatrix} & & & \mathbf{0}_{3\times 6} & & \\ & -\frac{\bar\delta^2}{2}u_1 & 0 & -\frac{\bar\delta^3}{6}u_1 & 0 \\ \mathbf{0}_{3\times 2} & 0 & 0 & 0 & 0 \\ & -\bar\delta u_1 & 0 & -\frac{\bar\delta^2}{2}u_1 & 0 \end{pmatrix}$$

$$B_0^{\bar\delta}(u_1, u_2) = \begin{pmatrix} \frac{\bar\delta^2 u_1}{2} & \bar\delta u_1 & \frac{\bar\delta^2 u_2}{2} & \frac{-\bar\delta^4(1+u_1)u_2}{24} & \bar\delta u_2 & \frac{-\bar\delta^3(1+u_1)u_2}{6} \end{pmatrix}^\top$$

with $\bar\delta \geq 0$ being the sampling period and $\delta = 4\bar\delta$.

Planning and control

For all $t = k\delta$ with $k \geq 0$ planning is made on the basis of the simplified equivalent model (5.9) so getting, for the original system (5.7) a sequence of admissible outputs $\{(\hat x^i(k+j), \hat z^i(k+j)),\quad i = 1, \ldots, 4$ and $j = 0, 1\}$ when setting $(\hat x^i(k+j), \dot{\hat x}^i(k+j), \hat z^i(k+j), \dot{\hat z}^i(k+j), \hat\theta^i(k+j), \dot{\hat\theta}^i(k+j))^\top = \varphi^{-1}(\hat\zeta^i(k))$.

Consequently, for all $t = k\delta + i\bar\delta$, the MPC computes the feedback $u^i(k)$ (for $i = 0, \ldots, 3$) with the sampled data SR model of the PVTOL used for prediction. This feedback is then applied to the simulation model of system (5.7) while recomputing the reference for all $t = k\delta$.

Simulations and Remarks

In the following we will compare the proposed control algorithm (denoted MR MPC) to both the stand-alone multi-rate deadbeat control (denoted MR) and MPC with the trajectory planner proposed by Biagiotti and Melchiorri (2019) (hereinafter denoted FIR MPC). In all simulations $\bar\delta = 1$ seconds while $n_p = n_c = 4$. In the exact steering scenarios, The PVTOL is required to perform the classical lateral maneuver of 10 m, namely a reference on the normalized position of $(x\ \ z)^\top = (1\ \ 0)^\top$. While in the time varying references case, a linear path is fixed on both the lateral and vertical displacements (that is x, z respectively) as a ramp signal with velocity $v_0 = 1$m/s to

be tracked at $t = k\delta, \delta = 4\bar{\delta}$.

Exact steering with Perturbation Here we perform the manuever of a lateral displacement, assuming the system is perturbed by a disturbance $w(t)$ where w is a randomly generated actuation white noise (that is $u(t) = u_{mpc}(t) + w(t)$). In that case, the following comparisons are made:

- Figure 5.7 compare the performance of this control scheme to that obtained in Di Giamberardino et al. (1994). Notice that in the figure the proposed planning and control algorithm is able to stabilize the vertical displacement to zero despite the disturbance, while the multi-rate deadbeat alone fails at doing so. On the other hand, the rotation is kept bounded by the proposed control scheme below 0.1 rads after 10 seconds.

- Figure 5.8 compare the performance of this control scheme to that obtained with an FIR MPC trajectory planner with a rest to rest motion. In this case, both control schemes perform similarly in the steady state keeping the desired position while also ensuring the stability of the θ dynamics (the PVTOL doesn't perform flips around its axis). It's worth mentioning that the FIR MPC does better in the transient compared to our scheme and requires less vertical movement to recover the required lateral manuever. Once stabilization is achieved, both control schemes stabilize the PVTOL.

Exact steering with γ variation Here we perform the same manuever above, without an actuation perturbation, and we assume that the value of $\gamma = 1.1$ in the actual model, while it's the nominal value for defining the MR planner simplified model and the MPC prediction models, we perform the following comparisons

- Figure 5.9 compare the performance of MR MPC to that obtained with an FIR MPC. Similar performances are recovered, although MR MPC performs slightly worse than FIR MPC in the transient as expected due to the fact that the feedback and coordinate change bringing (5.7) to (5.8) are not defined for $\gamma \neq 0.8$

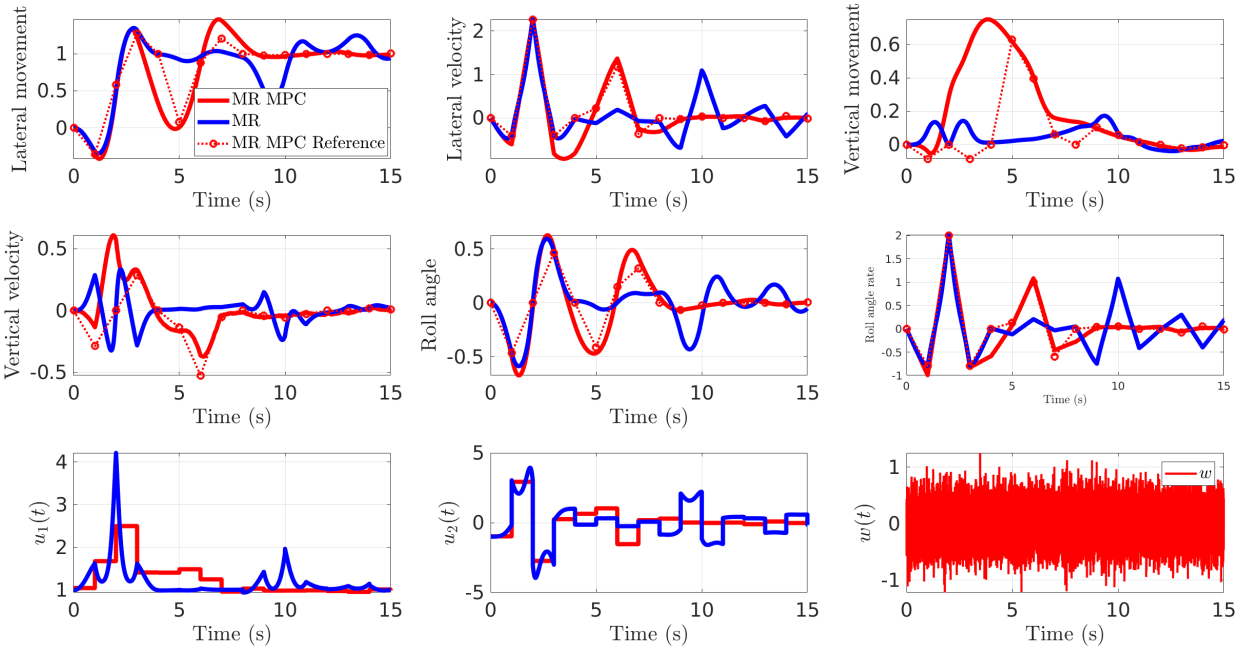

Figure 5.7: PVTOL perturbed steering to $(x, y) = (1, 0)$ MR VS MR MPC with $\epsilon = 0, Q = \mathrm{I}$

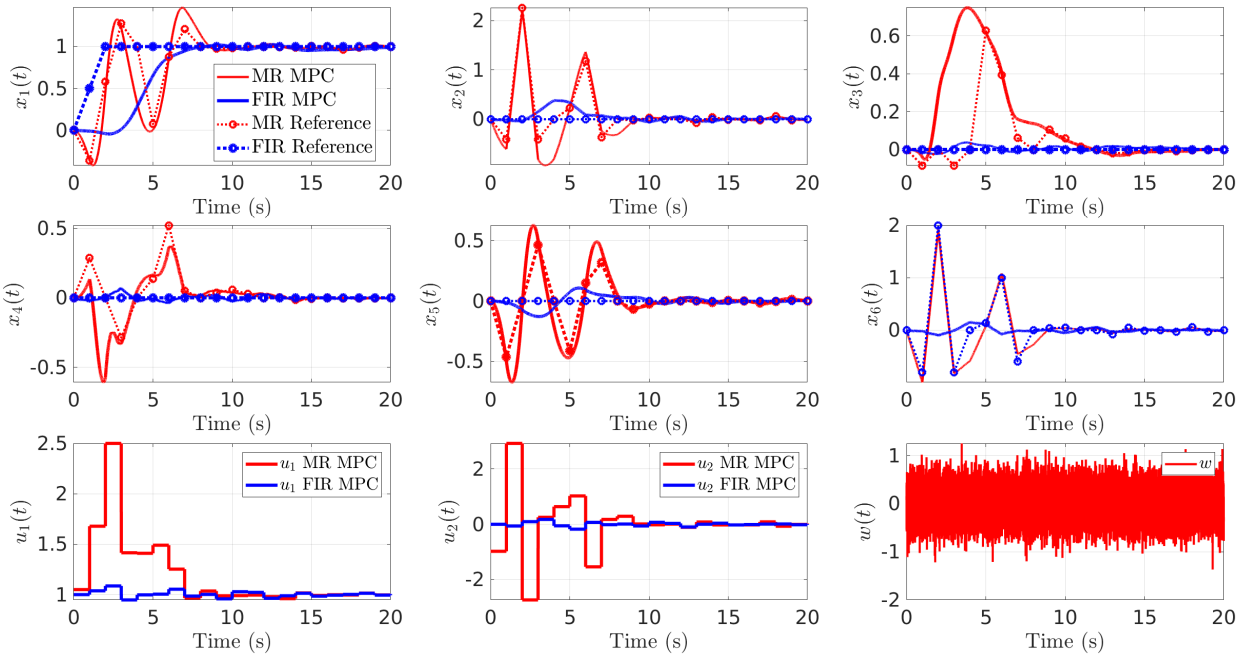

Figure 5.8: PVTOL perturbed steering to $(x, y) = (1, 0)$ FIR MPC VS MR MPC with $\epsilon = 0, Q = \mathrm{I}$

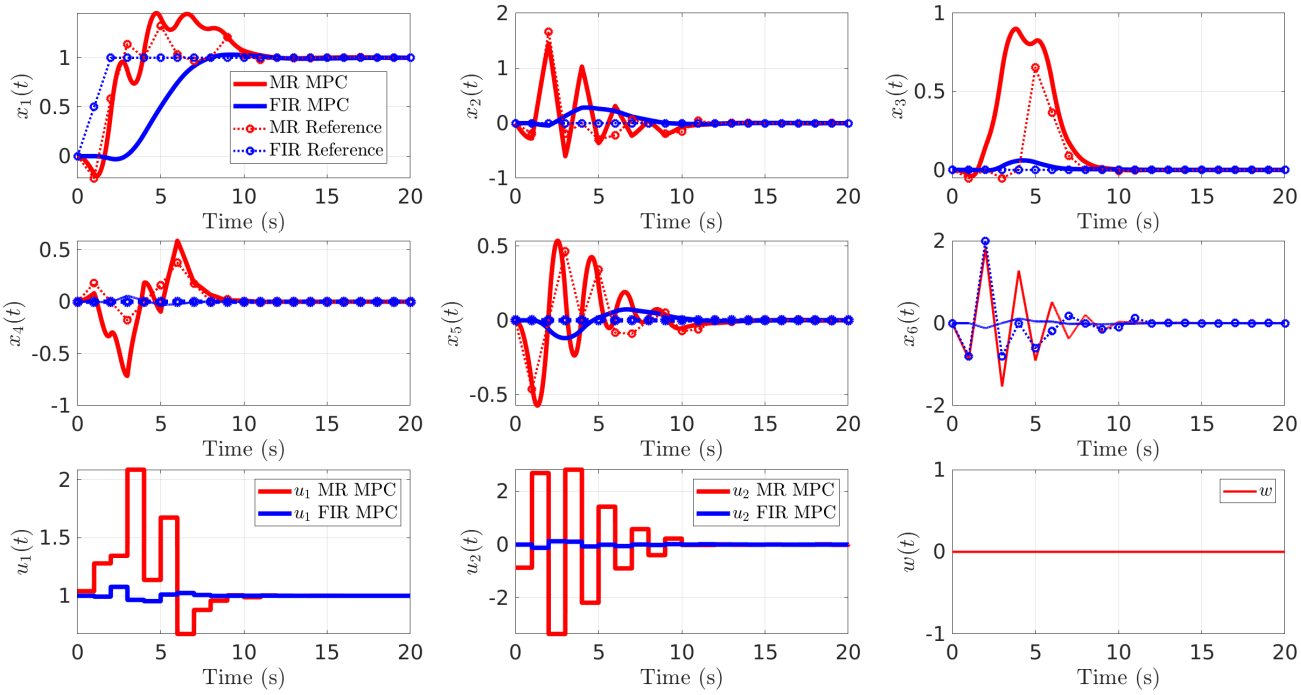

Figure 5.9: PVTOL perturbed steering to $(x, y) = (1, 0)$ FIR MPC VS MR MPC with $\gamma = 1.1, \epsilon = 0, Q = \mathrm{I}$

Time-varying references tracking

We require both the lateral x and vertical displacement z to follow a given reference, in this case, a ramp signal with velocity $v_0 = 0.1$ (i.e without normalization $v_0 = 1m/s$). We show that the proposed scheme outperforms both stand-alone MR control and FIR MPC one, and to this end, the following comparisons are made:

- In the nominal case depicted by Figure 5.10, we set $\gamma = 0$ in the cost (5.3) i.e. cheap control. Notice that, contrarily to the MR MPC scheme, the FIR MPC is unable to follow the reference over the larger steps δ, and for the same choices of Q, R, n_p, n_c an off-set is evident.

- Figure 5.11 shows that, even when there is actuation perturbation, and parameter variation, our proposed scheme outperforms the FIR MPC one, not just on the big sampling instants $k\delta$, but also during the smaller sub-intervals $k\bar{\delta}$.

- Figure 5.12 compares our scheme tracking a straight line, under the action of a perturbation, against the stand-alone MR control, and the benefit in using our proposed scheme is evident as expected, both in terms of tracking at the small sampling instants, and maintaining the variation in the θ dynamics small. This reflects the idea that MR MPC is a robust way to implement MR controls.

- Figure 5.13 shows the effect of weighting the output $R > 0$ and verifying that the MR MPC scheme performs better compared to FIR MPC in this case, under both the action of a perturbation and the parameter ϵ change.

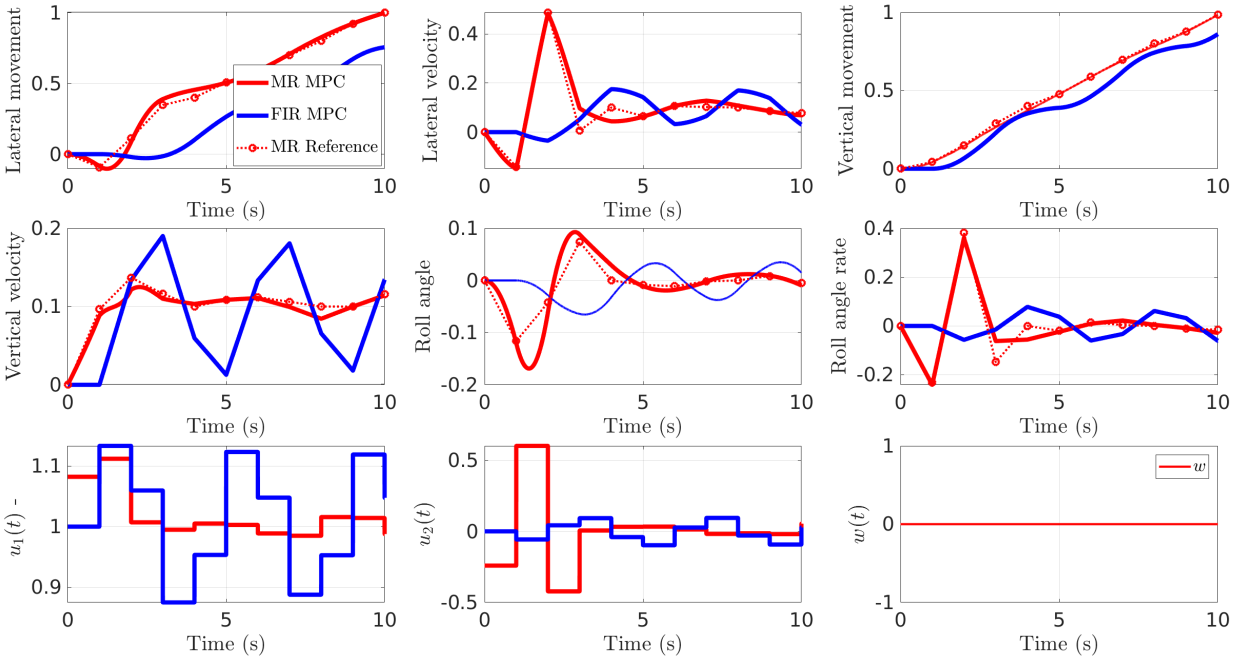

Figure 5.10: PVTOL nominal tracking of a straight line FIR MPC VS MR MPC with $R = 0, Q = \mathrm{I}$

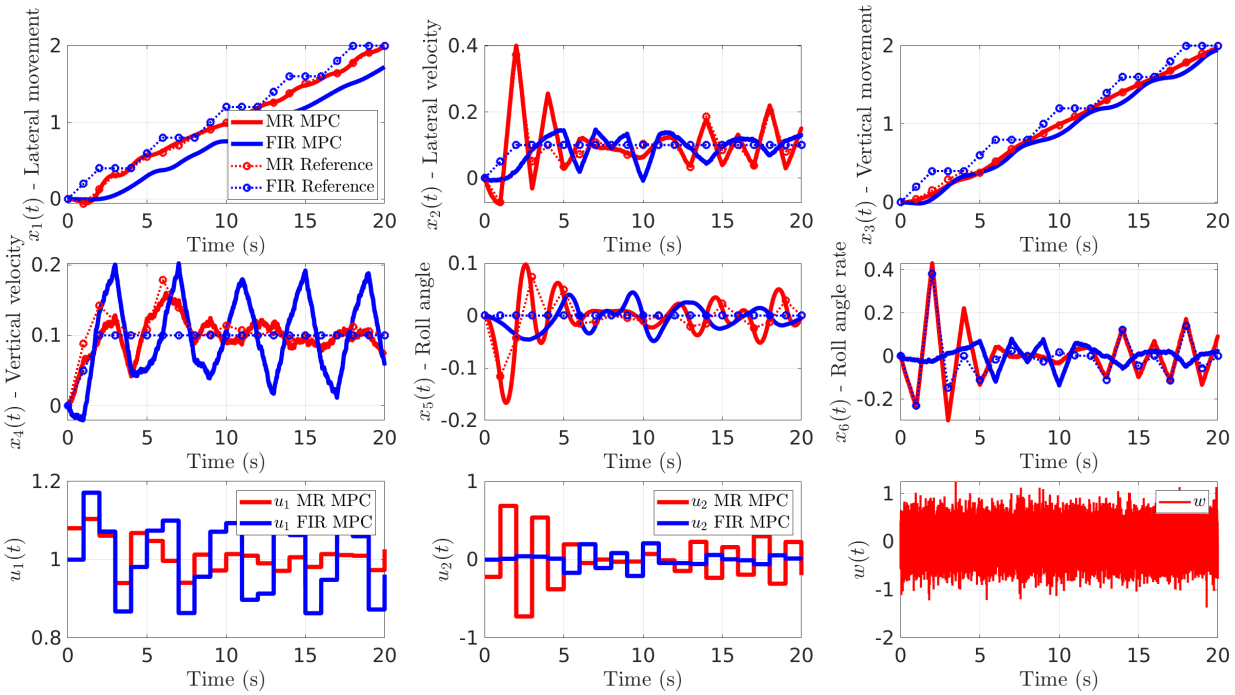

Figure 5.11: PVTOL perturbed tracking of a straight line FIR MPC VS MR MPC with $\gamma = 0.5, \epsilon = 0, Q = \mathrm{I}$

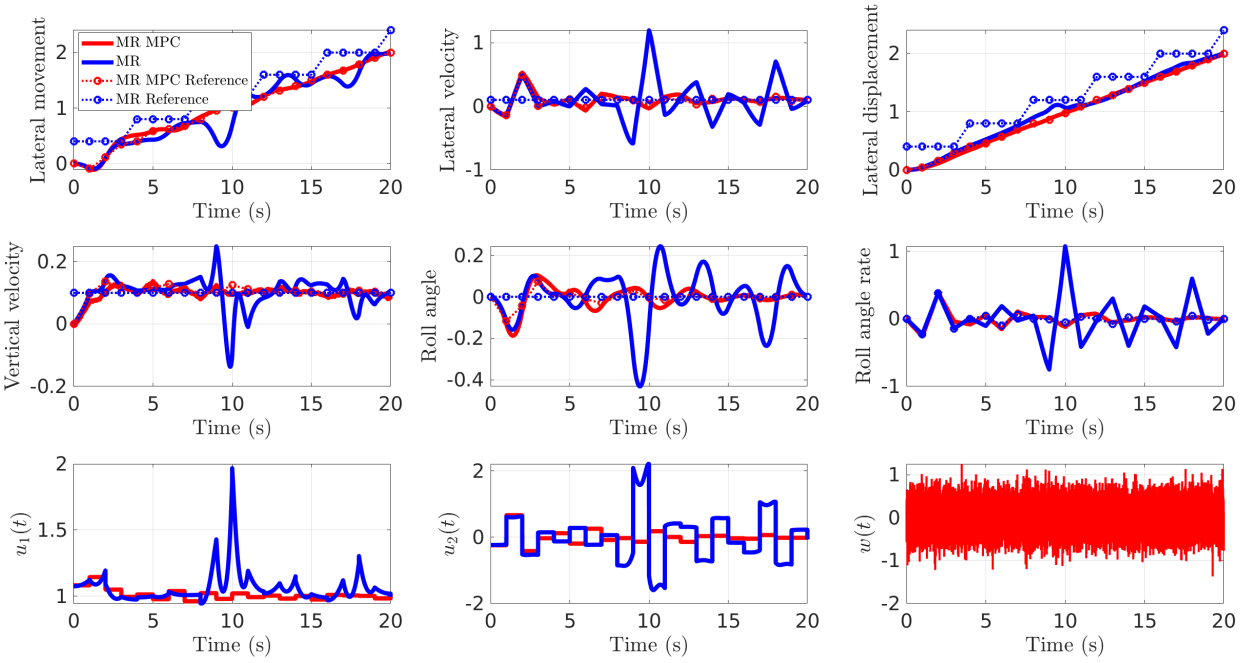

Figure 5.12: PVTOL perturbed tracking of a straight line MR VS MR MPC with $\gamma = 0.8, \epsilon = 0, Q = \mathrm{I}$

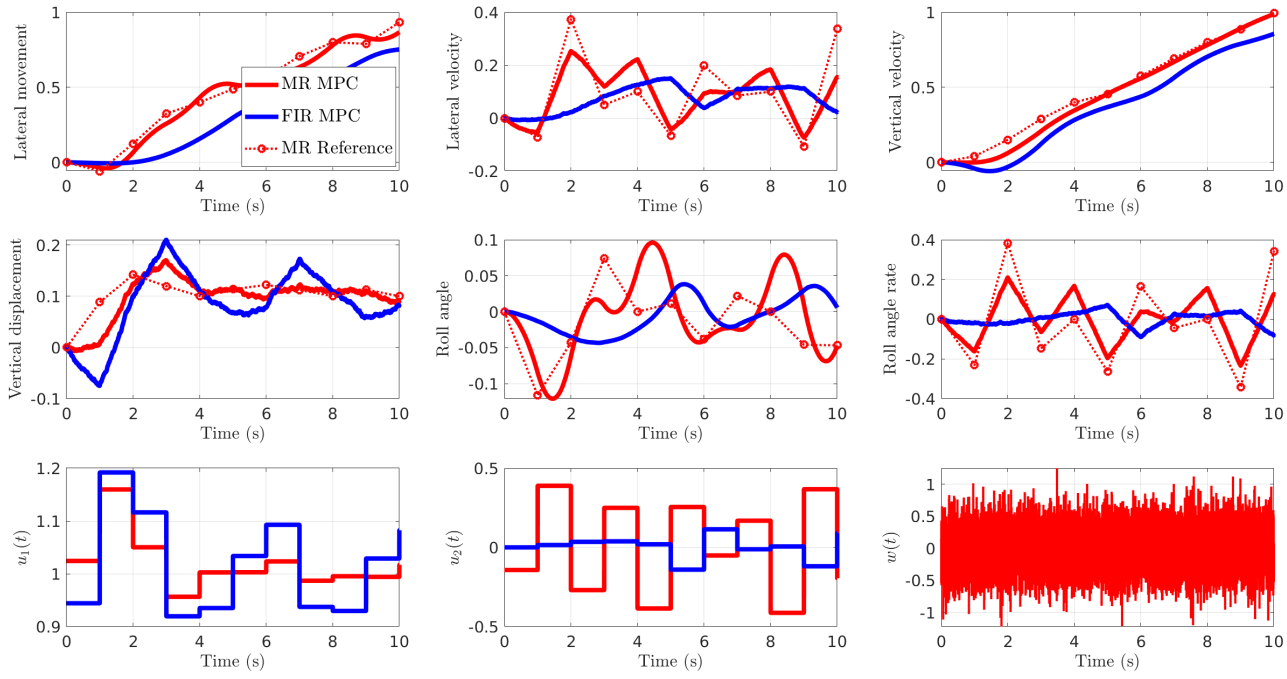

Figure 5.13: PVTOL perturbed tracking of a straight line FIR MPC VS MR MPC with $\gamma = 0.5, \epsilon = 0.5, R = \mathrm{I}, Q = \mathrm{I}$

5.6 Concluding remarks

A few concluding remarks to summarize this chapter are in order;

- Concerning the unconstrained MPC problem, utilizing a multi-rate sampled-data trajectory planner ensures the availability of *admissible* references by construction.
- Those planned references, when no additional constraints are present guarantee recursive feasibility when considering the cheap control variation of the optimization problem.
- Combining nonlinear MPC with multi-rate sampled-data planning ensures that the the closed loop inherits the nominal robustness of MPC. In essence *MPC robustifies multi-rate control, and multi-rate improves the performances achieved by MPC.*
- In this scheme, all the sampling and holding devices on the loop run at a synchronous rate. The asynchronous sampling rate is relegated to the planner level.
- In both solutions presented in this chapter and the previous one, we treated a specific variation of the unconstrained MPC problem under the hypothesis of cheap control. Effects of state and input constraints were not taken into account.

As already explained, this chapter barely touches upon the use of multi-rate sampled models as trajectory planners in MPC to avoid closed-loop instability. Aspects concerning the role of trajectory planners in ensuring recursive feasibility and stability at large are not discussed as well as the role of state and input constraints in the inversion-like nature of MPC. The interested reader is referred to Camacho and Alba (2013), Allgöwer and Zheng (2012), Grüne and Pannek (2017) and the references contained therein.

Available online at www.sciencedirect.com

ScienceDirect

IFAC PapersOnline CONFERENCE PAPER ARCHIVE

IFAC PapersOnLine 53-2 (2020) 3620–3625

Sampled-data tracking under model predictive control and multi-rate planning*

Mohamed Elobaid *,** **Mattia Mattioni** * **Salvatore Monaco** *
Dorothée Normand-Cyrot **

* *Dipartimento di Ingegneria Informatica, Automatica e Gestionale (La Sapienza University of Rome) Rome, 00185 Italy (e-mail: {mohamed.elobaid, mattia.mattioni, salvatore.monaco}@uniroma1.it).*
** *Laboratoire de Signaux et Systèmes (L2S, CNRS); 3, Rue Joliot Curie, 91192, Gif-sur-Yvette, France (e-mail: {mohamed.elobaid, dorothee.normand-cyrot}@centralesupelec.fr)*

Abstract: In this paper, a new control scheme for sampled-data nonlinear model predictive control is proposed making use of a multi-rate based trajectory planning for designing admissible references over the prediction horizon. The proposed controller is compared with existing reference generators for model predictive control through simulations over a benchmark example.

Keywords: Digital implementation; Nonlinear predictive control; Tracking

1. INTRODUCTION

Several control problems involve the cancellation of the so called zero-dynamics. This issue is even more evident in the nonlinear context when solving input-output feedback linearization or tracking problems (see Isidori (2013)).
The problem becomes more delicate under sampling and, in particular, when direct digital control approaches are employed to design the controller. In that case in fact, the minimum-phase property of the system can even be lost for small sampling periods, due to the appearance of the unstable so-called sampling zeros (Åström et al. (1984); Monaco and Normand-Cyrot (1988) for linear and nonlinear cases).
The idea of making use of a piecewise constant control over sub-intervals of the sampling interval, that is multi-rate control, has been properly introduced in the nonlinear context to overcome the aforementioned pathologies (Monaco and Normand-Cyrot (1992)). The possibility of varying the control several times in the sampling interval confers more degrees of freedom to the control action (Monaco and Normand-Cyrot (1991, 2001)).
A major limitation in the use of multi-rate control stands in its intrinsic dependence on the model so implying lack of robustness. Moreover, since the input signal changes over sub-intervals of the sampling period, the control works in open loop at all those sub-intervals since the corresponding measures of the states are not available.
On the other hand, model predictive control (MPC) represents a powerful and effective design technique that relies upon the solution of a constrained optimization problem subject to the system dynamics plus possible additional requirements over a finite time horizon. Indeed, it has now become the mainstay for regulation and tracking in the industry for constrained multi-input/multi-output (MIMO) systems (see Camacho and Alba (2013); García et al. (1989)). Additionally, under suitable assumptions, it has been proved that the feedback generated by a nominal nonlinear model predictive problem is *inherently robust* with respect to different perturbing actions and model uncertainties (e.g., Picasso et al. (2010); Grimm et al. (2004); Magni et al. (2009)). Still, as the intuition suggests, some difficulties may arise when discrete-time models are used by the MPC designer to ensure a prefixed reference profile for the output. As sampling induces unstable zero-dynamics, a naive implementation of MPC feedback might yield unboundedness of the internal trajectories and thus of the feedback. To overcome this issue, standard MPC implementations introduce further penalizing weights on the objective function and/or constraints (typically LMI) over the optimization problem (e.g., Bemporad and Morari (1999); Byun (1988)). As a drawback, such a stratagem is not based on the understanding of the source of unstability so that ad-hoc tuning is needed.
Motivated by these reasons, in Elobaid et al. (2019a) a first attempt to handle those aspects has been proposed by directly designing MPC utilizing multi-rate inputs and the equivalent multi-rate sampled-data model for prediction. Under small penalties on the input, this approach has been shown to be effective as no further modifications of the optimization problem are required for preserving boundedness of the closed loop; however it requires huger capabilities of the sample and hold devices.
In this respect, this work is aimed to weaken this demand by leaving the holding and sampling devices (i.e., actuators and sensors) synchronous. The new proposed control scheme combines a classical single-rate MPC controller with a multi-rate planner that computes, starting from samples of the desired output profile, a suitable admissible reference trajectory to be fed to the MPC. The inner MPC controller working on the fast sampling rate will now guarantee the prefixed boundedness of the internal behaviour of the overall system with no need of introducing further constraints. Roughly speaking, in the proposed control

* Partially funded by *Université Franco-Italienne/Università Italo-Francese* (UFI/UIF) through the Vinci program.

10.1016/j.ifacol.2020.12.2043

scheme, MPC is used to robustify multi-rate design, and multi-rate planning is used to improve MPC.
This work is organized as follows. In Section 2 recalls on single and multi-rate sampling and model predictive control are given. In Section 3 the main ideas and motivations behind multi-rate planning for MPC control are introduced. Section 4 is devoted to the proposed MPC-MR control scheme which is applied to the simplified model of a planar vertical take-off and landing in Section 5. Concluding remarks end the paper.

Notations: All functions and vector fields defining the dynamics are assumed smooth and complete over the respective definition spaces. In the paper T will be the length of the sampling period, and any suitable sub-interval will be denoted by δ. M_U denotes the space of measurable and locally bounded functions $u : \mathbb{R} \to U$ with $U \subseteq \mathbb{R}$. $\mathcal{U}_s \subseteq M_U$ denotes the set of piecewise constant functions over time intervals of fixed length $s \in]0, T^*[$ and T^* small enough; i.e. $\mathcal{U}_s = \{u \in M_U \text{ s.t. } u(t) = u_k, \forall t \in [ks, (k+1)s[; k \geq 0\}$. Given a vector field f, L_f denotes the Lie derivative operator, $\mathrm{L}_f = \sum_{i=1}^{n} f_i(\cdot)\frac{\partial}{\partial x_i}$. The Lie exponential operator is denoted as e^{L_f} and defined as $e^{\mathrm{L}_f} := \mathrm{I} + \sum_{i\geq 1} \frac{\mathrm{L}_f^i}{i!}$ with I being the identity operator. Finally, $\|x\|_P = x^\top P x$ denotes the seminorm of $x \in \mathbb{R}^n$ for some $P \geq 0$. A function $\beta(\cdot) : [0, \infty) \to [0, \infty)$ that is zero in zero and strictly increasing and unbounded is said to be of class κ_∞. A function $R(x, \delta) = O(\delta^p)$ is said to be of order $\delta^p, p \geq 1$ if, whenever it is defined, it can be written as $R(x, \delta) = \delta^{p-1}\tilde{R}(x, \delta)$ and there exists a function $\beta(\delta) \in \kappa_\infty$ and $\delta^\star > 0$ s.t. $\forall \delta \leq \delta^\star, |\tilde{R}(x, \delta)| \leq \beta(\delta)$

2. PRELIMINARIES AND RECALLS

2.1 Sampled-data systems

Single-rate (SR) and multi-rate (MR) sampled-data (SD) equivalent models of a continuous-time process are recalled in the sequel (Monaco and Normand-Cyrot (2001)). Consider a nonlinear continuous-time input-affine system

$$\dot{x} = f(x) + g(x)u, \quad y = h(x) \tag{1}$$

and let $u(t) \in \mathcal{U}_T$ and $y(t) = y_k$ for $t \in [kT, (k+1)T[$ (with $T \geq 0$ being the sampling period). Then, denoting $x_k := x(kT)$, $y_k := y(kT)$, $u_k := u(kT)$ for $k \geq 0$, the evolutions of (1) at the sampling instants $t = kT$ with $T \geq 0$, are described by its *single-rate* (SR) *sampled-data equivalent model*

$$x_{k+1} = F^T(x_k, u_k), \quad y_k = h(x_k) \tag{2}$$

where the mapping $F^T(\cdot, \cdot) : \mathbb{R}^n \times \mathbb{R} \to \mathbb{R}^n$ admits the following series expansion in powers of T

$$F^T(x_k, u_k) = e^{T(\mathrm{L}_f + u_k \mathrm{L}_g)} x\Big|_{x_k} = x_k + \sum_{i>0} \frac{T^i}{i!}(\mathrm{L}_f + u_k \mathrm{L}_g)^i\Big|_{x_k}. \tag{3}$$

Since a closed-form expression for the state and output evolutions of (1) does not exist in general, only approximated expansions in power of T can be computed. In this respect, if the series expansion (3) is characterized by a finite number of terms, then system (1) is said to be *finitely discretizable* (Monaco and Normand-Cyrot (2001)).
It is a matter of computations to verify that if (1) has well defined relative degree, say $r \leq n$, the relative degree of the sampled-data equivalent model always falls to $r_d = 1$; namely, one has

$$y_{k+1} = h(x_k) + \sum_{i=1}^{r} \frac{T^i}{i!}\mathrm{L}_f^i h(x)\Big|_{x_k} + \frac{T^r}{r!} u_k \mathrm{L}_g \mathrm{L}_f^{r-1} h(x)\Big|_{x_k} + O(T^{r+1})$$

so that $\frac{\partial y_{k+1}}{\partial u_k} \neq 0$. As a consequence, whenever $r > 1$, the sampling process induces a further zero-dynamics of dimension $r-1$ (the *sampling zero-dynamics*, Monaco and Normand-Cyrot (1988)) that is in general unstable for $r > 1$. In that case inversion-like techniques via single-rate sampling cannot be achieved while guaranteeing stability of the internal dynamics.
To overcome this pathology multi-rate (MR) sampling, corresponding to sample the state and output at lower frequency with respect to changes of the piecewise constant control, has been introduced in Monaco and Normand-Cyrot (1991). Accordingly, denoting by $u_k^i(t)$, $x_k^i(t)$ and $y_k^i(t)$ the input, state and output variables at any $t = kT + (i-1)\delta$ for $i = 1, \ldots, m$ (with $u_k = u_k^1$, $x_k = x_k^1$ and $y_k = y_k^1$), the multi-rate equivalent model of order m of (1) gets the form

$$x_{k+1} = F_m^T(x_k, u_k^1, \ldots, u_k^m) \tag{4}$$

with $T = m\delta$, $u(t) \in \mathcal{U}_\delta$ and

$$F_m^T(x_k, u_k^1, \ldots, u_k^m) = e^{\delta(\mathrm{L}_f + u_k^1 \mathrm{L}_g)} \ldots e^{\delta(\mathrm{L}_f + u_k^m \mathrm{L}_g)} x\Big|_{x_k} = F^\delta(\cdot, u_k^m) \circ \cdots \circ F^\delta(x_k, u_k^1).$$

It has been proved by the authors that, with $m = r$, the MR sampled-data model has vector relative degree $r^\delta = (1, \ldots, 1)$ under the choice of a suitable output vector specified by the output itself and its first $(r-1)$ derivatives. Accordingly, the corresponding zero-dynamics inherits the zero-dynamics stability properties of (1) (see Monaco and Normand-Cyrot (1988)). In addition in Mattioni et al. (2017), it has been shown that the minimum-phase condition can be relaxed by increasing the MR order.
This MR-SD equivalent model can then be used to design tracking controllers over the sampling interval T as developed in Section 3.

2.2 Sampled-data unconstrained MPC

The problem of tracking a reference $v(t)$ at the sampling instants is typically addressed within the framework of nonlinear model predictive control. Roughly speaking, the feedback is computed to minimize a quadratic cost function of the form

$$J = \sum_{i=1}^{n_p} \left(\|e_{k+i}\|_Q + \|u_{k+i-1}\|_R \right) \tag{5}$$

with $e_k(y_k, v_k)$ a suitable tracking error, $Q > 0, R \geq 0$ being appropriate penalizing weights and n_p, n_c the prediction and control horizons respectively. The functional cost (5) is repeatedly optimized at each sampling instant $t = k\delta$ over a finite horizon while the feedback is applied via a *receding horizon* implementation.
As well know, tracking control implicitly requires zero-dynamics cancellation. In this respect, as the above problem is formulated in the sampled-data context, instability of the closed loop system unavoidably arises due to the sampling zero-dynamics. To overcome this, the *uncon-*

strained MPC problem is typically enriched by redefining the cost function as

$$\mathcal{J} = \sum_{i=1}^{n_p-1} \left(\|e_{k+i}\|_Q + \|u_{k+i-1}\|_R\right) + V_{n_p}$$
$$s.t.\ \ x_{k+1} = F^T(x_k, u_k), \quad x_{n_p} \in \mathcal{X}_f$$

with V_{n_p} and $\mathcal{X}_f$ being the terminal cost and constraints set suitably constructed for keeping the state bounded (Camacho and Alba, 2013). This new formulation gives rise to possible feasibility issues so that solution might not exist for a given set of initial conditions.

On the other hand, reformulation of the tracking MPC problem under multi-rate sampling allows to overcome those unstability and feasibility issues while avoiding unnecessary complications. Indeed, it was proved in Elobaid et al. (2019a) that, given (1) with well-defined relative degree and the MPC problem over (5) subject to the MR-SD model (4), the optimal SD feedback always exists and is uniquely defined as a formal series in powers of δ for all $n_p = n_c \geq 1$. Thus using MR control at the implementation level of MPC allows to handle the issues arising due to sampling, without resorting to penalizing terminal costs and constraints. However, it places a greater burden on the sampling and hold devices, assumes a cheap control, and does not address the issue of working in open loop over intervals of length T; this motivates the proposed control scheme.

3. MULTI-RATE PLANNING FOR MPC CONTROL

For system (1), it is required to design a single rate piecewise constant state feedback (with sampling period δ) that tracks samples of suitable reference $v(\cdot)$ at prefixed sampling instants (that is $v_k = v(kT)$, $T = m\delta$) by minimizing the cost functional (5) at all $t = k\delta$, $k \geq 0$ and ensuring boundedness of the closed loop trajectories. In the nominal multi-rate scenario and when $R = 0$ and $Q = \mathrm{I}$, this can be achieved by considering (4) with $m \geq 1$ and solving in $(u_k^1, u_k^2, .., u_k^m)$ the following system of nonlinear algebraic equations

$$H(F_m^T(x_k, u_k^1, \ldots, u_k^m)) = \mathbf{V}_{k+1} \tag{6}$$

where $H : \mathbb{R}^n \to \mathbb{R}^m$ and the vector $\mathbf{V}$ are respectively suitable augmented output and reference vectors so as to guarantee that, by invoking the implicit function theorem, the solution exists.

As already commented, major limits of this stand in its lack of robustness with respect to model uncertainties and sampling approximations and to the fact it works in open loop over time intervals of length T. How to improve its effectiveness? We propose to design a sampled-data single-rate control law, acting at all $t = k\delta$ and based on the corresponding sampled measures of the state, through a sampled-data MPC procedure that makes use of the intermediate reference output values y_k^i resulting from the application of the nominal control sequence computed from (6) to the MR-SD model (4). This reference is said to be admissible in the sense of the definition below.

Definition 3.1. A sampled-data reference sequence $\{v_k, k \geq 0\}$ is said to be admissible for (1) from $x_0 \in \mathbb{R}^n$ if, for a suitable integer $m \leq n$, equality (6) has a solution $\{u_k^i, i = 1, \ldots, m\}$ which remains bounded. It will be said SR or MR admissible if $m = 1$ or $m > 1$, respectively.

Note that, from Definition 3.1 a MR admissible sequence can be suitably enriched to be SR admissible, as suggested by the following result.

Theorem 3.1. Consider the system (1) and let $v(t)$ be a reference signal to be tracked at $t = kT$ for $k \to \infty$. Denote by $\{v_k = v(kT), k \geq 0\}$ the sequence of samples of the reference that is assumed to be MR admissible for a suitable $m > 1$ under the input sequence $\{\hat{u}_k^i, \quad k \geq 0, i = 1, \ldots, m\}$ solution to (6) for all $k \geq 0$. Let $\{\hat{y}_k^i, \quad k \geq 0, i = 1, \ldots, m\}$ be the augmented reference generated by $\hat{y}_k^1 = v_k$, and for, $i = 2, \ldots, m$, $\hat{y}_k^i = h(\hat{x}_k^i)$ with $\hat{x}_k^1 = x(kT)$ $\hat{x}_k^i = F^\delta(\hat{x}_k^{i-1}, \hat{u}_k^{i-1})$. Then, the unconstrained MPC problem defined via the cost (5) with $e_{k+i} = \hat{y}_k^i - y_k^i$ subject to the SR-SD model (2) admits a solution which is bounded for $n_p = n_c \geq m$ and $R = 0$.

Proof: Whenever $\{v_k, k \geq 0\}$ is admissible, then there exists a solution sequence $\{\hat{u}_k^i, \quad k \geq 0, i = 1, \ldots, m\}$ such that (6) is solved and s.t $y_{k+1} = v_{k+1}, k \geq 0$. Then applying the solution to (2), one gets $\hat{x}_k^i = F^\delta(\hat{x}_k^{i-1}, \hat{u}_k^{i-1})$ and correspondingly the intermediate output values $\hat{y}_k^i = h(\hat{x}_k^i)$. Setting $\delta = \frac{T}{m}$ this sequence is SR admissible by construction, and by Definition 3.1 there exists a sequence of controls such that $y(kT) = \hat{v}_k$, so implying feasibility. To show that the MPC optimization problem recovers this solution, one sets $n_p = n_c$ and the proof proceeds along the lines of (Elobaid et al., 2019a, Th.2, Prop.7). ◁

Note that the statement above does not assume that the reference can be tracked in continuous time, but merely that it is MR admissible. Given a reference $v(t)$ that system (1) can exactly track (in the sense of Isidori (2013)[Chapter 4]), then a fast sampling of this reference v_k is MR admissible, namely one can define $H(x) = (h(x), L_f h(x), \ldots, L_f^{r-1} h(x))^\top, \mathbf{V} = (\mathbf{v}, \dot{\mathbf{v}}, \ldots, \mathbf{v}^{(r-1)})^\top$ as in (Monaco and Normand-Cyrot, 1991) corresponding to which which (6) admits a solution. The following result can be hence given.

Corollary 3.1. Suppose system (1) is minimum-phase and has a well defined relative degree $r \leq n$, then equality (6) always admits a solution with a multi-rate of order $m \geq r$.

Proof: Since (1) has a well defined relative degree, then the input-output feedback linearization problem is solvable so that, under feedback and change of coordinates, (1) reads

$$\dot{z} = Az + Bv, \quad \dot{\eta} = q(z, \eta) + p(z, \eta)v$$

with $A, B, q(\cdot), p(\cdot)$ as in Isidori (2013)[Chapter 4]. Accordingly, the MR equivalent model of order $m \geq r$ is given by

$$z_{k+1} = A_m^T z_k + B_m^T \underline{v}_k, \quad \eta_{k+1} = \tilde{F}_m^T(z_k, \eta_k, \underline{v}_k) \tag{7}$$

with $A_m^T = (e^{A\delta})^m, B_m^T = \left[A_{sr}^{m-1} B_{sr} \ \ldots \ B_{sr}\right]$ and $A_{sr} = e^{A\delta}, B_{sr} = \int_0^\delta e^{A\delta} u(\tau) d\tau$ and $\tilde{F}_m^T(z_k, \eta_k, \underline{v}_k) = e^{\delta(\mathrm{L}_q + v_k^1 \mathrm{L}_p)} \ldots e^{\delta(\mathrm{L}_q + v_k^m \mathrm{L}_p)} x\big|_{(z_k, \eta_k)}$. In this setting, z_k corresponds to H so that (6) reduces to a linear map on the multi-rate inputs $\underline{v}_k$. Because B_m^δ is full rank by construction and because the relative degree is invariant under feedback, one gets the solution $\underline{\hat{v}}_k = (B_m^T)^{-1}(\mathbf{V}_{k+1} - A_m^\delta z_k)$. Moreover, by the fact that $\dot{\eta} = q(z, \eta) + p(z, \eta)v$ is stable, and combined with Theorem 3.1 and the arguments in Monaco and Normand-Cyrot (1988), one gets that the

planned trajectories are admissible for the overall dynamics over the small interval $\delta = \frac{T}{m}$. ◁

Theorem 3.1 applies to finitely discritizable systems.

4. PLANNING AND CONTROL ALGORITHM

In this section, and referring to the discussion above, we present in a detailed manner the control scheme for designing a sampled-data feedback $u_k = u(x_k)$ ensuring tracking of a given output profile at the sampling instants $t = kT$ for all $k \geq 0$ by exploiting a planned *admissible* trajectory generated via the MR model (4).
We assume that the dynamics (1) is finitely descritizable with $F_m^T(\cdot, \hat{u}_k^1, \ldots, \hat{u}_k^r)$ denoting the corresponding multi-rate finite model of order m (possibily computed under coordinate change and preliminary feedback).
The following algorithm is proposed by using the admissible sequence $\{\hat{y}_k^i, \quad i = 1, \ldots, m, \ k \geq 0\}$ defined in Theorem 3.1 as a reference trajectory for the MPC with $n_p = m$. Such a trajectory is computed and updated at all $t = kT$ based on the nominal multi-rate solution defined through (4). Thus, for all $t \in \{kT, kT + \delta, \ldots, kT + (m-1)\delta\}$ the planned reference sequence is fed to the MPC for computing the optimizing controller which is guaranteed to exist for $R \geq 0$ small enough by virtue of Theorem 3.1. Specifically, the algorithm works over the steps depicted in Algorithm 1.

Algorithm 1 Planning and control algorithm

Initialization:
$\mathbf{V}_a \leftarrow (v_{k+1}, v_{k+2})^\top$
$x_k \leftarrow x(kT), Q \leftarrow Q, R \leftarrow R, m \leftarrow m$
while $t \geq 0$ **do**
  if $t = (k+j)T, j \in \mathbb{Z}_{\geq 0}$ **then**
    $k \leftarrow k + j$
    $(\hat{y}_k, \hat{y}) = \text{Planning}(x_k)$
    $u_k = \text{Control}(m, Q, R)$
  else
    for $t = kT + i\delta, i = 1, \ldots, m-1$ **do**
      $u_k^i = \text{Control}(m, Q, R)$
procedure $(\hat{y}_k, \hat{y}_{k+1}) = \textsc{Planning}(x_k, \mathbf{V}_a)$
  $\hat{x}_k^1 \leftarrow x_k$

$$\begin{pmatrix} \hat{u}_k^1 \\ \vdots \\ \hat{u}_k^m \\ \vdots \\ \hat{u}_{k+1}^m \end{pmatrix} = \begin{pmatrix} (h \circ F_m^T)^{-1}(\hat{x}_k, v_{k+1}) \\ (h \circ F_m^T)^{-1}(\cdot, v_{k+2}) \circ (F_m^T)^{-1}(\hat{x}_k, v_{k+1}) \end{pmatrix} \quad (8)$$

  for $j = 0 : 1$ **do**
    for $i = 1 : m$ **do**
      $\hat{x}_{k+j}^{i+1} = F^\delta(\hat{x}_{k+j}^i, \hat{u}_{k+j}^i), \quad \hat{y}_{k+j}^i = h(\hat{x}_{k+j}^i).$
procedure $u_k^\star = \textsc{Control}(m, Q, R, \hat{y}_k^1, \ldots, \hat{y}_k^{n_p})$
  $n_p \leftarrow m$

$$u_k = \text{argmin}_{u_k} \quad \sum_{i=1}^{n_p} \left(\|\hat{y}_k^i - y_k^i\|_Q + \|u_k^{i-1}\|_R \right)$$

  $u_k^\star = u_k^1$

Remark 4.1. From the previous arguments, we only exploit the samples of the reference over two big steps (that is v_{k+1}, v_{k+2} and correspondingly setting in the MR planner (6) an augmented output vector $H_a(x) = (y_k, y_{k+1})^\top$). This is due to the fact that in the implementation of a receding horizon algorithm, we will need explicitly the values of the desired reference sequence over $n_p = m$ steps, and writing the second iteration of the MPC (i.e., at time $t = kT + \delta$), one notes the explicit dependence of the (optimal) control on values of the desired output trajectories at $\hat{y}_k^{m+1} = \hat{y}_{k+1}^1$.

Remark 4.2. The design the planner can be worked out on a simplified sampled-data model so to reduce the computational burden related to solve equality (8). When the conditions of Corollary 3.1 are met, the computations associated with the planner are simply the inversion of a matrix B_m^T which is full rank by construction. Consequently, as shown in the case study, one in principle uses a simplified finite model for the planner, while a more exhaustive one is employed by MPC for prediction.

Remark 4.3. The proposed control scheme inherits the nominal robustness properties of MPC (e.g. Grimm et al. (2007); Picasso et al. (2010); Grimm et al. (2004)). This will be further demonstrated in the following case study.

5. THE PVTOL AS A CASE STUDY

Let the model of the PVTOL (planar vertical take-off and landing) aircraft take the form:

$$\begin{aligned} \ddot{x} &= -sin(\theta)v_1 + \epsilon cos(\theta)v_2 \\ \ddot{z} &= cos(\theta)v_1 - 1 + \epsilon sin(\theta)v_2 \\ \ddot{\theta} &= v_2 \end{aligned} \quad (9)$$

with output $y = h(x, \dot{x}, z, \dot{z}, \theta, \dot{\theta}) = (x, z)^\top$.

5.1 Construction of the simplified MR planner model

To use our control scheme, we first define the multi-rate sampled-data model of the PVTOL. To this end, it is known (e.g. Di Giamberardino and Djemai (1994)) that (9) is feedback equivalent to a finitely discretizable system, by setting

$$v = \begin{pmatrix} \frac{1}{cos\theta} + \varepsilon\dot{\theta}^2 \\ -2\dot{\theta}^2 \tan\theta \end{pmatrix} + \begin{pmatrix} \frac{1}{cos\theta} & 0 \\ 0 & \cos^2\theta \end{pmatrix} u$$

together with the coordinates change

$$\zeta = \varphi(x, \dot{x}, z, \dot{z}, \theta, \dot{\theta}) = \epsilon\varphi_1(\cdot) + \varphi_2(\cdot)$$

with $\varphi_1(\cdot) = \begin{pmatrix} \cos\theta & -\dot{\theta}\sin\theta & 0 & -\sin\theta & 0 & -\dot{\theta}\cos\theta \end{pmatrix}^\top$, $\varphi_2(\cdot) = \begin{pmatrix} z & \dot{z} & \tan\theta & x & \frac{\dot{\theta}}{\cos^2\theta} & \dot{x} \end{pmatrix}^\top$, thus obtaining

$$\dot{\zeta} = \tilde{f}(\zeta) + \tilde{g}_1(\zeta)u_1 + \tilde{g}_2(\zeta)u_2$$

$$\tilde{f}(\zeta) = \begin{pmatrix} \zeta_2 & 0 & \zeta_5 & \zeta_6 & 0 & -\zeta_3 \end{pmatrix}^\top, \tilde{g}_1(\zeta) = \begin{pmatrix} 0 & 1 & 0 & 0 & 0 & -\zeta_3 \end{pmatrix}^\top$$

$$\tilde{g}_2(\zeta) = \begin{pmatrix} 0 & 0 & 0 & 0 & 1 & 0 \end{pmatrix}^\top$$

A multi-rate of order 2 on u_1 and 4 on u_2 can be employed to ensure the invertibility of the sampled-data dynamics. Explicitly writing

$$u_1(t) = u_1^j(k),\ t \in [(k + \frac{j-1}{2})T, (k + \frac{j}{2})T[,\ j = 1, 2$$

$$u_2(t) = u_2^j(k),\ t \in [(k + \frac{j-1}{4})T, (k + \frac{j}{4})T[,\ j = 1, 2, 3, 4.$$

and developing the calculations and rearranging the terms, we obtain the MR SD equivalent model of the PVTOL as:

$$\begin{aligned}\zeta_{k+1} &= (A^\delta + B_1^\delta(u_1^2))^2(A^\delta + B_1^\delta(u_1^1))^2\zeta_k \\ &+ (A^\delta + B_1^\delta(u_1^2))^2(I + B_1^\delta(u_1^1))B_0^\delta(u_1^1, u_2^1) \\ &+ (A^\delta + B_1^\delta(u_1^2))^2 B_0^\delta(u_1^1, u_2^2) \\ &+ (I + B_1^\delta(u_1^1))B_0^\delta(u_1^2, u_2^3) + B_0^\delta(u_1^2, u_2^4)\end{aligned} \tag{10}$$

with $\zeta_k = \varphi(x_k, \dot{x}_k, z_k, \dot{z}_k, \theta_k, \dot{\theta}_k)$ for all $k \geq 0$ with

$$A^\delta = \begin{pmatrix} 1 & \delta & 0 & 0 & 0 & 0 \\ 0 & 1 & 0 & 0 & 0 & 0 \\ 0 & 0 & 1 & 0 & \delta & 0 \\ 0 & 0 & -\frac{\delta^2}{2} & 1 & -\frac{\delta^3}{6} & \delta \\ 0 & 0 & 0 & 0 & 1 & 0 \\ 0 & 0 & -\delta & 0 & -\frac{\delta^2}{2} & 1 \end{pmatrix}, B_0^\delta(v, w) = \begin{pmatrix} \frac{\delta^2 v}{2} & \delta v \\ \frac{\delta^2 w}{2} & \\ \frac{-\delta^4(1+v)w}{24} & \\ \frac{\delta w}{} & \\ \frac{-\delta^3(1+v)w}{6} & \end{pmatrix}$$

$$B_1^\delta(v) = \begin{pmatrix} & \mathbf{0}_{3\times 6} & \\ -\frac{\delta^2}{2}v & 0 & -\frac{\delta^3}{6}v \ 0 \\ \mathbf{0}_{3\times 2} \quad 0 & 0 & 0 \quad 0 \\ -\delta v & 0 & -\frac{\delta^2}{2}v \ 0 \end{pmatrix}$$

with $\delta \geq 0$ being the sampling period and $T = 4\delta$. The model (10) will be used for planning the admissible reference trajectories.

5.2 Planning and control

For all $t = kT$, planning of the intermediate output references is made on the basis of the simplified equivalent model (10). Hence one gets for all $t = kT + (i-1)\delta$, an admissible sequence $(\hat{x}^i_{k+j}, \dot{\hat{x}}^i_{k+j}, \hat{z}^i_{k+j}, \dot{\hat{z}}^i_{k+j}, \hat{\theta}^i_{k+j}, \dot{\hat{\theta}}^i_{k+j})^\top = \varphi^{-1}(\hat{\zeta}^i_k)$, and thus the intermediate reference output values $\{(\hat{x}^i_{k+j}, \hat{z}^i_{k+j}), \quad i = 1, 2, 3, 4 \text{ and } j = 0, 1\}$ for system (9). Consequently, for all $t = kT + (i-1)\delta$, the MPC computes the feedback u^i_k (for $i = 1, \ldots, 4$) with the sampled-data SR model of the PVTOL (in the form (2)) used for prediction. This feedback is then applied to the simulation model of system (9) while recomputing the reference for all $t = kT$.

5.3 Simulations

In the following we will compare the proposed control algorithm (denoted MR-MPC) to the stand-alone MPC with the trajectory planner proposed by Luigi Biagiotti (2019) (denoted FIR-MPC). Figure 1 depicts the nominal scenario (with no external perturbations nor model uncertainties), while in Figure 2 actuator disturbances as well as uncertainties on the parameter ϵ are considered. In all simulations $\delta = 1$ seconds while $n_p = n_c = 4$ seconds and $Q = \mathrm{I}$. Both schemes will utilize a sequential quadratic programming SQP based optimization solver. Time varying references are fixed on both the lateral and vertical displacements (that is x, z respectively) as a ramp signal (shown in black) with velocity $v_0 = 1$ m/s to be tracked at $t = kT, T = 4\delta$.

It results that the proposed control algorithm favourably compares to the FIR-MPC.

In the nominal case (Figure 1), we set $R = 0$. Contrarily to the MR-MPC scheme, the FIR-MPC is unable to follow the reference over the sampling steps δ and an off-set is evident. While the number of iterations in each instant to compute the minimizer is slightly more in the MR-MPC case, the minimum obtained is lower, namely it is $V_{n_p} = 0$ compared to 0.5 obtained by the FIR-MPC.

In Figure 2, $R > 0$ and a white noise is added on the actuation signal. In addition the parameter $\epsilon = 0.5$ in the simulation model, while the nominal value $\epsilon = 0.8$ is used to construct the planner and the prediction model for the MPC. In this case as well, the proposed algorithm is able to track the reference over the big intervals T, despite the effect of uncertainties being evident (although acceptable i.e. $|\theta| \leq 0.1$ rads) in the internal dynamics. Note also that while the number of iterations required to obtain the minimum is comparable between the two algorithms, the value function was still lower $V_{n_p} = 0.08$ for MR-MPC compared to 0.1 for FIR-MPC. Further simulations are reported in Elobaid et al. (2019b) comparing the MR-MPC with FIR-MPC and stand-alone MR control in different situations.

6. CONCLUSIONS

We establish an intuitive implementation of sampled-data tracking control through multi-rate planning utilizing discrete time nonlinear single-rate MPC for reference tracking. This is done by highlighting the role played by ensuring the availability of good and admissible references to the MPC controller so to improve the effectiveness of the two stand-alone design methodologies. Future works concern the study of the effect of incorporating constraints on the control, on the benefits incurred by the proposed scheme.

REFERENCES

Åström, K., Hagander, P., and Sternby, J. (1984). Zeros of sampled systems. *Automatica*, 20(1), 31 – 38.

Bemporad, A. and Morari, M. (1999). Robust model predictive control: A survey. In *Robustness in identification and control*, 207–226. Springer.

Byun, D.G. (1988). Predictive control: A review and some new stability results. *IFAC Proceedings Volumes*, 21(4), 81 – 87. IFAC Workshop on Model Based Process Control, Atlanta, GA, USA, 13-14 June.

Camacho, E.F. and Alba, C.B. (2013). *Model predictive control*. Springer Science & Business Media.

Di Giamberardino, P. and Djemai, M. (1994). Multirate digital control of a pvtol. In *Proc. 33th CDC*, 3844–3849.

Elobaid, M., Mattioni, M., Monaco, S., and Normand-Cyrot, D. (2019a). On unconstrained mpc through multirate sampling. *IFAC-PapersOnLine*, 52(16), 388–393.

Elobaid, M., Mattioni, M., Monaco, S., and Normand-Cyrot, D. (2019b). Sampled-data tracking under model predictive control and multirate planning: further simulations and remarks. Technical report, DIAG, Università degli Studi di Roma La Sapienza. URL `https://hal.archives-ouvertes.fr/hal-02365409`.

García, C.E., Prett, D.M., and Morari, M. (1989). Model predictive control: Theory and practice—a survey. *Automatica*, 25(3), 335 – 348.

Grimm, G., J. Messina, M., E. Tuna, S., and R. Teel, A. (2004). Examples when model predictive control is non-robust. *Automatica*, 40, 1729–1738.

Grimm, G., Messina, M.J., Tuna, S.E., and Teel, A.R. (2007). Nominally robust model predictive control with state constraints. *IEEE Transactions on Automatic Control*, 52(10), 1856–1870.

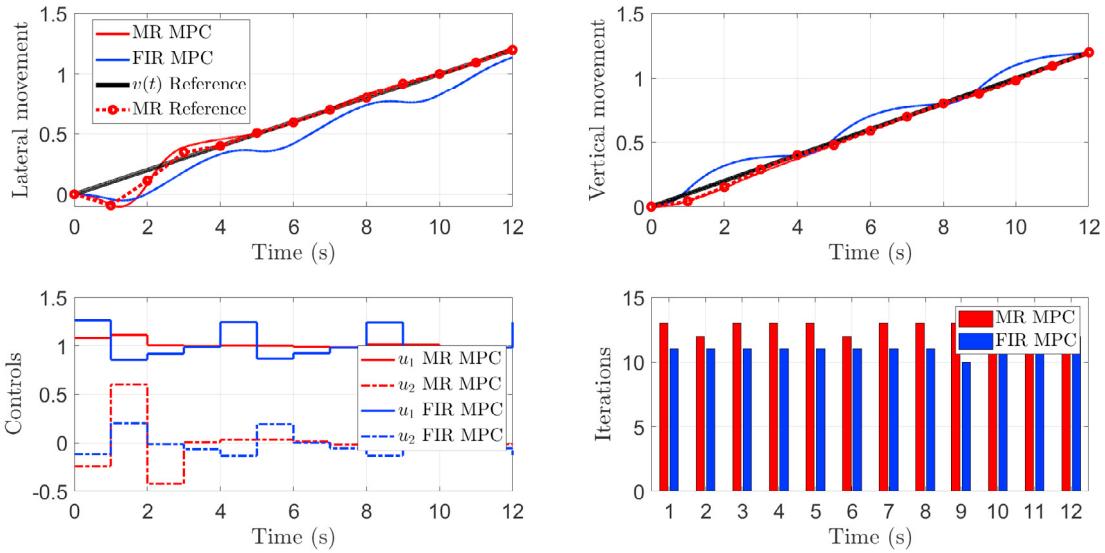

Fig. 1. Nominal tracking, $R = 0, Q = \mathrm{I}$

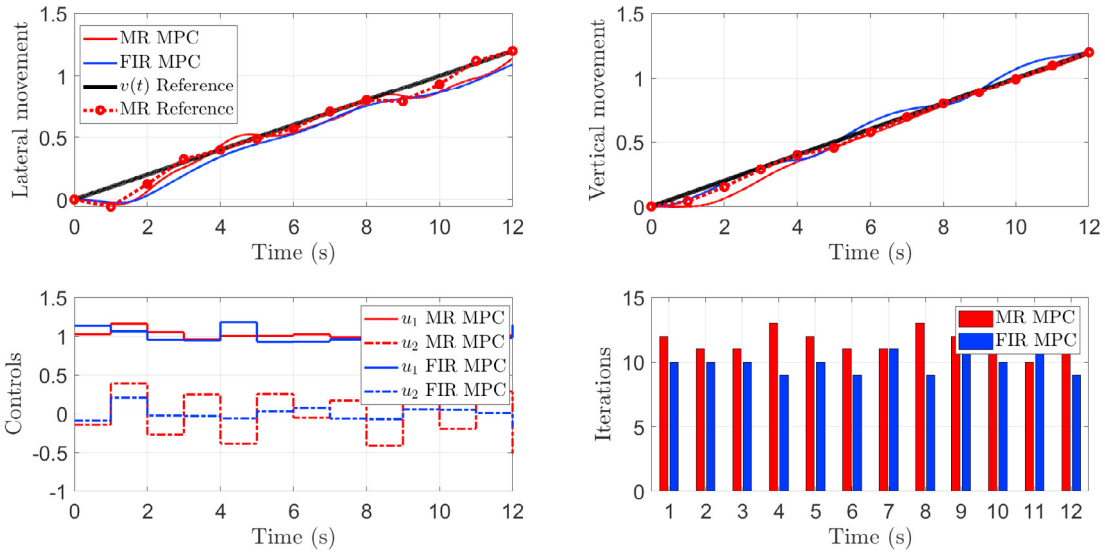

Fig. 2. Perturbed tracking, $\epsilon = 0.5, R = 0.5\mathrm{I}, Q = \mathrm{I}$ and white actuation noise with mean 10^{-3}

Isidori, A. (2013). *Nonlinear control systems*. Springer Science & Business Media.

Luigi Biagiotti, C.M. (2019). Trajectory generation via fir filters: A procedure for time-optimization under kinematic and frequency constraints. *Control Engineering Practice*, 87, 43 – 58.

Magni, L., Raimondo, D.M., and Allgöwer, F. (2009). Nonlinear model predictive control. *Lecture Notes in Control and Information Sciences*, (384).

Mattioni, M., Hassan, M., Monaco, S., and Normand-Cyrot, D. (2017). On partially minimum phase systems and nonlinear sampled-data control. In *2017 IEEE 56th Annual Conference on Decision and Control (CDC)*, 6101–6106.

Monaco, S. and Normand-Cyrot, D. (1988). Zero dynamics of sampled nonlinear systems. *Systems & control letters*, 11(3), 229–234.

Monaco, S. and Normand-Cyrot, D. (1991). Multirate sampling and zero dynamics: from linear to nonlinear. In *Nonlinear Synthesis*, 200–213. C. Byrnes, A. Isidori Eds., Birkauser.

Monaco, S. and Normand-Cyrot, D. (2001). Issues on nonlinear digital systems. *Semi-Plenary Conference, European Journal of Control*, 7(2-3), 160–178.

Monaco, S. and Normand-Cyrot, D. (1992). An introduction to motion planning using multirate digital control. 1780 – 1785 vol.2.

Picasso, B., Desiderio, D., and Scattolini, R. (2010). Robustness analysis of nominal model predictive control for nonlinear discrete-time systems. *IFAC Proceedings Volumes*, 43(14), 214 – 219. 8th IFAC Symposium on Nonlinear Control Systems.

Chapter 6

Application to halo orbits stabilization

Contents

BUILDING on the discussions found in the previous chapter, and having seen the benefit of using multi-rate sampling at the planning level of an MPC controller, this chapter will give a more complete case study. Referencing a constrained nonlinear MPC problem, Halo orbits station keeping under digital control is studied. In this instant a simplified, under an *assumed* regulation feedback, multi-rate model of the plant are used as trajectory generators. And while no theoretical guarantees on the equivalence to inversion and stability of the closed loop are provided due to the presence of state constraints, nonetheless better performances are achieved compared to a host of control techniques from the literature.

The notions appearing hereinafter are recalled and elaborated on based on the *contributions* found in

> Mohamed Elobaid, Mattia Mattioni, Salvatore Monaco and Dorothée Normand-Cyrot. *"Station-keeping of L_2 halo orbits under sampled-data model predictive control". Journal of Guidance, Control, and Dynamic, 2022 to appear.*

This chapter will conclude Part II with some remarks concerning the general constrained case, its equivalence to inversion at the limit of cheap control requirement, and ways to incorporate sampled-data methodologies in handling such situations. Indeed, this chapter, and the previous two, merely constitute an introduction into looking at ways that leverage the available and rich sampled-data tools to handle in tracking nonlinear MPC at large. And with the detailed applications provided in this chapter hopefully the reader will appreciate the practical validity of such ideas.

Introduction and context

The dynamics of a spacecraft in the Earth-Moon gravitational system (the so-called Restricted Three-Body Problem (RTBP) Poincaré (1893); Barrow-Green (1997)) exhibit equilibria commonly

known as Libration (or Lagrangian) points. This makes Lagrangian points excellent locations for spacecrafts in exploration applications Farquhar (1970). Among those the so-called *translunar* Libration point L_2 has been attracting particular interest for various satellite communication applications Wu et al. (2018) and deep space observation and exploration purposes Farquhar (1971) as also testified by the numerous space missions that have already taken place (e.g., NASA's ARTEMIS Woodard et al. (2009) and CNSA's Chang'e 5-T1 Harvey (2019)) and new ones are in schedule Bobskill and Lupisella (2012).

However, keeping a spacecraft close to L_2 requires an active control action because, as well-known, it is an unstable equilibrium point as are most equilibrium trajectories within the Halo family of orbits around it Gómez et al. (2001); Zimovan-Spreen et al. (2020). In this respect, several control design methods have been proposed throughout the last decades for stabilizing Halo orbits while mitigating the effect of perturbations and unmodelled dynamics (see Shirobokov et al. (2017) for a complete survey, and Howell and Pernicka (1993) for an earlier work). Among these and related to this work, the most important ones are based on optimization Simó et al. (1987); Folta and Vaughn (2004); Breakwell et al. (1974); Folta et al. (2014); Ulybyshev (2015); Rahmani et al. (2003); Bando and Ichikawa (2015), receding horizon Kalabic et al. (2015); Misra et al. (2018) and advanced nonlinear design (e.g. projection to the stable manifold Zhang and Li (2019), feedback linearization, nonlinear regulation Di Giamberardino and Monaco (1996) and backstepping Qi and de Ruiter (2019)). In the majority of the aforementioned works, a circular RTBP model is used to describe the dynamics of a spacecraft so neglecting the primaries motion perturbations whose effect, however, cannot be discarded in practice. Only few works consider the more realistic elliptic RTBPs in which the eccentricity is not zero (e.g. Farquhar (1970); Di Giamberardino and Monaco (1996)) possibly making use of ephemeris models considering the solar radiation pressure and other gravitational perturbations (e.g. Qi and de Ruiter (2019)).

In the sequel, we provide a new control scheme assuming the so-called elliptic RTBP model under the influence of solar radiation pressure which captures the principal feature of the dynamics while retaining simplicity Shirobokov et al. (2017). In addition, a modified model predictive control approach is proposed to cope with real-time implementation issues as, for instance, the digital nature of both actuation and sensing and possible limits on control, unavoidable in practice. In particular, we consider the case in which measures are available only at sporadic time instants whereas the control is piecewise constant over the sampling period (e.g. Celsi et al. (2015)). The approach we propose is based on the design of multi-rate (MR) strategies at the planning level providing a suitable reference governor for a model-predictive control (MPC) control scheme. The resulting control system enables to overcome the limits of small prediction horizons underlined in Misra et al. (2018), when the controller is designed under usual MPC. As a matter of fact, such limits would bring to unfeasible controllers for small prediction horizons when the design makes use of a the sampled-data model, due to the cancellation of the possibly unstable zero-dynamics under sampling Elobaid et al. (2019). Also, the use of large prediction horizons, typically used as a stratagem in practice, might introduce large computational delays.

This work is contextualized in this framework by proposing a new sampled-data MPC control scheme where the problem is simplified. This is achieved by generating a suitable reference trajectory based on a multi-rate planner which guarantees stability of the closed loop and feasibility of the optimization problem solved, at each step, by the MPC assuming cheap control. In particu-

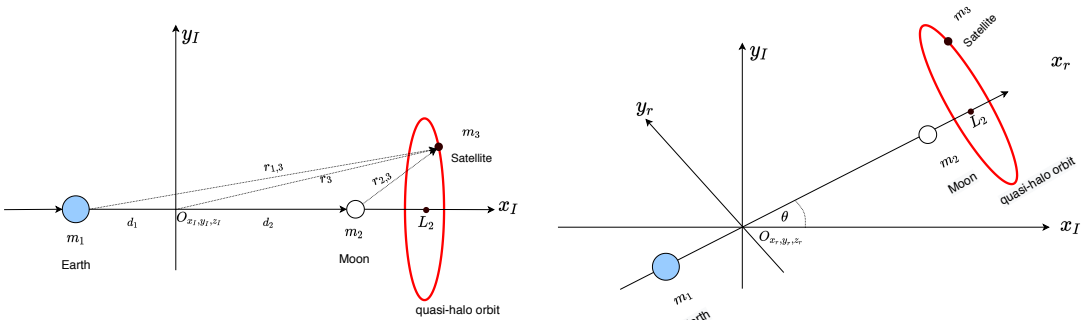

(a) Basic quantities in the inertial reference frame **(b)** Rotating frame

Figure 6.1: Figure showing the rotating and inertial reference frame in the EM three body system

lar, such a planner is designed starting from the nonlinear regulation-based controller proposed in Di Giamberardino and Monaco (1996) which yields, by construction, admissible and bounded trajectories which can be then fed to the MPC as reference to track. In this context, the contribution of this paper stands in the proposition of a new control scheme which employs at the low level an inherently robust nonlinear MPC fed by a references generated by a multi-rate sampled-data model of a control system designed making use of nonlinear regulation.

The choice of the proposed control scheme is motivated by the observation that MPC and nonlinear regulation can be employed together to mitigate each the deficiencies of the other: nonlinear regulation appears to be the natural context for setting the problem since the references and perturbations are periodic although it lacks in robustness to unmodelled disturbances; MPC is becoming a standard tool for handling tracking applications, it is inherently robust to bounded perturbations Grüne and Pannek (2017) despite it requiring reference signals pre-processing to guarantee convergence and recursive feasibility. Thus, the implementation of a nonlinear MPC fed by samples of a reference signal generated by the sampled-data model of the controlled circular RTBP under nonlinear regulation provides a natural solution.

6.1 Modelling and problem statement

The mathematical model describing the motion of a satellite under the gravitational pull of both the earth and moon referred in the current literature (see Shirobokov et al. (2017) and the references therein) takes the form:

$$\begin{aligned}
\ddot{x} - u_1 - 2\dot{y}(1+\beta(t)) - x(1+2\beta(t)+\beta(t)^2) - y\dot{\beta}(t) &= -\frac{(1-\mu)(x+\mu(1+\alpha(t)))}{r_1} \\
&\quad - \frac{\mu(x-(1-\mu)(1+\alpha(t)))}{r_2} + \frac{G_{sc}}{c}\cos^2(\zeta t) \\
\ddot{y} - u_2 + 2\dot{x}(1+\beta(t)) - y(1+2\beta(t)+\beta(t)^2) - x\dot{\beta}(t) &= -\frac{(1-\mu)y}{r_1} - \frac{\mu y}{r_2} + \frac{G_{sc}}{c} sin^2(\zeta t) \\
\ddot{z} - u_3 &= -\frac{(1-\mu)z}{r_1} - \frac{\mu z}{r_2}
\end{aligned} \tag{6.1}$$

where, with reference to Fig. 6.1: $x\,, y\,, z$ are the distance normalized[1] coordinates of the planetoid expressed in the rotating frame when the eccentricity e is assumed to be zero; $u_1\,, u_2\,, u_3$ are three axis thrusts in the corresponding direction, $\alpha(t)$ and $\beta(t)$ are periodic functions with zero mean value admitting the form of a series expansion in e given by

$$\alpha(t) = -e\cos(t+\phi) + 0.5e^2(1+\cos(2t+2\phi)) + O(e^3) \tag{6.2}$$

$$\beta(t) = 2e\cos(t+\phi) + 2.5e^2\cos(2t+2\phi) + O(e^3) \tag{6.3}$$

m_1, m_2 are the masses of the earth and moon respectively, and $\mu = \frac{m_2}{m_1+m_2}$; $r_i = \frac{|r_{i,3}|}{\|r_{i,3}\|^3}, i = 1,2$ are the norms, in the distance normalized rotating frame, of the vectors from the earth to the planetoid, and the moon to the planetoid respectively; G_{sc} is the solar constant and c the speed of light and $\frac{G_{sc}}{c} \approx 4.5^{-3} N/m^2$; finally $\zeta \approx 0.9252$ is the angular rate of the sun light line in non-dimensional units.

Some comments about the validity of the model are in order; as usual, in (6.1) it is assumed that the solar radiation pressure (SRP) is constant in magnitude throughout the earth-moon system. In addition, assuming the primaries (earth and moon) move in a circular path around the barycenter, one can set $\alpha(t) = \beta(t) = 0$ and the model above reduces to the well known approximated Circular Restricted Three Body Problem (CRTBP) model. The periodic functions $\alpha(t)$ and $\beta(t)$ are indeed used to capture the effect of eccentricity of the orbits. This effect is used to get better approximations, in the normalized coordinates, of the distance between earth and moon $d(t)$ and the angular rate of change between the rotating and inertial frame $\dot{\theta}(t)$. A reliable Elliptic Restricted Three Body Problem (ERTBP) model for our problem is obtained assuming $e \approx 0.0549$.

The motion equations (6.1) can be re-written in the control affine perturbed state-space form

$$\begin{aligned} \dot{q} &= f(q,\xi) + B(u+D) \\ p &= h(q) = Cq \end{aligned} \tag{6.4}$$

with

$$f(q,\xi) = \begin{bmatrix} f_1(q) \\ f_2(q,\xi) \end{bmatrix}, \quad f_1(q) = \begin{bmatrix} 0_{3\times 3} & I_3 \end{bmatrix} q, \quad B = \begin{bmatrix} 0_{3\times 3} \\ I_3 \end{bmatrix}, \quad C = \begin{bmatrix} I_3 & 0_{3\times 3} \end{bmatrix}$$

$$f_2(q,\xi) = -Mp - 2N\dot{p} - \xi_1(2Mp + 2N\dot{p}) - \xi_2 Mp - \xi_3 N\dot{p} - \frac{1-\mu}{\|p-d_1\|^3}(p-d_1) - \frac{\mu}{\|p-d_2\|^3}(p-d_2)$$

$$M = \begin{bmatrix} -1 & 0 & 0 \\ 0 & -1 & 0 \\ 0 & 0 & 0 \end{bmatrix}, \quad N = \begin{bmatrix} 0 & -1 & 0 \\ 1 & 0 & 0 \\ 0 & 0 & 0 \end{bmatrix}, \quad d_1 = \begin{bmatrix} -\mu - \frac{\xi_4}{1-\mu} \\ 0 \\ 0 \end{bmatrix}, \quad d_2 = \begin{bmatrix} 1-\mu+\frac{\xi_4}{\mu} \\ 0 \\ 0 \end{bmatrix}$$

where $p = (x\ y\ z)^T \in \mathbb{R}^3$ specifies the output, $q := (q_1\ \ldots\ q_6)^\top = (p^\top\ \dot{p}^\top)^\top \in \mathbb{R}^6$ the state, $u \in \mathbb{R}^3$ the control input,

$$\xi(t) = \begin{pmatrix} \beta(t) & \beta^2(t) & \dot{\beta}(t) & \mu(1-\mu)\alpha(t) \end{pmatrix}^\top \in \mathbb{R}^4 \tag{6.5}$$

[1] Following Farquhar (1970), the average distance between earth and moon is normalized (i.e., $d(t) = d_1(t) + d_2(t) = 1$) as well as the sum of masses of earth and moon (i.e., $m_1 + m_2$) and the average angular rate of change $\dot{\theta}(t)$ between the rotating and inertial frame.

and the vector of the eccentricity perturbation and the Solar Radiation Pressure (SRP)

$$D(t) = \begin{bmatrix} \frac{G_{sc}}{c}\cos^2(\zeta t) \\ \frac{G_{sc}}{c}\sin^2(\zeta t) \\ 0 \end{bmatrix}.$$

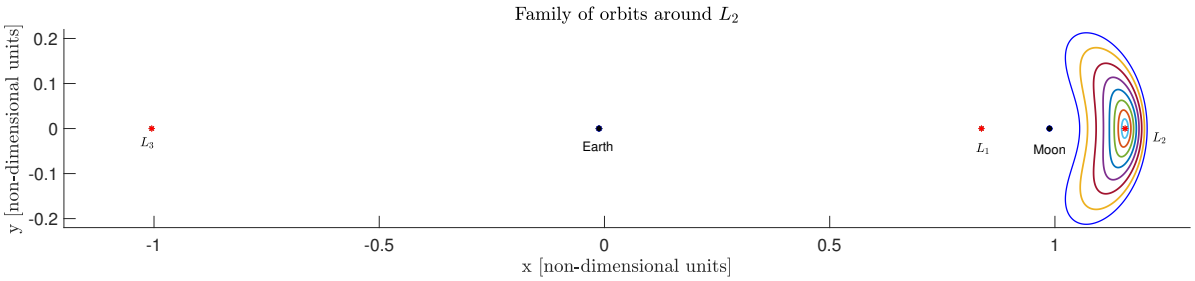

Figure 6.2: Family of Lyapunov planar orbits around the translunar point L_2.

When setting $\xi = 0_{4\times1}$, $D(t) = 0_{3\times1}$, the dynamics (6.1) reduces to the so-called circular RTBP model. In that case, the resultin dynamics possesses five equilibria with fixed location on the rotating frame and usually denoted by L_i, with $i = 1, \dots, 5$. Among these, L_1, L_2 and L_3 are the so-called collinear points with the corresponding x coordinates, in the distance normalized rotating frame, given by $L_3 = -1.0050627, L_1 = 0.8369147$, $L_2 = 1.155682$. As shown in Richardson (1980); Doedel et al. (2007) (see also Carletta et al. (2019); Gurfil and Meltzer (2007) for comments on the circular and elliptic RTBP cases respectively), the solutions of (6.4) close to the collinear equilibria, when suitably initialized, are periodic in nature as also underlined by the corresponding linear tangent model of (6.1).

The quasi-halo orbit model and L_2-station keeping

When neglecting external signals (i.e., $D = u = 0_{3\times1}$), the linear tangent model of (6.4) at $q^\star = (L_2\ 0\ 0\ 0\ 0\ 0)^\top$ gets the form

$$\dot{q} = Aq, \quad A = \begin{bmatrix} 0_{3\times3} & I_3 \\ A_{2,1} & A_{2,2} \end{bmatrix}, \quad A_{2,1} = \begin{bmatrix} 1+2\eta & 0 & 0 \\ 0 & 1-\eta & 0 \\ 0 & 0 & -\eta \end{bmatrix}, \quad A_{2,2} = \begin{bmatrix} 0 & 2 & 0 \\ -2 & 0 & 0 \\ 0 & 0 & 0 \end{bmatrix} \tag{6.6}$$

with $\eta = \frac{1-\mu}{(L_2+\mu)^3} + \frac{\mu}{(L_2-1+\mu)^3} = 3.194075$. Because A possesses periodic modes, for a suitable set of initial conditions $q_0 \in \mathbb{R}^6$, (6.6) admits periodic and bounded solutions of the form $q(t) =$

$(\nu(t)\ \dot{\nu}(t))^\top$ Richardson (1980) with

$$\nu(t) = \left[-\frac{k(1-\eta+\Omega^2)}{2\Omega}\cos(\Omega t+\phi) \quad k\sin(\Omega t+\phi) \quad k\cos(\Omega_z t)\right]^\top. \tag{6.7}$$

where, in addition, k being a constant depending on the initial displacement from L_2, ϕ a phase angle and Ω, Ω_z the in-plane and out-of-plane natural frequencies. It is assumed that $\Omega = \Omega_z = 1.8636$ for guaranteeing visibility from Earth. In addition, when simulating, ϕ is set to zero.

Expression (6.7) defines a *quasi* Halo orbit that is an approximate circular orbit in 3D centered around L_2. In this sense, the objective is to drive and maintain the satellite onto such an orbit. Formally, the control objective consists in designing a feedback law ensuring tracking of the quasi halo orbit described by (6.7) (i.e., that $p(t) \to \nu(t)$ as $t \to \infty$). In the concerned literature (e.g., Shirobokov et al. (2017) and references therein) such a problem is commonly referred to as *station-keeping* of the L_2 orbit and has found, as already mentioned, numerous solutions under different working assumptions. However none of them considers, at the same time, issues arising from both digital implementation of the control laws and the effect of unmodelled perturbations over the closed loop as formally set here below.

With this in mind and assuming the general case of thrusts inputs to be piecewise constant over the sampling period, we can now formally state the problem under investigation.

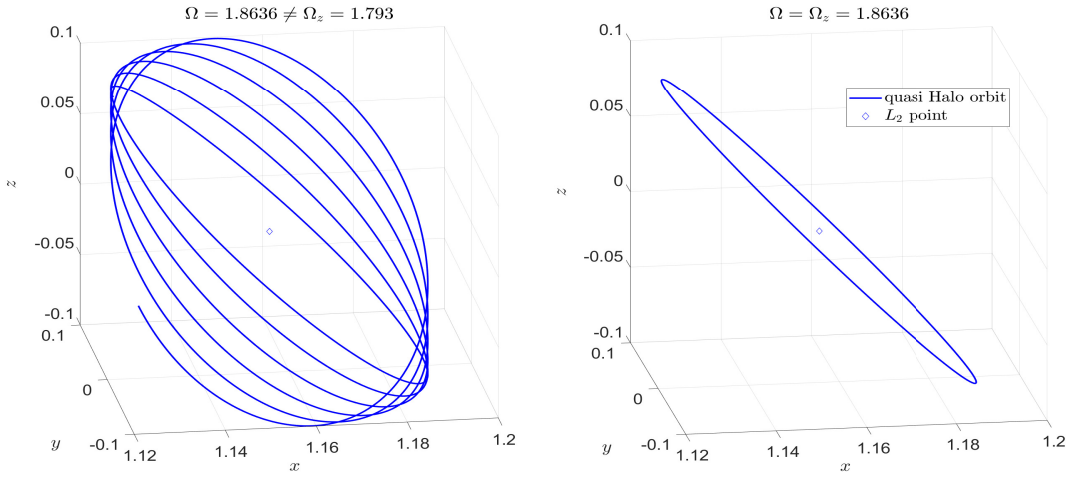

Figure 6.3: Approximated quasi Halo orbits around the translunar point L_2

Problem: station-keeping under digital control

Consider a spacecraft whose dynamics around L_2 is described by (6.4). Let measures of the state be available at periodic sampling instants $t = k\delta, k \in \mathbb{Z}_{\geq 0}$, with δ the sampling period, and the thrusts input be piecewise constant over δ that is, $u(t) = u(k\delta) = u(k)$ for $t \in [k\delta, (k+1)\delta[$. Design a piecewise constant control $u(k) = \gamma(q(k), \nu(k))$ such that the position of the satellite approaches and stays on the quasi-Halo orbit reference (6.7) at all sampling instants $t = k\delta$, $k \geq 0$; namely, $p(k\delta) \to \nu(k\delta)$ as $k \to \infty$.

Several solutions were found in the literature to the problem above when assuming, in most cases, a continuous control signal (i.e., $\delta \to 0$). The most relevant to the purpose of this paper are

recalled here below whereas the interested reader is referred to Shirobokov et al. (2017) for a more in deep discussion.

6.2 Background material on station-keeping techniques

Continuous-time nonlinear regulation for Halo orbits stabilization

When neglecting the effects of the SRP, a good solution to the L_2-station-keeping control is achieved under regulation by fixing the exosystem as

$$\dot{\omega} = S\omega \tag{6.8a}$$
$$\xi = T_\xi \omega \tag{6.8b}$$
$$\nu = T_\nu \omega \tag{6.8c}$$

with $\omega \in \mathbb{R}^4$ and

$$S = \begin{bmatrix} S_1 & 0_{2\times 2} \\ 0_{2\times 2} & S_2 \end{bmatrix}, \; S_1 = \begin{bmatrix} 0 & -1 \\ 1 & 0 \end{bmatrix}, \; S_2 = \Omega S_1, \tag{6.9}$$

$$T_\nu = \begin{bmatrix} & -\frac{k(1-\eta+\Omega^2)}{2\Omega} & 0 \\ 0_{3\times 2} & 0 & k \\ & k\cos\phi & k\sin\phi \end{bmatrix}, \quad T_\xi = \begin{bmatrix} 2 & 0 & \\ 0 & 0 & \\ 0 & -2 & 0_{4\times 2} \\ -\mu(1-\mu) & 0 & \end{bmatrix} e. \tag{6.10}$$

The so-defined exosystem dynamically generates, when setting the initial condition

$$\omega_0 = \begin{pmatrix} \cos\phi & \sin\phi & \cos\phi & \sin\phi \end{pmatrix}^\top$$

the external signals feeding (6.4) and, in particular, the quasi Halo orbits (6.7), the reference trajectories to track, and the periodic eccentricity perturbations (6.8b) to asymptotically reject.

As the intuition suggests, the exosystem satisfies the internal model principle Francis and Wonham (1976) so that the problem reduces to stabilizing the internally admissible trajectory (6.8c) while negating the effect of the eccentricity perturbations (6.8b); namely, one seeks for a control law ensuring the regulation error falls to zero asymptotically, i.e.,

$$e(t) = Cq(t) - T_\nu \omega(t) \to 0 \text{ as } t \to \infty.$$

This argument is at the basis of the controller proposed in Di Giamberardino and Monaco (1996) deduced by assuming $\xi(t) \approx 0$ and approximating (6.4) as

$$\dot{q} = f_0(q) + P(q)\xi + Bu \tag{6.11}$$

with

$$f_0(q) = f(q, 0), \quad P(q) = \frac{\partial f}{\partial \xi}\Big|_{\xi=0}.$$

In this way, one gets the feedback law

$$u = c(\omega) + K(q - \pi(\omega)) \tag{6.12}$$

with: $\pi : \mathbb{R}^4 \to \mathbb{R}^6$ and $c : \mathbb{R}^4 \to \mathbb{R}^3$, solutions to the Francis-Byrnes-Isidori equations **??**,

$$\begin{aligned} \frac{\partial \pi(\omega)}{\partial \omega} S\omega &= f_0(\pi(\omega)) + P(\pi(\omega))\omega + Bc(\omega) \\ 0 &= C\pi(\omega) - T_\nu \omega, \end{aligned}$$

given by

$$\pi(\omega) = \Pi\omega, \quad \Pi = \begin{bmatrix} T_\nu \\ T_\nu S \end{bmatrix}, \quad c(\omega) = -\begin{bmatrix} 0_{3\times 3} & I_3 \end{bmatrix} \Big(f_0(\pi(\omega)) + P(\pi(\omega)) T_\xi \omega \Big) + \Pi S \omega \tag{6.13}$$

with K ensuring $\sigma(A + BK) \subset \mathbb{C}^-$, $A = \frac{\partial f_0(q)}{\partial q}\Big|_{q=q^\star}$. In Di Giamberardino and Monaco (1996), this control was shown to provide good results both in terms of quasi-Halo orbit station-keeping error (also when considering higher order terms in (6.2)) and energy expenditure in the sense of $\|u(t)\|$ in the nominal case of $D(t) = 0$. However, such a controller lacks in robusteness with respect to unmodelled uncertainties (e.g., the effect of the SRP) and digital implementation of the control laws as demanded from more recent practical scenarios Farquhar (1971). To make regulation robust with respect to sampling, a solution based on direct digital design has been proposed in Celsi et al. (2015) solving the regulation problem on the sampled-data multi-rate equivalent model of (6.4). Still, in this setting, measures are available only at the sampling periods while the control switches at suitably defined sub-intervals, so making it work in open loop during such sub-intervals.

Multi-rate L_2-station under sampling

When $D = 0_{3\times 1}$, the corresponding unperturbed model (6.4) possesses a well-defined (vector) relative degree $r = (2\ 2\ 2)$; i.e., the following holds:

- $L_B h(q) = CB = 0_{3\times 3}$ while $L_B L_f(\cdot, \xi)h(q) = C\frac{\partial f(q,\xi)}{\partial q}B \neq 0_{3\times 3}$;
- the decoupling matrix $U(q, \xi) = C\frac{\partial f(q,\xi)}{\partial q}B$ is non-singular.

Let us now assume that measurements are available only at $t = k\delta$ (i.e., the sampling instants) with $k \geq 0$ and the control and the eccentricity perturbation are piecewise constant over the sampling period $\delta \geq 0$; i.e., $\xi(t) = \xi(k)$ and $u(t) = u(k)$ for $t \in [k\delta, (k+1)\delta($. Then, the dynamics are described at all sampling instants by the so-called single-rate (SR) equivalent sampled-data model which takes the form of a map

$$\begin{aligned} q(k+1) &= F^\delta(q(k), \xi(k), u(k)) \\ p(k) &= h(q(k)) = Cq(k) \end{aligned} \tag{6.14}$$

with $q(k) = q(k\delta)$ and

$$F^\delta(q, \xi, u) = e^{\delta \mathrm{L}_{f(\cdot,\xi)+Bu}} q = q + \sum_{j>0} \frac{\delta^j}{j!} (L_{f(\cdot,\xi)+Bu})^j q. \tag{6.15}$$

It is a matter of computation to verify that, independently on the continuous-time vector relative degree r, the relative degree of each output channel of the sampled-data equivalent model (6.14) always falls to $r_d = (1\ 1\ 1)$; namely, one gets

$$\frac{\partial p(k+1)}{\partial u(k)} = \frac{\delta^2}{2!} \mathrm{L}_B \mathrm{L}_{f(\cdot,\xi)} h(q) + \mathcal{O}(\delta^3) = \frac{\delta^2}{2!} C \frac{\partial f(q,\xi)}{\partial q} B + \mathcal{O}(\delta^3) \neq 0.$$

As a consequence, the sampled dynamics (6.14) possesses a further unstable zero dynamics (the so-called sampling zero-dynamics) of dimension 3. For this reason, inversion-like techniques via single-rate sampling cannot be achieved while guaranteeing stability of the internal dynamics. This fact induces some obstructions due to the appearance of the sampling zero-dynamics. To overcome this pathology, *multirate sampling* has been introduced and developed in a nonlinear context Monaco and Normand-Cyrot (1992).

In detail, fixing $\bar{\delta} = \frac{\delta}{2}$ and $u(t) = u^i(k),\ t \in [k\delta, k\delta + i\bar{\delta}(,\ i = 1, 2$ one gets the multirate (MR) equivalent model of order 2 of the form

$$q(k+1) = F_2^\delta(q(k), \xi(k), \underline{u}(k)) \tag{6.16}$$

with

$$F_2^\delta(q, \xi, \underline{u}) = F^{\bar{\delta}}(\cdot, \xi, u^2) \circ F^{\bar{\delta}}(q, \xi, u^1) = \sum_{j_1, j_2 \geq 0} \frac{\bar{\delta}^{j_1+j_2}}{j_1! j_2!} (L_{f(\cdot,\xi)+Bu^1})^{j_1} \circ (L_{f(\cdot,\xi)+Bu^2})^{j_2} q.$$

At this point, the multi-rate design model used for regulation is deduced by approximating (6.16) as

$$q(k+1) = q(k) + \frac{\delta}{2}\big(f^\delta(q(k), \omega(k)) + g^\delta(\omega(k))\underline{u}(k)\big) \tag{6.17}$$

with

$$\begin{aligned} f^\delta(q, \omega) &= f(q, T_\xi \omega) + f(q, T_\xi e^{\frac{\delta}{2} S} \omega) + \frac{\delta}{2} \frac{\partial f}{\partial q}(q, T_\xi e^{\frac{\delta}{2} S} \omega) f(q, T_\xi \omega) \\ g^\delta(\omega) &= \Big[\big(I + \tfrac{\delta}{2} \tfrac{\partial f}{\partial q}(q, T_\xi e^{\frac{\delta}{2} S} \omega)\big) B \quad B\Big] \end{aligned}$$

where we have used the exosystem (6.8) for predicting the disturbance at the small sampling instants $t = k\delta + \bar{\delta}$; namely, $\xi(k\delta + \bar{\delta}) = T_\xi e^{\frac{\delta}{2} S} \omega(k)$ and $\omega(k) = \omega(k\delta)$.

Because $g^\delta(\omega)$ is non-singular the regulation problem is solved by the feedback

$$\underline{u} = \big(g^\delta(\omega)\big)^{-1} \Big(A_d(q - \pi(\omega)) - f^\delta(q, \omega) + \pi(e^{\delta S} \omega)\Big)$$

with $\pi(\omega)$ as in (6.13) and A_d any Schur stable matrix (i.e., with $\sigma(I + \bar{\delta} A_d) \in \mathbb{S}^1$). In this sense a MR feedback was used to solve the station-keeping problem in an approximate sense. This feedback was shown to give better results when applied to the simulation model (6.4) without SRP compared to the emulation-based implementation of the continuous-time regulation feedback (6.12) (i.e., when directly implemented via zero-order-holding (ZOH) and no redesign). On the other hand, a known limitation of MR sampled-data control is the lack of robustness.

L_2-station keeping under nonlinear MPC

With reference to the SR sampled-data model (6.14) and assuming $\xi = 0_{4\times1}$, a station-keeping nonlinear MPC has been proposed in Misra et al. (2018) based on the online solution, at all sampling instants, of a finite horizon optimal control problem of the form;

$$\min \left\{ V_{n_p}(q(k+n_p)) + \sum_{i=1}^{n_p-1} \|p(k+i) - \nu(k+i)\|_Q^2 + \|u(k+i-1)\|_R^2 \right\} \tag{6.18a}$$

$$\text{s. t.} \quad q(k+1) = F^\delta(q(k), 0, u(k)) \tag{6.18b}$$

$$q(k+i) \in \mathcal{X}, \quad u(k+j) \in \mathcal{U}, \quad i = 1\ldots, n_p - 1, j = 0, \ldots, n_c - 1 \tag{6.18c}$$

$$q(k+n_p) \in \mathcal{X}_{n_p} \tag{6.18d}$$

where: the sampled-data equivalent model is used as prediction model Grüne and Pannek (2017); $\nu(k) = \nu(k\delta)$ is the sample of the reference trajectory in (6.7); $Q \succeq 0$ and $R \succ 0$ are the penalizing weights; n_p, n_c are the prediction and control horizons; $\mathcal{X}$,$\mathcal{U}$ are the states and control constraints sets assumed, as usual, compact, convex and containing the origin; V_{n_p} and $\mathcal{X}_{n_p}$ represent the terminal cost and terminal constraint set respectively. Those terminal ingredients are incorporated into the optimization problem (6.18) for providing closed-loop stability and convergence Mayne et al. (2000b). Instability in closed loop, when no further constraint is included, arises due to the generally unstable zero-dynamics induced by single-rate sampling Monaco et al. (1986b).

Remark 6.1 *In Halo-orbit station-keeping applications usually one has box constraints on the controls Shirobokov et al. (2017).*

The nonconvex *nonlinear programming* (NLP) problem (6.18) can be recast into a polynomial optimization problem Raff et al. (2006); Misra et al. (2018) of the form

$$V^\star = \max_{U \in \mathcal{U}, \lambda \in \mathbb{R}} \lambda \tag{6.19a}$$

$$s.t \quad p_0(U) - \lambda \geq 0 \tag{6.19b}$$

with $\lambda \in \mathbb{R}$, $U = (u(k), \ \ldots \ u(k+n_p-1))^\top$ being the decision variable, and denoting the single-shooting prediction of the output for i steps by $H_i(U)$;

$$\begin{aligned}
p_0(U) &= H_1(U) + H_2(U) + \ldots + H_{n_p}(U) \\
H_1(U) &= \|\nu(k+1) - CF^\delta(q(k), 0, u(k))\|_Q \\
H_2(U) &= \|\nu(k+2) - CF^\delta(\cdot, 0, u(k+1)) \circ F^\delta(q(k), 0, u(k))\|_Q \\
&\vdots \\
H_{n_p}(U) &= \|\nu(k+n_p) - CF^\delta(\cdot, 0, u(k+n_p-1)) \circ \cdots \circ F^\delta(q(k), 0, u(k))\|_Q
\end{aligned}$$

so to guarantee, if any, convergence to a solution in finite time and the corresponding global optimality. The above problem is a Sum-Of-Squares (SOS) polynomial minimization problem Putinar (1993) subject to convex polynomial constraints, for which one can utilize a Semi-Definite Programming (SDP) solver to reach global optimal solutions in polynomial time. However, as noted in

Misra et al. (2018), when solving (6.25) via SDP solvers two issues arise: semi-definite programming solutions to (6.25) are computationally demanding (depending on the degree of the sum of squares polynomial relaxations for $p_0(U) - \lambda$), and the closed loop system may lack in robustness since the employed prediction model neglects both eccentricity and SRP and for which no reference signal pre-processing is done.

In the context of tracking known limitations with nonlinear MPC are related to two main aspects: recursive feasibility of the optimization problem that is linked to admissibility of the reference trajectory for the dynamics, and boundedness of the closed-loop trajectories Gilbert and Tan (1991).

6.3 Station-keeping under sampled-data model predictive control

With reference to Fig. 6.4 below, we detail the proposed single-rate sampled-data quasi Halo orbit station-keeping control scheme. This proposed scheme solves Problem 6.1 combining an outer trajectory planner together with an inner nonlinear MPC controller working at different sampling rates. More In detail, the trajectory is planned at all $t = 2k\bar{\delta}$ (the so-called planning instants), whereas the control is computed by the MPC inner controller at all $t = k\bar{\delta}$ (the sampling instants).

- **MR reference planner**. Given the samples of the quasi Halo orbit reference generated by the exosystem (6.8c). This MR reference planner produces a sequence of admissible position trajectories, denoted $\hat{p}(k)$, based on a simplified model of the spacecraft under the regulation feedback (6.12) neglecting SRP.

- **Inner-loop MPC controller**. A simplified nonlinear MPC control problem is obtained by feeding the reference generated by the MR reference planner to the stage cost function (6.18a) in place of $\nu(k)$, thus ensuring tracking, while mitigating the effect of the unmodelled additive SRP disturbance.

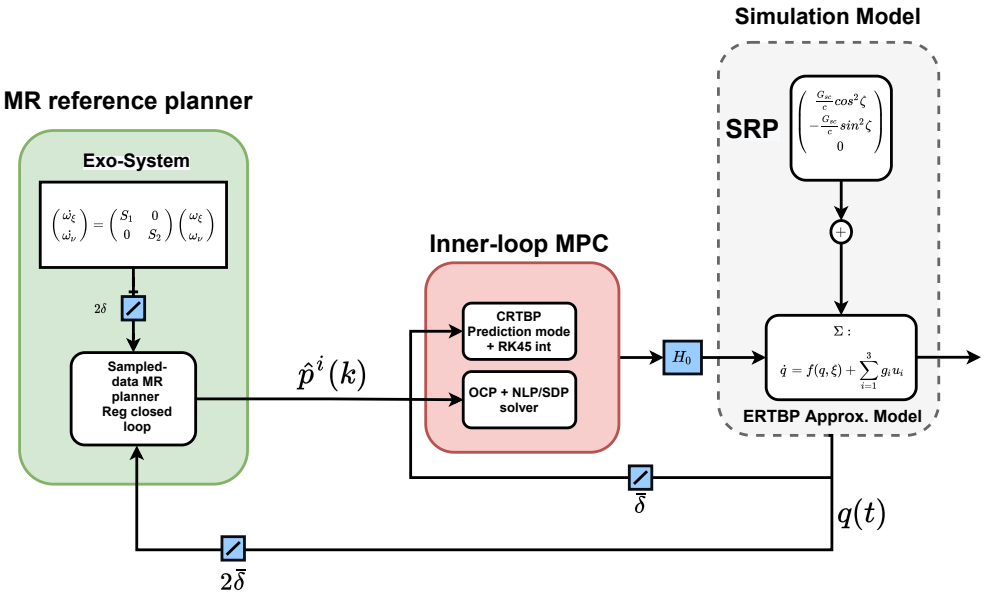

Figure 6.4: The proposed control scheme MR MPC

Construction of the MR planner model

Consider the feedback system (6.4) under the control (6.12) computed for $K = 0$ and $D \equiv 0$; namely, we get

$$\dot{q}(t) = \tilde{f}(q(t), \omega(t)) + B\tilde{u}_i(k) \tag{6.20}$$

for $t \in [(k + \frac{i-1}{2}\delta, (k + \frac{i}{2})\delta[$ and $i = 1, 2$ and $\tilde{f}(q, \omega) = f(q, T_\xi\omega) + Bc(\omega)$. Accordingly, the corresponding MR sampled-data equivalent model is approximately provided by

$$q(k+1) = \tilde{F}_2^\delta(q(k), \omega(k), \underline{\tilde{u}}(k)) \tag{6.21}$$

with $\underline{\tilde{u}} = (u_1^\top \; u_2^\top)^\top \in \mathbb{R}^6$, the map

$$\tilde{F}_2^\delta(q, \omega, \underline{\tilde{u}}) = q + \frac{\delta}{2}\Big(\tilde{f}^\delta(q, \omega) + \tilde{g}^\delta(\omega)\underline{\tilde{u}}\Big)$$

and

$$\begin{aligned}
\tilde{f}^\delta(q, \omega) &= \Big(I + \frac{\delta}{4}(A + \frac{\partial \Gamma}{q}(q, T_\xi e^{\frac{\delta}{2}S}\omega))\Big)Aq \\
\tilde{g}^\delta(\omega) &= \Big[B + \tfrac{\delta}{4}AB \quad \tfrac{\delta}{4}\tfrac{\partial \Gamma}{q}(q, T_\xi e^{\frac{\delta}{2}S}\omega)B\Big] \\
\Gamma(q, \omega) &= -M(p + T_\nu\omega) - 2N(\dot{p} + T_\nu S\omega) - (2Mp + 2N\dot{p})(e_1 T_\xi\omega) - Mp(e_2 T_\xi\omega) - N\dot{p}(e_3 T_\xi\omega) \\
&\quad - (1-\mu)[\frac{p - \tilde{d}_1}{\|p - \tilde{d}_1\|^3} + \frac{T_\nu\omega - \tilde{d}_1}{\|T_\nu\omega - \tilde{d}_1\|^3}] - \mu[\frac{p - \tilde{d}_2}{\|p - \tilde{d}_2\|^3} + \frac{T_\nu\omega - \tilde{d}_2}{\|T_\nu\omega - \tilde{d}_2\|^3}] + P(\pi(\omega))T_\xi\omega - T_\nu\omega \\
\tilde{d}_1 &= \Big[-\mu - \tfrac{e_4 T_\xi\omega_\xi}{1-\mu} \quad 0 \quad 0\Big]^\top, \quad \tilde{d}_2 = \Big[1 - \mu + \tfrac{e_4 T_\xi\omega_\xi}{\mu} \quad 0 \quad 0\Big]^\top, \quad A = \begin{bmatrix} 0 & I \\ 0 & 0 \end{bmatrix}
\end{aligned}$$

Accordingly, station keeping is guaranteed for the discrete-time model (6.21) by the planned feedback law

$$\underline{\tilde{u}}(q, \omega) = \big(\tilde{g}^\delta(\omega)\big)^{-1}\Big(A_d(q - \pi(\omega)) + \pi(e^{\delta S}\omega) - \tilde{f}^\delta(q, \omega))\Big) \tag{6.22}$$

and A_d being such that $\sigma(I + \delta A_d) \subset \mathbb{S}^1$. for all $\delta > 0$.

Remark 6.2 *It can be verified that $\Gamma(q, \omega)$ vanishes as $p \to T_\nu\omega$ that is, as the satellite reaches the Halo orbit, apart from the external perturbation. More in detail, one computes at the Halo orbit (i.e., $p = T_\nu\omega$)*

$$\Gamma(q, \omega) = -(e_1 T_\xi\omega_\xi)(2Mp + 2N\dot{p}) - (e_2 T_\xi\omega_\xi)Mp - (e_3 T_\xi\omega_\xi)N\dot{p} + P(\pi(\omega))T_\xi\omega_\xi = \bar{\Gamma}(q)\omega_\xi.$$

Moreover, denoting $\omega_\xi = \Big[I \quad 0\Big]\omega$, one gets $\|\bar{\Gamma}(q)\omega_\xi\|$ is bounded at the quasi Halo orbit since $\|\omega_\xi\| \leq c, c \in (0, 1]$.

At all planning instants $t = k\delta$, the simplified MR model (6.21) under the feedback (6.22) provides an admissible sequence of bounded references $\hat{p}^i(k) = \hat{p}(k\delta + \frac{i\delta}{2})$ with $k = 1, \ldots, \hat{n}_p$, $i = 1, 2$ for the original dynamics (6.4) over the prediction horizon of length $n_p = 2\hat{n}_p$ and $\hat{n}_p > 1$.

More rigorously, for $i = 1, 2$, $k = 1, \dots, \hat{n}_p$ and $q^0(k) = q(k\delta)$ the multi-rate planner gets the form

$$q^i(k) = \tilde{F}^{\bar{\delta}}(q^{i-1}(k), \tilde{u}_i(k)) \tag{6.23a}$$
$$\hat{p}^i(k) = Cq^i(k) \tag{6.23b}$$

with the single-rate map associated to (6.20) given by

$$\tilde{F}^{\bar{\delta}}(q, \tilde{u}) = q + \bar{\delta}\Big(\tilde{f}(q, \omega) + B\tilde{u}\Big) + O(\bar{\delta}^2)$$

Accordingly, such references can be directly fed to MPC controller for which, then, the optimization problem can be notably simplified by discarding the terminal ingredients when the penalty on the control is small as discussed in Chapter 5.

The inner-loop MPC controller

Assuming now the references computed by the planner (6.23), the actual single-rate control is computed via MPC solving at all sampling instants $t = k\bar{\delta}$ the modified optimization problem (6.18) of the form

$$V^\star = \min_U \Big\{ \sum_{\ell=0}^{\hat{n}_p - 1} \sum_{i=1}^{2} \|p((2k + \ell + i)\bar{\delta}) - \hat{p}^i((2k + \ell)\bar{\delta})\|_Q^2 + \|u(2k + \ell + i - 1))\|_R^2 \Big\} \tag{6.24a}$$
$$\text{s. t.} \quad q(k + 1) = F^\delta(q(k), 0, u(k)) \tag{6.24b}$$
$$lb \le u(k + i - 1) \le ub, \quad i = 1, \dots, n_p \text{ and } n_p = 2\hat{n}_p \tag{6.24c}$$

Some comments are in order.

The MPC problem we propose is notably simplified discarding terminal ingredients. This is due to the fact that the references $\hat{p}(\cdot)$ provide bounded and admissible trajectories for the dynamics by construction of the multi-rate planner (6.21). This is specially true for ϵ small enough, when neglecting (6.24c) Elobaid et al. (2020b). In this sense, the admissible references $\hat{p}^i(k)$ are specifically designed to ensure better performances while simplifying the optimization problem. The generated references are generated depend on the quasi Halo references obtained from (6.8c).

Expression (6.24b) represents a simplified prediction model for MPC being an approximate sampled-data equivalent CRTBP model.

The constraint (6.24c) takes into account possible saturations and physical limitations of the actuators and safety margins on thrusts. Note that (6.24c) are simple algebraic convex box constraints. Consequently, polynomial optimization reformulation of the nonlinear MPC problem above is possible by noting that this problem can be rewritten as

$$V^\star = \max_{U \in \mathcal{U}, \lambda \in \mathbb{R}} \lambda \tag{6.25a}$$
$$s.t \quad L\begin{pmatrix} U & \mathrm{I} \end{pmatrix} \le 0 \tag{6.25b}$$

with $\lambda \in \mathbb{R}$, $U = (u(k), \ \dots \ u(k+n_p-1))^\top$ being the decision variable and

$$L = \begin{bmatrix} I & 0 & \dots & 0 & -ub \\ I & 0 & \dots & 0 & lb \\ \vdots & \vdots & \ddots & \vdots & \vdots \\ I & 0 & \dots & 0 & -ub \\ I & 0 & \dots & 0 & lb \end{bmatrix} \in \mathbb{R}^{3n_p \times 3n_p+3} \tag{6.26}$$

The above problem is a Sum-Of-Squares (SOS) polynomial minimization problem Putinar (1993) subject to convex polynomial constraints, one can utilize a Semi-Definite Programming (SDP) solver to reach global optimal solutions in polynomial time. To sum up, the control scheme we propose is summarized in the algorithm below applying algorithm (A1) in Chapter 5.

Algorithm 2 Halo orbit station keeping algorithm

Solving Problem 6.1: $p(k) \to \nu(k)$
initialization $q(k) \leftarrow q(t = k\delta), Q \leftarrow Q, R \leftarrow R, ub \leftarrow u_{MAX}, lb \leftarrow u_{MIN}$
while $t \geq 0$ **do**
  if $t = (k+j)\delta, j \in \mathbb{Z}_{\geq 0}$ **then** $k \leftarrow k + j$
    $\hat{p} = \text{Planning}(q(k), T_\nu \omega(k))$
    $u(k) = \text{SolveNMPC}()$
  for $t = k\delta + i\bar{\delta}, i = 1, 2$ **do**
    $u(k) = \text{SolveNMPC}()$

Remark 6.3 *In the algorithm above, the SolveNMPC() routine is a NLP (equivalently SDP routing) routine that solves the optimization problem 6.24. This can be any off the shelf routine. The implementation details and a brief discussion on the computational aspects associated with this routine are deferred to the next section. The if statement in the algorithm specifies that planning and control are carried at different sampling rates as already discussed. This is precisely why we need to propagate the MR planner (6.21) and compute the admissible reference $\hat{p}^i(k)$ over double the prediction horizon.*

Combined in this way, it will be illustrated through simulations depicting various realistic scenarios, how utilizing a simplified MR model to provide admissible references for a nonlinear MPC with a simplified prediction model solves problem (6.1) while addressing the limitations discussed associated with the lack in robustness associated with nonlinear regulation.

6.4 Simulations and comparative discussions

Utilizing Matlab/Simulink©, a comparative study is carried out testing the proposed control scheme (later on denoted by MR MPC) with respect to nonlinear MPC via polynomial optimization (PolyNMPC, Misra et al. (2018); Shirobokov et al. (2017)), nonlinear regulation and feedback linearization proposed in Di Giamberardino and Monaco (1996). In particular, the nonlinear controllers (regulation and feedback linearization) are implemented via sampling and hold devices with no sampled-data redesign. For PolyNMPC, a polynomial approximation of the CRTBP model is used for prediction deduced from Runge–Kutta (RK) numerical integrator of (6.4) assuming $D(t) \equiv 0$

and $\xi \equiv 0$. Consequently the nonlinear MPC problem (6.24a)-(6.24b)-(6.24c) is transformed into a polynomial optimization problem using sum of squares (SOS), as detailed in (6.25)-(6.25b). This equivalent optimization problem is then solved in a receding horizon approach utilizing SOSTools© Prajna et al. (2002).

We assume as simulation time $T \approx 2.7days = m\bar{\delta}$ coinciding the time needed for at least two revolutions around the orbit and $\bar{\delta} > 0$ being the sampling period of the sampling and hold devices. The comparison is aimed at showing how the various controllers succeed in keeping the spacecraft on the Halo orbit based, also, on Key Performance Indicators (KPIs) below.

- **Tracking Error** in terms of the root-mean-square value of the spatial tracking error; namely, $e_{RMS}(t) = \sqrt{\frac{1}{3}(\|\nu(t) - p(t)\|}$ and $e_{RMS}(T) = \sqrt{\frac{1}{3}(\|\nu(T) - p(T)\|}$ in non-dimensional units.

- **Energy Expenditure** based on the $\mathcal{L}_2$-norm of the controls for the duration of the flight (i.e., T); i.e., $EE_T = \sqrt{\int_0^T \|u(t)\|^2 \mathrm{d}t} = \bar{\delta}\sqrt{\sum_{k=0}^{m} \|u(k)\|^2}$ with $u(k) = u(k\bar{\delta})$ and $k \geq 0$ in m/s^2. Additionally, the instantaneous control norm (i.e., $\|u(t)\|$) is reported as well as an indicator of the so-called *velocity budget*.

More in details, starting from several initial conditions (e.g. near L_2, close to the quasi-Halo orbit), the proposed MR MPC scheme is compared with different control strategies available in the literature in terms of robustness with respect to the effect of:

- **unmodelled perturbations and actuator saturations** (Sections 6.4-6.4) that is, when the spacecraft starts from various initial conditions (e.g. near L_2, close to the quasi-Halo orbit) in nominal conditions (i.e., $D(t) \equiv 0$ in (6.4)) and when assuming SRP terms and saturation of the actuators which were neglected during the design;

- **sampling** (Section 6.4) in presence of perturbations but no limits on the thrusts.

The computational aspects and the application of a Real Time Iteration MPC (RTI MPC) solver to the proposed control scheme conclude the comparative study (Section 6.4).

First comparison starting from L_2 in nominal conditions

The spacecraft is assumed to start in the translunar point i.e. $q(0) = (L_2\ 0\ 0\ 0\ 0\ 0)^\top$ in the rotating frame with no SRP terms. The proposed MR MPC and the PolyMPC are set with penalizing weights $Q = diag\{10, 10, 10, 1, 1, 1\}, R = 0.1\mathrm{I}$. The sampling period $\bar{\delta} \equiv 0.65\mathrm{hr}$ in dimensional time (this is a reasonable sampling period for this application see Sec. 4.A.7 in Shirobokov et al. (2017)). Figure 6.5 shows the emulated Feedback linearization controller, while Fig. 6.6 depicts the feedback nonlinear regulation feedback. These two control schemes are compared to the proposed MR MPC (Fig 6.7) and polynomial based NMPC (Fig. 6.8). The results show that all the control schemes are comparable, with nonlinear regulation outperforming others in terms of tracking error at the expense of marginally higher energy demand. It is of note however that the proposed MR MPC outperforms PolyMPC in tracking at the expense of relatively higher energy demand. Table 6.1 summarizes the main KPIs and performances of the various controllers tested in this scenario.

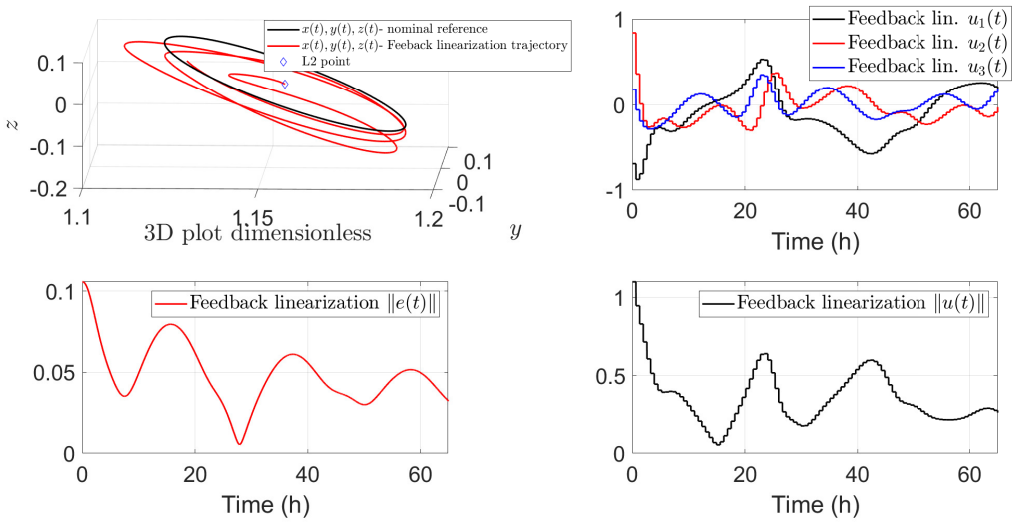

Figure 6.5: Station-keeping under feedback linearization (emulated)

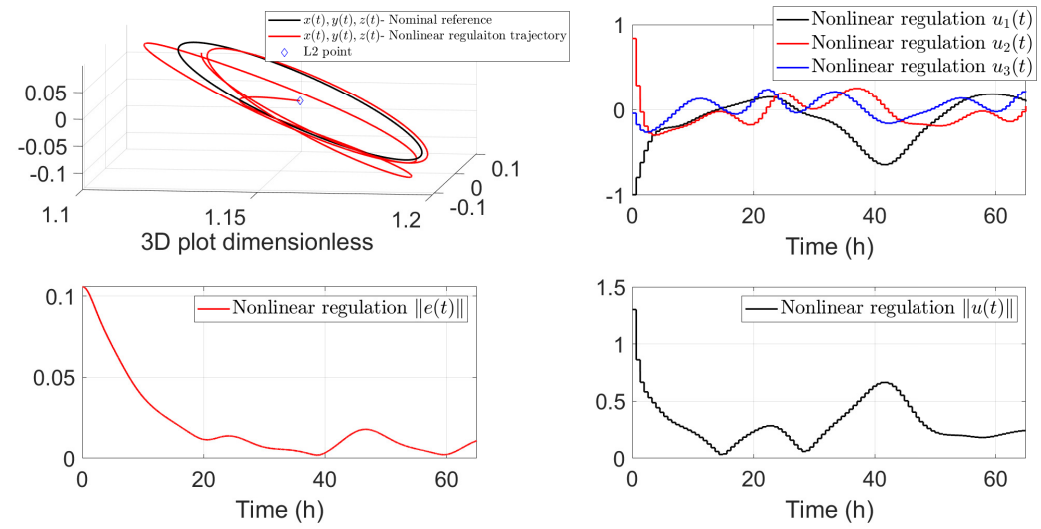

Figure 6.6: Station-keeping under nonlinear regulation (emulated)

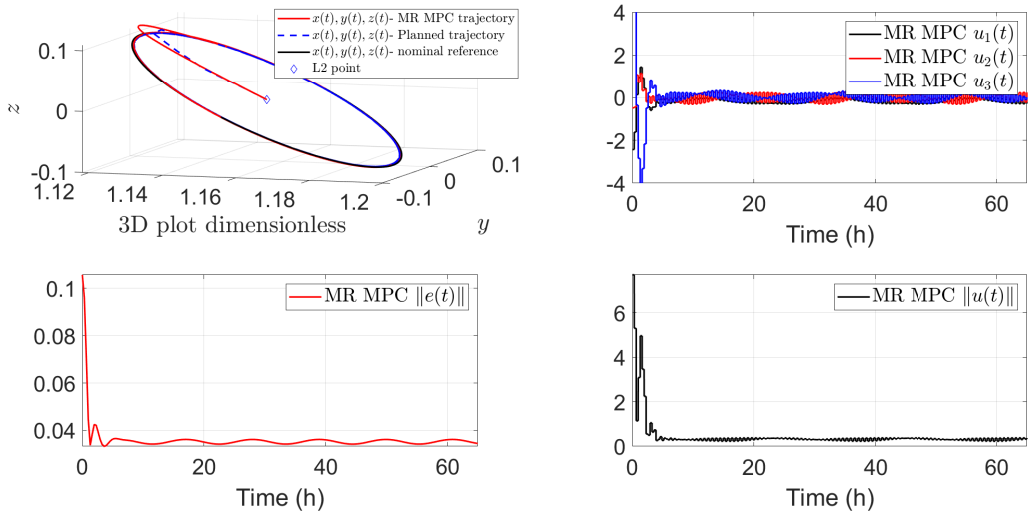

Figure 6.7: Station-keeping under the proposed MR MPC control scheme

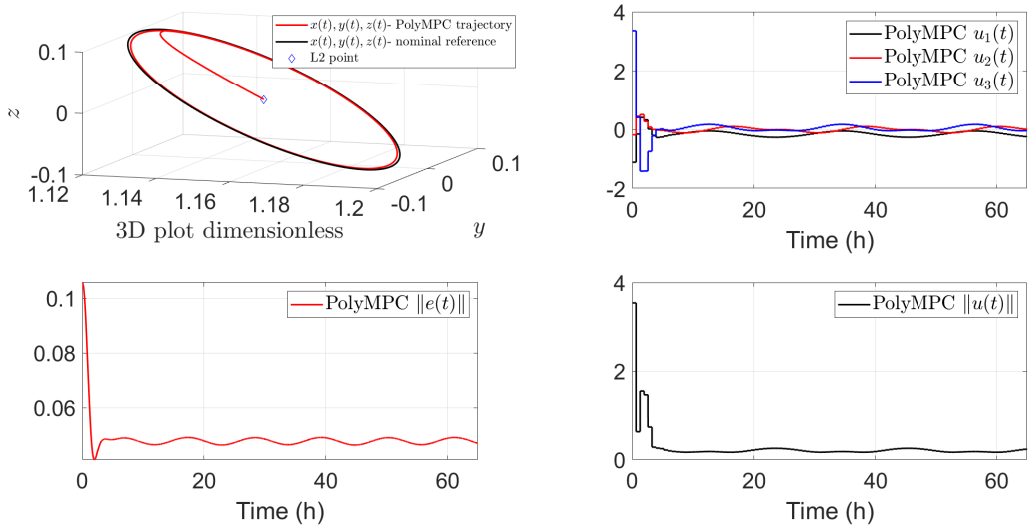

Figure 6.8: Station-keeping under nonlinear MPC in the nominal case

	FL	NL regulation	MR MPC	PolyMPC
$e_{RMS}(T)$	0.04	0.002	0.047	0.069
EE_T	2.238 m/s^2	2.29 m/s^2	1.927 m/s^2	0.98 m/s^2

Table 6.1: Summary of main KPI comparisons in scenario 1 at $T = 65$hours

Second comparison starting from L_2 with SRP and control limits

This is a more realistic scenario in which the spacecraft start at the translunar libration point. In this situation however, the spacecraft is subject to the primaries perturbations, solar radiation pressure as well as assuming each thrust being able to provide a maximum of 0.55[ND]. The sampling period is maintained at $\bar{\delta} = 0.65$hr. While emulation of the standard feedback linearization fails

with this limit on the control (Figure 6.9), emulation of nonlinear regulation feedback yields better results in terms of tracking error and control effort. Similar performance is obtained when utilizing the proposed MR MPC approach (Figure 6.11) with $Q = diag\{10, 10, 10, 1, 1, 1\}, R = 0.1\text{I}$, and PolyMPC (Figure 6.12). Unlike the previous case, the propose control scheme yields the best tracking performance, even outperforming nonlinear regulation. This is achieved at the expense of a relatively higher control effort over the station-keeping simulation period. Table 6.2 summarizes the main KPIs and performances of the various controllers tested in this scenario.

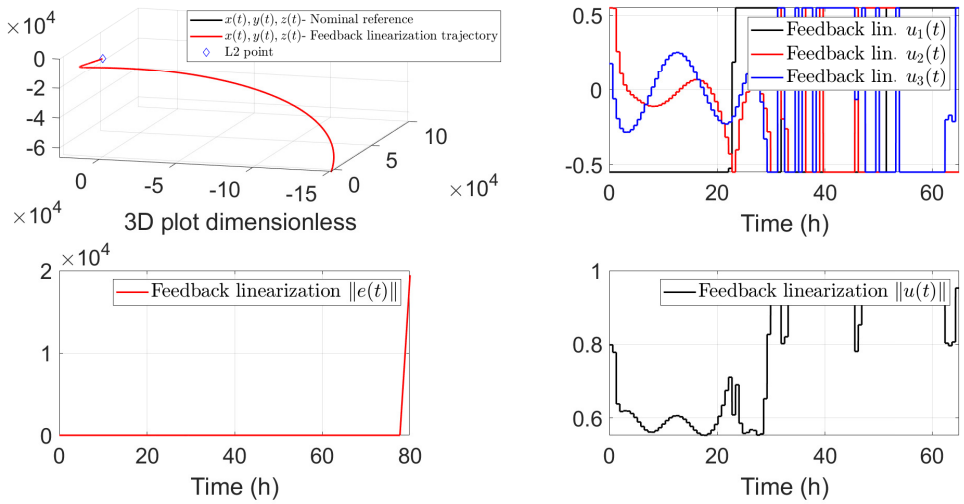

Figure 6.9: Failure of station-keeping under feedback linearization (emulated) with SRP and control limits

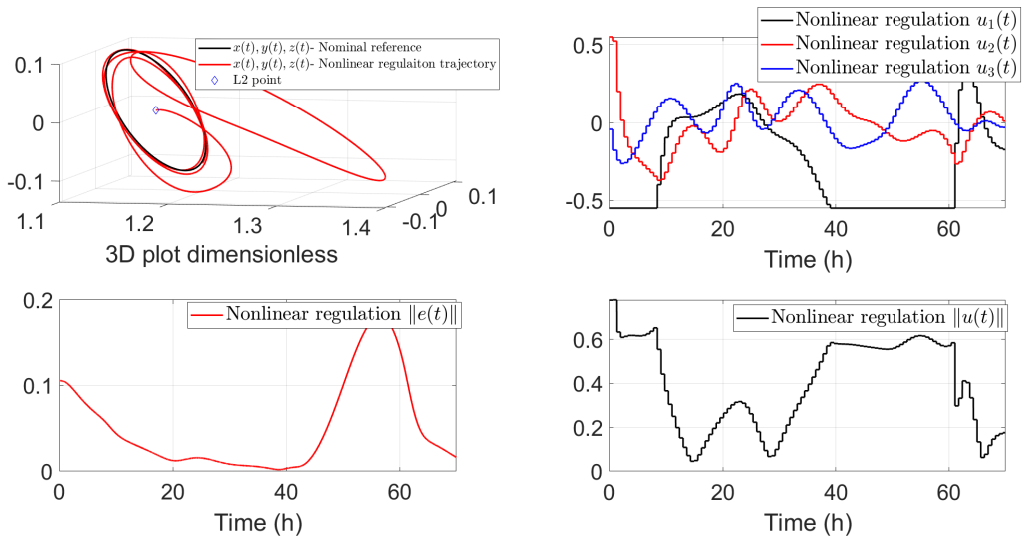

Figure 6.10: Station-keeping under nonlinear regulation (emulated) with SRP and control limits

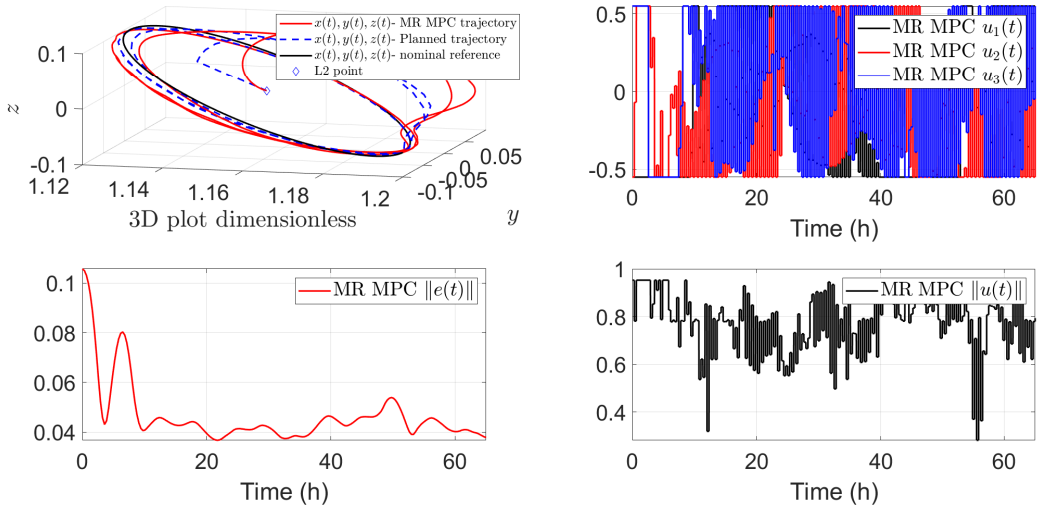

Figure 6.11: Station-keeping under the proposed control scheme with SRP and control limits

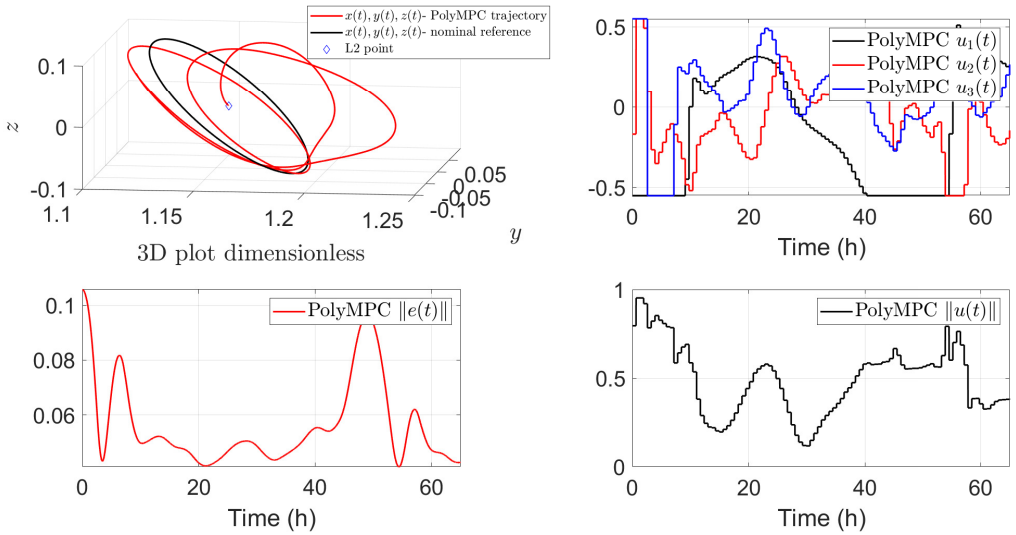

Figure 6.12: Station-keeping under nonlinear MPC with SRP and control limits

	FL	NL regulation	MR MPC	PolyMPC
$e_{RMS}(T)$	N/A	0.044	0.0255	0.0323
EE_T	N/A	4.2001 m/s^2	6.0708 m/s^2	5.3414 m/s^2

Table 6.2: Summary of the main KPI comparisons in scenario 2 at $T = 65$hours

Third comparison starting away from the orbit with SRP and control limits

In this scenario, we start away from the orbit with a so called insertion error of 300km in dimensional units and the same control limit imposed previously. While at the end of simulation period, the nonlinear regulation seems closer to the orbit (Figure 6.13), yet, it is clear from Figure 6.14 that the proposed controller maintains the space craft closer to the Halo orbit consistently during the

whole simulation period with no jumps in $\|e(t)\|$ value. It is also worth mentioning that in this scenario, the proposed controller, while being comparable to the emulated nonlinear regulation, the PolyMPC controller suffers both in terms of energy expenditure and tracking error (Figure 6.15). Emulated feedback linearization fails to maintain the spacecraft in the vicinity of the orbit, and thus omitted for the sake of space. Table 6.3 reflects the previous discussion.

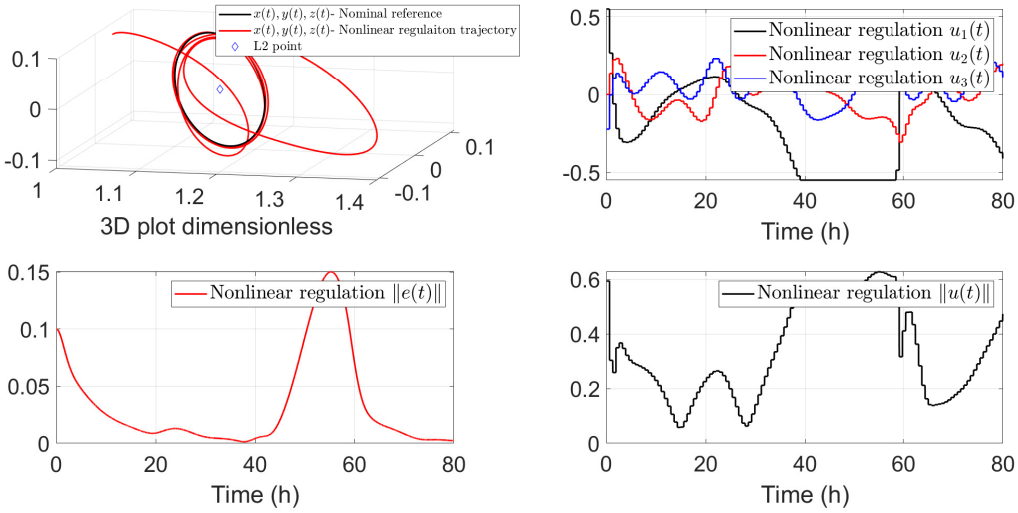

Figure 6.13: Station-keeping under nonlinear regulation (emulated) with SRP and control limits

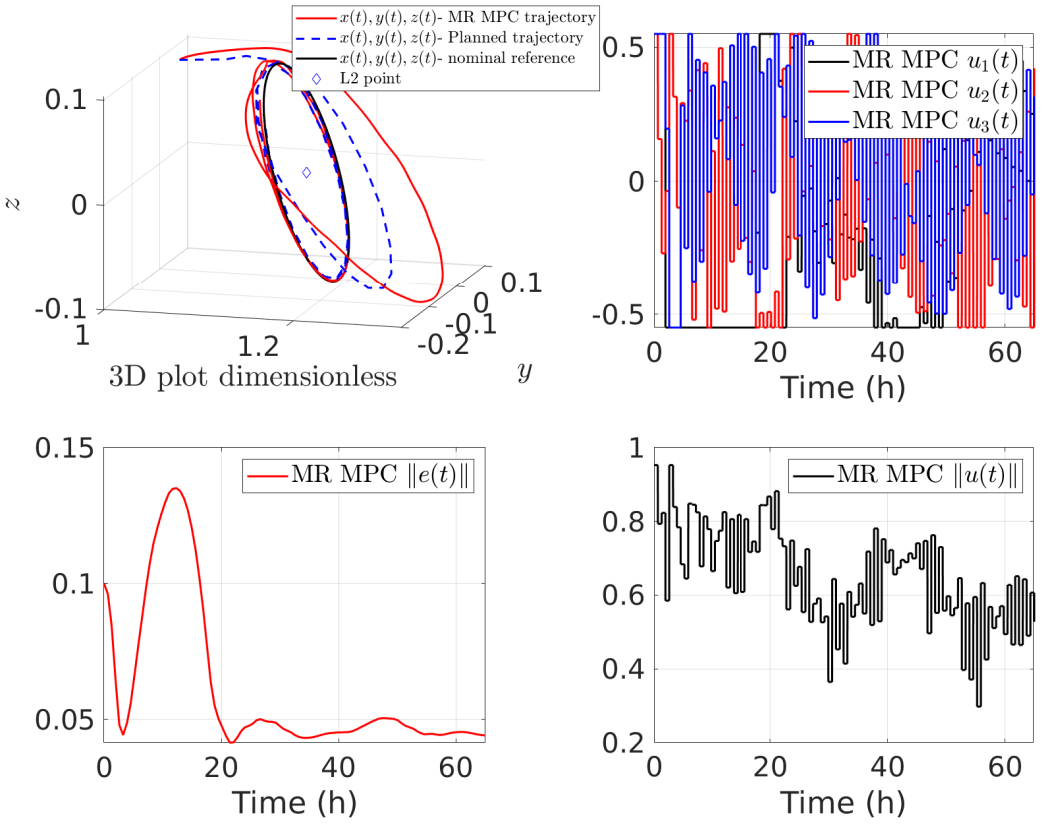

Figure 6.14: Station-keeping under the proposed control scheme with SRP and control limits

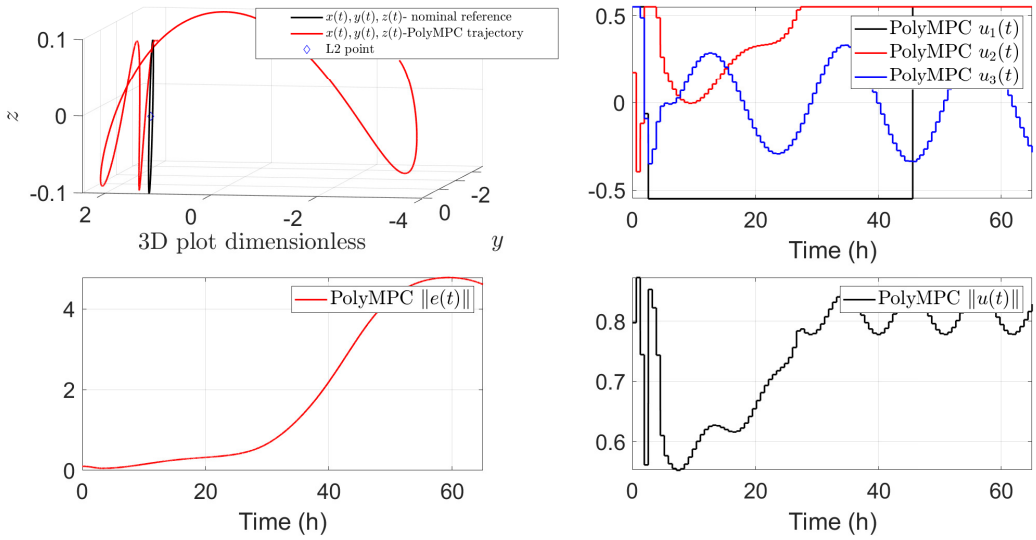

Figure 6.15: Station-keeping under nonlinear MPC with SRP and control limits

	FL	NL regulation	MR MPC	PolyMPC
$e_{RMS}(T)$	N/A	0.0174	0.0255	4.61
EE_T	N/A	5.4 m/s^2	6.5410 m/s^2	7.479 m/s^2

Table 6.3: Summary of the main KPI comparisons in scenario 3 at $T = 65$hours

Fourth comparison on the effect of δ

A major benefit for the proposed MR MPC is the robustness with respect to higher sampling intervals. In fact Fig. 6.16 depicts how the proposed MR MPC maintains the spacecraft close to the quasi Halo orbit when increasing the sampling interval length to $\bar{\delta} = 1.2$hr in dimensional units (still lower than that reported in 4.A.7 in Shirobokov et al. (2017)), starting close to the orbit, namely $q(0) = (L_2\ 0\ 0.12\ 0\ 0.186\ 0)^\top$. Indeed, in this comparison we assume nominal conditions, i.e. $D(t) \equiv 0$. At this sampling rate, both feedback linearization (through emulation) and emulated nonlinear regulation fail to keep the spacecraft in the vicinity of the quasi Halo orbit, as well as the polynomial optimization based PolyMPC.

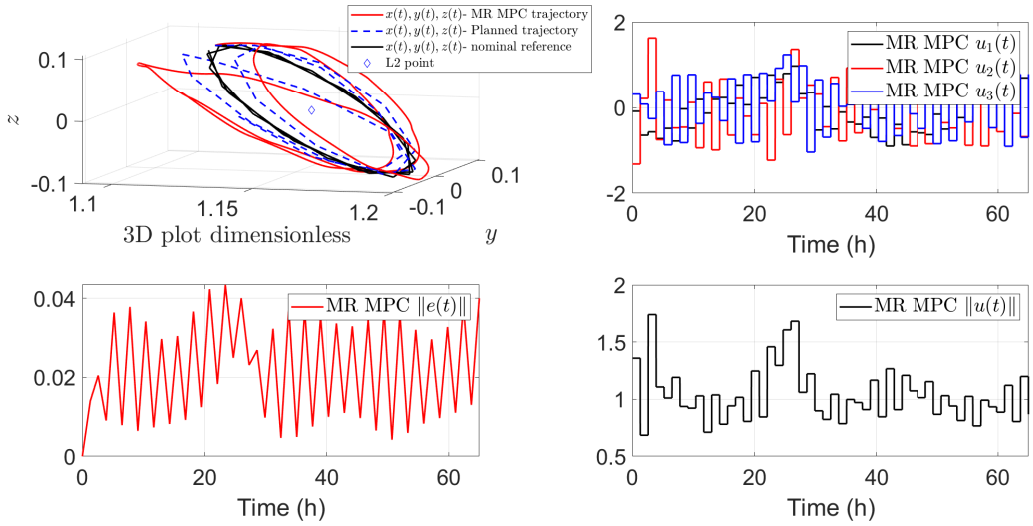

Figure 6.16: Station-keeping under MR MPC with $\bar{\delta} = 1.2$hr

Computational aspects and RTI MPC

To study the real time implementation question, we opt to utilize the real time iteration model predictive control Diehl et al. (2002), together with the multirate sampled-data planner. The simulations are carried out using ACADO'S Houska et al. (2011) Matlab Interface. Simulations were run on a PC running Windows 10 with an Intel i7 9^{th} generation CPU and 16 GB of RAM. For testing reasons, Horizon lengths up to 40 steps were used for the 3 different simulation scenarios discussed in the previous section. Figure 6.17 shows the performance of MR MPC in the RTI framework, together with time to QP solution corresponding to scenario 6.4. Indeed fast QP solution times are possible, at the expense of degraded tracking performance. Table 6.4 shows QP solution time for a prediction horizon length of $n_p = 30$. This indicates that the MR MPC, with an RTI MPC solver can be implemented to solve the problem of station-keeping in real time provided some trade off is admissible in terms of quasi Halo orbit station-keeping performance.

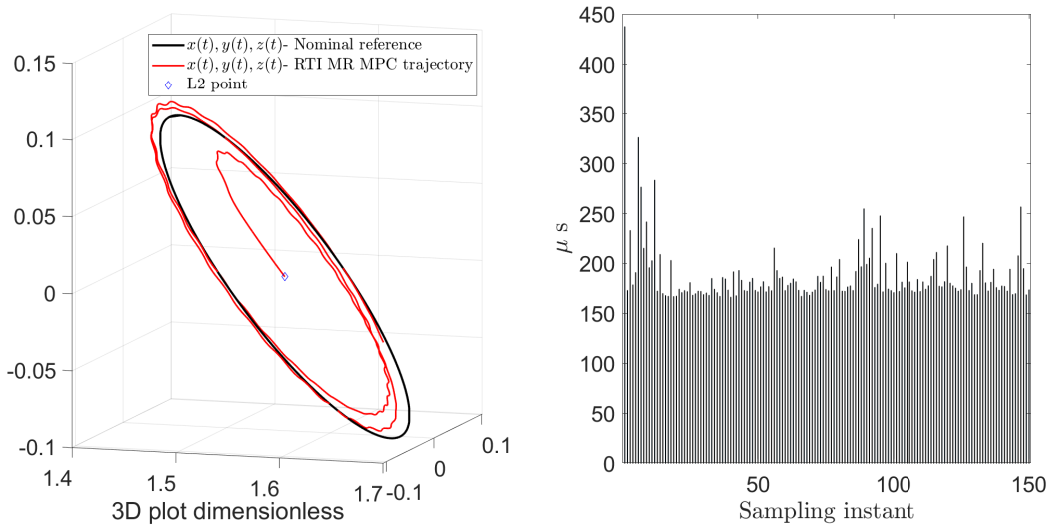

Figure 6.17: Figure shows time required by the CPU to solve the QP in the RTI in Scenario 1

	Average time to QP solution
Scenario 1	187 μs
Scenario 2	191 μs
Scenario 3	220 μs

Table 6.4: Table showing average time to QP solution when using RTI

Final comments on the simulations

A sampled-data controller based on the algorithm introduced in Chapter 5 was proposed for allowing a spacecraft to track a quasi Halo orbit around the L_2 point in the earth-moon system. In particular, the control is composed of two main components: a multi-rate trajectory planner which, based on a simplified feedback equivalent discrete-time model, generates admissible and bounded references guiding the space-craft to the orbit; a model predictive controller which, based on the aforementioned trajectories and a suitably defined sampled-data prediction model, solves at each sampling instants a constrained optimization problem. Because of the generated references, such a problem is feasible and the closed-loop trajectories are bounded.

Simulations based on realistic scenarios highlight that the performances achieved under the proposed control scheme are significantly improved when compared to standard digital implementations (that is through zero order holding) of standard nonlinear control laws (e.g., based on regulation, feedback linearization control) and polynomial optimization based nonlinear MPC in station-keeping of quasi Halo orbits applications. Several aspects were considered such as eccentricity related perturbations and saturation limits on the control inputs. Key performance indicators enforce the validity of the proposed control scheme, both in terms of orbit tracking root-mean-square error and the $\mathcal{L}_2$ norm of the accelerations required for station-keeping as a measure of energy expenditure. Furthermore, robustness to both solar radiation pressure, as modelled by an additive periodic perturbation, and slower sampling rates, is illustrated. Finally, it results that the proposed scheme is suitable for real time digital implementation on modern hardware, even with longer prediction horizon for the MPC than is typically reported to be possible in the literature (e.g. longer than 40 time steps), through small adjustment to the online optimization solver.

Since the methodology here proposed is general in nature, an additional conclusion that can be drawn is that this methodology can be used, with the appropriate changes, to handle a variety of Halo and Lyapunov orbits around liberation points both in the Earth-Moon and Sun-Earth systems. Of course the results here reported are preliminary in nature albeit paving the way for sampled-data approaches in station-keeping applications

6.5 Conclusions to Part II and further comments

A few concluding remarks to this chapter, and by extension our discussion of stable inversion in unconstrained sampled-data model predictive control are in order;

- In this part of the thesis we concerned ourselves with the problem of tracking a desired reference via unconstrained finite time cheap optimal control. Furthermore, the design of the

controller followed a receding horizon approach (MPC) in which the prediction and control horizons were assumed to coincide.

- From the point of view of achieving zero ideal performance, this control design faces limitations even when the system is minimum phase in continuous-time due to the rise of unstable sampling zero dynamics. Not surprisingly, tracking with zero ideal performance implies the cancellation of the internal dynamics when no penalty on the control is imposed.

- In this sense, this part introduced two possible multi-rate sampled-data solutions to the problem; (*i*) utilizing multi-rate sampling at the prediction model level as carried out in Chapter 4, or (*ii*) utilizing multi-rate sampling to modify the reference signals coming to the MPC as carried out in Chapter 5.

- For the first solution, application to the class of non-holonomic systems admitting chained forms was studied. This example was repeated again for the second proposed solution to illustrate the benefits of working at the reference planning level.

- This part was concluded with two bench-marking examples on the use of multi-rate reference planners with MPC.

What remains, for this work to constitute a somewhat complete framework for *sampled-data model predictive control* is to study the effects of state (and input) constraints on the achieved zero ideal performance. This is indeed a big gap that, while interesting in its own merit, is not strictly pertinent to the sampled-data nature of the controller, in particular concerning the use of multi-rate sampling. It can, by the way, noted that possible over-dimensioning of the multi-rate order can be fruitfully employed to address additional state constraints Di Giamberardino et al. (1996a).

Additionally, some ideas on the use of a multi-rate sampled-data trajectory planner as an *extended command governer* to (*i*) enforce those constraints and (*ii*) provide some stable inversion guarantees will be highlighted briefly at the end of the thesis. Those ideas, while being proposed in a rather superficial way, can form a starting point for possible extensions.

As the reader may have noted, this work is rather written as a companion to the published articles. As a consequence, the author makes no claims of this part being complete, self-contained or formally rigorous. To this effect, different strategies, and combinations thereof of designing the terminal ingredients to ensure stability of MPC controlled systems are omitted. For example the use of terminal strict equality constraints can be found in Keerthi and Gilbert (1988) and Chen and Shaw (1982), while the use of set inclusion for the terminal constraint can be studied in Michalska and Mayne (1993). On the other hand, other methods of enforcing stability using an extra stability constraint Sznaier and Damborg (1990), bounds on the horizons length Limón et al. (2008) and a combination thereof Allgöwer and Zheng (2012) are well documented in the literature and the interested reader is advised to refer to the cited works and the references therein.

Sampled-data transverse feedback linearization

Chapter 7

Approximate transverse feedback linearization via single-rate sampling

Contents

The assignment of a prefixed behavior to a given control system can be assured by confining, through feedback, its evolution to a submanifold specifying the required performances. In other words, the target submanifold is rendered attractive and invariant through feedback.

Transverse Feedback Linearization - TFL solves this problem through linear feedback equivalence, linearizing and stabilizing the dynamics transverse to the desired sub-manifold. In this respect, TFL implements the solution through two main steps: (1) define function(s) with respect to which the performances are set and the sub-manifold specifying those performances is the zero dynamics sub-manifold. (2) Compute a feedback linearizing and stabilizing the transverse dynamics to the characterized zero dynamics sub-manifold.

In this context, TFL is equivalent to the zero dynamics assignment problem and thus poses two issues to the control designer. On the one hand, TFL implies restricting the motion to a "desired" zero dynamics sub-manifold in continuous-time and hence boundedness of the evolution of the internal dynamics is paramount. On the other hand, even when the problem admits a satisfactory solution in continuous-time, it is clear that the pathology put in light in Chapter 2 may destroy the feedback equivalence desired by TFL under sampling. To make this discussion more concrete, and as is usual by now, we start with an example reported first in Nielsen and Maggiore (2008), that we use to also highlight the obstructions caused by sampling.

Example 7.1 Consider the dynamics

$$\dot{x} = \begin{pmatrix} -x_2 \\ x_1 \\ x_3 x_4 \\ 0 \end{pmatrix} + \begin{pmatrix} 0 \\ 0 \\ x_3 \\ 1 \end{pmatrix} u_1 + \begin{pmatrix} -x_2 \\ x_1 \\ 0 \\ 0 \end{pmatrix} u_2$$

and assume we want to confine its evolution to an elliptic paraboloid immersed in the subspace $\{x \in \mathbb{R}^4 : x_4 = 0\}$, namely the controlled invariant submanifold

$$\Gamma^\star = \{x \in \mathbb{R}^4 : x_1^2 + x_2^2 - x_3 = x_4 = 0\}$$

Note that $n^\star = \dim(\Gamma^\star) = 2$, and consider the function

$$\alpha(x) = ln(\frac{x_3}{x_1^2 + x_2^2}) - x_4$$

which indeed has relative degree $r = 2$ over $\mathbb{R}^4/\{x \in \mathbb{R}^4 : x_1 = x_2 = 0; x_3 = 0\}$. Additionally, this function is transverse to $\Gamma^\star$, i.e. in $\Gamma^\star$, $\alpha(x) = \dot{\alpha}(x) = 0$. Consequently, the coordinates change

$$\begin{pmatrix} z_1 \\ z_2 \\ \eta_1 \\ \eta_2 \end{pmatrix} = \phi(x) = \begin{pmatrix} \alpha(x) \\ \dot{\alpha}(x) \\ x_1 \\ x_2 \end{pmatrix}$$

puts the system in the normal form

$$\begin{aligned} \dot{z}_1 &= z_2 \\ \dot{z}_2 &= u_1 \\ \dot{\eta}_1 &= -\eta_2(1 + u_2) \\ \dot{\eta}_2 &= \eta_1(1 + u_2) \end{aligned}$$

from which setting

$$u_1 = -k_1 z_1 - k_2 z_2, \quad k_1, k_2 > 0$$

confines the evolution to $\Gamma^\star$ on which the dynamics are described by the η sub-dynamics. However, the ASR sampled-data equivalent model of the normal form above is;

$$\begin{aligned} z_1(k+1) &= z_1(k) + \delta z_2(k) + \frac{\delta^2}{2} u_1(k) \\ z_2(k+1) &= z_2(k) + \delta u_1(k) \\ \eta_1(k+1) &= \eta_1(k) - \delta\eta_2(1 + u_2) - \frac{\delta^2}{2}\eta_1(1 + u_2)^2 + O(\delta^3) \\ \eta_2(k+1) &= \eta_2(k) + \delta\eta_1(1 + u_2) - \frac{\delta^2}{2}\eta_2(1 + u_2)^2 + O(\delta^3) \end{aligned}$$

and for which, as detailed in Chapter 2, the discrete relative degree of $\alpha(\cdot) = z_1$ falls to $r_d = 1$ and the zero-dynamics submanifold of the sampled-data model does not coincide with $\Gamma^\star$. Consequently, stabilizing z_1 sub-dynamics does not confine the evolution to $\Gamma^\star$ as desired.

With reference to the above discussion, and example, two different design approaches are proposed in this chapter and the next. The first solution, working on the first step of the above mentioned TFL program, is based on a redesign of the functions with respect to which the performances of the feedback system are defined in a single-rate sampled data context. The second solution, on the other hand, works over the second step keeping the functions specifying the performances intact, and working over the feedback computation via multi-rate sampling.

This chapter will focus on the first solution; a single rate sampled-data approximate solution (that can be made arbitrarily accurate via an iterative procedure). This solution will be shown to exist whenever a continuous-time solution does. The results, discussion and example presented in this chapter serve as a *more elaborate* companion to the formal statements found in;

> Mohamed Elobaid, Salvatore Monaco and Dorothée Normand-Cyrot. *"Approximate transverse feedback linearization under digital control". IEEE Control System Letters (L-CSS), 2021, 6, 13 - 18. DOI: 10.1109/LCSYS.2020.3046539.*

The notions and concepts appearing in this chapter are based on Banaszuk and Hauser (1995),Nielsen and Maggiore (2008), Nielsen and Maggiore (2006), Akhtar et al. (2015) and the references therein. It is important here to remind the reader how useful TFL, and set stabilization techniques in general are. For it is enough to consider the case in which the set to be stabilized is physically meaningful (e.g. the *lift* of a path on the plane to the state-space, or the synchronization *hyper plane*) and the usefulness of those techniques becomes apparent.

Our point of departure is a general nonlinear control affine system of the form;

$$\dot{x} = f(x) + \sum_{i=1}^{m} g_i(x) u_i \tag{7.1}$$

where the vector fields are assumed complete and $g_i(x),\ i = 1, \dots, m$ are independent over $\mathbb{R}^n$.

7.1 Transverse feedback linearization in continuous-time

As already alluded to from the discussion, and the academic example above; transverse feedback linearization essentially refers to equivalence under feedback to a system characterized by a linear controllable sub-dynamics transverse to a given closed, controlled invariant, embedded sub-manifold in the system state-space. Formally from Nielsen and Maggiore (2008), one sets the problem below.

Problem: (Local) TFL in continuous-time

Let $\Gamma^\star \subset \mathbb{R}^n$ be a closed, controlled invariant sub-manifold for dynamics (7.1) and let $x_0 \in \Gamma^\star$; TFL is said to be locally solvable if there exist a feedback $u = \gamma(x, \nu)$ and a coordinates change $\phi(x) = \text{col}(\phi_1(x),\ \phi_2(x)) : x \to \text{col}(\xi,\ z)$, defined in a neighbourhood U of x_0, such that (7.1) rewrites

$$\begin{aligned} \dot{z} &= Az + B\nu_1 \\ \dot{\eta} &= f_\eta(z,\eta) + g^1_\eta(z,\eta)\nu_1 + g^2_\eta(z,\eta)\nu_2 \end{aligned} \tag{7.2}$$

where $z \in \mathbb{R}^{n-n^\star}, \eta \in \mathbb{R}^{n^\star}, \nu = col(\nu_1, \nu_2) \in \mathbb{R}^m$, $n^\star = \dim(\Gamma^\star)$, $g^1_\eta(\cdot), g^2_\eta(\cdot)$ are smooth (matrix) valued functions, B full column rank, the pair (A, B) controllable, $\phi(\Gamma^\star \cap U) = \{(z,\eta) : z = 0\}$. When U is a tubular neighbourhood of the whole $\Gamma^\star$, then TFL is said to hold *globally*.

The following comments are in order;

- $\dot{z} = Az + B\nu_1$ specifies the *transverse dynamics* and ν_1 the *transverse control*;
- the dynamics of η, restricted to $\phi(\Gamma^\star \cap U)$, $\dot{\eta} = f_\eta(0,\eta) + g^2_\eta(0,\eta)\nu_2$, is referred to as the *tangential dynamics* with ν_2 the *tangential control*;
- setting $\nu_1 = -Kz$ for a suitable $K : \sigma(A - BK) \subset \mathbb{C}^-$, (local) stabilization of $\Gamma^\star$ is achieved. If the trajectories of the closed loop system (under ν_1) are bounded, stabilization of $\Gamma^\star$ holds.

Thanks to the decoupling of the control components, one independently forces the state evolutions towards $\Gamma^\star$ via the control ν_1 and assigns a desired behaviour over $\Gamma^\star$ through ν_2.

Nielsen and Maggiore (2006) showed that Problem (7.1) is equivalent to the well known *zero dynamics assignment problem with relative degree* through output redefinition. The necessary and sufficient conditions for the solvability of the zero dynamics assignment problem, and hence (L)TFL problem, set in Nielsen and Maggiore (2008),Nielsen and Maggiore (2006) and recalled in the sequel, rely on the notion of a well defined vector relative degree in continuous-time as detailed in Section 1.2.

Theorem: TFL equivalence to zero dynamics assignment

The LTFL Problem 7.1 is solvable if and only if there exist ρ smooth $\mathbb{R}$-valued functions $(\alpha_1(x), \dots, \alpha_\rho(x))$, $\rho \leq m$, defined on U such that:

1. $\Gamma^\star \cap U \subset \{x \in U : \alpha_i(x) = 0, i = 1, \dots \rho\}$;
2. the dynamics (7.1) with output $\alpha(x) = col(\alpha_1(x), \dots, \alpha_\rho(x))$, has a well defined vector relative degree $r = (r_1, \dots, r_\rho)$ at x_0 with $\sum_{i=1}^{\rho} r_i = n - n^\star$.

When the vector relative degree is defined everywhere in a tubular neighbourhood of $\Gamma^\star$, then TFL holds globally.

Note that the above result is not constructive; it does not provide a method for finding the functions $\alpha_i, i = 1, \dots, \rho$ solving the problem, nor does it provide structural and verifiable conditions on the dynamics (7.1) to admit a solution to TFL. To this effect, we recall the following result which provides such verifiable necessary and sufficient conditions;

Theorem: TFL necessary and sufficient conditions

Consider the distributions $G_i = span\{ad_f^j g_k, 0 \leq j \leq i, 1 \leq k \leq m\}$, and suppose the involutive closure $\bar{G}_i$ are regular at x_0, then the (L)TFL problem is solveable if and only if;

1. $\dim(T_{p_0}\Gamma^\star + span\{G_{n-n^\star-1}\}) = n$.
2. $\exists U : (\forall x \in \Gamma^\star \cap U)\dim(T_p\Gamma^\star + G_i(p)) = \dim(T_p\Gamma^\star + \bar{G}_i(p)) = \text{constant}, 1 \leq i \leq n - n^\star - 2$.

Remark 7.1 *While the solvability of the (L)TFL problem is addressed by the Theorem above, the construction of the functions $\alpha_i(x)$, $i = 1, \dots, \rho$ is not. A constructive result to that effect, based on the annihilator of some controlled invariant distributions coinciding with the tangent bundle of the set $\Gamma^\star$ can be found in (Nielsen and Maggiore, 2008, Th 3.5). Informally, the (L)TFL problem is typically solved in continuous time in the following steps:*

1. *Find the coordinate transformation $\phi(x)$. This is done through the following steps*
   - *Check the necessary and sufficient conditions on the dynamics for the solvability of the problem.*
   - *If yes, try to write the set $\Gamma^\star$ as the $0-$level set of some $n - n^\star$ functions, and check if there exists a subset of those meeting the requirements of the zero dynamics assignment result.*
   - *If not possible, utilize the result in (Nielsen and Maggiore, 2008, Th 3.5) to construct the dummy output.*
2. *Once the required outputs are found with well defined vector relative degree, one uses the usual transformation to put the system in normal form. Then it is always possible to use a decoupling static state feedback to split the control into transverse and tangential components, Figure 7.1 illustrates this fact.*

Remark 7.2 *As depicted in Figure 7.1 below, the decoupling of the controls into transverse and tangential controls is done in the following manner: by the definition of the vector relative degree of the output functions $\alpha_i(x)$ solving the TFL problem in continuous-time, the $\rho \times m$ decoupling matrix $D(x)|_{x=\phi^{-1}(z,\eta)}$ is full row rank. One can re-write this matrix as $D(\cdot) = [M(\cdot) \;\; N(\cdot)]$ where the $\rho \times \rho$ matrix $M(\cdot)$ is non-singular, and $N(\cdot) = span\{\ker D(\cdot)\}$. Thus, setting*

$$u_1 = M^{-1}(x)\Big(\nu_1 - N(x) - \tilde{f}(x)\Big)|_{x=\phi^{-1}(z,\eta)}$$
$$u_2 = \nu_2$$

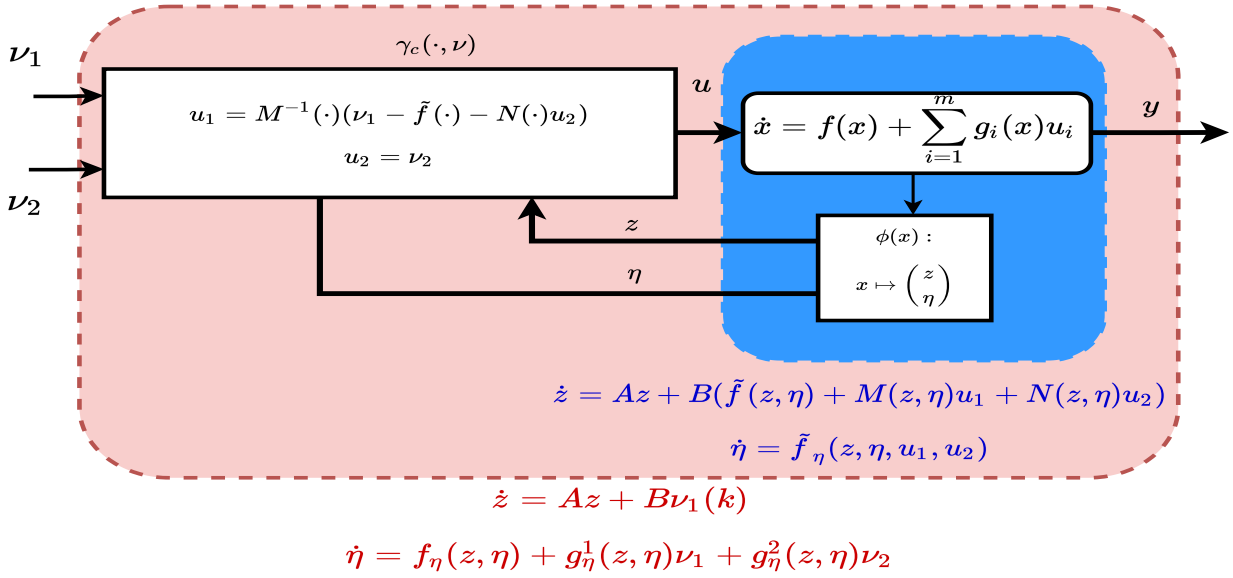

Figure 7.1: Solution of TFL in continuous time

with $\tilde{f}(\cdot) = col(L_f^{r_1}\alpha_1(x), \ \ldots, \ L_f^{r_\rho}\alpha_\rho(x))$ *performs the desired effect. Consequently, one gets the TFL normal form as in Figure 7.1*

At this point, it is imperative to stress that to the best of the author's knowledge, TFL has never been addressed in the digital context. Motivated by this fact, in what follows, we will attempt to address this gap first in an approximate sense under single-rate sampling, and later in a more complete manner under multi-rate sampling.

7.2 Preservation of the relative degree under single-rate sampling

Starting from the observations made in Chapter 2 concerning the loss of relative degree and appearance of extra zero dynamics under sampling, it is clear that the TFL normal form structure is lost under sampling as depicted in the figure below. Indeed the sampled equivalent model to a system in normal form is a nonlinear map as depicted in red losing the structure of a linear controllable dynamics transverse to the desired sub-manifold.

As discussed in Section 2.3, and detailed for SISO systems in Barbot et al. (1996) (see also Barbot et al. (1992)), it is possible to preserve the relative degree and the normal form structure in a predefined approximate order. In the sequel, we adapt these developments found in Barbot et al. (1996) to the general MIMO case posed by the dynamics (7.1) in the context of TFL.

To this end, let the continuous-time dynamics (7.1) have a well defined vector relative degree $r = (r_1 \ r_2 \ \ldots \ r_\rho)$ in a neighbourhood of a point x_0, with respect to an output function

$$y = \begin{pmatrix} \alpha_1(x) & \alpha_2(x) & \ldots & \alpha_\rho(x) \end{pmatrix}^\top \tag{7.3}$$

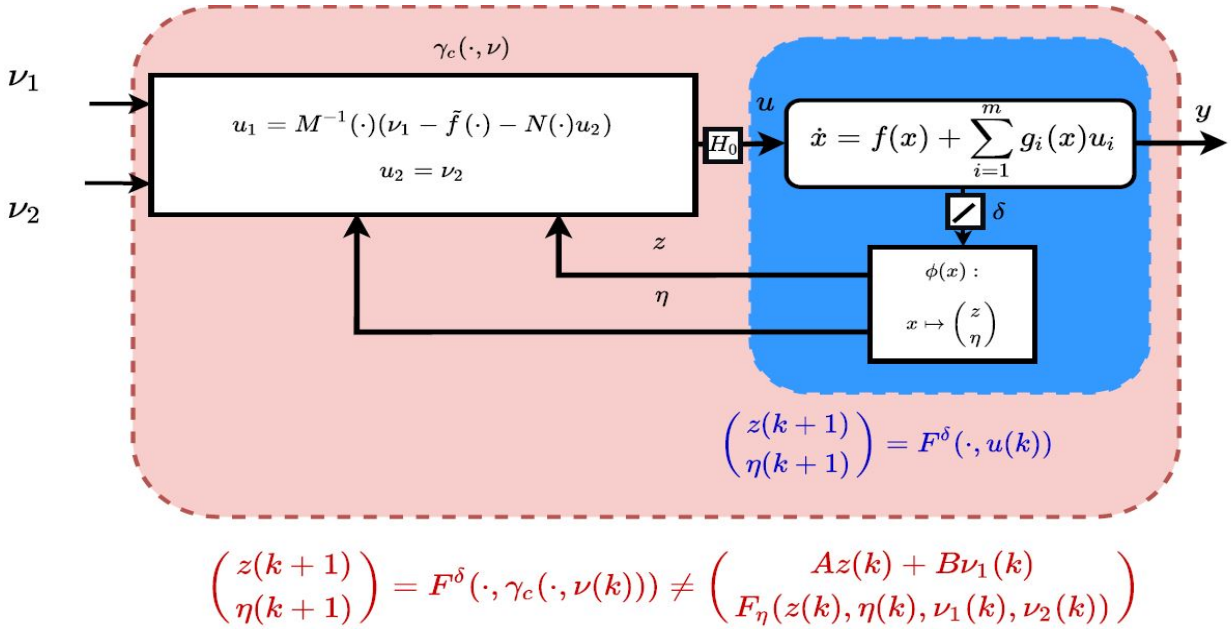

Figure 7.2: Failure of TFL emulation via sample and zero order holding to preserve the TFL normal form

Consequently, there exists a continuous-time coordinates change

$$\begin{aligned} z_1 = \phi_1(x) &= \begin{pmatrix} \alpha_1(x) & L_f\alpha_1(x) & \dots & L_f^{r_1-1}\alpha_1(x) \end{pmatrix}^\top && \in \mathbb{R}^{r_1} \\ &\vdots \\ z_\rho = \phi_\rho(x) &= \begin{pmatrix} \alpha_\rho(x) & L_f\alpha_\rho(x) & \dots & L_f^{r_\rho-1}\alpha_\rho(x) \end{pmatrix}^\top && \in \mathbb{R}^{r_\rho} \\ \eta = \phi_{\rho+1}(x) & && \in \mathbb{R}^{n-r_1-\dots-r_\rho} \end{aligned} \tag{7.4}$$

under which the system takes the normal form;

$$\begin{aligned} \dot{z}_1 &= A_{r_1} z_1 + b_{r_1}(b_1(z,\eta) + a_1(z,\eta)u) \\ &\vdots \\ \dot{z}_\rho &= A_{r_\rho} z_\rho + b_{r_\rho}(b_\rho(z,\eta) + a_\rho(z,\eta)u) \\ \dot{\eta} &= q(z,\eta) + p(z,\eta)u \end{aligned}$$

with A_{r_i}, b_{r_i} as in (2.10) and $b_i(z,\eta) = L_f^{r_i}\alpha_i(x)$ and

$$a_i(z,\eta) = \begin{pmatrix} L_{g_1}L_f^{r_i-1}\alpha_i(x) & \dots & L_{g_m}L_f^{r_i-1}\alpha_i(x) \end{pmatrix} \tag{7.6}$$

Under piecewise constant control, and applying the definition (2.6), the single-rate sampled

equivalent model reads;

$$z_1(k+1) = A^\delta_{r_1} z_1(k) + b^\delta_{1,r_1}(b_1(z(k),\eta(k)) + a_1(z(k),\eta(k))u(k)) + \sum_{i\geq 2} b^\delta_{i,r_1} L^{i-1}_{f+\sum_{i=1}^m g_i u_i(k)}(b_1(z(k),\eta(k)) + a_1(z(k),\eta(k))u(k))|_{x=\phi^{-1}(z(k),\eta(k))} \tag{7.7a}$$

$$\vdots$$

$$z_\rho(k+1) = A^\delta_{r_\rho} z_\rho(k) + b^\delta_{1,r_\rho}(b_\rho(z(k),\eta(k)) + a_\rho(z(k),\eta(k))u(k)) + \sum_{i\geq 2} b^\delta_{i,r_\rho} L^{i-1}_{f+\sum_{i=1}^m g_i u_i(k)}(b_\rho(z(k),\eta(k)) + a_\rho(z(k),\eta(k))u(k))|_{x=\phi^{-1}(z(k),\eta(k))} \tag{7.7b}$$

$$\eta(k+1) = \eta(k) + \delta\Big(q(z(k),\eta(k)) + p(z(k),\eta(k))u(k)\Big) + O(\delta^2) \tag{7.7c}$$

$$y_i(k) = c_{r_i} z_i(k), \quad i = 1 \dots \rho \tag{7.7d}$$

with c_{r_i} as in (2.10), the δ-dependent matrix $A^\delta_{r_i}$ as in (2.12) and for $j \geq 1$

$$b^\delta_{j,r_i} = \begin{pmatrix} \frac{\delta^{r_i+j-1}}{(r_i+j-1)!} & \frac{\delta^{r_i+j-2}}{(r_i+j-2)!} & \dots & \frac{\delta^j}{j!} \end{pmatrix}^\top \tag{7.8}$$

As mentioned earlier, it can be verified that the discrete vector relative degree with respect to the output (7.7d) falls to $r_{d,i} = (1,\ 1,\ \dots, 1)$ when truncating the SR sampled equivalent model at the order $\mathrm{col}(p_1,\ \dots, p_n)$ with $p_i \geq \max(r_j)$ or higher in δ because

$$\frac{\partial y_i(k+1)}{\partial u(k)} = \frac{\partial c_{r_i} z_i(k+1)}{\partial u(k)} = \frac{\delta^{r_i}}{r_i!} a_i(z(k),\eta) \neq 0$$

To weaken this pathology, it has been proposed in Barbot et al. (1996) (see also the work by the same authors Barbot et al. (1992)) to modify the continuous-time output function in a δ dependent manner, namely setting

$$y^\delta = \begin{pmatrix} \alpha^\delta_1(x) & \dots & \alpha^\delta_\rho(x) \end{pmatrix}^\top = C^\delta z \tag{7.9}$$

Where $C^\delta = \mathrm{blkdiag}\{c^\delta_1,\ \dots, c^\delta_\rho\}$ and

$$c^\delta_i = \delta^{r_i} \begin{pmatrix} 0 & 0 & \dots & 1 \end{pmatrix} \begin{pmatrix} b^\delta_{1,r_i} & A^\delta_{r_i} b^\delta_{1,r_i} & \dots & (A^\delta_{r_i})^{(r_i-1)} b^\delta_{1,r_i} \end{pmatrix}^{-1} \tag{7.10}$$

corresponding to this output, one can obtain a coordinates change;

$$\begin{pmatrix} z^\delta_1 \\ \vdots \\ z^\delta_\rho \\ \eta^\delta \end{pmatrix} = \phi^\delta(x) = \left(\begin{array}{ccc|c} T_{r_1}(\delta) & \dots & 0 & \\ & \ddots & & 0_{(n-n^\star)\times n^\star} \\ 0 & \dots & T_{r_\rho}(\delta) & \\ \hline \multicolumn{3}{c|}{0_{n^\star\times(n-n^\star)}} & \mathrm{I}_{n^\star\times n^\star} \end{array}\right) \begin{pmatrix} z_1 \\ \vdots \\ z_\rho \\ \eta \end{pmatrix} \tag{7.11}$$

where z, η are as in (7.4), and

$$T_{r_i}(\delta) := \begin{pmatrix} c_{r_i}^{\delta} \\ \frac{1}{\delta} c_{r_i}^{\delta}(A_{r_i}^{\delta} - I) \\ \vdots \\ \frac{1}{\delta^{r_i-1}} c_{r_i}^{\delta}(A_{r_i}^{\delta} - I)^{(r_i-1)} \end{pmatrix} \tag{7.12}$$

and we have the following statement **extending** that of Proposition 3.2 in Barbot et al. (1996).

Result: MIMO Sampled normal form of order $p = 1$

The sampled-data system (7.7a),(7.7b),(7.7c),(7.7d), has a DT vector relative degree $(r_{d,1}, \ldots, r_{d,\rho})$ with respect to the dummy output (7.9) up to approximation in $\mathrm{col}\{O(\delta^{r_1+1}), \ldots, O(\delta^{r_\rho+1})\}$ and is transformed under the coordinates change (7.11),(7.12) into the *approximate sampled normal form* of order $p = 1$

$$z_1^{\delta}(k+1) = (I + \delta A_{r_1}) z_1^{\delta}(k) + \delta b_{r_1}(b_1(\cdot, \eta^{\delta}(k)) + a_1(\cdot, \eta^{\delta}(k))u(k)) + O(\Delta_1^2) \tag{7.13a}$$

$$\vdots$$

$$z_\rho^{\delta}(k+1) = (I + \delta A_{r_\rho}) z_\rho^{\delta}(k) + \delta b_{r_\rho}(b_\rho(\cdot, \eta^{\delta}(k)) + a_\rho(\cdot, \eta^{\delta}(k))u(k)) + O(\Delta_\rho^2) \tag{7.13b}$$

$$\eta^{\delta}(k+1) = \eta^{\delta}(k) + \delta\Big(q(z^{\delta}(k), \eta^{\delta}(k)) + p(z^{\delta}(k), \eta^{\delta}(k))u(k)\Big) + O(\delta^2) \tag{7.13c}$$

$$y_i^{\delta}(k) = c_{r_i} z_i^{\delta}(k) \tag{7.13d}$$

with

$$\Delta_i^{p+1} = \begin{pmatrix} \frac{\delta^{r_i+p}}{(r_i+p)!} & \frac{\delta^{r_i+p-1}}{(r_i+p-1)!} & \cdots & \frac{\delta^{p+1}}{(p+1)!} \end{pmatrix}^{\top} \tag{7.14}$$

One should emphasize that the coordinates change (7.11) allows for the definition of an *approximate* sampled data normal form (7.13a) — (7.13d) in $O(\Delta_i^2)$ **which corresponds to preserving the relative degree of each output at** $O(\delta^{r_i+1})$ unlike in Euler's approximation. This normal form preserves the relative degree of the continuous-time system in an approximate sense in a prefixed order of approximation, and consequently recover linear feedback equivalence via inversion under digital control despite sampling.

Remark 7.3 *the dummy output (7.9), and the coordinates change (7.12) for the first values of r explicitly are*

- **the case** $r = 2$*:*

$$y^{\delta} = y - \frac{\delta}{2}\dot{y} = (1 \quad 0) z^{\delta}$$

$$z^{\delta} = T_2(\delta) z = \begin{pmatrix} 1 & \frac{-\delta}{2} \\ 0 & 1 \end{pmatrix} \begin{pmatrix} z_1 \\ z_2 \end{pmatrix}$$

- **the case** $r = 3$

$$y^\delta = y - \delta\dot{y} + \frac{\delta^2}{3}\ddot{y} = (1 \quad 0 \quad 0)z^\delta$$
$$z^\delta = T_3(\delta)z = T_3(\delta) = \begin{pmatrix} 1 & -\delta & \frac{\delta^2}{3} \\ 0 & 1 & \frac{-\delta}{2} \\ 0 & 0 & 1 \end{pmatrix} \begin{pmatrix} z_1 \\ z_2 \\ z_3 \end{pmatrix}$$

Preserving the relative degree in higher order approximations

For preserving the relative degree, and the sampled normal form structure in higher orders of approximations, i.e col$\{O(\Delta_1^{p+1}),\ \ldots,\ O(\Delta_\rho^{p+1})\}$ with $p \geq 2$, an iterative procedure was proposed in Barbot et al. (1996) in the SISO case and hereinafter extended to the MIMO setting. In this context, the first successive term of the approximation is detailed and the general iterative procedure is outlined.

To this end, let $p = 2$ and consider the sampled normal form (7.13a) — (7.13d) and let

$$u(x(k)) = u^0(x(k)) + \delta u^1(x(k)) \tag{7.15}$$

equivalently, rewrite the control adding a single successive so-called corrective term. With this in place, and considering higher truncations in (7.13a) — (7.13d) i.e.;

$$\begin{aligned}
z_1^\delta(k+1) &= (I + \delta A_{r_1})z_1^\delta(k) + \delta b_{r_1}\Big[b_1(\cdot,\eta^\delta(k)) + a_1(\cdot,\eta^\delta(k))(u^0(k) + \delta u^1(k))\Big] \\
&\quad + \underline{T_{r_1}(\delta)b_{2,r_1}^\delta L_{f+\sum_{i=1}^m g_i u_i(k)}(b_1(\cdot,\eta^\delta(k)) + a_1(\cdot,\eta^\delta(k))u^0(k))} + O(\Delta_1^3) \\
&\vdots \\
z_\rho^\delta(k+1) &= (I + \delta A_{r_\rho})z_\rho^\delta(k) + \delta b_{r_\rho}\Big[b_\rho(\cdot,\eta^\delta(k)) + a_\rho(\cdot,\eta^\delta(k))(u^0(k) + \delta u^1(k))\Big] \\
&\quad + \underline{T_{r_\rho}(\delta)b_{2,r_\rho}^\delta L_{f+\sum_{i=1}^m g_i u_i(k)}(b_\rho(\cdot,\eta^\delta(k)) + a_\rho(\cdot,\eta^\delta(k))u^0(k))} + O(\Delta_\rho^3) \\
\eta^\delta(k+1) &= \eta^\delta(k) + \delta\Big(q(z^\delta(k),\eta^\delta(k)) + p(z^\delta(k),\eta^\delta(k))u(k)\Big) + O(\delta^2)
\end{aligned}$$

so one is interested in finding a corrective term $u^1(k)$ such that the underlined terms are compensated for. Equivalently, after gathering terms in a compact way, a corrective term solving the following equality

$$\delta^2 \begin{pmatrix} a_1(\cdot,\eta^\delta(k)) \\ \vdots \\ a_\rho(\cdot,\eta^\delta(k)) \end{pmatrix} u^1(k) = - \begin{pmatrix} T_{r_1}(\delta)b_{2,r_1}^\delta L_{f+\sum_{i=1}^m g_i u_i(k)}(b_1(\cdot,\eta^\delta(k)) + a_1(\cdot,\eta^\delta(k))u^0(k)) \\ \vdots \\ T_{r_\rho}(\delta)b_{2,r_\rho}^\delta L_{f+\sum_{i=1}^m g_i u_i(k)}(b_\rho(\cdot,\eta^\delta(k)) + a_\rho(\cdot,\eta^\delta(k))u^0(k)) \end{pmatrix} \tag{7.16a}$$

which admits a solution since simple calculations yield $T_{r_i}(\delta)b_{2,r_i}^\delta = \delta^2 b_{r_i}$ and the matrix multiplying $u^1(k)$ from the right is full row rank by construction considering truncations, at least locally where the continuous-time vector relative degree is assumed defined. Consequently solving for $u^1(k)$ one obtains the approximate sampled normal form;

$$
\begin{aligned}
z_1^\delta(k+1) &= (I+\delta A_{r_1})z_1^\delta(k) + \delta b_{r_1}\Big[b_1(\cdot,\eta^\delta(k)) + a_1(\cdot,\eta^\delta(k))u^0(k))\Big] + O(\Delta_1^3)\\
&\vdots\\
z_\rho^\delta(k+1) &= (I+\delta A_{r_\rho})z_\rho^\delta(k) + \delta b_{r_\rho}\Big[b_\rho(\cdot,\eta^\delta(k)) + a_\rho(\cdot,\eta^\delta(k))u^0(k))\Big] + O(\Delta_\rho^3)\\
\eta^\delta(k+1) &= \eta^\delta(k) + \delta\Big(q(z^\delta(k),\eta^\delta(k)) + p(z^\delta(k),\eta^\delta(k))u(k)\Big) + O(\delta^2)\\
y_i^\delta(k) &= c_{r_i} z_i^\delta(k), \qquad i=1,\dots,\rho
\end{aligned}
\tag{7.17}
$$

Result: MIMO sampled normal form in order $p>1$

The sampled-data model (7.7a) — (7.7d) has a DT vector relative degree $(r_{d,1},\ \dots, r_{d,\rho})$ with respect to the dummy output (7.9) up to approximation in $\text{col}\{O(\delta^{r_1+p}),\ \dots,\ O(\delta^{r_\rho+p})\}$ when considering p additional corrective terms in the control, namely

$$
u(k) = u^0(k) + \delta u^1(k) + \ldots + \frac{\delta^p}{p!}u^p(k) = \sum_{i=0}^{p}\frac{\delta^i}{i!}u^i(k) \tag{7.18}
$$

and the single-rate sampled-data system, under the coordinates change (7.11),(7.12) is transformed into the *approximate sampled data normal form*

$$
\begin{aligned}
z_1^\delta(k+1) &= (I+\delta A_{r_1})z_1^\delta(k) + \delta b_{r_1}\Big[b_1(\cdot,\eta^\delta(k)) + a_1(\cdot,\eta^\delta(k))u^0(k))\Big] + O(\Delta_1^{p+1})\\
&\vdots\\
z_\rho^\delta(k+1) &= (I+\delta A_{r_\rho})z_\rho^\delta(k) + \delta b_{r_\rho}\Big[b_\rho(\cdot,\eta^\delta(k)) + a_\rho(\cdot,\eta^\delta(k))u^0(k))\Big] + O(\Delta_\rho^{p+1})\\
\eta^\delta(k+1) &= \eta^\delta(k) + \delta\Big(q(z^\delta(k),\eta^\delta(k)) + p(z^\delta(k),\eta^\delta(k))u(k)\Big) + O(\delta^2)\\
y_i^\delta(k) &= c_{r_i} z_i^\delta(k), \qquad i=1,\dots,\rho
\end{aligned}
\tag{7.19}
$$

Remark 7.4 *note that solving for the first corrective term requires predictions of the states and the control $u^0(k+1)$ because of the operator $L_{f+\sum_{i=1}^m g_i u_i(k)}$. This requirement is not restrictive as can be seen extending the statements in Barbot et al. (1992).*

It is perhaps obvious to the reader by now that a byproduct of the approximate sampled normal form is the preservation of the zero dynamics structure at the first approximation. This motivates the use of this normal form to the purpose of preserving TFL in an approximate sense under single rate sampling as will be detailed in the sequel.

7.3 Approximate transverse feedback linearization under single rate sampling

Following on from the discussion above we can set the problem addressed in this chapter, namely;

Problem: (Local) TFL under single-rate sampling

Let $\Gamma^\star \subset \mathbb{R}^n$ be a closed, controlled invariant sub-manifold for dynamics (7.1) and let $x_0 \in \Gamma^\star$. **Find** for any $\delta \in]0, T^\star[$, $T^\star > 0$ small enough, a piecewise constant feedback $u^\delta = \gamma^\delta(x, v)$ and a coordinates change $\phi^\delta(\cdot) : x \mapsto (z^\delta, \eta^\delta)$ defined in a neighbourhood U of $x_0 \in \Gamma^\star$, under which the sampled-data closed loop dynamics takes the normal form below

$$z^\delta(k+1) = (Id + \delta A)z^\delta(k) + \delta B\nu_1(k) \tag{7.20a}$$
$$\eta^\delta(k+1) = F_\eta^\delta(z^\delta(k), \eta^\delta(k), \nu_1(k), \nu_2(k)) \tag{7.20b}$$

with $z^\delta \in \mathbb{R}^{n-n^\star}$, $\eta^\delta \in \mathbb{R}^{n^\star}$, $\nu = \text{col}\{\nu_1,\ \nu_2\} \in \mathbb{R}^m$ and $\phi^\delta(\Gamma^\star \cap U) = \{(z^\delta, \eta^\delta) : z^\delta = 0\} \equiv \{(z, \eta) : z = 0\} = \phi(\Gamma^\star \cap U)$. If instead (7.20a) is approximated in $O(\Delta^{p+1})$;

$$z^\delta(k+1) = (Id + \delta A)z^\delta(k) + \delta Bv_1(k) + O(\Delta^{p+1}) \tag{7.21}$$

with

$$\Delta^{p+1} = \begin{pmatrix} \Delta_1^{p+1} & \dots & \Delta_\rho^{p+1} \end{pmatrix}^\top \tag{7.22}$$

with Δ_i^{p+1} as in (7.14), the solution is said to be *approximate of order p*. If the relative degree is well defined for all $x \in \Gamma^\star$ we will say, with a little abuse of nomenclature, that the problem is globally solved around $\Gamma^\star$.

The utilization of approximate sampled normal forms to preserve feedback equivalence is coupled with the observation that the zero dynamics sub-manifold of the sampled-data model associated with the continuous-time dummy outputs $\alpha_i(\cdot), i = 1, \dots, \rho$ contains $\Gamma^\star$ because;

$$\mathcal{Z}_{SD} = \{\tilde{x} : \alpha_1(x) = \dots = \alpha_\rho(x) = 0\} \subseteq \mathbb{R}^{n-\rho}$$
$$\mathcal{Z}_{SD} \supset \Gamma^\star = \{x : \alpha_1(x) = L_f\alpha_1(x) = L_f^{r_1}\alpha_1(x) = \dots = \alpha_\rho(x) = L_f\alpha_\rho(x) = L_f^{r_\rho}\alpha_\rho(x) = 0\} \subseteq \mathbb{R}^{n^\star}$$

This is a byproduct of the transformation defining the sampled-normal form being a linear transformation with constant matrix $z^\delta = T(\delta)z$, $\eta^\delta = \eta$ so that $z = 0 \implies z^\delta = 0$. ■

Indeed, for an approximate solution at the order $p = 1$ it is enough to directly apply the result concerning the sampled normal form as the following figure suggests;

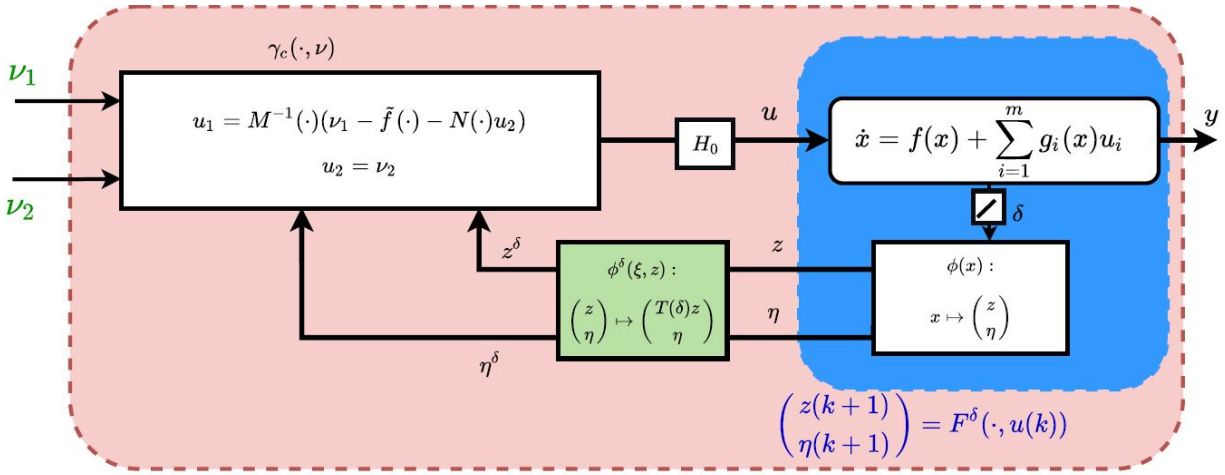

$$z^\delta(k+1) = (I + \delta A)z^\delta(k) + \delta B\nu_1(k) + O(\Delta^2)$$
$$\eta^\delta(k+1) = F^\delta_\eta(z^\delta(k), \eta^\delta(k), \nu_1(k), \nu_2(k))$$

Figure 7.3: Approximate preservation of TFL via single-rate sampling for $p = 1$

with the above discussion we can make the following statement generalizing that in (Elobaid et al., 2020c, Theorem 1)

Result: approximate SD-TFL

Let $\Gamma^\star \subset \mathbb{R}^n$ be a closed, controlled invariant sub-manifold for dynamics (7.1) and specifying the TFL problem. Assume there exists output functions $\alpha_i(\cdot), i = 1, \dots, \rho$ solving the TFL problem in continuous-time. Then there exist a small enough $T^\star > 0$, and for any $\delta \in]0, T^\star[$, a δ-dependent coordinates change $\phi^\delta(x)$ and a sampled-data feedback $\gamma^\delta(x, v)$ under which the sampled-data equivalent model takes the following approximate normal form

$$z^\delta(k+1) = (Id + \delta A)z^\delta(k) + \delta B\nu_1(k) + O(\Delta^{p+1})$$
$$\eta^\delta(k+1) = F^\delta_\eta(z^\delta(k), \eta^\delta(k), \nu_1(k), \nu_2(k))$$

where $O(\Delta^{p+1})$, $p \geq 1$ is the vector approximation of the form (7.22). Moreover, $\Gamma^\star$ is the zero dynamics sub-manifold associated with the modified output function of the form (7.9), and the zero dynamics coincide with the dynamics of η^δ at the first order. .

Some comments are in order;

- The sub-manifold $\Gamma^\star$ is given a priori, and in this context the problem above concerns the preservation of the (L)TFL property under single-rate sampling. It does not concern the existence and the computation, for the equivalent sampled-data dynamics, of a closed controlled invariant sub-manifold for which the problem is solvable.
- The sampled-data tangential η^δ-dynamics on $\Gamma^\star$ recovers the continuous-time η-dynamics in the first approximation i.e $O(\delta^2)$.

- The sampled-data transverse dynamics recovers the transverse dynamics in the vector approximation $O(\Delta^{p+1})$ **drastically improving over Euler's approximation.** In fact, this is precisely the reason we obtain better performances compared to ZOH of the continuous-time solution.

- As the previous section suggests, an approximate solution could be obtained preserving the TFL normal form structure by modifying the dummy outputs solving the problem in continuous-time. The modification stands in adding $\delta-$dependent additional terms, suitable combinations of the higher derivatives, to the original dummy outputs thus preserving the relative degrees at prefixed orders.

- From Figure 7.3 above, it is clear that the proposed solution, **at least at the order $O(\Delta^2)$ is very simple, with the modification highlighted in green in Figure 7.3 requiring only a change of coordinates that can be pre-calculated offline. The feedback linearizing the transverse dynamics comes to be the emulation one, and the stabilizing external transverse control comes to depend on the new coordinates change and thus on δ explaining the better performances compared to emulation of the external stabilizing control.**

- For a sketch of the proof one can refer to the statements and results in Elobaid et al. (2020c).

7.4 Illustrative example

To demonstrate the effectiveness of using approximate sampled normal forms to preserve TFL under digital control as compared to holding the continuous-time solution via ZOH, an academic example *complementing* the ones already reported in Elobaid et al. (2020c) is presented below. Note that, in the cited reference, both a treatment of Example 7.1 using the developed machinery in this chapter, and a path following application for a differential drive are reported for the interested reader.

Example 7.2 Consider the following academic example due to Banaszuk and Hauser (1995)

$$\dot{x} = f(x) + g_1(x)u \tag{7.23}$$

with

$$f(x) = \begin{pmatrix} x_2 + x_1 x_3 \\ -x_1 + x_2 x_3 \\ 0 \end{pmatrix}, \qquad g(x) = \begin{pmatrix} x_1 \\ x_2 \\ 1 \end{pmatrix}$$

The TFL problem has been set and solved in Banaszuk and Hauser (1995) with the control goal of stabilizing the family of orbits given by $\Gamma^\star = \{x \in \mathbb{R}^3 : x_1^2 + x_2^2 - R^2 = x_3 = 0\}$ where $R \in \mathbb{R}$. It has been shown that the function

$$\alpha(x) = \frac{1}{2}\ln(x_1^2 + x_2^2) - \ln R - x_3$$

has relative degree $r = 2 = n - n^\star$, so defining the coordinates change

$$\begin{aligned} z_1 &= \frac{1}{2}\ln(x_1^2 + x_2^2) - \ln R - x_3 \\ z_2 &= x_3 \\ \eta_1 &= -\tan^{-1}\frac{x_2}{x_1} \end{aligned}$$

puts the system, approperiately defining $\tan^{-1}(\cdot)$, in the form;

$$\begin{aligned} \dot{z}_1 &= z_2 \\ \dot{z}_2 &= u \\ \dot{\eta}_1 &= 1 \end{aligned}$$

Under sampling, setting according to (7.9)

$$y^\delta = y - \frac{\delta}{2}\dot{y} = \alpha(x) - \frac{\delta}{2}\dot{\alpha}(x)$$

one defines the sampled coordinates change as

$$\begin{aligned} z^\delta &= T_2(\delta)z = \begin{pmatrix} \frac{1}{2}\ln(x_1^2 + x_2^2) - \ln R - (1 + \frac{\delta}{2})x_3 \\ x_3 \end{pmatrix} \\ \eta^\delta &= \eta = \tan^{-1}\frac{x_2}{x_1} \end{aligned}$$

under which (7.23) is transformed, after sampling, into

$$\begin{aligned} z_1^\delta(k+1) &= z_1^\delta(k) + \delta z_2^\delta(k) \\ z_2^\delta(k+1) &= z_2^\delta(k) + \delta u(k) \\ \eta^\delta(k+1) &= \eta^\delta(k) + \delta \end{aligned} \tag{7.24}$$

Accordingly, setting the (single) transverse control

$$u^\delta(k) = -k_1 z_1^\delta - k_2 z_2^\delta \tag{7.25}$$

with $k, k2$ such that the closed loop transverse dynamics poles are located at the corresponding closed loop ideal continuous-time ones. This feedback stabilizes the transverse dynamics over $\Gamma^\star = \{x \in \mathbb{R}^4 : \alpha(x) = \dot{\alpha}(x) = 0\} = \{x \in \mathbb{R}^4 : z_1^\delta = z_2^\delta = 0\}$.

In Figure 7.4, the initial condition is $x_0 = col(0.1,\ 0.2,\ 0)^\top \notin \Gamma^\star$ and the continuous-time feedback is set to

$$u = -z_1 - \sqrt{3}z_2$$

thus placing the poles of the linearized transverse dynamics at $p_d = \{-0.8660{+}0.5i,\ -0.8660{-}0.5i\}$. The sampling period is set to $\delta = 0.5$ and the feedback (7.25) is set with gains $k_1 = 0.4387,\ k_2 = 1.2617$ placing the linearized sampled transverse dynamics poles at $\{e^{(-0.8660-0.5i)\delta},\ e^{(-0.8660+0.5i)\delta}\}$. This feedback stabilizes the system to the periodic orbit solution.

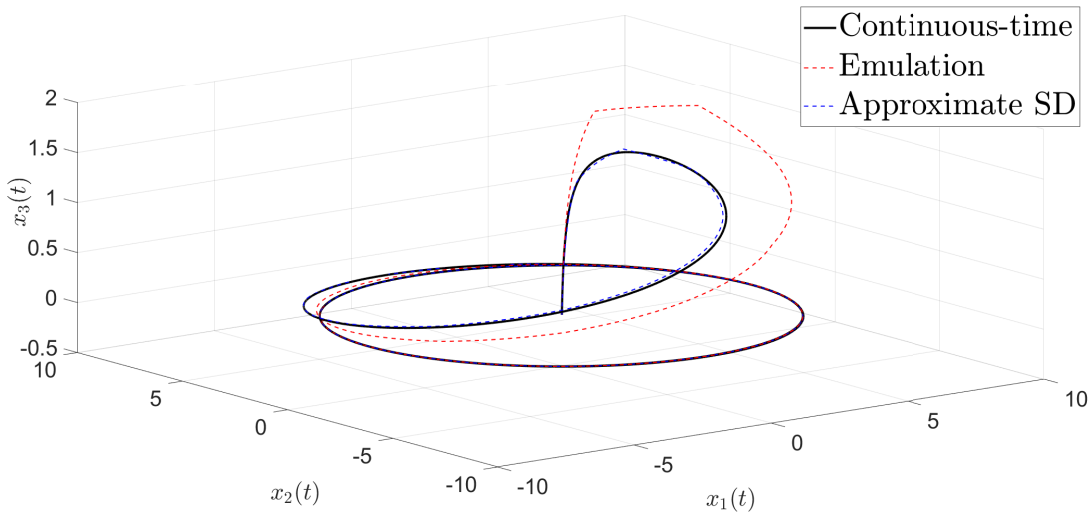

Figure 7.4: States Evolution approaching $\Gamma^\star, \delta = 0.5$

Figure 7.5 illustrates that the same situation when the sampling period is increased $\delta = 1$. Note that the approximate sampled solution, at the first approximation order (7.25) manages to follow the continuous-time ideal performance while the emulation fails when holding constant (ZOH) the CT control.

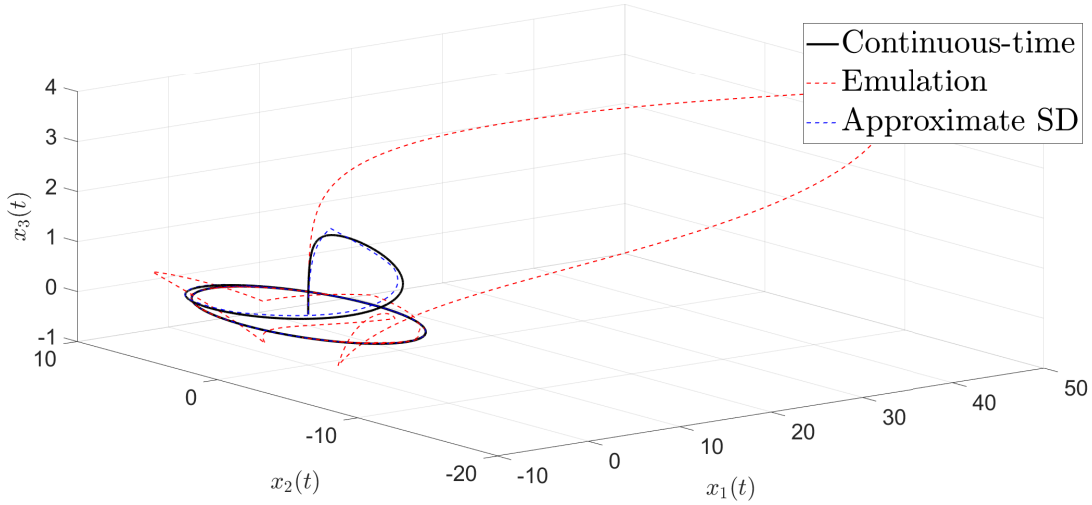

Figure 7.5: Failure of the emulation with $\delta = 1$

Finally, 7.6 depicts the interesting situation where we start on the set $\Gamma^\star$ with the sampling period increased to $\delta = 3$. Indeed both the ideal continuous-time solution and the proposed method coincide managing to maintain invariance, emulation fails to maintain invaraince of the periodic orbit.

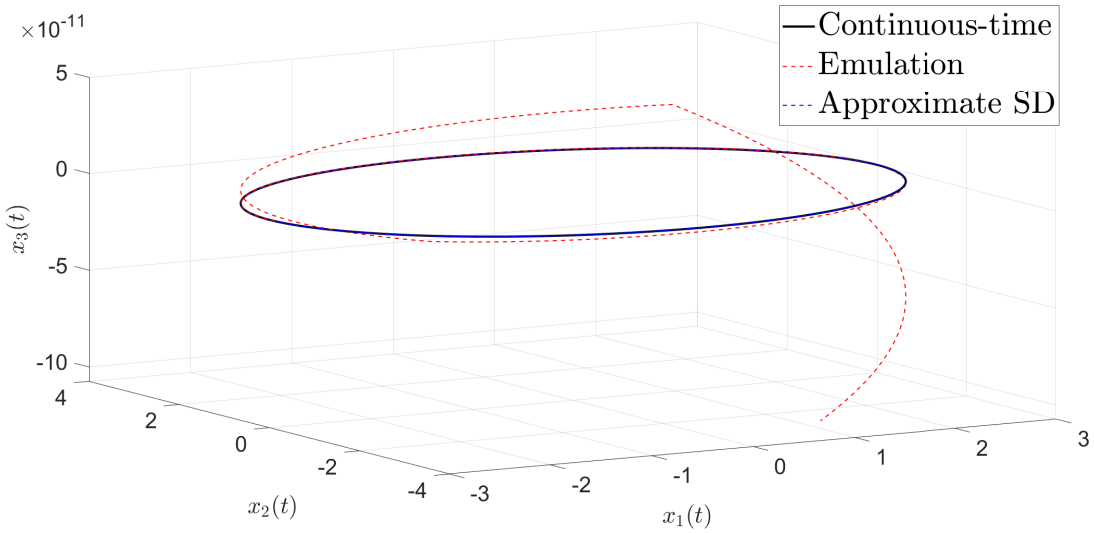

Figure 7.6: Invariance of $\Gamma^\star, \delta = 3$

7.5 Concluding remarks

A few comments to summarize this chapter are in order;

- A single-rate sampled-data solution that preserves TFL up to suitably defined approximations has been described based on similar results for linearization under feedback Barbot et al. (1996), Monaco et al. (1986a).
- The proposed solution leads to the redefinition of a transverse output function that depends on delta and allows to preserve in the so defined approximate sense the continuous-time relative degree. Then the digital stabilizing control (negative output feedback plus stabilizing terms) is easily computed on the sampled data normal form.
- The proposed solution recovers $\Gamma^\star$ as the zero dynamics sub-manifold of the sampled-data model.
- By construction the proposed digital scheme outperforms a simple emulated one that does not preserve for the same order of approximation the invariance of $\Gamma^\star$
- The degree of approximation can be arbitrarily enhances by adding additional corrective terms in the control.

While the solution proposed in this chapter is attractive, it has a few disadvantages, namely;

- The solution proposed is approximate in nature. Thus no general statements on the existence of an exact solution preserving the continuous-time one was made.
- Even if the order of approximation can be arbitrarily enhanced leading to a "*quasi-exact*" solution, the price is quite heavy computations depending on the nonlinearities.

With these observation we ask if one can obtain: First, guarantees of existence of an exact solution recovering TFL under sampling using multi-rate. And second, if this multirate solution, even when approximated for implementation purposes at the first order, improves upon the approximate single-rate solution in practical situations. These aspects will lead us to the next and final core chapter of this work.

Approximate Transverse Feedback Linearization Under Digital Control

Mohamed Elobaid, Salvatore Monaco, *Fellow, IEEE*, and Dorothée Normand-Cyrot, *Fellow, IEEE*

***Abstract*—Thanks to a suitable redesign of the maps involved in the continuous-time solution, a digital design procedure preserving transverse feedback linearization up to a prefixed order of approximation in the sampling period is described. Simulated examples illustrate the results.**

***Index Terms*—Sampled-data control, feedback linearization, algebraic/geometric methods.**

I. Introduction

SEVERAL control problems, as for instance synchronization, path following or manoeuvring electro-mechanical systems, can be naturally cast in the context of *set stabilization*, relying on stabilization over surfaces that specify the control goals (e.g., [1], [2], [3], [4]). Various approaches have been proposed in the recent literature for solving set stabilization problems; among them the ones based on Lyapunov arguments (e.g., [1]), immersion and invariance (e.g., [5], [6]) and, more relevant for this letter, those based on the notion of *feedback linearization* (e.g., [7], [8]).

Generalizing the idea proposed in Banaszuk and Hauser [9] for solving a periodic orbit stabilization problem, Nielsen and Maggiore introduced in [2] the *Transverse feedback linearization - TFL* - approach. The underlying idea is to make the closed sub-manifold to be stabilized the zero-dynamics manifold associated to a suitable set of dummy output functions. Stabilization is then achieved by stabilizing the transverse linearized dynamics to this sub-manifold. The formalization and solution proposed in [2] provide an elegant framework for solving problems which can be reduced to constrain and control the evolutions over a suitable sub-manifold of the state space.

It is well known that in a digital context, i.e., under piecewise constant controls and periodical sampled measures, holding the continuous-time feedback solution constant over the sampling intervals significantly degrades the performances as the sampling period increases. On the other hand, a direct digital design based on the sampled-data model suffers from limitations induced by the loss of crucial control properties under sampling (e.g., feedback equivalence and zero-dynamics stability [10], [11]). Consequently, ad hoc schemes and design procedures are needed [12], [13].

In this letter, under the assumption that a continuous-time feedback exists, we propose a digital solution that preserves transverse feedback linearization in an approximate sense. The result is achieved through a suitable sampling-dependent redesign of the functions which define the invariant sub-manifold. The procedure is based on the generalization to set stabilization of multi-input multi-output (MIMO) dynamics, of an iterative approach proposed in [14] for preserving the relative degree under sampling.

This letter is organized as follows. Section II recalls the continuous-time solution, motivates and sets the problem. The proposed control strategy is developed in Section III in a constructive way. Simulated examples are discussed in Section IV. Concluding remarks end the manuscript.

Notations: Functions and vector fields are assumed smooth and complete. Given f and g, vector fields on $\mathbb{R}^n$, L_f denotes the first order differential operator $\mathrm{L}_f = \sum_{i=1}^{n} f_i(\cdot)\frac{\partial}{\partial x_i}$, $\mathrm{L}_f\mathrm{L}_g$ their composition, $e^{\mathrm{L}_f} := \mathrm{Id} + \sum_{i\geq 1} \frac{\mathrm{L}_f^i}{i!}$ the exponential Lie series operator with Id the identity operator and L_f^i iterative composition i times of L_f. Given a real valued function $h(\cdot)$ on $\mathbb{R}^n$, $e^{\mathrm{L}_f}h(x)|_{x(k)}$ denotes the application of the Lie series operator e^{L_f} to the function $h(x)$ evaluated at the state $x(k)$ so recovering the equality $e^{\mathrm{L}_f}h(x)|_{x(k)} = h(e^{\mathrm{L}_f}(x(k))$ where for simplicity one writes $e^{\mathrm{L}_f}(x)|_{x(k)} = e^{\mathrm{L}_f}(x(k))$. I_r indicates the identity square matrix of order r. Given a manifold M and a closed connected set $N \subset M$, N is said to be invariant under the dynamics $\dot{x} = f(x)+g(x)u$ if $\forall x_0 \in N$ and any control $u(\cdot)$, $x(t) \in N$, $\forall t$. N is *controlled* invariant if there exists a feedback $u^\star$ making N invariant for the closed loop system. Given a pair of matrices (A, B), one sets $col(A, B) = \begin{pmatrix} A^\top & B^\top \end{pmatrix}^\top$ and similarly, $blkdiag(A_i)$ the block diagonal matrix formed by the matrices A_i. A continuous function $\beta(\cdot) : [0, \infty) \to [0, \infty)$,

Manuscript received September 14, 2020; revised November 19, 2020; accepted December 8, 2020. Date of publication December 22, 2020; date of current version June 23, 2021. The work of Mohamed Elobaid was partly supported by Université Franco-Italienne/Università Italo-Francese (Vinci Grant 2019). Recommended by Senior Editor L. Menini. *(Corresponding author: Mohamed Elobaid.)*

Mohamed Elobaid is with the Dipartimento di Ingegneria Informatica, Automatica e Gestionale A. Ruberti, Sapienza University of Rome, 00185 Rome, Italy, and also with the Laboratoire de Signaux et Systèmes, L2S, CNRS, University Paris Saclay, 91192 Gif-sur-Yvette, France (e-mail: mohamed.elobaid@uniroma1.it).

Salvatore Monaco is with the Dipartimento di Ingegneria Informatica, Automatica e Gestionale A. Ruberti, Sapienza University of Rome, 00185 Rome, Italy (e-mail: salvatore.monaco@uniroma1.it).

Dorothée Normand-Cyrot is with the Laboratoire de Signaux et Systèmes, L2S, CNRS, University Paris Saclay, 91192 Gif-sur-Yvette, France (e-mail: dorothee.normand-cyrot@centralesupelec.fr).

Digital Object Identifier 10.1109/LCSYS.2020.3046539

that is zero at zero and strictly increasing and unbounded is said to be of class κ_∞. A continuous function $R(x,\delta)$ is of order $O(\delta^p)$ with $p \geq 1$ if, whenever it is defined, it can be written as $R(x,\delta) = \delta^{p-1}\tilde{R}(x,\delta)$ and there exists a function $\beta(\delta) \in \kappa_\infty$ and $\delta^\star > 0$ such that $\forall \delta \leq \delta^\star, |\tilde{R}(x,\delta)| \leq \beta(\delta)$. Given $x_0 \in M$, U denotes a *connected neighbourhood* of x_0 in M.

II. Preliminaries and Recalls

We consider the input-affine dynamics defined on $\mathbb{R}^n$

$$\dot{x} = f(x) + \sum_{i=1}^{m} g_i(x)u_i = f(x) + g(x)u \tag{1}$$

with $u \in \mathbb{R}^m$ and independent vector fields $g_1(x), \ldots, g_m(x)$.

A. Recalls on Transverse Feedback Linearization

Transverse feedback linearization essentially refers to equivalence under feedback to a system characterized by a linear controllable sub-dynamics transverse to a given closed, controlled invariant, embedded sub-manifold in the system state-space. Formally from [2], one sets the problem below.

Problem 1 [(L)TFL]: Let $\Gamma^\star \subset \mathbb{R}^n$ be a closed, controlled invariant sub-manifold for dynamics (1) and let $x_0 \in \Gamma^\star$; TFL is said to be locally solvable if there exist a feedback $u = \gamma(x,v)$ and a coordinates change $\phi(x) = col(\phi_1(x), \phi_2(x)) : x \mapsto (\xi, z)$, defined in a neighbourhood U of x_0, such that (1) rewrites

$$\begin{aligned} \dot{\xi} &= A\xi + Bv_1 \\ \dot{z} &= f_z(\xi, z) + g_z^1(\xi, z)v_1 + g_z^2(\xi, z)v_2 \end{aligned} \tag{2}$$

where $\xi \in \mathbb{R}^{n-n^\star}, z \in \mathbb{R}^{n^\star}, v = col(v_1, v_2) \in \mathbb{R}^m$, $n^\star = dim(\Gamma^\star)$, $g_z^1(\cdot), g_z^2(\cdot)$ are smooth (matrix) valued functions, B full column rank, the pair (A,B) controllable, $\phi(\Gamma^\star \cap U) = \{(\xi, z) : \xi = 0\}$. When U is a tubular neighbourhood of the whole $\Gamma^\star$, then TFL is said to hold *globally*.

The following comments are in order:

- $\dot{\xi} = A\xi + Bv_1$ specifies the *transverse dynamics* and v_1 the *transverse control*;
- the dynamics of z, restricted to $\phi(\Gamma^\star \cap U)$, $\dot{z} = f_z(0,z) + g_z^2(0,z)v_2$, is referred to as the *tangential dynamics* with v_2 the *tangential control*;
- setting $v_1 = -K\xi$ for a suitable K, (local) stabilization of $\Gamma^\star$ is achieved. If the trajectories of the closed loop system (under v_1) are bounded, stabilization of $\Gamma^\star$ holds.

Thanks to the decoupling of the control components, one independently forces the state evolutions towards $\Gamma^\star$ under v_1 and assigns a desired behaviour over it through v_2.

Before stating the necessary and sufficient conditions solving the (L)TFL problem given in [2], the well known notion of well defined vector relative degree is recalled [7].

Definition 1: The dynamics (1), with output $y = col(h_1(x), \ldots, h_q(x))$, $q \leq m$, $h_i(\cdot) : \mathbb{R}^n \to \mathbb{R}$ has *well-defined* vector relative degree $r = (r_1 \ \ldots \ r_q)$ at x_0 if $L_{g_j}L_f^k h_i(x) = 0$ on U for $k = 1, \ldots, r_i - 2$, $i = 1, \ldots, q$, $j = 1, \ldots, m$, while $L_{g_j}L_f^{r_i-1}h_i(x_0) \neq 0$ for some j and the $(q \times m)$ decoupling matrix $[D(x)]_{i,j} = L_{g_j}L_f^{r_i-1}h_i(x)$ is full rank at x_0; r is globally defined if the rank condition holds on $\mathbb{R}^n$ with respect to a fixed decoupling sub-matrix.

Theorem 1 [2], [15]: The LTFL Problem 1 is solvable if and only if there exist ρ smooth $\mathbb{R}$-valued functions $(\alpha_1(x), \ldots, \alpha_\rho(x))$, $\rho \leq m$, defined on U such that:

1) $\Gamma^\star \cap U \subset \{x \in U : \alpha_i(x) = 0, i = 1, \ldots \rho\}$;
2) the dynamics (1) with output $\alpha(x) = col(\alpha_1(x), \ldots, \alpha_\rho(x))$, has a well defined vector relative degree $r = (r_1, \ldots, r_\rho)$ at x_0 with $\sum_{i=1}^{\rho} r_i = n - n^\star$.

When $\phi(x)$ and $\alpha(x)$ are defined everywhere in a tubular neighbourhood of $\Gamma^\star$, then TFL holds globally.

Theorem 1 specifies that Problem 1 is indeed equivalent to partial feedback linearization and zero dynamics assignment with respect to a suitable dummy output vector.

Remark 1: Finding the functions α_i, $i = 1, \ldots, \rho$, from the given control specifications may be a difficult task. A procedure based on the annihilator of some *controlled invariant distributions* coinciding with the tangent bundle to $\Gamma^\star$ is developed in [2].

Without loss of generality, we assume in the sequel that the matrices (A,B) are in the Brunowsky canonical form with

$$\begin{aligned} &A \coloneqq blkdiag(A_1, \ldots, A_\rho) \in \mathbb{R}^{n-n^\star} \times \mathbb{R}^{n-n^\star} \\ &B \coloneqq blkdiag(B_1, \ldots, B_\rho) \in \mathbb{R}^{(n-n^\star)\times m} \\ &A_i \in \mathbb{R}^{r_i \times r_i} = \begin{pmatrix} 0 & 1 & 0 & \ldots & 0 \\ 0 & 0 & 1 & \ldots & 0 \\ & & \vdots & & \\ 0 & 0 & 0 & \ldots & 1 \\ 0 & 0 & 0 & \ldots & 0 \end{pmatrix}, \ B_i \in \mathbb{R}^{r_i \times 1} = \begin{pmatrix} 0 \\ 0 \\ \vdots \\ 0 \\ 1 \end{pmatrix}. \end{aligned} \tag{3}$$

B. Recalls on Sampled-Data Dynamics

The sampled-data model we are dealing with is characterized by a dynamics for which the measures are available at periodic sampling instants and the controls kept constant over the sampling period. This naturally arises in presence of digital actuation and sensing devices. More precisely in this letter, dynamics (1) is fed by constant controls over time intervals of length δ, i.e., $u_i(t) = u_i(k\delta) = u_i(k)$ for $t \in [k\delta, (k+1)\delta[$, $k \geq 0$. Accordingly, the sampled-data dynamics equivalent to (1) takes the form

$$\begin{aligned} x(k+1) &= F^\delta(x(k), u(k)) = e^{\delta(\mathrm{L}_f + \sum_{i=1}^m u_i(k)\mathrm{L}_{g_i})}(x(k)) \\ &= x(k) + \sum_{j \geq 1} \frac{\delta^j}{j!}(\mathrm{L}_f + \sum_{i=1}^{m} u_i(k)\mathrm{L}_{g_i})^j(x(k)) \end{aligned} \tag{4}$$

with $u(k) = col(u_1(k), \ldots, u_m(k))$ and the function $F^\delta(\cdot, u)$ defined by its series expansion in powers of δ, [16]. When truncating each row of this expansion at any fixed order $col(p_1, \ldots, p_n)$ in δ, so neglecting row-wise the remaining terms in $(O(\delta^{p_1+1}), \ldots, O(\delta^{p_n+1}))$ in the infinite series expansion, the sampled-data model is said to be *approximated at the order* $col(p_1, \ldots, p_n)$. Given a real valued output function $y_i = h_i(x)$, starting from $x(k)$ at time $t = k\delta$, one computes the output at any sampling instant $t = (k+j)\delta, j > 0$, under the control sequence $(u(k), \ldots, u(k+j-1))$, through the usual composition of functions so getting

$$\begin{aligned} y_i(k+j) &= h_i(x(k+j)) \\ &= h_i \circ F^\delta(\cdot, u(k+j-1)) \circ \ldots \circ F^\delta(x(k), u(k)). \end{aligned}$$

For sampled-data dynamics, the notion of relative degree reads as follows.

Definition 2 [16]: The MIMO sampled data dynamics (4) with output vector $y = col(h_1(x), \dots, h_q(x))$ has a well defined vector relative degree $r = (r_1, \dots, r_q)$ at x_0, if the following holds true for $x \in U$, $i = 1, \dots, q$

$$\begin{aligned} &\frac{\partial y_i(l)}{\partial u_j(0)}(x) = 0, \quad l = 1, \dots r_i - 1; \ j = 1, \dots m \\ &\frac{\partial y_i(r_i)}{\partial u_j(0)}(x_0) \neq 0 \quad \text{for some } j \end{aligned} \tag{5}$$

and the sampled data $(q \times m)$ decoupling matrix $[D^\delta(x)]_{i,j} = \frac{\partial y_i(r_i)}{\partial u_j(0)}(x)$ is full rank at x_0. If the p_i's are the highest orders of the expansions in power of δ at which the conditions above hold, the system (4) is said to have a vector relative degree $r = (r_1, \dots, r_q)$ at x_0 at the order $p = col(p_1, \dots, p_q)$ in δ (truncation with error in $col(O(\delta^{p_1+1}), \dots, O(\delta^{p_q+1}))$.

The falling to one of the relative degree is a well known fact, which is emblematic of the appearance of extra sampling zero-dynamics responsible for serious limitations in feedback design (see [17] for the linear framework and (e.g., [11], [18]) for the nonlinear one). The following result from [16] is recalled.

Lemma 1: Given dynamics (1) with output vector $y = col(h_1(x), \dots, h_q(x))$ and well defined vector relative degree at x_0 then, there exists $T^\star > 0$ such that for any $\delta \in]0, T^*[$, its sampled-data equivalent model (4) has well defined vector relative degree equal to $r = (1, \dots, 1)$ at x_0, whenever one takes into account for each respective output y_i, approximations in δ of order at least r_i, the continuous-time relative degree.

The result easily follows from (4) by computing

$$\frac{\partial y_i(1)}{\partial u_j(0)} = \frac{\delta^{r_i}}{r_i!} L_{g_j} L_f^{r_i-1} h_i(x)\big|_{x_0} + O(\delta^{r_i+1})$$

because $\forall i = (1, \dots, q)$, $L_{g_j} L_f^{r_i-1} h_i(x_0) \neq 0$ for some j.

C. Problem Statement

Assuming that a solution to the (L)TFL Problem 1 exists, does a sampled-data solution exist ? How to compute it and what about its performances ? With this in mind and recalling that, because of (3), the coordinates ξ in Theorem 1 are

$$\xi = col(\xi_1, \dots, \xi_\rho) \quad with \quad \xi_i = col(\alpha_i, \dots, L_f^{r_i-1}\alpha_i)(x) \tag{6}$$

the sampled-data (L)TFL problem is set.

Problem 2 [SD-(L)TFL]: Given dynamics (1) satisfying the conditions of Theorem 1, find for any $\delta \in]0, T^\star[$, $T^* > 0$ small enough, a piecewise constant feedback $u^\delta = \gamma^\delta(x, v)$ and a coordinates change $\phi^\delta(\cdot) : x \mapsto (\xi^\delta, z)$ defined in a neighbourhood U of $x_0 \in \Gamma^\star$, under which the sampled-data closed loop dynamics takes the normal form below

$$\xi^\delta(k+1) = (Id + \delta A)\xi^\delta(k) + \delta B v_1(k) \tag{7a}$$
$$z(k+1) = F_z^\delta(\xi^\delta(k), z(k), v(k)) \tag{7b}$$

with $\xi^\delta \in \mathbb{R}^{n-n^\star}$, $\xi^\delta = col(\xi_1^\delta, \dots, \xi_\rho^\delta)$, $z \in \mathbb{R}^{n^\star}$, $v = col(v_1, v_2) \in \mathbb{R}^m$ and $\phi^\delta(\Gamma^\star \cap U) = \{(\xi^\delta, z) : \xi^\delta = 0\} = \{(\xi, z) : \xi = 0\} = \phi(\Gamma^\star \cap U)$. The approximate SD-(L)TFL is solvable at degree $p \geq 1$, if (7a) is approximated in $O(\Delta^{p+1})$

$$\xi^\delta(k+1) = (Id + \delta A)\xi^\delta(k) + \delta B v_1(k) + O(\Delta^{p+1}) \tag{8}$$

with $\Delta^{p+1} = col(\delta^{r_1+p}, \dots, \delta^{p+1}, \dots, \delta^{r_\rho+p}, \dots, \delta^{p+1})$. If the relative degree is well defined for all $x \in \Gamma^*$ we will say, with a little abuse of nomenclature, that the problem is globally solved around Γ^*.

Some remarks are in order.

- Problem 2 should be understood as the preservation of the (L)TFL property under sampling. It does not concern the existence and the computation, for the equivalent sampled-data dynamics, of a closed controlled invariant sub-manifold. This data of the design is assumed to be known from the continuous-time solution. Note that, with a little abuse, the same notation, U, is used to denote the set over which the continuous-time and the sampled-data solutions are defined.
- The sampled-data tangential z-dynamics on $\Gamma^\star$ (setting $\xi^\delta = 0$) is not constrained and recovers the continuous-time z-dynamics in $O(\delta^2)$.
- The (L)TFL solution described in Theorem 1 relies on partial feedback linearization with respect to outputs with suitable well defined vector relative degrees. It is clear from Lemma 1 that (L)TFL is lost under sampling except when these relative degrees are all equal to 1.
- The approximation in (8) must be understood as an approximation at the Δ^p-vector's order; i.e., the j^{th} component of $\xi_i^\delta = col(\xi_{i,1}^\delta, \dots, \xi_{i,r_i}^\delta)$ in ξ^δ, is approximated at the order $(p + r_i - j)$. Such a non homogeneous approximation reflects the preservation of each relative degree r_i of the respective ξ_i^δ at an order of approximation that has to be at least r_i itself. This is at the basis of the result here proposed and reveals to be profitable in the achieved performances illustrated through simulations.

III. Approximate Transverse Feedback Linearization Under Digital Control

In this section, making use of a suitable sampling-dependent redesign of the output functions, we propose an approximated solution which combines computational simplicity with a significant improvement with respect to the zero-order-holding implementation of the continuous-time control law.

Let us start by pointing out why the continuous-time design approach cannot be directly applied in the sampled-data context. As noted before, the continuous-time solution is achieved by stabilizing Γ^*, rendered the zero dynamics sub-manifold of (1) with respect to a set of $(\rho \leq m)$ suitably chosen dummy output functions, the $\alpha_i(\cdot)$'s, that have a well defined vector relative degree $r = (r_1, \dots, r_\rho)$. The control goal is then assured under input-to-output feedback linearization and linear stabilization. Such an approach cannot be applied to the sampled-data model as Γ^*, the subset of the state-space to stabilize and to make invariant, is not a zero dynamics sub-manifold of the sampled-data model (4) associated to the $\alpha_i(\cdot)$'s. Moreover, because of Lemma 1, even the dimension of the sampled-data zero dynamics sub-manifold is not the

same as that of Γ^*. The main result stated below, relying on the extension to MIMO systems of a procedure proposed in [14], shows how starting from the $\alpha_i(\cdot)$'s, a new set of delta-dependent functions, the $\alpha_i^\delta(\cdot)$'s , can be designed for preserving the relative degrees and, at the same time, the zero dynamics sub-manifold. In addition, by working on the approximated sampled-data model it is shown that solutions, at increasing degrees of approximation can be computed.

With this in mind, under the conditions of Theorem 1, in the coordinates $\xi = \phi_1(x)$ as in (6) and $z = \phi_2(x)$, with $col(\phi_1(x), \phi_2(x))$ defining a smooth deffeomeorphism, (1) takes the form

$$\begin{aligned}\dot{\xi} &= A\xi + B(f_a(\xi, z) + g_a(\xi, z)u)\\ \dot{z} &= f_z(\xi, z) + g_z(\xi, z)u\end{aligned} \tag{9}$$

with $\xi = col(\xi_1, \dots, \xi_\rho) \in \mathbb{R}^{n-n^\star}, z \in \mathbb{R}^{n^\star}$, $\xi_i = col(\xi_{i,1}, \dots, \xi_{i,r_i}) \in \mathbb{R}^{r_i}$, (A, B) as in (3), $B(f_a(\xi, z) + g_a(\xi, z)u) := col(B_1(f_{a_1} + g_{a_1}u), \dots, B_\rho(f_{a_\rho} + g_{a_\rho}u)) \in \mathbb{R}^{(n-n^\star)\times m}$, $f_a = col(f_{a_1}, \dots, f_{a_\rho})$, $g_a(\xi, z) = col(g_{a_1}, \dots, g_{a_\rho})$, $g_{a_i} = (g_{a_i}^1, \dots, g_{a_i}^m)$ and

$$\begin{aligned}&f_{a_i}(\xi, z) = L_{f(x)}^{r_i}\xi_i^1|_{x=\phi^{-1}(\xi,z)}, \quad i = 1, \dots, \rho\\ &g_{a_i}^j(\xi, z) = L_{g_j(x)}L_{f(x)}^{r_i-1}\xi_i^1|_{x=\phi^{-1}(\xi,z)}, i = 1, \dots, \rho, j = 1, \dots, m\\ &f_z(\xi, z) + g_z(\xi, z)u = \frac{\partial\phi_2}{\partial x}(f(x) + g(x)u)|_{x=\phi^{-1}(\xi,z)}.\end{aligned}$$

In these coordinates, the sampled-data dynamics equivalent to (9) reads as (dropping the k-index in the right hand side)

$$\begin{aligned}\xi(k+1) &= A^\delta\xi + B_1^\delta(f_a(\xi, z) + g_a(\xi, z)u) + O(\Delta^2)\\ z(k+1) &= z + \delta(f_z(\xi, z) + g_z(\xi, z)u) + O(\delta^2)\end{aligned} \tag{10}$$

with $A^\delta = blkdiag(A_1^\delta, \dots, A_\rho^\delta)$, $B_j^\delta = blkdiag(B_{j,1}^\delta, \dots, B_{j,\rho}^\delta)$ with $A_i^\delta = e^{\delta A_i}$ and $B_{1,i}^\delta = \int_0^\delta e^{\tau A_i}B_i d\tau$, $B_{j,i}^\delta = \sum_{k\geq j}\frac{\delta^k}{k!}(A_i)^{k-j}B_i$, so getting

$$A_i^\delta = \begin{pmatrix}1 & \delta & \frac{\delta^2}{2!} & \dots & \frac{\delta^{r_i-1}}{(r_i-1)!}\\ 0 & 1 & \delta & \dots & \frac{\delta^{r_i-2}}{(r_i-2)!}\\ & & \vdots & & \\ 0 & 0 & 0 & \dots & 1\end{pmatrix}, \quad B_{j,i}^\delta = \begin{pmatrix}\frac{\delta^{r_i+j-1}}{(r_i+j-1)!}\\ \vdots\\ \frac{\delta^j}{j!}\end{pmatrix}. \tag{11}$$

The main result can now be stated.

Theorem 1: Under the conditions of Theorem 1, there exist a small enough $T^\star > 0$, and for any $\delta \in]0, T^\star[$, a δ-dependent coordinates change $\phi^\delta(x)$ and a sampled-data feedback $\gamma^\delta(x, v)$ solving Problem 2 in $O(\Delta^2)$.

Proof: Under the assumption of well-defined vector relative degree and without loss of generality (possibly after a reordering of the control variables in ξ), $g_a(\xi, z)$ in (9) takes the form of a full rank matrix $D(\xi, z) = \begin{bmatrix}M(\xi, z) & N(\xi, z)\end{bmatrix}$ with $M(\xi, z)$, $\rho \times \rho$ full rank, and $N(\xi, z)$ spanning $ker(D(\xi, z))$. Thus, with a little abuse of notations, the continuous-time normal form rewrites as

$$\begin{aligned}\dot{\xi} &= A\xi + B(f_a(\xi, z) + M(\xi, z)u_1 + N(\xi, z)u_2)\\ \dot{z} &= f_b(\xi, z) + g_b(\xi, z)u\end{aligned}$$

with $u = col(u_1, u_2), u_1 \in \mathbb{R}^\rho, u_2 \in \mathbb{R}^{m-\rho}$. Accordingly, the linearizing continuous-time feedback reads as

$$\begin{aligned}u_1 &= \gamma_1(\xi(k), z(k), v_1(k), u_2(k))\\ &= M^{-1}(\xi, z)(-f_a(\xi, z) - N(\xi, z)u_2(k) + v_1(k))\end{aligned} \tag{12}$$

with external control vector $v_1 \in \mathbb{R}^\rho$. The second part of the proof stands in the computation of a reshaped δ-dependent dummy output, $\alpha^\delta(x) = col(\alpha_1^\delta(x), \dots, \alpha_\rho^\delta(x))$, under which the vector relative degree $r = (r_1, \dots, r_\rho)$ is preserved under sampling, up to approximations in $col(O(\delta^{r_1+1}), \dots, O(\delta^{r_\rho+1}))$. Moreover, the zero dynamics sub-manifold is preserved at the same orders of approximation. For, let us associate to each function α_i, $i = 1, \dots, \rho$

$$\alpha_i^\delta(x) = \alpha_i(x) + \sum_{j=1}^{r_i-1}\delta^j c_{i,j}\alpha_i^{(j)}(x) = C_i^\delta\xi_i(x) \tag{13}$$

where $\alpha_i^{(j)} = L_f^j(\alpha_i)$ is the j^{th}-time derivative of α_i and the real coefficients $c_{i,j}$ are the entries of the row matrix

$$\begin{aligned}C_i^\delta &= col(1, \delta c_{i,1}, \dots, \delta^{r_i-1}c_{i,r_i-1})\\ &= \delta^{r_i}B_i^T\begin{pmatrix}B_{1,i}^\delta & A_i^\delta B_{1,i}^\delta & \dots & (A_i^\delta)^{(r_i-1)}B_{1,i}^\delta\end{pmatrix}^{-1}\end{aligned} \tag{14}$$

with A_i^δ and $B_{1,i}^\delta$ as in (11). The so defined δ-dependent functions are used to define the first $(r_1 + \dots + r_\rho)$ coordinates of a block diagonal transformation to be applied to the approximated sampled-data representation (10). For, we define

$$\phi^\delta(x) = col(\xi^\delta, z) := \begin{pmatrix}T_{n-n^\star}(\delta) & 0\\ 0 & I_{n^\star}\end{pmatrix}\begin{pmatrix}\xi\\ z\end{pmatrix}$$

with $T_{n-n^\star}(\delta) = blkdiag(T_1(\delta), \dots, T_\rho(\delta)) \in \mathbb{R}^{(n-n^\star)\times(n-n^\star)}$

$$\xi_i^\delta(x) = T_i(\delta)\xi_i(x) := \begin{pmatrix}C_i^\delta\\ \frac{1}{\delta}C_i^\delta(A_i^\delta - I_{r_i})\\ \vdots\\ \frac{1}{\delta^{r_i-1}}C_i^\delta(A_i^\delta - I_{r_i})^{(r_i-1)}\end{pmatrix}\xi_i(x). \tag{15}$$

It is a matter of computation to verify that the vector relative degree of the functions (13) is $r = (r_1, \dots, r_\rho)$ and that the feedback (12), with v_1^δ in the place of v_1, transforms (10) into

$$\begin{aligned}\xi^\delta(k+1) &= (I_{(n-n^*)} + \delta A)\xi^\delta(k) + \delta B v_1^\delta(k) + O(\Delta^2)\\ z(k+1) &= z(k) + \delta(f_b(\xi, z) + g_b(\xi, z)col(v_1^\delta, u_2) + O(\delta^2).\end{aligned} \tag{16}$$

Hence, the posed problem is solved at the fixed approximated order. Moreover, setting $v_1^\delta(k) = -K\xi^\delta(k)$, with gains $k_{i,j}$'s, $i = 1, \dots, \rho$, $j = 1, \dots, n - n^*$, suitably chosen to assign Hurwitz polynomials, stabilization of Γ^* is attained at the same order of approximation, since the sampled-data zero dynamics manifold recovers the continuous-time one, i.e., $\phi^\delta(\Gamma^\star \cap U) = \{(\xi^\delta, z); \xi^\delta = 0\} = \{(\xi, z); \xi = 0\} = \phi(\Gamma^\star \cap U)$. The sampled-data feedback so far designed is thus

$$u_1^\delta(k) = \gamma_1^\delta(\xi(k), z(k), -K\xi^\delta(k), u_2(k)). \tag{17}$$

It provides a local solution around any point at which the vector relative degree is well defined; it provides a global solution

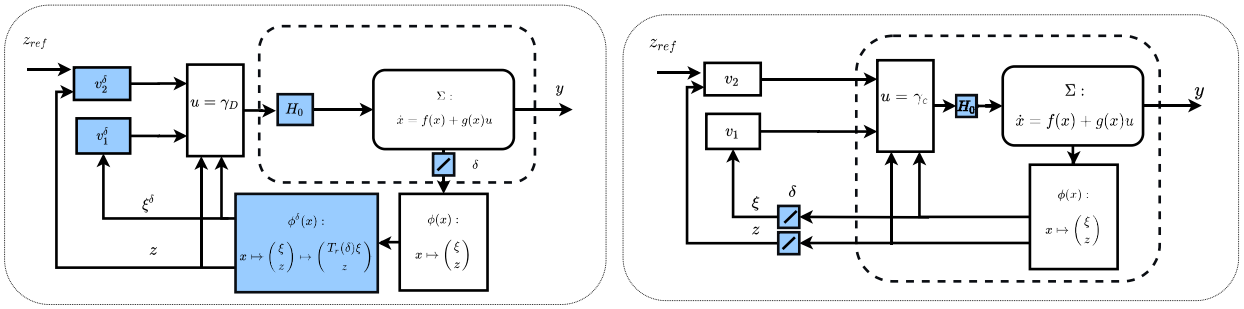

(a) (b)

(a) Proposed SDTFL (b) Zero-order holding (ZOH) of TFL

Fig. 1. Implementation of the proposed sampled-data solution (a), compared to zero-order-holding of the continuous-time solution (b). The modified coordinates change and feedback of the proposed solution are highlighted in blue.

around Γ^* if the vector relative degree is defined at any point of Γ^*. ■

The approach could be further developed to increase the approximation order along the lines of the proof of Theorem 1 and extending the SISO procedure in [14]. Starting from an higher order approximation of the sampled-data model (10), the idea is to add a δ-dependent part to the control law to compensate the effects of the additional terms occuring at the corresponding degree of approximation. Iteratively, a controller of the form $u_1(k) = u_{1,0}(k) + \delta u_{1,1}(k) + \cdots + \frac{\delta^p}{p!} u_{1,p}(k)$ is built, with $u_{1,0}$ as in (17), to reach a solution approximated in $O(\Delta^{p+1})$. Detailed computations are left out for the sake of space.

Remark 2: It is worth to note that the controller (17) can be easily computed since $\xi^\delta = T(\delta)\xi$ depends on $r_1, \ldots, r_\rho$ only and can be precomputed offline. Each function $\alpha_i^\delta(\cdot)$ is a polynomial in the first r_i time derivatives of $\alpha_i(\cdot)$, with real δ-depend coefficients. For the first values of r_i, one computes

$$r_i = 2: \quad \alpha_i^\delta = \alpha_i - \frac{\delta}{2}\dot{\alpha}_i = \xi_{i,1} - \frac{\delta}{2}\xi_{i,2}$$

$$r_i = 3: \quad \alpha_i^\delta = \alpha_i + \delta\dot{\alpha}_i - \frac{\delta^2}{3}\ddot{\alpha}_i = \xi_{i,1} + \delta\xi_{i,2} - \frac{\delta^2}{3}\xi_{i,3}$$

$$T_2(\delta) = \begin{pmatrix} 1 & \frac{-\delta}{2} \\ 0 & 1 \end{pmatrix}; \quad T_3(\delta) = \begin{pmatrix} 1 & \delta & -\frac{\delta^2}{3} \\ 0 & 1 & \frac{-\delta}{2} \\ 0 & 0 & 1 \end{pmatrix}.$$

IV. Examples

In this section two examples from [2] and [19] are worked out to illustrate the benefits of the proposed digital design procedure. Figure 1 depicts the implementation schemes.

Example 1 (SISO): Consider the unicycle model

$$\dot{x} = v\cos\theta, \quad \dot{y} = v\sin\theta, \quad \dot{\theta} = w \tag{18}$$

with $v = 1$, under the control goal of tracking a circular path $\{(x, y, \theta) : x^2 + y^2 - 1 = 0\}$. Following [19], one sets the transversal output as $\alpha(x, y, \theta) = x^2 + y^2 - 1$, with relative degree $r = 2 = n - n^\star$ over $\mathbb{R}^3 \backslash \{\theta = \tan^{-1}\frac{y}{x}\}$. Then, under the coordinates change $\phi(x, y, \theta) = col(x^2 + y^2 - 1, 2(x\cos\theta + y\sin\theta), \theta) = (\xi_1, \xi_2, z)$, the dynamics (18) is transformed into the normal form

$$\dot{\xi}_1 = \xi_2; \quad \dot{\xi}_2 = 2(1 + b(\xi, z)u); \quad \dot{z} = u \tag{19}$$

with $b(\xi, z) = 2(y\cos\theta - x\sin\theta)|_{(x,y,\theta)=\phi(\xi,z)^{-1}}$. Under sampling, because $(n = 3, n^\star = 1, m = 1)$, one reshapes the transversal output as in (13), so getting

$$\alpha^\delta(x, y, \theta) = \alpha(x, y, \theta) - \frac{\delta}{2}\dot{\alpha}(x, y, \theta) = x^2 + y^2 - \delta(x\cos\theta + y\sin\theta).$$

Accordingly, under the coordinates change

$$\phi^\delta(\cdot) = col(\xi_1^\delta, \xi_2^\delta, z) = col(T_2(\delta)\xi, z) = col(\xi_1 - \frac{\delta}{2}\xi_2, \xi_2, z)$$

the sampled-data equivalent model to (19) is transformed into

$$\begin{aligned} \xi_1^\delta(k+1) &= \xi_1^\delta(k) + \delta\xi_2^\delta(k) + O(\delta^3) \\ \xi_2^\delta(k+1) &= \xi_2^\delta(k) + 2\delta(1 + b(\xi, z)u(k)) + O(\delta^2) \\ z(k+1) &= z(k) + \delta u(k). \end{aligned}$$

Finally, the sampled-data feedback law

$$u(k) = (2b(\xi(k), z(k)))^{-1}(-2 + v^\delta(k)) \tag{20}$$

with $v^\delta(k) = -k_1\xi_1^\delta - k_2\xi_2^\delta$ and suitably chosen $k_1 = 16.6, k_2 = -11.1$, stabilizes the dynamics onto $\Gamma^\star$ ($\xi^\delta = 0$). Setting $x_0 = (-1.5, 1, \frac{\pi}{4})$, comparative simulations between the continuous-time CT design (in red), ZOH of the CT feedback (in black) and the sampled-data proposed solution (in blue) are plotted, for a sampling period $\delta = 0.3$. As clearly illustrated through the simulations (Figure 2), the proposed design outperforms ZOH of the CT solution.

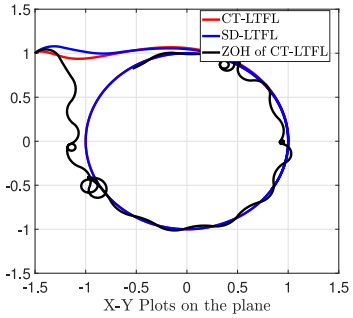

Fig. 2. SD feedback VS ZOH of the CT feedback $\delta = 0.3$.

Example 2 (MIMO): Let the input-affine dynamics

$$\dot{x} = f(x) + g_1(x)u_1 + g_2(x)u_2 \tag{21}$$

with $f(x) = \begin{pmatrix} -x_2 & x_1 & x_3x_4 & 0 \end{pmatrix}^\top$, $g_1(x) = \begin{pmatrix} 0 & 0 & x_3 & 1 \end{pmatrix}^\top$, $g_2(x) = \begin{pmatrix} -x_2 & x_1 & 0 & 0 \end{pmatrix}^\top$. The LTFLP has been set and solved in [2] with the control goal of reaching and traversing an elliptic paraboloid immersed in the subspace $x_4 = 0$; i.e.,

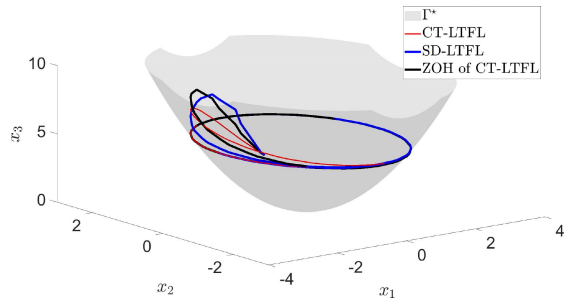

Fig. 3. States Evolution approaching $\Gamma^\star$, $\delta = 0.4$.

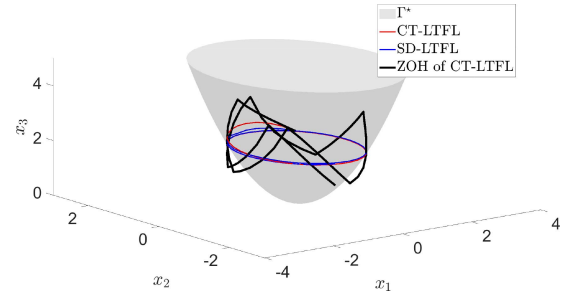

Fig. 4. Invariance of $\Gamma^\star$, $\delta = 1$.

$\{x \in \mathbb{R}^4 : x_1^2 + x_2^2 - x_3 = x_4 = 0\}$ around $x_0 = col(4, 0, 2, 0)$. Because $(n = 4, n^\star = 2, m = 2)$, it has been shown that the function $\alpha(x) = ln(\frac{x_3}{x_1^2+x_2^2}) - x_4$, has relative degree $2 = n - n^\star$ over $\mathbb{R}^4/\{x \in \mathbb{R}^4 : x_1 = x_2 = 0; x_3 = 0\}$, so defining the coordinates change $col(\xi_1, \xi_2, z) = \phi(x) = col(ln(\frac{x_3}{x_1^2+x_2^2}) - x_4, x_4, x_1, x_2)$ and $u^\star = (0, 0)^\top$. Under sampling, setting according to (13) $\alpha^\delta(x) = \alpha(x) - \frac{\delta}{2}\dot{\alpha}(x)$, one defines the sampled coordinates change as $col(\xi_1^\delta, \xi_2^\delta, z) = \phi^\delta(x) = col(\phi_1^\delta(x), x_1, x_2)$, with

$$\phi_1^\delta(x) = col(ln(\frac{x_3}{x_1^2+x_2^2}) - (1+\frac{\delta}{2})x_4, x_4) = T_2(\delta)col(\alpha(x), \dot{\alpha}(x))$$

under which (21) is transformed, after sampling, into

$$\begin{aligned}
\xi_1^\delta(k+1) &= \xi_1^\delta(k) + \delta\xi_2^\delta(k)\\
\xi_2^\delta(k+1) &= \xi_2^\delta(k) + \delta u_1(k)\\
z_1(k+1) &= z_1(k) - \delta z_2(k)(1+u_2(k)) + O(\delta^3)\\
z_2(k+1) &= z_2(k) + \delta z_1(k)(1+u_2(k)) + O(\delta^3).
\end{aligned} \tag{22}$$

Accordingly, the control

$$u_1^\delta(k) = -k_1\xi_1^\delta - k_2\xi_2^\delta \tag{23}$$

with $k = 2, k_2 = -1.5$, stabilizes the transverse dynamics over $\Gamma^\star = \{x \in \mathbb{R}^4 : \alpha(x) = \dot{\alpha}(x) = 0\} = \{x \in \mathbb{R}^4 : \xi_1^\delta = \xi_2^\delta = 0\}$.

In Figure 3, the initial condition is $x_0 = col(1, 2, 2, 0.5) \notin \Gamma^\star$ and the feedback (23) stabilizes the system to $\Gamma^\star$. Figure 4 illustrates that the invariance of $\Gamma^\star$ is preserved under the proposed feedback (23) while it fails when holding constant (ZOH) the CT control; the initial state being $x = col(1, 1, 2, 0) \in \Gamma^\star$. In both simulations, the motion on $\Gamma^\star$ is free, i.e., $u_2(k) = 0$.

V. Conclusion

A procedure to preserve transverse feedback linearization under digital control has been proposed. The first step of this iterative procedure leads to the redefinition of a linearizing output which comes out to depend in a polynomial way on the sampling period and allows for the design of a digital stabilizing control which outperforms simple zero-order holding of the continuous-time solution. Accordingly, attractivity and invariance of the set $\Gamma^\star$ is preserved under digital feedback with arbitrary orders of approximation. An exact solution to the (L)TFL-SD problem can be obtained using multi-rate sampling techniques, special care is needed when selecting the multirate orders on the input channels, this is deferred to a different work.

Acknowledgment

The authors wish to thank the Associate Editor and the anonymous Reviewers for their helpful comments when preparing the final manuscript.

References

[1] A. S. Shiriaev, "The notion of v-detectability and stabilization of invariant sets of nonlinear systems," *Syst. Control Lett.*, vol. 39, no. 5, pp. 327–338, 2000.
[2] C. Nielsen and M. Maggiore, "On local transverse feedback linearization," *SIAM J. Control Optim.*, vol. 47, no. 5, pp. 2227–2250, 2008.
[3] A. Hladio, C. Nielsen, and D. Wang, "Path following for a class of mechanical systems," *IEEE Trans. Control Syst. Technol.*, vol. 21, no. 6, pp. 2380–2390, Nov. 2013.
[4] A. Doosthoseini and C. Nielsen, "Local nested transverse feedback linearization," *Math. Control Signals Syst.*, vol. 27, no. 4, pp. 493–522, 2015.
[5] A. Astolfi and R. Ortega, "Immersion and invariance: A new tool for stabilization and adaptive control of nonlinear systems," *IEEE Trans. Autom. Control*, vol. 48, no. 4, pp. 590–606, Apr. 2003.
[6] M. Mattioni, S. Monaco, and D. Normand-Cyrot, "Immersion and invariance stabilization of strict-feedback dynamics under sampling," *Automatica*, vol. 76, pp. 78–86, Feb. 2017.
[7] A. Isidori, *Nonlinear Control Systems*. London, U.K.: Springer-Verlag, 2013.
[8] A. J. Krener, "On the equivalence of control systems and the linearization of nonlinear systems," *SIAM J. Control*, vol. 11, no. 4, pp. 670–676, 1973.
[9] A. Banaszuk and J. Hauser, "Feedback linearization of transverse dynamics for periodic orbits," *Syst. Control Lett.*, vol. 26, no. 2, pp. 95–105, 1995.
[10] A. Arapostathis, B. Jakubczyk, H.-G. Lee, S. Marcus, and E. Sontag, "The effect of sampling on linear equivalence and feedback linearization," *Syst. Control Lett.*, vol. 13, no. 5, pp. 373–381, 1989.
[11] S. Monaco and D. Normand-Cyrot, "Zero dynamics of sampled nonlinear systems," *Syst. Control Lett.*, vol. 11, no. 3, pp. 229–234, 1988.
[12] J. Grizzle and P. Kokotovic, "Feedback linearization of sampled-data systems," *IEEE Trans. Autom. Control*, vol. 33, no. 9, pp. 857–859, Sep. 1988.
[13] S. Monaco and D. Normand-Cyrot, "Issues on nonlinear digital control," *Eur. J. Control*, vol. 7, nos. 2–3, pp. 160–177, 2001.
[14] J.-P. Barbot, S. Monaco, and D. Normand-Cyrot, "A sampled normal form for feedback linearization," *Math. Control Signals Syst.*, vol. 9, no. 2, pp. 162–188, 1996.
[15] C. Nielsen and M. Maggiore, "Output stabilization and maneuver regulation: A geometric approach," *Syst. Control Lett.*, vol. 55, no. 5, pp. 418–427, 2006.
[16] S. Monaco and D. Normand-Cyrot, "On nonlinear digital control," in *Nonlinear Systems*. Boston, MA, USA: Springer, 1997, pp. 127–155.
[17] K. J. Åström, P. Hagander, and J. Sternby, "Zeros of sampled systems," *Automatica*, vol. 20, no. 1, pp. 31–38, 1984.
[18] J. I. Yuz and G. C. Goodwin, "On sampled-data models for nonlinear systems," *IEEE Trans. Autom. Control*, vol. 50, no. 10, pp. 1477–1489, 2005.
[19] C. Nielsen and M. Maggiore, "Maneuver regulation via transverse feedback linearization: Theory and examples," in *Proc. IFAC Symp. Nonlinear Control Syst. (NOLCOS)*, Stuttgart, Germany, 2004, pp. 59–66.

Chapter 8

Exact transverse feedback linearization via multi-rate sampling

Contents

The second, and more advantageous, solution to the problem of preserving the TFL normal form under sampling is detailed in this chapter. As briefly alluded to in the introduction of Chapter 7, this solution utilizes multi-rate sampling working over the second step of the general TFL two-step program. Namely, instead of modifying the functions specifying the zero dynamics sub-manifold and solving the problem in continuous-time, we modify the computation of the feedback that linearizes and stabilizes the dynamics transverse to the desired sub-manifold.

This multi-rate sampled solution to the problem of preserving TFL under sampling relies on the fact that multi-rate, as detailed in Chapter 2 preserves the zero dynamics structure of a continuous-time plant.

The main advantage of using multi-rate sampled solution is two fold: First, it allows one to demonstrate that whenever a continuous-time solution to the TFL problem exists, an exact digital solution exists, even if the implementation is carried over approximations. Second, and more interestingly, it allows one to find a piecewise constant state solution in particular cases where no static feedback continuous-time solution exists. This later aspect is demonstrated on the application to the path following problem serving as a companion to the results obtained in;

> Mohamed Elobaid, Mattia Mattioni, Salvatore Monaco and Dorothée Normand-Cyrot. *"Digital path-following for a car-like robot". Control Conference Africa IFAC CCA 2021, 174-179, DOI: 10.1016/j.ifacol.2021.12.030*

> Mohamed Elobaid, Mattia Mattioni, Salvatore Monaco and Dorothée Normand-Cyrot. *"Virtual Holonomic Constraints for Euler-Lagrange systems under sampling" ECC 2022, to appear*

The notions and concepts appearing in this chapter are based on Banaszuk and Hauser (1995),Nielsen and Maggiore (2008), Nielsen and Maggiore (2006), Akhtar et al. (2015) and the references therein together with the referenced paper.

8.1 Linear feedback equivalence under multi-rate sampling

In this section we recall how preservation of linear equivalence under feedback for nonlinear continuous-time systems can be done via multi-rate sampling. This idea is precisely the one applied, with some care, to the problem of preserving the TFL normal form under sampling. To this end, consider a continuous-time system of the form (3.1),(1.1b), having a well defined relative degree r together with feedback $u = \gamma_c(x, \nu)$ of the form (1.4) that renders the input-output link a chain of r integrators.

As discussed in Chapter 2, the multi-rate sampled model of order r is

$$\begin{aligned} x(k+1) &= F_r^{\delta}(x(k), \underline{u}(k)) = e^{\bar{\delta}(L_f + u^1(k)L_g)} \circ \ldots \circ e^{\bar{\delta}(L_f + u^r(k)L_g)} x|_{x(k)} \\ y(k) &= h(x(k)) \end{aligned} \tag{8.1}$$

with $\delta = r\bar{\delta}$. The question is then to find a multi-rate digital feedback

$$\underline{u} = \gamma_d(x, \nu) = \begin{pmatrix} \gamma_d^1(x,\nu) & \ldots & \gamma_d^r(x,\nu) \end{pmatrix}^\top$$

such that the sampled data system under this feedback recovers the input-output linearaization of the original continuous-time system. Considering the extended output vector (2.15), namely $H(x) = (h(x),\ L_f h(x),\ \ldots, L_f^{r-1}h(x))^\top$, then our question is equivalent to asking for a digital feedback such that;

$$H(F_r^{\delta}(x(k), \gamma_d(\cdot, \nu(k)))) = A_r^{\delta} H(x(k)) + b_r^{\delta}\nu(k) \tag{8.2}$$

for A_r^{δ}, b_r^{δ} as in (2.12). It turns out that such feedback solution preserving input-output linearization exists. In fact, expanding the equality (8.2), one has (droppping time arguments for clarity)

$$e^{\bar{\delta}(L_f+\gamma_d^1 L_g)} \circ \ldots \circ e^{\bar{\delta}(L_f+\gamma_d^r L_g)} h(x) = h(x) + \delta L_f h(x) + \ldots + \frac{\delta^{r-1}}{(r-1)!} L_f^{r-1} h(x) + \frac{\delta^r}{r!}\nu \tag{8.3a}$$

$$e^{\bar{\delta}(L_f+\gamma_d^1 L_g)} \circ \ldots \circ e^{\bar{\delta}(L_f+\gamma_d^r L_g)} L_f h(x) = L_f h(x) + \delta L_f^2 h(x) + \ldots + \frac{\delta^{r-2}}{(r-2)!} L_f^{r-2} h(x) + \frac{\delta^{r-1}}{(r-1)!}\nu \tag{8.3b}$$

$$\vdots$$

$$e^{\bar{\delta}(L_f+\gamma_d^1 L_g)} \circ \ldots \circ e^{\bar{\delta}(L_f+\gamma_d^r L_g)} L_f^{r-1} h(x) = L_f^{r-1} h(x) + \delta\nu \tag{8.3c}$$

The left hand side of the r equations above can be rearranged, for the i^{th} equation as

$$\begin{aligned} e^{\bar{\delta}(L_f+\gamma_d^1(k) L_g)} \circ \ldots \circ e^{\bar{\delta}(L_f+\gamma_d^r(k) L_g)} L_f^i h(x(k)) &= L_f^i h(x(k)) + \delta L_f^{i+1} h(x(k)) + \ldots \\ &\quad + L_f^{r-i-1} h(x(k)) + \frac{\delta^{r-i}}{(r-i)!} P_{i-1}(\bar{\delta}, \gamma_d^1, \ldots, \gamma_d^r) \end{aligned} \tag{8.4}$$

where $P_i(\bar{\delta}, \gamma_d^1, \ldots, \gamma_d^r)$ is an infinite series collected, term by term, according to the powers of $\bar{\delta}$ Monaco and Normand-Cyrot (1997). In this sense, the equations (8.2) reduces to setting

$$P_i(\bar{\delta}, \gamma_d^1, \ldots, \gamma_d^r) = \nu(k), \quad i = 0, \ldots, r-1 \tag{8.5}$$

for which we can recall the following;

Lemma: linear feedback equivalence under multi-rate sampling

The equations (8.2) admits a digital feedback solution of the form

$$\gamma_d(x,\nu) = \gamma_{d,0}(x,\nu) + \sum_{j\geq 1} \frac{\bar{\delta}^j}{(j+1)!}\gamma_{d,j}(x,\nu) \tag{8.6}$$

infinite series expansion in powers of δ around the continuous-time input-output linearizing feedback.

Remark 8.1 *The multi-rate digital feedback (8.6) preserving feedback equivalence under sampling is an infinite series expansion around the continuous-time feedback. Because of this, in practice, only approximations can be computed obtained by truncating the feedback (8.6) at a finite power of δ so getting for the $p-th$ order approximate feedback*

$$\gamma_d^p(x,\nu) = \gamma_{d,0}(x,\nu) + \sum_{j=1}^{p} \frac{\bar{\delta}^j}{(j+1)!}\gamma_{d,j}(x,\nu) \tag{8.7}$$

In the next section, we revisit an example treated using the single rate approximate solution to the TFL preservation problem in Elobaid et al. (2020c) and demonstrate the effectiveness of multi-rate.

The example of the differential drive revisited

To show explicitly the computations involved we revisit the example of a differential drive with constant forward velocity treated in (Elobaid et al., 2020c, Example 1). This unpublished example complements the results with single-rate and provides further insights into the differences with respect to multi-rate. Consider

$$\dot{q} = f(q) + g(q)\omega = \begin{pmatrix} v\cos q_3 \\ v\sin q_3 \\ 0 \end{pmatrix} + \begin{pmatrix} 0 \\ 0 \\ 1 \end{pmatrix}\omega \tag{8.8}$$

Let

$$y = \alpha(q) = (q_1^2 + q_2^2 + a^2)^2 - 4a^2q_1^2 - b^4$$

with $a, b \in \mathbb{R}$ describe the Casini oval, a geometric path on the plane with no self-intersections. This output has relative degree $r = 2$. In this sense, there exist a linearizing feedback of the form;

$$\omega_c = \frac{\nu - [4\,v^2\,\left(a^2\,\cos\left(2\,q_3\right) + {q_1}^2\,\cos\left(2\,q_3\right) - {q_2}^2\,\cos\left(2\,q_3\right) + 2\,a^2 + 2\,{q_1}^2 + 2\,{q_2}^2 + 2\,q_1\,q_2\,\sin\left(2\,q_3\right)\right)]}{4\,q_1\,v\,\sin\left(q_3\right)\,\left(3\,a^2 + {q_1}^2 + {q_2}^2\right) - 4\,q_2\,v\,\cos\left(q_3\right)\,\left(a^2 + {q_1}^2 + {q_2}^2\right)}$$

Setting

$$\nu = -k_1\alpha(q) - k_2\dot{\alpha}(q)$$

with $k_1,\ k_2 > 0$ stabilizes the linear input-output link allowing the differential drive to follow the path. Now define the multi-rate sampled equivalent model of order $r = 2$ on ω, equivalently setting $\omega^i(k) = \omega(t), t \in [k\frac{\delta}{2} + (i-1)\frac{\delta}{2}, (k+i)\frac{\delta}{2}[, i = 1, 2$ and applying the identity (8.1) so getting

$$\begin{aligned} q(k+1) &= F_2^{\delta}(q(k), \omega^1(k), \omega^2(k)) = e^{\bar{\delta}(L_f + \omega^1(k)L_g)} \circ e^{\bar{\delta}(L_f + \omega^2(k)L_g)} q|_{q(k)} \\ \alpha(k) &= h(q(k)) \end{aligned} \tag{8.9}$$

and the equations (8.2) reduces to

$$\begin{aligned} e^{\bar{\delta}(L_f + \omega^1(k)L_g)} \circ e^{\bar{\delta}(L_f + \omega^2(k)L_g)} \alpha(q)|_{q(k)} &= \alpha(q) + \delta L_f\alpha(q) + \frac{\delta^2}{2}\nu \\ e^{\bar{\delta}(L_f + \omega^1(k)L_g)} \circ e^{\bar{\delta}(L_f + \omega^2(k)L_g)} L_f\alpha(q)|_{q(k)} &= L_f\alpha(q) + \delta\nu \end{aligned}$$

Expanding the left hand side of the above one has for the expansions P_i in (8.5) the expressions;

$$\begin{aligned} P_0 = &\frac{3}{16}(L_f + \omega^1 L_g)L_f\alpha + \frac{1}{16}(L_f + \omega^2 L_g)L_f\alpha + \frac{\bar{\delta}}{12}(L_f + \omega^1 L_g)^2 L_f\alpha \\ &+ \frac{\bar{\delta}}{16}\bar{\delta}(L_f + \omega^1 L_g)(L_f + \omega^2 L_g)L_f\alpha + \frac{\bar{\delta}}{48}(L_f + \omega^2 L_g)^2 L_f\alpha + O(\bar{\delta}^2) \\ P_1 = &\frac{1}{2}(L_f + \omega^1 L_g)L_f\alpha + \frac{1}{2}(L_f + \omega^2 L_g)L_f\alpha + \frac{\bar{\delta}}{8}(L_f + \omega^1 L_g)^2 L_f\alpha \\ &+ \frac{\bar{\delta}}{8}\bar{\delta}(L_f + \omega^1 L_g)(L_f + \omega^2 L_g)L_f\alpha + \frac{\bar{\delta}}{4}(L_f + \omega^2 L_g)^2 L_f\alpha + O(\bar{\delta}^2) \end{aligned}$$

Following (8.7), and taking the first two terms by substituting in the above the expressions

$$\omega^1 = \omega^1_{d,0} + \frac{\bar{\delta}}{2}\omega^1_{d,1}, \qquad \omega^2 = \omega^2_{d,0} + \frac{\bar{\delta}}{2}\omega^2_{d,1}$$

and collecting terms in similar powers of $\bar{\delta}$, one has

$$\begin{aligned} \omega^1_{d,0} &= \omega_c(\cdot, \nu(k)), \qquad & \omega^2_{d,0} &= \omega_c(\cdot, \nu(k)) \\ \omega^1_{d,1} &= \frac{2}{3}\dot{\omega}_c(\cdot, \nu(k)), \qquad & \omega^2_{d,1} &= \frac{10}{3}\dot{\omega}_c(\cdot, \nu(k)) \end{aligned}$$

Setting in our example a constant forward velocity of $v = 0.5m/s$, with the curve parameters being $a = 3,\ b = 1.05a$ and for the continuous-time feedback gains $k_1 = 2,\ k_2 = 3$ and $\delta = 0.2$ we note in Figure (8.1) that at the cusps of the oval, the emulation slightly leaves the curve while the multi-rate solution preserves invariance tracing the ideal continuous-time performance.

In Figure 8.2, the initial conditions were changed to $x_0 = (2,\ 0,\ \frac{2\pi}{3})^\top$ and $\delta = 0.5$. Both the gains of the continuous-time controller and its corresponding digital gains are kept the same. The forward velocity is kept the same. Significant deterioration in the performances observed from the emulation controlled system are reported in the figure.

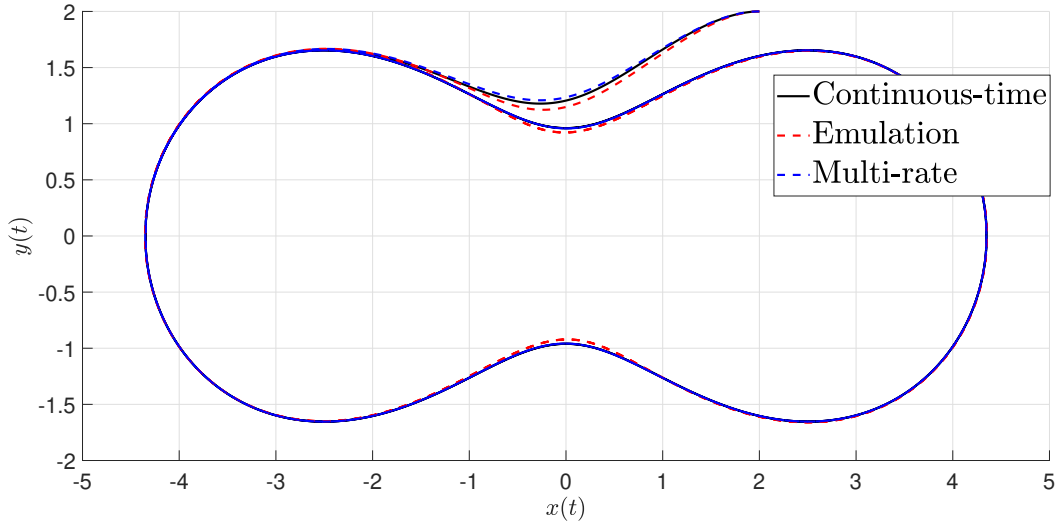

Figure 8.1: Tracing the Casini oval with $\delta = 0.2$

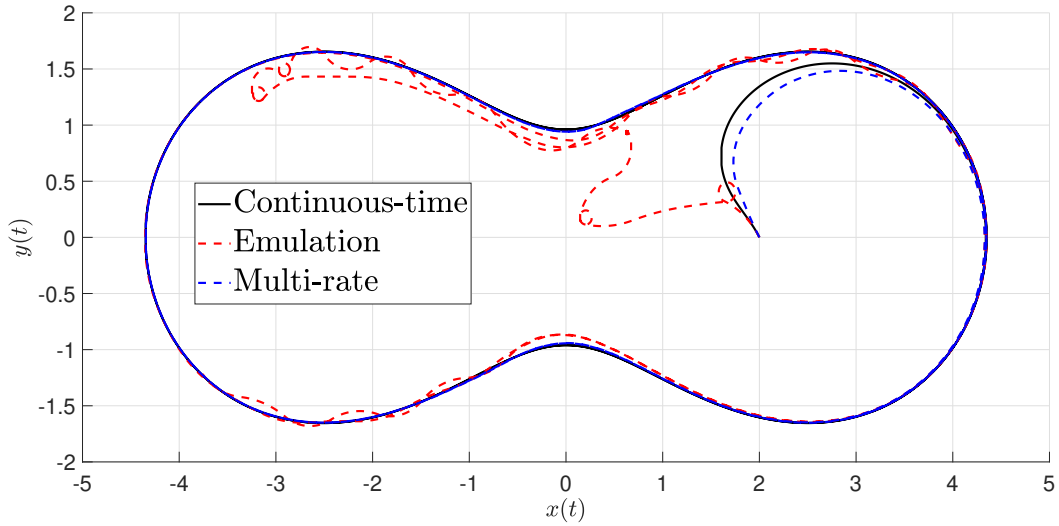

Figure 8.2: Tracing the Casini oval with $\delta = 0.5$

The above example showed that when there exists a continuous-time inversion control linearizing the input-output link of a given system, a multi-rate digital feedback exists preserving this property. This sampled feedback is of the form (8.6), an infinite series expansion in powers of δ around the continuous-time solution. This idea can then be specialized to the context of TFL as done in the sequel.

8.2 Exact transverse feedback linearization via multi-rate sampling

Following from the discussion presented in the previous section, we can now draw some general conclusions concerning the preservation of TFL under sampling. In the case of a SISO system, the following statement, not published anywhere, is straightforward

Result: TFL under multi-rate sampling for SISO systems

Given a SISO continuous-time system and $\Gamma^\star$, a controlled invariant sub-manifold of dimension $n^\star$. Let there exists a function $\alpha(x)$ solving TFL in continuous-time, i.e. having relative degree $r = n - n^\star$ and for which $\Gamma^\star = \{x \in \mathbb{R}^n : \alpha(x) = L_f\alpha(x) = \ldots = L_f^{n-n^\star-1}\alpha(x) = 0\}$. Then there exists $T^\star$ such that for any $\delta \in [0,\ T^\star[$, the multi-rate equivalent dynamics (8.1) together with the output;

$$H(x) = \begin{pmatrix} \alpha(x) & L_f\alpha(x) & \ldots & L_f^{n-n^\star-1}\alpha(x) \end{pmatrix}^\top \tag{8.10}$$

under the feedback (8.6) preserves TFL under sampling and $\Gamma^\star$ will be its zero dynamics sub-manifold. Additionally, the zero dynamics, motions on $\Gamma^\star$ are preserved in the first order.

The proof of this claim follows directly from applying (Monaco and Normand-Cyrot, 1997, Theorem 5.2) and its subsequent corollary. Additionally, in this setting, the (single) control is used to derive the evolutions to $\Gamma^\star$ thus stabilizing $\Gamma^\star$ and the tangential dynamics are uncontrolled.

In the more interesting and general MIMO scenario, things are more delicate as the reader can predict. To this end consider the following dynamics

$$\dot{x} = f(x) + \sum_{i=1}^{m} g_i(x)u_i \tag{8.11}$$

with $x \in \mathbb{R}^n$ and $u_i \in \mathbb{R}, i = 1, \ldots, m$ real analytic. Assume the vector fields describing the dynamics are complete and $g_i(x), i = 1, \ldots, m$ are independent. Let there exists ρ functions $\alpha_i(x)$ solving TFL in continuous-time for the controlled invariant sub-manifold $\Gamma^\star$, i.e.

$$\Gamma^\star = \{x \in \mathbb{R}^n : \alpha_1(x) = \ldots = L_f^{r_1-1}\alpha_1 = 0, \ldots, \alpha_\rho(x) = \ldots = L_f^{r_\rho-1}\alpha_\rho = 0\} \tag{8.12}$$

and the dummy output

$$y = \begin{pmatrix} \alpha_1(x) & \ldots & \alpha_\rho(x) \end{pmatrix}^\top \tag{8.13}$$

has a well defined vector relative degree $r = (r_1,\ \ldots,\ r_\rho)$ with $\sum_{i=1}^{\rho} \rho_i = n - n^\star$. As discussed in Chapter 7, after possibly rearranging the columns, the $\rho \times m$ decoupling matrix can be written as $D(x) = [M(x)\ N(x)]$ with the $\rho \times \rho$ matrix M full rank. Then a coordinates change similar to that reported in Section 1.2 and a feedback $u = \gamma_c(x, \nu)$ of the form;

$$\begin{aligned} u_1 &= M^{-1}(x)\Big(\nu_1 - N(x) - \tilde{f}(x)\Big) \\ u_2 &= \nu_2 \end{aligned}$$

where $\tilde{f}(x) = (L_f^{r_1}\alpha_1(x)\ \ldots\ L_f^{r_\rho}\alpha_\rho(x))^\top$, stabilizes the trajectories to $\Gamma^\star$ by appropriately setting $\nu_1 \in \mathbb{R}^\rho$, the transverse control.

Under sampling, let the multi-rate order on the control u_1 linearizing the transverse dynamics

be $m = \ell cm(r_i),\ i = 1, \ldots, r_\rho$, i.e. the least common multiple of the relative degrees, while u_2 kept constant over the larger sampling period $\delta = m\bar{\delta}$. One obtains a multi-rate sampled equivalent dynamics being

$$x(k+1) = F_m^\delta(x(k), \underline{u}_1(k), u_2(k)) \tag{8.14}$$

with

$$\begin{aligned} F_m^\delta(x, \underline{u_1}, u_2) &= F^{\bar{\delta}}(\cdot, u_1^m, u_2) \circ \ldots \circ F^{\bar{\delta}}(x, u_1^1, u_2) \\ &= \sum_{j_1, \ldots, j_m \geq 0} \frac{\bar{\delta}^{j_1+j_2+\ldots,+j_m}}{j_1! j_2! \ldots, j_m!} (u_1^1 L_{G_1} + u_2 L_{G_2})^{j_1} \circ \ldots \circ (u_1^m L_{G_1} + u_2 L_{G_2})^{j_m} x. \end{aligned}$$

where, after possible rearrangement, $G_1(x), G_2(x)$ are the first $\rho, (m-\rho)$ vector fields of the set $g_i(x)$ respectively corresponding to the controls u_1, u_2. Define now the extended output vector

$$H_e(x) = \begin{pmatrix} \alpha(x) & L_f\alpha_1(x) & \ldots & L_f^{r_1-1}\alpha_1(x) & \ldots & \alpha_\rho(x) & L_f\alpha_\rho(x) & \ldots & L_f^{r_\rho-1}\alpha_\rho(x) \end{pmatrix}^\top \tag{8.15}$$

with these machinery settled we can now make the following statement;

Result: TFL under multi-rate sampling for MIMO systems

Given the dynamics (8.11) and $\Gamma^\star$, a controlled invariant sub-manifold of dimension $n^\star$. Let there exists a function (8.13) solving TFL in continuous-time. Then there exists $T^\star$ such that for any $\delta \in [0,\ T^\star[$, the multi-rate equivalent dynamics (8.14) together with the output (8.15) admit a feedback of the form (8.6) preserving TFL under sampling, i.e. solving an equality of the form

$$H_e(F_m^\delta(x(k), \gamma_d(\cdot, \nu_1(k)), u_2(k))) = A^\delta H_e(x(k)) + B^\delta \nu_1(k) \tag{8.16}$$

with $A^\delta = \text{blkdiag}(A_{r_1}, \ldots, A_{r_\rho})$, $B^\delta = \text{blkdiag}(b_{r_1}, \ldots, b_{r_\rho})$ and $\nu_1 \in \mathbb{R}^\rho$ the transverse control. Moreover, $\Gamma^\star$ will be its zero dynamics sub-manifold of the sampled dynamics associated to (8.15), and the zero dynamics, motion on $\Gamma^\star$, is preserved in the first order.

It is clear that this is, albeit intuitive, a very strong claim for which the author provides no rigorous proof. The existence of a multi-rate solution follows from the application of the Implicit function theorem, however the difficulty stands on showing that the choice of the multi-rate order $m = \ell cm(r_i),\ i = 1, \ldots, r_\rho$ is sufficient. In anycase, in the sequel we verify, through application to different control problems, the existence and efficacy of multi-rate sampled solutions preserving TFL.

8.3 Applications to path following without dynamic extension

In this section we apply the above statements to two the important control problem of allowing a nonholonomic system to follow a given path.

Moreover, through the treatment of the specific example of the car-like robot, it is demonstrated

that the multi-rate solution, in addition to preserving TFL under sampling allow to find a state feedback when the problem admits only a dynamic feedback solution in continuous-time.

Given a car-like robot kinematics be described as(Siciliano et al. (2010))

$$\begin{aligned} \dot{q} &= g_1(q)v + g_2(q)\omega \\ p &= \begin{pmatrix} x & y \end{pmatrix}^\top \end{aligned} \tag{8.17}$$

with (see Figure 8.3)

$$g_1(q) = \begin{pmatrix} \cos\theta \\ \sin\theta \\ \frac{1}{\ell}\tan\phi \\ 0 \end{pmatrix}, \quad g_2(q) = \begin{pmatrix} 0 \\ 0 \\ 0 \\ 1 \end{pmatrix}$$

$q = \begin{pmatrix} q_1 & q_2 & q_3 & q_4 \end{pmatrix}^\top = \begin{pmatrix} x & y & \theta & \phi \end{pmatrix}^\top \in \mathbb{R}^4$, $v \in \mathbb{R}$, the forward linear velocity, $\omega \in \mathbb{R}$, the angular velocity and ℓ the distance between the wheels. The position on the plane $p = h(q) := (q_1\ q_2)^\top \in \mathbb{R}^2$ is the output of the system.

Figure 8.3: The car-like kinematics.

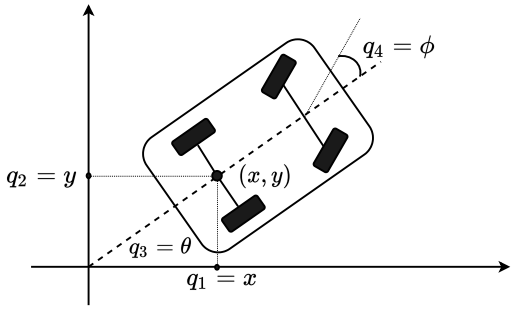

The desired path is given by $\varrho : \mathbb{D} \mapsto \mathbb{R}^2 = \{w \in \mathbb{R}^2 \text{ s.t. } s(w) = 0\}$ a regular parameterized curve on the plane with no self-intersections. The path following problem formally asks;

Problem: Path following for the car-like kinematics

Find if possible, a feedback law for the car-like kinematics (8.17) such that for a set of some initial conditions containing the path the following holds true.

1. *Invariance*: if the robot starts on the path it remains on the path.
2. *Attractivity*: if the robot starts close enough to the path, it reaches the path asymptotically.
3. *Motion on the curve*: the robot traverses the path with a given desired velocity or acceleration profile.

It is known that, because of requirement (3) above, TFL can not be applied directly to solve the problem with static feedback. Indeed the $n^\star = 3$ dimensional *path following sub-manifold* characterized by $\Gamma^\star \subseteq \{q \in \mathbb{R}^4 : q = (s \circ h)^{-1}(0)\}$ can *not* be made into the zero dynamics sub-manifold for a physically meaniful output map while also satisfying (3) Nielsen and Maggiore (2006), Akhtar et al. (2015) because

$$L_{g_1}\alpha(q_1, q_2) \neq 0, \qquad L_{g_2}\alpha(q_1, q_2) \neq 0$$

for any $\alpha(q_1, q_2)$ related to the path parametrization. The workaround, in continuous-time, is to

define a dynamics extension of order 2 on the linear velocity v;

$$\dot{\xi} = \xi_2, \quad \dot{\xi}_2 = u_1$$
$$v = \xi_1, \quad \omega = u_2$$

Such that for the dynamically extended system;

$$\dot{\tilde{q}} = \tilde{f}(\tilde{q}) + \tilde{g}_1(\tilde{q})u_1 + \tilde{g}_2(\tilde{q})u_2$$

with

$$\tilde{f} = \begin{pmatrix} \xi_1 \cos q_3 \\ \xi_1 \sin q_3 \\ \frac{\xi_1}{\ell} \tan q_4 \\ 0 \\ \xi_2 \\ 0 \end{pmatrix}, \quad \tilde{g}_2 = \begin{pmatrix} 0 \\ 0 \\ 0 \\ 0 \\ 0 \\ 1 \end{pmatrix}, \quad \tilde{g}_2 = \begin{pmatrix} 0 \\ 0 \\ 0 \\ 1 \\ 0 \\ 0 \end{pmatrix}$$

the dummy physically meaningful output function

$$y = \begin{pmatrix} \alpha(\tilde{q}) \\ \pi(\tilde{q}) \end{pmatrix} = \begin{pmatrix} (s \circ h)(\tilde{q}) \\ \arctan(\frac{\tilde{q}_2}{\tilde{q}_1}) \end{pmatrix} \tag{8.18}$$

being the parametrization of the curve and the projection of the position on the curve, have a well defined vector relative degree $r = (n - n^\star \; n^\star) = (3 \; 3)$. Because of this, there exists a coordinates change $z = \phi_1(\tilde{q}),\ \eta = \phi_2(\tilde{q})$ and

$$\phi_1 = (\alpha \; L_{\tilde{f}}\alpha \; L^2_{\tilde{f}}\alpha)^\top, \quad \phi_2 = (\pi \; L_{\tilde{f}}\pi \; L^2_{\tilde{f}}\pi)^\top$$

and linearizing feedback as the one reported in Section 1.2 of the form;

$$u = \gamma_c(\tilde{q}, \nu) \tag{8.19}$$

such that the system takes the form

$$\dot{z} = A_3 z + b_3 \nu_1 \tag{8.20}$$
$$\dot{\eta} = A_3 \eta + b_3 \nu_2 \tag{8.21}$$

with A_3, b_3 as in (2.10), and TFL is solved simply by setting $\nu_1 = Kz$ with $K : \sigma(A + BK) \subset (\mathbb{C}^-)$. As is obvious, in these coordinates $\Gamma^\star = \{(z, \eta) : z = 0\}$. In this sense, requirement (1), (2) in the path following problem are solved by the transverse control, while requirement (3) is solved by the tangential control.

Path following under multi-rate sampling

It is clear that, in the digital context, if one wants to preserve TFL using the approximate single-rate solution presented in Chapter 7, one needs the preliminary dynamic extension thus obtaining

a piecewise continuous feedback. This puts us in the position to highlight an additional benefit of the exact solution offered by multi-rate sampling, namely a workaround the need for the dynamic extension.

Following the claim stated in the previous section, and setting $\bar{\delta} = \frac{\delta}{3}$ and $\omega(t) = \omega^i(k)$ for $t \in [k\delta + (i-1)\bar{\delta}, k\delta + i\bar{\delta}[$ with $i = 1, 2, 3$ and $v(t) = v(k)$ for $t \in [k\delta, (k+1)\delta[$ we get the multi-rate dynamics of order $n - n^\star = 3$ equivalent to the the car-like kinematics;

$$\begin{aligned} q(k+1) =& F_3^\delta(q(k), v(k), \underline{\omega}(k)) \\ F_3^{\bar{\delta}}(q, v, \underline{\omega}) =& F^{\bar{\delta}}(\cdot, v, \omega^1) \circ F^{\bar{\delta}}(\cdot, v, \omega^2) \circ F^{\bar{\delta}}(q, v, \omega^3) \\ =& \sum_{j_1, j_2, j_3 \geq 0} \frac{\bar{\delta}^{j_1+j_2+j_3}}{j_1! j_2! j_3!} (vL_{g_1} + \omega^3 L_{g_2})^{j_1} \circ (vL_{g_1} + \omega^2 L_{g_2})^{j_2} \circ (vL_{g_1} + \omega^1 L_{g_2})^{j_3} q. \end{aligned} \tag{8.22}$$

As discussed in the previous section, and because the linear velocity v is constant over the large sampling period, define the extended transverse output;

$$H(q) = \begin{pmatrix} \alpha(q) & \dot{\alpha}(q) & \ddot{\alpha}(q) \end{pmatrix}^\top \tag{8.23}$$

$$\dot{\alpha} = v \cos q_3 \frac{\partial}{\partial q_1}\alpha + v \sin q_3 \frac{\partial}{\partial q_2}\alpha \tag{8.24}$$

$$\begin{aligned} \ddot{\alpha} = \frac{v^2}{\ell} [\ell \cos^2 q_3 \frac{\partial^2}{\partial q_1^2}\alpha + 2\,\ell \cos q_3 \sin q_3 \frac{\partial}{\partial q_2}\frac{\partial}{\partial q_1}\alpha - \\ \tan q_4 \left(\sin q_3 \frac{\partial}{\partial q_1}\alpha + \cos q_3 \frac{\partial}{\partial q_2}\alpha \right) + \ell \sin^2 q_3 \frac{\partial^2}{\partial q_2^2}\alpha] \end{aligned} \tag{8.25}$$

With this output, the equality (8.16) becomes;

$$\begin{aligned} e^{\bar{\delta}(vL_{g_2} + \omega^1(k) L_{g_1})} \circ e^{\bar{\delta}(v(k)L_{g_1} + \omega^2(k)L_{g_2})} \circ e^{\bar{\delta}(v(k)L_{g_1} + \omega^3(k)L_{g_2})} \alpha|_{q(k)} &= \alpha + \delta\dot{\alpha} + \frac{\delta^2}{2}\ddot{\alpha} + \frac{\delta^3}{6}\nu_1 \\ e^{\bar{\delta}(vL_{g_2} + \omega^1(k) L_{g_1})} \circ e^{\bar{\delta}(v(k)L_{g_1} + \omega^2(k)L_{g_2})} \circ e^{\bar{\delta}(v(k)L_{g_1} + \omega^3(k)L_{g_2})} \dot{\alpha}|_{q(k)} &= \dot{\alpha} + \delta\ddot{\alpha} + \frac{\delta^2}{2}\nu_1 \\ e^{\bar{\delta}(vL_{g_2} + \omega^1(k) L_{g_1})} \circ e^{\bar{\delta}(v(k)L_{g_1} + \omega^2(k)L_{g_2})} \circ e^{\bar{\delta}(v(k)L_{g_1} + \omega^3(k)L_{g_2})} \ddot{\alpha}|_{q(k)} &= \ddot{\alpha} + \delta\nu_1 \end{aligned}$$

Denoting $f(q) \equiv g_1(q)v$ since $v(k)$ is constant during the large interval by definition, we have $L_f \equiv vL_{g_1}$. With this notation, expanding the left hand side of the above equality and setting as in (8.7);

$$\omega^i = \omega_{d,0}^i + \frac{\bar{\delta}}{2}\omega_{d,1}^i \tag{8.26}$$

we have for the terms (8.5);

$$
\begin{aligned}
P_0 &= [\left(\frac{19}{27}\,\omega^1_{\mathrm{d},1} + \frac{7}{27}\omega^2_{\mathrm{d},1} + \frac{1}{27}\omega^3_{\mathrm{d},1}\right)\,\mathrm{L_g}\mathrm{L_f}^2 + \frac{1}{24}\,\left(\mathrm{L_f} + \omega^1_{\mathrm{d},0}\mathrm{L_g}\right)^2\mathrm{L_f}^2 \\
&+ \frac{1}{120}\,\left(\mathrm{L_f} + \omega^2_{\mathrm{d},0}\mathrm{L_g}\right)^2\mathrm{L_f}^2]\,\bar{\delta} + \frac{19}{27}\,\left(\mathrm{L_f} + \omega^1_{\mathrm{d},0}\mathrm{L_g}\right)\mathrm{L_f}^2 + \frac{7}{27}\,\left(\mathrm{L_f} + \omega^2_{\mathrm{d},0}\mathrm{L_g}\right)\mathrm{L_f}^2 \\
&+ \frac{1}{27}\,\left(\mathrm{L_f} + \omega^3_{\mathrm{d},0}\mathrm{L_g}\right)\mathrm{L_f}^2 + O(\bar{\delta}^2) \\
P_1 &= [\left(\frac{5}{9}\,\omega^1_{\mathrm{d},1} + \frac{3}{9}\omega^2_{\mathrm{d},1} + \frac{1}{9}\omega^3_{\mathrm{d},1}\right)\,\mathrm{L_g}\mathrm{L_f}^2 + 5\,\left(\omega^1_{\mathrm{d},0} + \omega^2_{\mathrm{d},0} + \omega^3_{\mathrm{d},0}\right)\,\mathrm{L_g}\mathrm{L_f}^3 \\
&+ 8\,\mathrm{L_f}^4]\,\bar{\delta} + \frac{5}{9}\,\left(\mathrm{L_f} + \omega^1_{\mathrm{d},0}\mathrm{L_g}\right)\mathrm{L_f}^2 + \frac{3}{9}\,\left(\mathrm{L_f} + \omega^2_{\mathrm{d},0}\mathrm{L_g}\right)\mathrm{L_f}^2 + \frac{1}{9}\,\left(\mathrm{L_f} + \omega^3_{\mathrm{d},0}\mathrm{L_g}\right)\mathrm{L_f}^2 + O(\bar{\delta}^2) \\
P_2 &= [\left(\frac{1}{3}\,\omega^1_{\mathrm{d},1} + \frac{1}{3}\omega^2_{\mathrm{d},1} + \frac{1}{3}\gamma^3_{\mathrm{d},1}\right)\,\mathrm{L_g}\mathrm{L_f}^2\mathrm{L_g}\mathrm{L_f}^2 + \frac{39}{2}\,\mathrm{L_f}^4 + 12\,\left(\omega^1_{\mathrm{d}1} + \omega^1_{\mathrm{d},1} + \omega^3_{\mathrm{d},1}\right)\,\mathrm{L_g}\mathrm{L_f}^2 \\
&+ 18\,\left(\omega^1_{\mathrm{d},0} + \omega^2_{\mathrm{d},0} + \omega^3_{\mathrm{d}0}\right)\mathrm{L_g}\mathrm{L_f}^3 + 6\,\left(\omega^1_{\mathrm{d},0}\,\omega^2_{\mathrm{d},0} + \omega^1_{\mathrm{d},0}\,\omega^3_{\mathrm{d},0} + \omega^2_{\mathrm{d},0}\,\omega^3_{\mathrm{d},0}\right)\,\mathrm{L_g}^2\mathrm{L_f}^2]\bar{\delta} \\
&+ \frac{1}{3}\,\left(\mathrm{L_f} + \omega^1_{\mathrm{d},0}\mathrm{L_g}\right)\mathrm{L_f}^2 + \frac{1}{3}\,\left(\mathrm{L_f} + \omega^2_{\mathrm{d},0}\mathrm{L_g}\right)\mathrm{L_f}^2 + \frac{1}{3}\,\left(\mathrm{L_f} + \omega^3_{\mathrm{d},0}\mathrm{L_g}\right)\mathrm{L_f}^2 + O(\bar{\delta}^2)
\end{aligned}
$$

which, solving for the terms with the same power in $\bar{\delta}$ we obtain the statement simplifying that made in (Elobaid et al., 2021, Proposition 3.1);

Result: stabilizing the path following sub-manifold

Consider the kinematic model of the car-like robot and a regular parameterized curve $\varrho : \mathbb{D} \mapsto \mathbb{R}^2$ for which the path following problem admits a solution in continuous-time. Then, requirement (1) of the path following problem is guaranteed, at all $t = k\delta$ with $k \geq 0$, by the feedback $\omega = \underline{\omega}^{\bar{\delta}}(q, v, \nu_1)$ of the form

$$
\underline{\omega}^{\bar{\delta}}(q, v, \nu_1) = \underline{\omega}_0(q, v, \nu_1) + \sum_{i>0} \frac{\bar{\delta}^i}{(i+1)!}\underline{\omega}_i(q, v, \nu_1) \tag{8.27}
$$

defined as the unique solution to (8.16). In addition, requirement (2) of the path following problem is guaranteed, at all $t = k\delta$ with $k \geq 0$, setting

$$
\nu_1(k) = -K^{\bar{\delta}} H(q(k)) \tag{8.28}
$$

with $K^{\bar{\delta}}$ is a suitable stabilizing gain.

Remark 8.2 *It turns out that the digital feedback solving the first two requirements of the path following problem is an expansion around the continuous-time solution when assuming v constant. Intuitively we use the angular velocity to stabilize the path following sub-manifold, thus satisfying*

requirements (1),(2) at all sampling instants. For the first terms, one has;

$$\omega^1_{d,0} = \omega^2_{d,0} = \omega^3_{d,0} = \gamma(q,\nu_1) = \frac{vL^3_{g_1}\alpha - \nu_1}{vL_{g_2}L^2_{g_1}\alpha} \tag{8.29}$$

$$\omega^1_{d,1} = \frac{15}{4}\dot{\gamma}(q,\nu_1), \quad \omega^2_{d,1} = -\frac{15}{4}\dot{\gamma}(q,\nu_1), \quad \omega^3_{d,1} = \frac{87}{4}\dot{\gamma}(q,\nu_1) \tag{8.30}$$

which stabilizes the car-like robot to the path at all $t = k\delta$.

Since the linear velocity is kept constant and free during the big interval, it ***can then be used to assign a desired motion*** (velocity and acceleration $\pi(k) = \pi(q(k))$, $\dot{\pi}(k) = \dot{\pi}(q(k))$) on the path by thus satisfying requirement (3). In fact setting the discrete-time feedback

$$v(k+1) = v(k) + \delta a(k) + \frac{\delta^2}{2}\nu_2(k) \tag{8.31a}$$

$$a(k+1) = a(k) + \delta\nu_2(k) \tag{8.31b}$$

over the tangential component with $v(k), a(k)$ are the linear velocity and acceleration over the path respectively and

$$\begin{aligned}\nu_2(k) = &\begin{pmatrix}\frac{1}{\delta^2}(a^\delta_0 - a^\delta_1 - 1) & \frac{1}{2\delta}(a^\delta_0 + a^\delta_1 - 3)\end{pmatrix} e(k) \\ &+ \ddot{\pi}_{ref}(k+1) - \ddot{\pi}_{ref}(k)\end{aligned} \tag{8.32}$$

so to guarantee, asymptotically,

$$\lim_{k\to\infty} e(k) = \begin{pmatrix} v(k) - \dot{\pi}_{ref}(k) \\ a(k) - \ddot{\pi}_{ref}(k)\end{pmatrix} = 0$$

for a^δ_0, a^δ_1 given by

$$\begin{aligned} a^\delta_0 &= e^{-\lambda_1\delta}e^{-\lambda_2\delta} \\ a^\delta_1 &= -(e^{-\lambda_1\delta} + e^{-\lambda_2\delta}), \quad \lambda_1, \lambda_2 > 0.\end{aligned}$$

Simulations

In Figure 8.4, the car-like robot is made to follow a Casini oval , i.e. $\alpha(q) = (q_1^2+q_2^2+a^2)^2 - 4a^2q_1^2 - b^4$ with $a = 3$, $b = 1.05a$. The sampling period is set to $\delta = 0.32$. And a desired velocity on the path being a step signal $\dot{\pi}_{ref} = 2$. The external transverse continuous-time control was computed via pole placement, placing the desired closed loop poles of the linearized transverse dynamics as roots to the polynomial $p = s^3 + 3s^2 + 4s + 1$, i.e. $(-0.317,\ -1.34 + 1.16i,\ -1.34 - 1.16i)$. Correspondingly, one finds the corresponding discrete time roots $(0.96,\ 0.86 + 0.1i,\ 0.86 - 0.1i)$, for which one computes the external transverse controls ν_1 through pole placement for both the single rate solution (depicted in dashed orange as Approximate SR) and the multi-rate solution depicted in dashed blue. It is clear that for this sampling period, emulation depicted in dashed red fails to achieve path following.

Changing the path to a circle of radius $R = 2$ by setting $\alpha(q) = q_1^2 + q_2^2 - R^2$ and maintaining the same external controls gains we have that for $\delta = 0.3235$ again the emulation fails at achieving

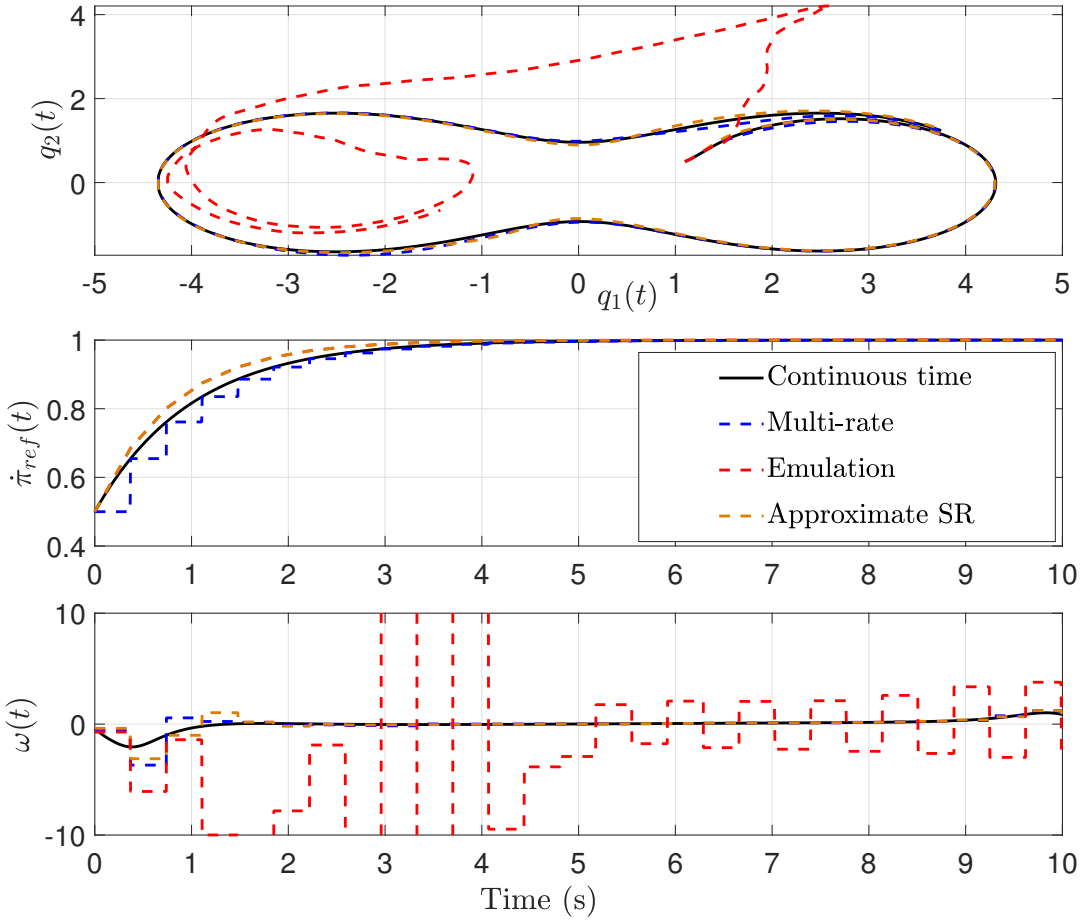

Figure 8.4: Tracing the Casini oval with $\delta = 0.32$

path following as depicted in Figure 8.5.

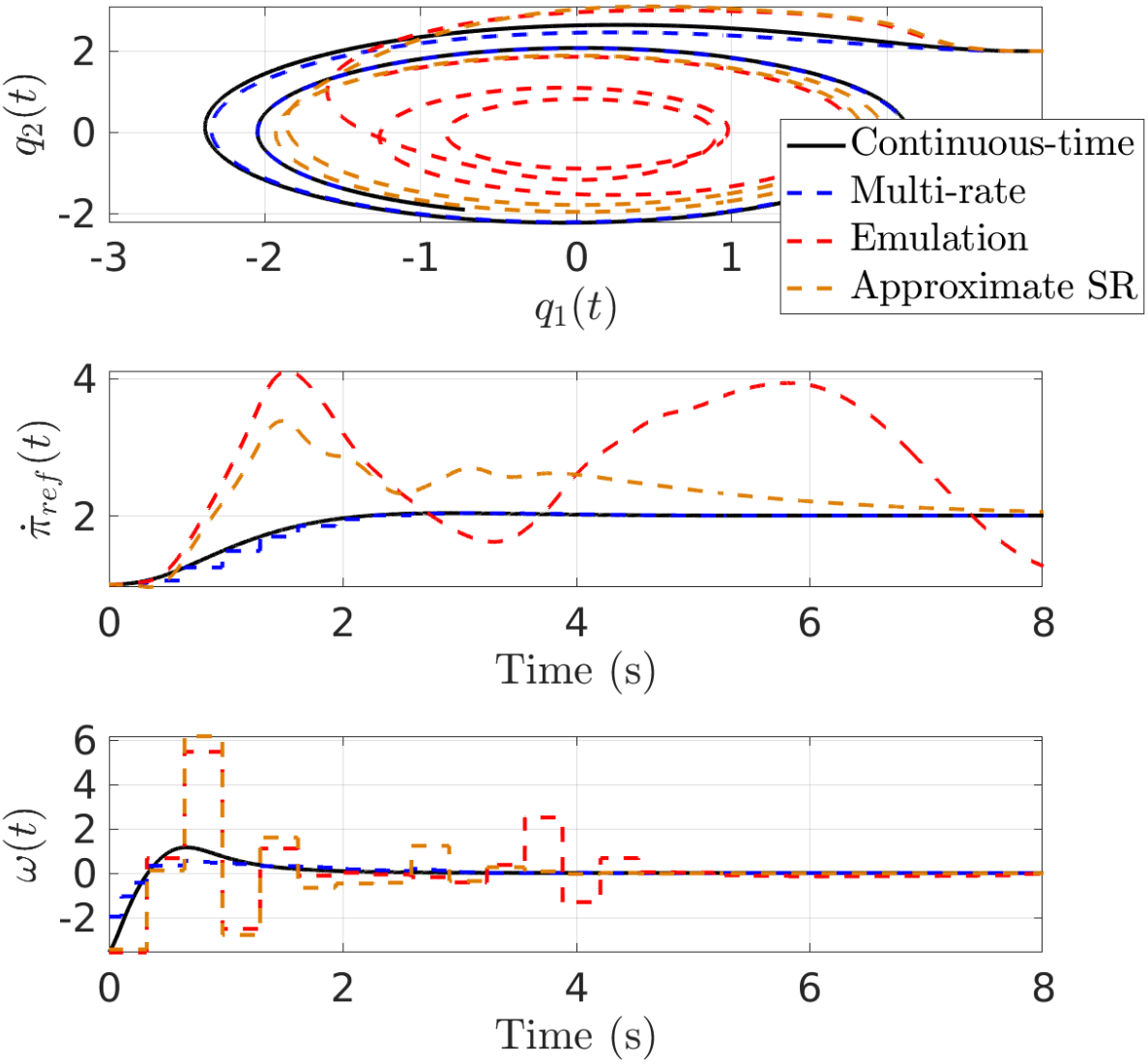

Figure 8.5: Tracing a circle with $\delta = 0.3235$

More simulations, formal statements and proofs can be found, for the interested reader, in the work Elobaid et al. (2021) which is attached at the end of this chapter. In the next section we tackle another interesting control problem through which we specify an additional benefit to preserving TFL via multi-rate sampling.

8.4 Application to periodic orbits stabilization for the Pendubot

In this section we specialize the results of preserving TFL under sampling to the case of underactuated mechanical systems under collocated feedback in the sense of Spong and Block (1995) (see also Pucci et al. (2015)). To this end, consider the dynamics of a Pendulum robot (Pendubot) depicted in Figure 8.6 which can be written as Spong and Block (1995), Romero and Yi (2021);

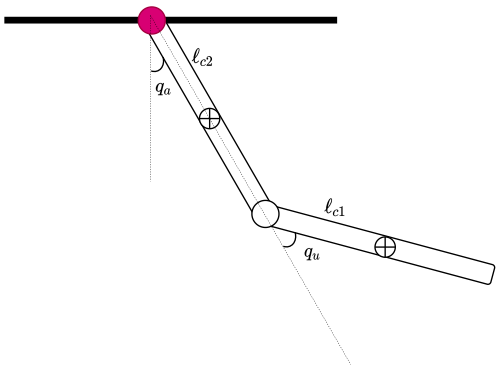

Figure 8.6: The Pendubot robot

$$
\begin{aligned}
m_{uu}(q_u)\ddot{q}_u + m_{ua}\ddot{q}_a + c_u(q,\dot{q})\dot{q} + \frac{\partial V(q)}{\partial q_u} &= 0 \\
m_{au}(q_u)\ddot{q}_u + m_{aa}\ddot{q}_a + c_a(q,\dot{q})\dot{q} + \frac{\partial V(q)}{\partial q_a} &= \tau
\end{aligned}
$$

where

$$
\begin{aligned}
m_{uu}(q_u) &= m_2\ell_{c2}^2 + I_2 \\
m_{ua}(q_u) &= m_2\ell_{c2}^2 + I_2 + m_2\ell_1\ell_{c2}\cos q_u \\
m_{au}(q_u) &= m_2\ell_{c2}^2 + I_2 + m_2\ell_1\ell_{c2}\cos q_u \\
m_{aa}(q_u) &= m_1\ell_{c1}^2 + m_2\ell_1^2 + I_1 + m_2\ell_{c2}^2 + I_2 + 2m_2\ell_1\ell_{c2}\cos q_u
\end{aligned}
$$

are the entries of the inertia matrix. The parameters $m_i, I_i\ell_i, \ell_{ci}$ are the mass, inertia, length and length to center of mass for link $i = 1, 2$ respectively. Additionally, the Coriolis terms and potential energy reads;

$$
\begin{aligned}
c_u(q,\dot{q}) &= (m_2\ell_1\ell_{c2}\sin q_u)\dot{q}_a \\
c_a(q,\dot{q}) &= (m_2\ell_1\ell_{c2}\sin q_u)\dot{q}_a - 2(m_2\ell_1\ell_{c2}\sin q_u)\dot{q}_u \\
\frac{\partial V(q)}{\partial q_u} &= m_2\ell_{c2}g_r\sin(q_a + q_u) \\
\frac{\partial V(q)}{\partial q_a} &= (m_1\ell_{c1} + m_2\ell_{c2})g_r\sin q_a + m_2\ell_{c2}g_r\sin(q_a + q_u)
\end{aligned}
$$

where g_r is the gravity constant. Under a preliminary collocation feedback

$$
\tau = c_a(q,\dot{q}) + \frac{\partial V(q)}{\partial q_a} + \frac{m_{au}(q_u)}{m_{uu}(q_u)}(c_u(q,\dot{q}) + \frac{\partial V(q)}{\partial q_u}) + \tilde{u} \tag{8.34}
$$

we have;

$$
\begin{aligned}
\ddot{q}_a &= u \\
\ddot{q}_u &= \frac{-1}{m_{uu}(q_u)}(c_u(q,\dot{q}) + \frac{\partial V(q)}{\partial q_u} - m_{ua}(q_u)u)
\end{aligned} \tag{8.35}
$$

with $u = \frac{1}{\tilde{m}_{aa}}\tilde{u}$ and $\tilde{m}_{aa}(q_u) > 0$ a parameter depending on the entries of the inertia matrix as in Spong and Block (1995). Note that because of underactuation, forcing a behaviour on the actuated

joint q_a through the external control u also defines a behaviour for the underactuated joint q_u.

Problem: periodic orbits stabilization for the Pendubot

Find if possible, a feedback law u for the Pendubot under collocation feedback such that the underactuated link in (8.35) admits a stable periodic solution.

Let the states vector be $x = \begin{pmatrix} q_u & q_a & \dot{q}_u & \dot{q}_a \end{pmatrix}^\top$ and define the set of desired stable periodic orbit solutions to the dynamics in the state-space as ;

$$\Gamma^\star = \{x \in \mathbb{S}^1 \times \mathbb{R}^1 \times \mathbb{S}^1 \times \mathbb{R}^1 : x_2 + k_2 x_1 = 0, x_4 + k_2 x_1 = 0\} \tag{8.36}$$

where $k_2 \in \mathbb{R}$ is a parameter as in Romero and Yi (2021). This set can be made controlled invariant in continuous-time using TFL by setting the output

$$\alpha(x) = x_2 + k_2 x_1 \tag{8.37}$$

which has a well defined relative degree $r = 2 = n - n^\star$ with respect to the dynamics rewritten in state-space format;

$$\dot{x} = f(x) + g(x)u \tag{8.38}$$

with

$$f(x) = \begin{pmatrix} x_3 \\ x_4 \\ \frac{-1}{m_{uu}(x_1)}(c_u(x,\dot{x})\dot{x} + \frac{\partial V(x)}{\partial x_1}) \\ 0 \end{pmatrix}, \qquad g(x) = \begin{pmatrix} 0 \\ 0 \\ \frac{m_{ua}(x_1)}{m_{uu}(x_1)} \\ 1 \end{pmatrix}$$

In fact it is enough to set

$$u = \gamma_c(x,\nu) = -\frac{(c_1 + c_2 + 2\,c_3\,\cos(x_1))\,\left(c_3\,k_2\,\sin(x_1)\,{x_4}^2 + c_2\,\nu + c_5\,\mathrm{g_r}\,k_2\,\sin(x_1 + x_2)\right)}{c_2\,\left(c_1 + c_2 - c_2\,k_2 + 2\,c_3\,\cos(x_1) - c_3\,k_2\,\cos(x_1)\right)} \tag{8.39}$$

with c_i as reported in Romero and Yi (2021), namely

$$\begin{aligned} c_1 &= m_1\ell_{c1}^2 + m_2\ell_1^2 + I_1 \\ c_2 &= m_2\ell_{c2}^2 + I_2 \\ c_3 &= m_2\ell_1\ell_{c2} \\ c_4 &= m_1\ell_{c1} + m_2\ell_1 \\ c_5 &= m_2\ell_{c2} \end{aligned}$$

To solve the problem then one sets

$$\nu = -f_1\alpha(x) - f_2\dot{\alpha}(x) \tag{8.40}$$

with $f_1, f_2 > 0$ and the Pendubot is forced to perform periodic motions above the horizontal.

Periodic orbits stabilization under multi-rate sampling

Being a SISO system, the results in Section 8.2 directly applies and one sets a multi-rate of order $m = r = 2$ on u and directly, similar to the differential drive example, obtain a feedback;

$$\begin{aligned} \underline{u} &= \begin{pmatrix} u^1 & u^2 \end{pmatrix}^\top \\ u^1 &= u^1_{d,0} + \frac{\bar{\delta}}{2!} u^1_{d,1} \quad = \gamma_c(x,\nu) + \frac{\bar{\delta}}{3}\dot{\gamma}_c(x,\nu) \\ u^2 &= u^2_{d,0} + \frac{\bar{\delta}}{2!} u^2_{d,1} \quad = \gamma_c(x,\nu) + \frac{5\bar{\delta}}{3}\dot{\gamma}_c(x,\nu) \end{aligned} \tag{8.41}$$

Simulations

To validate the approach proposed, simulations are performed with the following parameters

$m_1\ [kg]$	0.2	$m_2\ [kg]$	0.052
$I_1\ [kgm^2]$	3.38×10^{-1}	$I_2\ [kgm^2]$	1.17×10^{-1}
$\ell_1\ [m]$	0.2	$\ell_2\ [m]$	0.28
$\ell_{c1}\ [m]$	0.13	$\ell_{c2}\ [m]$	0.15

The parameter $k_2 = -1$ following Romero and Yi (2021) and $g_r = 10[m/s^2]$. Figure 8.7 depicted the transient behaviour under multi-rate control depicted in blue for and dashed blue, following the ideal continuous-time control depicted in black and dashed black for different initial conditions. The sampling period is set to $\delta = 0.5$ and the continuous-time external gains $f_1 = 1, f_2 = \sqrt{3}$ while the corresponding digital ones are set to $f_1 \approx 0.4387, f_2 \approx 1.2617$. It is clear that the multi-rate digital solution manages to stabilize the periodic orbit, following closely the ideal continuous-time solution

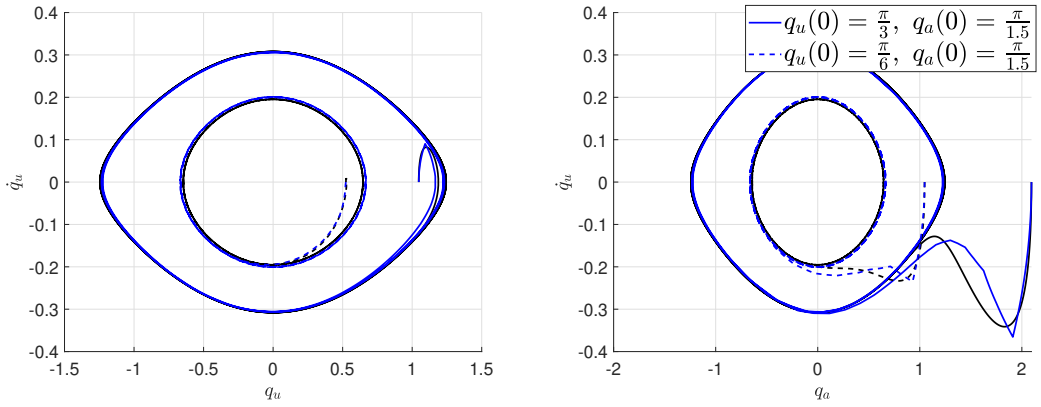

Figure 8.7: Multi-rate stabilizing the periodic orbit for different initial conditions $\delta = 0.5$

Figures 8.8, 8.9 depicted the transient behaviour under multi-rate control compared to the Emulation depicted in dashed red, and the approximate single rate solution depicted in dashed orange as the sampling period δ increases. Both sampled solution manage to stabilize the periodic orbit while the emulation, for $\delta = 1.2$ fails. The situations depicted are initialized at $x_0 = (\frac{\pi}{3},\ \frac{\pi}{1.5},\ 0,\ 0)^\top$.

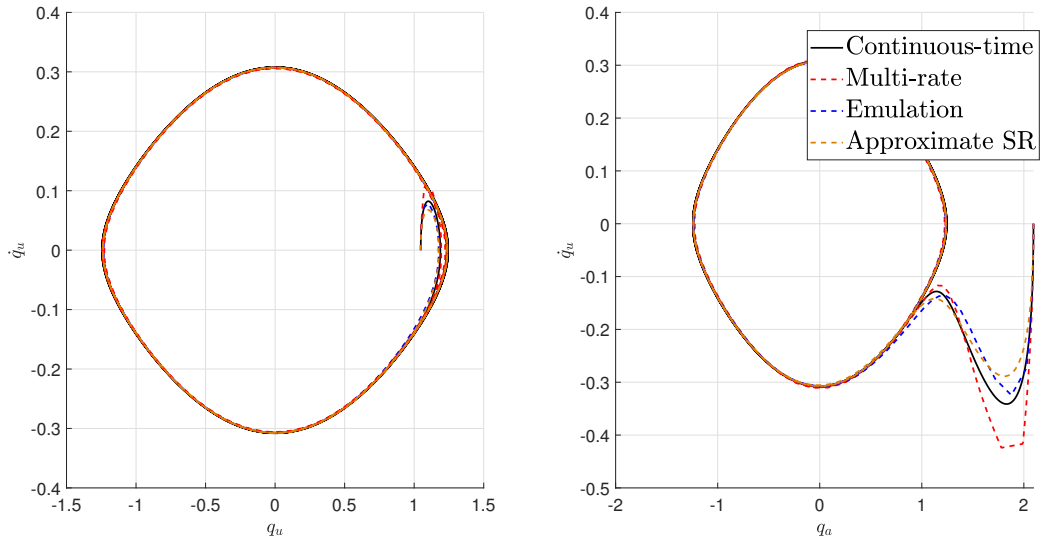

Figure 8.8: Comparing transient behaviour of q_u, q_a and their velocities $\delta = 0.5$

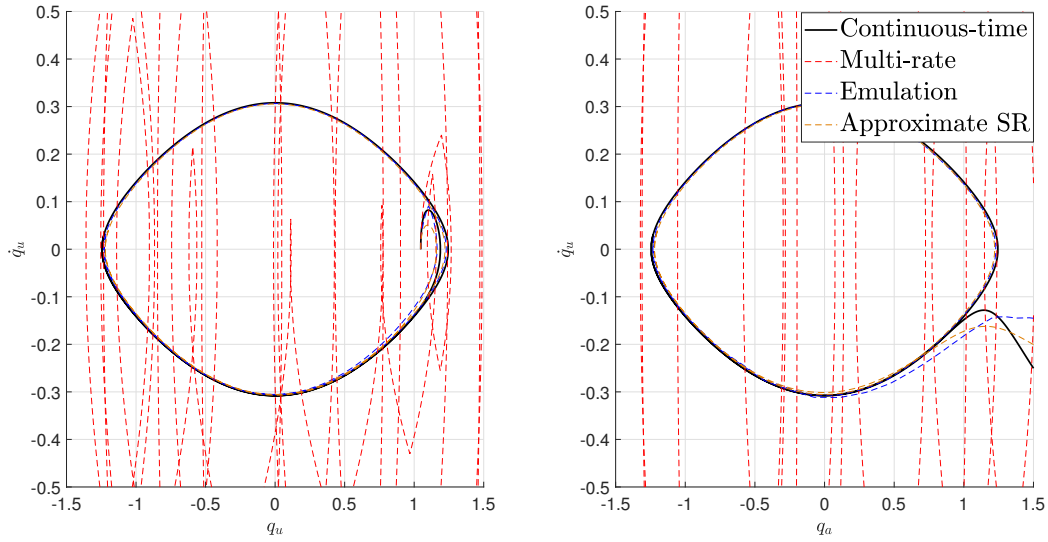

Figure 8.9: Failure of emulation $\delta = 1.2$

The above example suggests a very interesting application for the proposed methodology. Namely, the resulting set describing the periodic orbit was obtained through Immersion and Invariance techniques as in Romero and Yi (2021). This suggests a close link between immersion and invariance, once the implicit sub-manifold was characterized, and TFL both in continuous-time and under sampling. This point brings us to some concluding remarks and future works discussion.

While writing this manuscript, an additional and closely related paper herein attached was submitted. The paper deal with the **stabilization of *Virtual Holonomic Constraints - VHC* under digital control**. The feedback designed is of the linearizing type and which, as demonstrated in Chapter 8 can be preserved under sampling using multi-rate techniques. Being of this type, the work generalizes the intuition obtained dealing with periodic orbit stabilization for the pendubot. In fact; it is shown that one can impose Virtual Holonomic Constraints (VCHs) to a mechanical

systems in Euler-Lagrangian form **under sampling**. The provided feedback solution is exact based on a multi-rate sampling device of order two over each input channel. This work is submitted to the upcoming European Control Conference and is under review. For the interested reader the work is attached below.

8.5 Conclusions to Part III and further comments

In this part of the thesis we concerned ourselves with the problem of preserving TFL both under single rate and multi-rate sampling schemes.

- In Chapter 7, under single-rate sampling, an approximate solution relying on a previous result due to Barbot et al. (1996) was developed. Additionally, arbitrary higher orders of approximation was shown to follow provided an iterative procedure is carried out Elobaid et al. (2020c).
- In this chapter, we further proposed that an exact multi-rate solution exists whenever a continuous-time solution to the TFL problem exists. Moreover, through the application to the well studies path following problem, this solution was shown to have the additional benefit of mitigating the need for a preliminary dynamics extension.
- This part was concluded with two important control problems demonstrating how to use multi-rate to preserve TFL.

Some comments and self-criticisms are in order;

- What remains, for this work to constitute a somewhat complete framework for *Transverse feeback linearization under digital control* is to; starting from a purely discrete-time system and a set $\Gamma^\star$, the question of necessary and sufficient conditions for the solvability of TFL, as opposed to simply preserving a continuous-time solution, remains open.
- Finally, the application of the results obtained in Chapter 7 and the current chapter to different set stabilization problems is a worthy endeavour in and of itself. As an example to possible applications we mention nested sets stabilization and hierarchical control Doosthoseini and Nielsen (2015b), coordinated path following Doosthoseini and Nielsen (2015a) and stabilization of virtual holonomic constraints. It is also of interest to study the equivalence of those solutions to the feedback obtained using Immersion and Invariance Astolfi and Ortega (2003), Mattioni et al. (2017b) and those obtain through energetic techniques Moreschini et al. (2020), Ortega et al. (2008), Hilairet et al. (2013). This last aspect is motivated by the example developed in the previous section as the reader may have gathered. Indeed, for the Pendubot, once the set characterizing the desired periodic orbits solution was parametrized via I&I, applying TFL solutions both in continuous-time and digitally becomes a matter of computations. This motivates the question of such equivalence.

As the reader may have noted, this work is rather written as a companion to the published articles. As a consequence, the author makes no claims of this work being complete or self-contained. To this end the reader is advised to consult the seminal work of Banaszuk and hauser Banaszuk

and Hauser (1995) and the more recent and elegant formulation and solution of the problem of TFL in continuous time by Nielsen and Maggiore Nielsen and Maggiore (2008), Nielsen and Maggiore (2006). Additionally, for general treatment of linear equivalence under feedback, the reader may consult the important book by Isidori Isidori (1995) and for the digital treatment of the subject the monographs Monaco and Normand-Cyrot (1983b), Arapostathis et al. (1989), Grizzle and Shor (1988) and the references therein.

Digital path-following for a car-like robot ⋆

Mohamed Elobaid [*,**] **Mattia Mattioni** [*] **Salvatore Monaco** [*]
Dorothée Normand-Cyrot [**]

[*] *Dipartimento di Ingegneria Informatica, Automatica e Gestionale* A. Ruberti *(Università degli Studi di Roma* La Sapienza*); Via Ariosto 25, 00185 Rome, Italy (e-mail: {mohamed.elobaid,mattia.mattioni,salvatore.monaco}@uniroma1.it).*
[**] *Laboratoire de Signaux et Systèmes (L2S, CNRS-CentraleSupelèc); 3, Rue Joliot Curie, 91192, Gif-sur-Yvette, France (e-mail: {mohamed.elobaid,dorothee.normand-cyrot}@centralesupelec.fr).*

Abstract: This paper deals with path following under digital control for a car-like robot via TFL. Assuming the existence of a continuous-time feedback, a multi-rate sampled-data control strategy is proposed and its effectiveness validated through simulations.

Keywords: Robotic systems, Novel control theory and techniques, Sampled-data nonlinear control

1. INTRODUCTION

Path following control deals with the confinement of the evolutions of a nonholonomic mechanical system to a prescribed geometric path. The assignment of time requirements on the way the system moves along the path represent an extra constraint which can be handled separately from the geometric requirement, allowing for better performances compared to trajectory tracking design (Aguiar et al. (2008)).
Several approaches solving path following problems are discussed in the continuous-time literature. Among others, let us mention the work relying on energy shaping through Immersion and Invariance by Yi et al. (2020), sliding mode path following by Dagci et al. (2003), smooth time-varying feedback and input scaling by De Luca et al. (2001) and, more relevant to this work, Transverse Feedback Linearization (TFL) by Banaszuk and Hauser (1995); Altafini (2002); Nielsen and Maggiore (2008).
Among these, the latter one aims to stabilize a general set which is made the zero dynamics sub-manifold associated with a suitable output function with well-defined relative degree. Accordingly, static (or possibly dynamic) feedback linearization is applied to stretch the trajectories onto the target set (Nielsen and Maggiore (2006)). In this sense, path following admits a solution via TFL when the path can be implicitly represented by the equations which specify the zero-dynamics sub-manifold (Akhtar et al. (2015)).
When approaching these problems in a digital context, one has to face well-known limitations due to the sampling process as, for instance, the loss of the relative degree and the rise of the unstable sampling zero-dynamics (see Aström et al. (1984); Monaco et al. (1986)) so directly affecting TFL in general. For those reasons, a first single rate solution preserving TFL in an approximate sense was proposed in Elobaid et al. (2020) providing, under suitable assumptions, a solution to the path following problem as well. For instance, when dealing with the car-like robot approximate TFL under sampling is preserved for the kinematic model under a preliminary continuous-time dynamic extension (Akhtar et al. (2015)). Beyond TFL, a multi-rate technique has been proposed in Di Giamberardino et al. (1996) to solve steering problems for mobile robots, when assuming a preliminary continuous-time feedback making the dynamics finitely discretizable. In the method we propose, both these demands are weakened.
In this work, following Monaco and Normand-Cyrot (1992), we propose a solution which circumvents the need for the dynamic extension, making use of a multi-rate sampled-data control strategy. Simulation results validate the proposed design approach in a comparative way with respect to the continuous-time solution and its direct implementation through Zero Order Holding (ZOH) referred to as emulation as well as the design approach previously recalled (Elobaid et al. (2020)). The proposed multi-rate solution provides efficient and improving results with respect to the preliminary ones.

The paper is organized as follows: Section II provides some background material and states the problem. The proposed control solution is developed in Section III in a constructive way. Simulations are discussed in Section IV. Concluding remarks end the manuscript.

Notations: $\mathbb{S}^1$ denotes the unit disk, i.e. $\mathbb{S}^1 = \{z \in \mathbb{C} : |z| \leq 1\}$. $\mathbb{Z}_{\geq 0}$ denotes the set of non-negative integers. Given a pair of matrices (A, B), $\text{col}(A, B) = \begin{pmatrix} A^\top & B^\top \end{pmatrix}^\top$ while $\text{diag}(A, B)$ is the block diagonal matrix with blocks A, B. The couple (A_n, B_n) with

$$A_n = \begin{pmatrix} \mathbf{0}_{(n-1)\times 1} & I_{n-1} \\ 0 & \mathbf{0}_{1\times(n-1)} \end{pmatrix}, B_n = \begin{pmatrix} \mathbf{0}_{(n-1)\times 1} \\ 1 \end{pmatrix}$$

is said to be in Brunovský's canonical form with I_{n-1} being the identity matrix of dimension $n-1$ and $\mathbf{0}_{m\times n}$ the zero matrix of dimension $m \times n$. Given a manifold M and a closed connected set $N \subset M$, N is said to be invariant under the dynamics $\dot{q} = f(q) + g(q)u$ if for all $q(0) \in N$

⋆ Partially funded by *Université Franco-Italienne/Università Italo-Francese* (UFI/UIF) through the Vinci program.

and any control $u(\cdot)$, $q(t) \in N, \forall t$. N is *controlled* invariant if there exists a feedback $u^\star$ making N invariant for the closed loop system. The point-to-set distance is denoted $\|q_0\|_M = \inf\|q - q_0\|, q \in M$. L_f denotes the operator $\mathrm{L}_f = \sum_{i=1}^{n} f_i(\cdot)\frac{\partial}{\partial q_i}$, $\mathrm{L}_f\mathrm{L}_g$ their composition. Given a real valued function $h(\cdot)$ on $\mathbb{R}^n$, $e^{\mathrm{L}_f} h(q)|_{q(k)}$ denotes the application of the Lie series operator e^{L_f} to the function $h(q)$ evaluated at the state $q(k)$. A continuous function $R(x,\delta)$ is of order $O(\delta^p)$ with $p \geq 1$ if, whenever it is defined, it can be written as $R(x,\delta) = \delta^{p-1}\tilde{R}(x,\delta)$ and there exists a function $\beta(\delta)$ of class κ_∞ and $\delta^\star > 0$ such that $\forall \delta \leq \delta^\star, |\tilde{R}(x,\delta)| \leq \beta(\delta)$.

2. PRELIMINARIES AND PROBLEM STATEMENT

2.1 Path following for a car-like robot in continuous time

Consider the kinematic model of a car-like robot (Siciliano et al. (2010))

$$\begin{aligned} \dot{q} &= g_1(q)v + g_2(q)\omega \\ p &= (x \;\; y)^\top \end{aligned} \tag{1}$$

with (see Figure 1)

$$g_1(q) = \begin{pmatrix} \cos\theta \\ \sin\theta \\ \frac{1}{\ell}\tan\phi \\ 0 \end{pmatrix}, \quad g_2(q) = \begin{pmatrix} 0 \\ 0 \\ 0 \\ 1 \end{pmatrix}$$

$q = (q_1 \;\; q_2 \;\; q_3 \;\; q_4)^\top = (x \;\; y \;\; \theta \;\; \phi)^\top \in \mathbb{R}^4$, $v \in \mathbb{R}$, the forward linear velocity, $\omega \in \mathbb{R}$, the angular velocity and ℓ the distance between the wheels. The position on the plane $p = h(q) := (q_1 \;\; q_2)^\top \in \mathbb{R}^2$ is the output of the system.

The desired path is given by a regular parameterized curve $\varrho : \mathbb{D} \mapsto \mathbb{R}^2$ with no self-intersections. Following Nielsen and Maggiore (2004); Akhtar et al. (2015), we refer to for a precise characterization, let the path $\varrho(\mathbb{D})$ be an embedded sub-manifold of $\mathbb{R}^2$ of dimension 1; i.e., there exists a function $s(\cdot) : \mathbb{R}^2 \to \mathbb{R}$ such that 0 is a regular value of s and $\varrho(\mathbb{D}) = \{w \in \mathbb{R}^2 \text{ s.t. } s(w) = 0\}$.

The path following problem for a car-like robot asks for the design of a feedback control law maneuvering the output of system (1) to approach and move along a given curve in a desired way. The problem is formally stated below.

Problem 2.1. Given a regular parameterized curve $\mathcal{C} = Im\{\varrho(\mathbb{D})\}$, find if possible, a smooth feedback law for system (1) such that for a set of some initial conditions $\mathcal{X}$, with $\mathcal{C} \subset \mathcal{X}$ the following holds true.

(1) *Invariance*: if $p(0) = h(q(0)) \in \mathcal{C}$ then $\forall t \geq 0$ $\|p(t)\|_\mathcal{C} = 0$.
(2) *Attractivity*: system (1) under feedback is s.t $\forall t \geq 0$, $\|p\|_\mathcal{C} \to 0$ as $t \to \infty$.
(3) *Motion on the curve*: system (1) traverses the curve $\mathcal{C}$ with a given desired velocity or acceleration profile $(\dot{\pi}_{ref}(t), \ddot{\pi}_{ref}(t))$.

It is known (Altafini (2002); Nielsen and Maggiore (2006)) that TFL is a natural tool to handle path following problems. To see this, denote the $n^\star = 3$ dimensional sub-manifold $\Gamma^\star \subseteq \{q \in \mathbb{R}^4 : q = (s \circ h)^{-1}(0)\}$ as the control invariant subset for (1); i.e., the set of all initial

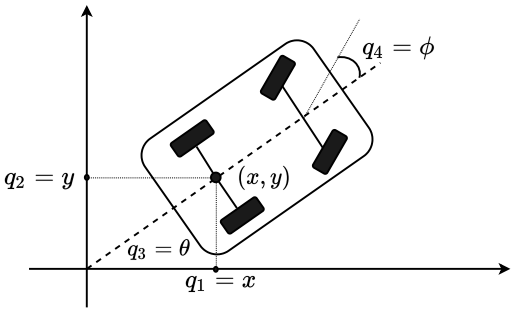

Fig. 1. Kinematics of a car-like robot

conditions $q_0 \in \mathbb{R}^4$ under which the car-like robot is forced to remain on the curve (i.e., $p(t) \in \mathcal{C}$ for all $t \geq 0$) under a suitably designed feedback. Consequently, $\Gamma^\star$ is referred to as the *path following sub-manifold* associated with the curve. With this in mind, Problem 2.1 is equivalent in the context of TFL to the problems of stabilizing $\Gamma^\star$ and zero dynamics assignment. The problem has been solved in Akhtar et al. (2015) making use of continuous-time TFL through dynamic control defining the function $\beta : \mathbb{R}^4 \to \mathbb{R}^2$

$$\beta(q) = (\alpha(q) \;\; \pi(q))^\top \tag{2}$$

with $\alpha(q) = (s \circ h)(q) \in \mathbb{R}$ the *transverse output function* (i.e., the curve implicit function) and $\pi(q) = \arctan(\frac{q_2}{q_1})$ is the *tangent output function*. Under the control dynamic extension

$$\begin{aligned} \dot{\eta}_1 = \eta_2, \quad \dot{\eta}_2 = u_1 \\ v = \eta_1, \quad \omega = u_2 \end{aligned} \tag{3}$$

the feedback system

$$\begin{aligned} \dot{\tilde{q}} &= \tilde{f}(\tilde{q}) + \tilde{g}_1(\tilde{q})u_1 + \tilde{g}_2(\tilde{q})u_2 \\ \tilde{f}(\tilde{q}) &= \left(\eta_1\cos\theta \;\; \eta_1\sin\theta \;\; \frac{\eta_1}{\ell}\tan\phi \;\; 0 \;\; \eta_2 \;\; 0\right)^\top \\ \tilde{g}_1(\tilde{q}) &= (0 \;\; 0 \;\; 0 \;\; 0 \;\; 0 \;\; 1)^\top, \tilde{g}_2(\tilde{q}) = (0 \;\; 0 \;\; 0 \;\; 1 \;\; 0 \;\; 0)^\top \end{aligned} \tag{4}$$

with $\tilde{q} = (q \;\; \eta_1 \;\; \eta_2)^\top \in \mathbb{R}^{\tilde{n}}, \tilde{n} = 6$ possesses strong vector relative degree $r = (\tilde{n} - n^\star \;\; n^\star) = (3 \;\; 3)$ with respect to the output function (2). Accordingly, the following result is recalled.

Theorem 2.1. (Akhtar et al. (2015)). Given a regular, three times differentiable curve $\mathcal{C}$ in the plane with $\Gamma^\star$ the path following sub-manifold associated with $\mathcal{C}$. Consider the dummy output function (2), then the Path-Following Problem 2.1 is solved by the feedback (3) with

$$u = \gamma(\tilde{q}, \nu) = A^{-1}(\tilde{q})(\nu - B(\tilde{q})) \tag{5}$$

with $u = (u_1, u_2)^\top$,

$$A(\tilde{q}) = \begin{pmatrix} L_{\tilde{g}_1}L_{\tilde{f}}^2\alpha(q) & L_{\tilde{g}_2}L_{\tilde{f}}^2\alpha(q) \\ L_{\tilde{g}_1}L_{\tilde{f}}^2\pi(q) & L_{\tilde{g}_2}L_{\tilde{f}}^2\pi(q) \end{pmatrix}, \; B(\tilde{q}) = \begin{pmatrix} L_{\tilde{f}}^3\alpha(q) \\ L_{\tilde{f}}^3\pi(q) \end{pmatrix}$$

and $\nu = (\nu_1, \;\; \nu_2)$ are respectively the transverse and tangential external stabilizing controls.

In the continuous-time case, dynamic extension is necessary for guaranteeing a well-defined relative degree $\tilde{n} - n^\star$ and, thus, TFL with respect to $\Gamma^\star$ via the input $\omega \in \mathbb{R}^n$.

Remark 2.1. Setting the feedback (5), and the coordinates change $\phi(\tilde{q}) = (\phi_1(\tilde{q}) \;\; \phi_2(\tilde{q}))^\top$ with $\xi = \phi_1(\tilde{q}) =$

$(\alpha(\tilde{q})\ L_{\tilde{f}}\alpha(\tilde{q})\ L^2_{\tilde{f}}\alpha(\tilde{q}))^\top, z = \phi_2(\tilde{q}) = (\pi(\tilde{q})\ L_{\tilde{f}}\pi(\tilde{q})\ L^2_{\tilde{f}}\pi(\tilde{q}))^\top$ the extended system (4) takes the form

$$\dot{\xi} = A_3\xi + B_3\nu_1 \tag{6a}$$
$$\dot{z} = A_3 z + B_3\nu_2 \tag{6b}$$

where $A_3 \in \mathbb{R}^{3\times 3}, B_3 \in \mathbb{R}^3$. From the result above, $\xi \in \mathbb{R}^3$ is the *transverse* component to $\Gamma^\star$ while z describes the motion when the dynamics is restricted to $\Gamma^\star$ i.e. $\Gamma^\star = \{(\xi\ \ z)^\top : \xi = 0\}$. It is intuitively understood that $\Gamma^\star$ is precisely the zero dynamics sub-manifold of the system (4) with output $\alpha(\tilde{q})$.

Remark 2.2. Theorem 2.1 states that, under TFL with dynamics extension, (1) and (2) in Problem 2.1 are solved by $\nu_1 = -K\xi$ so to make (6a) asymptotically stable. Denoting $z = (z_1\ z_2\ z_3)^\top$, requirement (3) is solved setting

$$\nu_2 = -f_2(z_3 - \dddot{\pi}_{ref}(t)) - f_1(z_2 - \ddot{\pi}_{ref}(t)) + \dddot{\pi}_{ref}(t)$$

with $f_1, f_2 > 0$ over the tangential dynamics (6b).

2.2 Path following for the car-like robot under sampling

In the sequel, we provide a solution to the path following problem for the car-like robot under sampled-data control and digital transverse feedback linearization as set in the following problem.

Problem 2.2. Design *a digital control* $(v(k)\ \ \omega(k)) = \gamma^{3\bar{\delta}}(q(k), \nu(k))$ with external inputs ν solving the Path Following Problem 2.1 for the car-like robot (1) at all sampling instants $t = k\delta$, $k \geq 0$ and $\delta > 0$ the sampling period.

In the present context, *digital control design* refers to design over the *sampled-data equivalent model* for which measures of the states are available at periodic sampling instants $t = k\delta, k \in \mathbb{Z}_{\geq 0}$, where δ is the sampling period, and controls kept constant over δ. A first solution to Problem 2.2 can be carried out over the extended model (4) with inputs (u_1, u_2) by directly applying the results in Elobaid et al. (2020). More in detail, let $u_i(t), i = 1, 2$ be constant over the sampling period, i.e. $u_i(t) = u_i(k\delta) = u_i(k)$ for $t \in [k\delta, (k+1)\delta[$. Then the sampled-data model equivalent to (4) takes he form

$$\tilde{q}(k+1) = \tilde{F}^\delta(\tilde{q}(k), u(k)) \tag{7}$$

with

$$\begin{aligned}\tilde{F}^\delta(\tilde{q}, u) =& e^{\delta(\mathrm{L}_{\tilde{f}} + u_1\mathrm{L}_{\tilde{g}_1} + u_2\mathrm{L}_{\tilde{g}_2})}\tilde{q}\\ =& \tilde{q} + \sum_{j\geq 1}\frac{\delta^j}{j!}(\mathrm{L}_{\tilde{f}} + u_1\mathrm{L}_{\tilde{g}_1} + u_2\mathrm{L}_{\tilde{g}_2})^j\tilde{q}\end{aligned}$$

with the function $\tilde{F}^\delta(\cdot, u)$ defined by its series expansion in powers of δ, Monaco and Normand-Cyrot (1997).

At this point, it is easily verified that the relative degree of the sampled-data model (7) with the output (2) falls to (1 1) for all $\delta > 0$ (Monaco and Normand-Cyrot (1987)). As a matter of facts, one gets that

$$\frac{\partial\alpha(\tilde{q}(k+1))}{\partial u_j(k)} = \frac{\delta^{\tilde{n}-n^\star}}{(\tilde{n}-n^\star)!}L_{\tilde{g}_j}L_{\tilde{f}}^{\tilde{n}-n^\star-1}\alpha(\tilde{q})\big|_{\tilde{q}(k)} + O(\delta^{\tilde{n}-n^\star+1})$$
$$\frac{\partial\pi(\tilde{q}(k+1))}{\partial u_j(k)} = \frac{\delta^{\tilde{n}^\star}}{n^\star!}L_{\tilde{g}_j}L_{\tilde{f}}^{\tilde{n}^\star-1}\pi(\tilde{q})\big|_{\tilde{q}(k)} + O(\delta^{\tilde{n}^\star+1})$$

for $n - n^\star = 3$ $j = 1, 2$ are non-zero (at least not simultaneously) by definition of the continuous-time relative degree. Thus, the path following sub-manifold $\Gamma^\star$ is no longer the zero dynamics sub-manifold for the sampled-data model (7) with output $\alpha(\tilde{q})$. In fact, the (typically unstable) zero dynamics of the sampled-data equivalent model evolves over a sub-manifold containing $\Gamma^\star \subset \mathbb{R}^3$ that is given by

$$\mathcal{Z}_{SD} = \{\tilde{q} : \alpha(\tilde{q}) = 0\} \subset \mathbb{R}^5$$
$$\mathcal{Z}_{SD} \supset \Gamma^\star = \{\tilde{q} : \alpha(\tilde{q}) = L_f\alpha(\tilde{q}) = L_f^2\alpha(\tilde{q}) = 0\}.$$

Accordingly, transverse feedback linearization is lost for the sampled-data model (7) with respect to the output function (2).

In Elobaid et al. (2020) TFL under sampling is achieved, up to a prescribed approximation order, by means of a δ-dependent dummy output computed from (2) as

$$\alpha^\delta(\tilde{q}) = \alpha(\tilde{q}) + \delta L_{\tilde{f}}\alpha(\tilde{q}) - \frac{\delta^2}{3}L^2_{\tilde{f}}\alpha(\tilde{q}) + O(\delta^3) \tag{8a}$$
$$\pi^\delta(q) = \pi(\tilde{q}) + \delta L_{\tilde{f}}\pi(\tilde{q}) - \frac{\delta^2}{3}L^2_{\tilde{f}}\pi(\tilde{q}) + O(\delta^3). \tag{8b}$$

The vector relative degree (3 3) is preserved under the dynamics (7) together with the zero dynamics sub-manifold $\Gamma^\star$ in $O(\delta^4)$, so that a digital solution can be computed to approximately solve the TFL problem under single-rate sampling. In fact, consider the coordinates change $q \mapsto (\xi^\delta\ \ z^\delta)$, with $\xi^\delta = T_3(\delta)\phi_1(\tilde{q})$, $z^\delta = T_3(\delta)\phi_2(\tilde{q})$, where $\phi_1(\cdot), \phi_2(\cdot)$ are as in Remark 2.1, and $T_3(\delta)$ as in Elobaid et al. (2020). This coordinates change, together with the piecewise continuous feedback for $t \in [k\delta, (k+1)\delta[$

$$\dot{\eta}(t) = A_2\eta(t) + B_2u_1(k) \tag{9a}$$
$$u(k) = A^{-1}(\tilde{q}(k))(\nu^\delta(k) - B(\tilde{q}(k))) \tag{9b}$$

recovers the TFL normal form in an approximate sense, with (v, ω) piecewise continuous. The control $\nu^\delta = -K^\delta\mathrm{col}(\xi^\delta,\ z^\delta)$, $K^\delta : \sigma(I_3 + \delta(A_3 + B_3K^\delta)) \subset \mathbb{S}^1$ stabilizes the system to the path following sub-manifold and allows for solving Problem 2.2 in an approximate sense.

In the following we present an exact (and fully digital) solution for Problem 2.2 based on multi-rate sampling with no need of a preliminary continuous-time dynamic extension. Namely, we design a digital control $(v(k)\ \ \omega(k)) = \gamma^{3\bar{\delta}}(q(k), \nu(k))$ for solving path following based on the sampled-data equivalent model to the kinematic car-like robot in (1); i.e., one gets for $\omega(t) = \omega(k)$ and $v(t) = v(k)$ for $t \in [k\delta, (k+1)\delta[$ the sampled-data equivalent kinematics

$$q(k+1) = F^\delta(q(k), v(k), \omega(k)) \tag{10}$$

with

$$F^\delta(q, v, \omega) = e^{\delta(v\mathrm{L}_{g_1} + \omega\mathrm{L}_{g_2})}q = q + \sum_{j\geq 1}\frac{\delta^j}{j!}(v\mathrm{L}_{g_1} + \omega\mathrm{L}_{g_2})^j q.$$

3. EXACT PATH FOLLOWING FOR A CAR-LIKE ROBOT UNDER MULTI-RATE SAMPLING

As shown in the previous section, dynamic extension is used over system (1) to guarantee $v^2L_{g_2}L^2_{g_1}\alpha(q) \neq 0$, that is relative degree 3 with respect to the dummy output component in (2) associated with $\Gamma^\star$ (i.e., $\alpha(q)$). However, the relative degree can also be guaranteed for the kinematic model (1) under multi-rate sampling without dynamic extension, as shown in Monaco and Normand-Cyrot (1992). To this end, we set in (10) a multi-rate of

order $n - n^\star = 3$ over the input ω that is $\bar\delta = \frac{\delta}{3}$ and $\omega(t) = \omega_i(k)$ for $t \in [k\delta + (i-1)\bar\delta, k\delta + i\bar\delta[$ with $i = 1, 2, 3$ and $v(t) = v(k)$ for $t \in [k\delta, (k+1)\delta[$. Accordingly, the multi-rate model of (1) gets the form

$$q(k+1) = F_3^{\bar\delta}(q(k), v(k), \underline{\omega}(k)) \tag{11}$$

with

$$\begin{aligned} F_3^{\bar\delta}(q, v, \underline{\omega}) =& F^{\bar\delta}(\cdot, v, \omega_3) \circ F^{\bar\delta}(\cdot, v, \omega_2) \circ F^{\bar\delta}(q, v, \omega_1) \\ =& \sum_{j_1, j_2, j_3 \geq 0} \frac{\bar\delta^{j_1+j_2+j_3}}{j_1! j_2! j_3!} (vL_{g_1} + \omega_1 L_{g_2})^{j_1} \\ & \circ (vL_{g_1} + \omega_2 L_{g_2})^{j_2} \circ (vL_{g_1} + \omega_3 L_{g_2})^{j_3} q. \end{aligned}$$

In this respect, with reference to Problem 2.2, we seek for a digital piecewise constant control that preserves TFL with respect to $\Gamma^\star$ for the multi-rate equivalent model (11) based on the dummy output (2).

The problem is set for (11) based on the augmented output vector (Monaco and Normand-Cyrot (1992))

$$H(q) = \left(\alpha(q) \;\; \dot\alpha(q) \;\; \ddot\alpha(q)\right)^\top \tag{12}$$

ensuring that the multi-rate model (11) possesses vector relative degree $(1, 1, 1)$ so that transverse feedback linearizability under sampling is guaranteed. Accordingly, requirements (1),(2) of Problem 2.1 at all sampling instants are satisfied by a digital feedback $\underline{\omega} = \underline{\omega}^{\bar\delta}(q)$ solution to the equality

$$H(F_3^{\bar\delta}(q, v, \underline{\omega})) = A^{3\bar\delta} H(q(k)) + B^{3\bar\delta} \nu_1(k) \tag{13}$$

with $A^{3\bar\delta} = e^{3\bar\delta A_3}$, $B^{3\bar\delta} = \int_0^{3\bar\delta} e^{\tau A_3} B_3 d\tau$, A_3, B_3 as in (6a) and ν_1 the external stabilizing *transverse* control. More in detail, the TFL feedback solution to (13) is the one making the $H(q) - \nu_1$ link in (11) linear. The following result asserts the existence of such feedback.

Proposition 3.1. Consider the kinematic model of the car-like robot (1), and a regular parameterized curve $\varrho : \mathbb{D} \mapsto \mathbb{R}^2$ under the hypotheses of Theorem 2.1. Then, requirement (1) of Problem 2.1 is guaranteed, at all $t = k\delta$ with $k \geq 0$, by the feedback $\omega = \underline{\omega}^{\bar\delta}(q, v, \nu_1)$ of the form

$$\underline{\omega}^{\bar\delta}(q, v, \nu_1) = \underline{\omega}_0(q, v, \nu_1) + \sum_{i>0} \frac{\bar\delta^i}{(i+1)!} \underline{\omega}_i(q, v, \nu_1) \tag{14}$$

defined as the unique solution to (13). In addition, requirement (2) of Problem 2.1 is guaranteed, at all $t = k\delta$ with $k \geq 0$, setting

$$\nu_1(k) = -K^{\bar\delta} H(q(k)) \tag{15}$$

with $K^{\bar\delta}$ such that $\sigma(A^{3\bar\delta} - B^{3\bar\delta} K^{\bar\delta}) \subset \mathbb{S}^1$.

Proof: Rewriting (13) as a formal series equality in powers of $\bar\delta$ so getting

$$\begin{aligned} &\begin{pmatrix} e^{\bar\delta(v(k)L_{g_1} + \omega_1(k)\mathrm{L}_{g_2})} \ldots e^{\bar\delta(v(k)L_{g_1} + \omega_3(k)\mathrm{L}_{g_2})} \alpha(q) \\ e^{\bar\delta(v(k)L_{g_1} + \omega_1(k)\mathrm{L}_{g_2})} \ldots e^{\bar\delta(v(k)L_{g_1} + \omega_3(k)\mathrm{L}_{g_2})} \dot\alpha(q) \\ e^{\bar\delta(v(k)L_{g_1} + \omega_1(k)\mathrm{L}_{g_2})} \ldots e^{\bar\delta(v(k)L_{g_1} + \omega_3(k)\mathrm{L}_{g_2})} \ddot\alpha(q) \end{pmatrix} \\ &= A^{3\bar\delta} H(q(k)) + B^{3\bar\delta} \nu_1(k) \end{aligned} \tag{16}$$

The equations (16) rewrite as $S^{\bar\delta}(q, \underline{\omega}, v, \nu_1) = \mathbf{0}$ with

$$\begin{aligned} &S^{\bar\delta}(q, \underline{\omega}, v, \nu_1) \\ &= \left(\bar\delta^3 S_1^\delta(q, \underline{\omega}, v, \nu_1) \;\; \bar\delta^2 S_2^\delta(q, \underline{\omega}, v, \nu_1) \;\; \bar\delta S_3^\delta(q, \underline{\omega}, v, \nu_1)\right)^\top \end{aligned} \tag{17}$$

and

$$\begin{aligned} \bar\delta^{4-i} S_i^{\bar\delta} =& e^{\bar\delta(vL_{g_1} + \omega_1 L_{g_2})} \circ \ldots \circ e^{\bar\delta(vL_{g_1} + \omega_3 L_{g_2})} \alpha^{(i-1)}(q) \\ & - \alpha^{(i-1)}(q) - \sum_{\ell=i}^{2} \frac{3^\ell \bar\delta^\ell}{\ell!} \alpha^{(\ell)}(q) - \frac{3^{4-i} \bar\delta^{4-i}}{(4-i)!} \nu_1 \end{aligned}$$

Accordingly, because $v(k)$ constant over the sampling interval, denoting $f(q) = g_1(q)v$, one looks for $\underline{\omega}$ satisfying (17), where each term can be written as $S_i(q, \underline{\omega}, v, \nu_1) = \sum_{j \geq 0} \bar\delta^j S_{i,j}(q, \underline{\omega}, v, \nu_1)$ with $i = 1, 2, 3$ and

$$S_{i,0}(q, \underline{\omega}, v, \nu_1) = \Delta_{4-i} \left(\mathrm{L}_{g_2} \mathrm{L}_f^2 \alpha(q) \underline{\omega} + \mathbf{1} \mathrm{L}_f^3 \alpha(q) - \mathbf{1} \nu_1(k)\right)$$

where $\mathbf{1} = (1 \; 1 \; 1)^\top$, $\Delta = \mathrm{col}(\Delta_3 \;\; \Delta_2 \;\; \Delta_1)$, and

$$\Delta_j = \frac{1}{j!} \left(j^{4-j} - (j-1)^{4-j}, \; (j-1)^{4-j} - (j-2)^{4-j}, \; 1\right)$$

with $j = 1, 2, 3$. Following Monaco and Normand-Cyrot (1997) , it results that the matrix

$$\frac{\partial}{\partial \underline{\omega}} S^{\bar\delta}(q, v, \underline{\omega})|_{\bar\delta \to 0} \to \Delta L_{g_2} L_f^2 \alpha(q)$$

is full rank because $L_{g_2} L_f^2 \alpha(q) \neq 0$ and Δ is invertible. Hence, by the Implicit Function Theorem, the existence of $\underline{\omega}^{\bar\delta}$ unique solution to (13) of the form (14) can be deduced (Mattioni et al., 2017, Proposition 4.1). Under the coordinates transformation $(\xi \;\; \bar z)^\top := q \mapsto \phi(q) = (H(q) \;\; \pi(q))^\top$, the controlled dynamics reads

$$\begin{aligned} \xi(k+1) &= A^{3\bar\delta} \xi(k) + B^{3\bar\delta} \nu_1(k) \\ \bar z(k+1) &= \psi(\xi(k), \bar z(k), v(k), \nu_1(k)) \end{aligned}$$

where $\psi(\xi, \bar z, v, \nu_1) = \arctan \frac{q_2(k+1)}{q_1(k+1)}|_{(\xi \;\; \bar z)^\top = \phi^{-1}(q)}$ bounded on the curve by definition and hence the result follows. ◁

From the statement above, denoting $\dot\pi_{ref}(k) = \dot\pi_{ref}(k\delta)$ and $\ddot\pi_{ref}(k) = \ddot\pi_{ref}(k\delta)$, requirement (3) at all $t = k\delta$ is fulfilled by the discrete-time feedback

$$v(k+1) = v(k) + \delta a(k) + \frac{\delta^2}{2} \nu_2(k) \tag{18a}$$

$$a(k+1) = a(k) + \delta \nu_2(k) \tag{18b}$$

over the tangential component with $v(k), a(k)$ are the linear velocity and acceleration over the path respectively and

$$\begin{aligned} \nu_2(k) =& \left(\frac{1}{\delta^2}(a_0^\delta - a_1^\delta - 1) \;\; \frac{1}{2\delta}(a_0^\delta + a_1^\delta - 3)\right) e(k) \\ & + \ddot\pi_{ref}(k+1) - \ddot\pi_{ref}(k) \end{aligned} \tag{19}$$

so to guarantee, asymptotically,

$$e(k) = \begin{pmatrix} v(k) - \dot\pi_{ref}(k) \\ a(k) - \ddot\pi_{ref}(k) \end{pmatrix} \to 0$$

for a_0^δ, a_1^δ given by

$$\begin{aligned} a_0^\delta &= e^{-\lambda_1 \delta} e^{-\lambda_2 \delta} \\ a_1^\delta &= -(e^{-\lambda_1 \delta} + e^{-\lambda_2 \delta}), \quad \lambda_1, \lambda_2 > 0. \end{aligned}$$

Those arguments, together with Proposition 3.1, constitute the proof of the result below.

Theorem 3.1. Consider the kinematic model of the car-like robot (1), and a regular parameterized curve $\varrho : \mathbb{D} \mapsto \mathbb{R}^2$ under the hypotheses of Theorem 2.1. Then, Problem 2.2 admits a solution under multi-rate control that is given by the feedback (v, ω) with: (i) $\omega = \underline{\omega}^{\bar\delta}(q, v, \nu_1)$ defined as in Proposition 3.1 with transverse control (15); (ii) v generated by the discrete dynamics (18) with tangential control (19).

Remark 3.1. It is important to stress the fact that, in the digital context, TFL is achieved working directly on the kinematic model of the car-like robot with no preliminary dynamic extension, contrarily to the continuous-time case.

The above discussion ascertains the intuitive expectation that whenever the path following problem is solvable in continuous time using TFL, a digital multi-rate feedback solution under sampling exists. As noted, the feedback component $\omega = \underline{\omega}^{\bar{\delta}}(q, v, \nu_1)$ soltion to (13) comes in the form of a series expansion in powers of $\bar{\delta}$. All terms of such an expansion (14) are computable through an iterative and constructive procedure solving, at each step, a linear equality in the corresponding unknown. For the first terms, one gets

$$\underline{\omega}_0(q, v, \nu_1) = \mathbf{1}\omega(q, v, \nu_1),\ \omega(q, v, \nu_1) = \frac{L_f^3\alpha(q) - \nu_1}{L_{g_2}L_f^2\alpha(q)} \tag{20a}$$

$$\underline{\omega}_1(q, v, \nu_1) = \begin{pmatrix} \frac{15}{4} & -\frac{15}{2} & \frac{87}{4} \end{pmatrix}^\top \dot{\omega}(q, v, \nu_1) \tag{20b}$$

when denoting $f(q) = g_1(q)v$ and $\dot{\omega}(q, v, \nu_1) = (vL_{g_1} + \omega(q, v, \nu_1)L_{g_2})\omega(q, v, \nu_1)$.

Remark 3.2. From the expression below, it is clear that the digital feedback $\omega = \underline{\omega}^{\bar{\delta}}(q, v, \nu_1)$ solution to (13) is an expansion around the continuous-time (static) TFL solution when no velocity and acceleration requirements on the path are enforced (i.e., when only (1) and (2) in Problem 2.1 are given).

Because a closed-form of (14) cannot be computed, only approximations can be implemented in practice as the truncation of the series at a finite order $\rho > 0$, i.e.,

$$\underline{\omega}^{\bar{\delta},[\rho]}(q, v, \nu_1) = \underline{\omega}_0(q, v, \nu_1) + \sum_{i=1}^{\rho} \frac{\bar{\delta}^i}{(i+1)!}\underline{\omega}_i(q, v, \nu_1). \tag{21}$$

Such approximate controllers (21) with (18)-(19) solve Problem 2.2 in a practical sense with trajectories of the closed-loop system converging to a neighbourhood of target set $\Gamma^\star$ in $O(\delta^{p+1})$, Mattioni et al. (2017).

4. SIMULATIONS

Consider the case where the car-like robot is required to follow a circle of radius $r = 2$. In this case; $\varrho : \mathbb{D} \mapsto \mathbb{R}^2,\ \lambda \mapsto (r\cos q_3\ \ r\sin q_3)^\top$, satisfies the hypotheses of Theorem 2.1. Consequently, one has $\alpha(q) = q_1^2 + q_2^2 - r^2$. Suppose we are given a constant reference on the linear velocity $\dot{\pi}_{ref}(q) = 2$ with zero acceleration (i.e., $\ddot{\pi}_{ref}(q) = 0$). To follow the path, let $v(k)$ be as in (18)-(19), with $\lambda_i = 5, i = 1, 2$, and the first order approximate feedback be as in (21) with $\rho = 1$. In addition, for the transverse dynamics, let $\nu_1(k)$ be as in (15) with $K^{\bar{\delta}}$ placing the poles of $(A^{3\bar{\delta}} + B^{3\bar{\delta}}K^{\delta})$ in $(e^{-0.317\delta},\ e^{(-1.34+1.16i)\delta),}\ e^{(-1.34-1.16i)\delta)})$ for $\delta = 3\bar{\delta}$.

Simulation compare, for different initial conditions and increasing values of δ, the proposed multi-rate controller (21) with $\rho = 1$ (MR Sampling) with both the emulation-based (ZOH emulation) and the one proposed in Elobaid et al. (2020) (Approx Sampling), based on the continuous-time preliminary dynamic extension. For completeness, the results under continuous-time control are reported as well.

In Figures 2 and 3, the initial condition is fixed as $q_0 = (1\ 1\ \pi\ 0)^\top$ with increasing values of δ. The former one highlights that, albeit all controllers ensure convergence to the circle, the results under multi-rate control are slightly better compared to the other controllers. The latter one shows that as δ increases one notices deteriorated performances by both the approximate feedback in Elobaid et al. (2020) as well as emulation based control with higher peak values for the control effort. In all cases, the multi-rate control ensures satisfactory performances with improved control effort even with respect to the continuous time control law. In Figure 4, the initial condition is fixed as $q_0 = (3\ 2\ \pi\ 0)$ and $\delta = 0.3235s$. Whereas similar comments hold true in this case for the emulation and the approximate single-rate controllers (which strongly rely on the continuous-time design), for such initialization (outside the circle) both the aforementioned controllers are significantly sensible to variations of δ, with no guarantee for convergence to the path under emulation. In this case, the multi-rate solution provides still notable performances with a desired velocity profile and limited control effort.

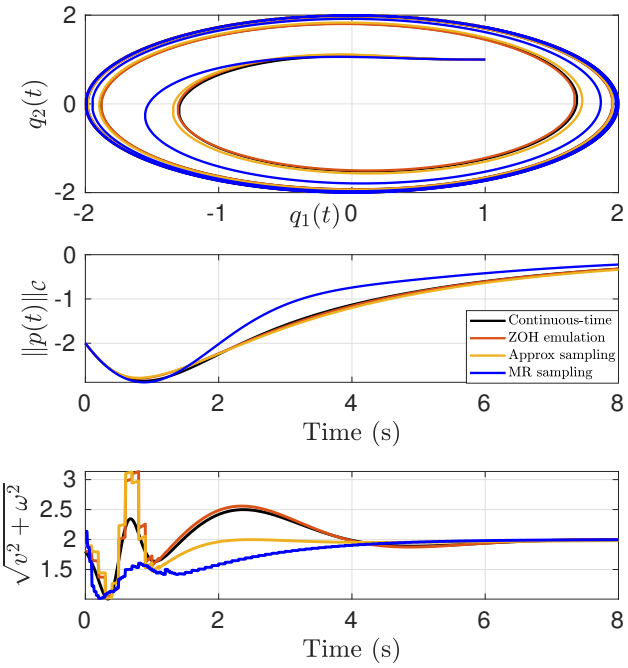

Fig. 2. From top to bottom: position on the plane, path-following error, control effort for $\delta = 0.1s$

5. CONCLUSIONS

Existence of a multi-rate digital feedback solution to the path following problem for a car-like robot via transverse feedback linearization was studied assuming a continuous time solution to the problem exists. In addition, this multi-rate solution was shown, through simulations, to provide better performances, both in terms of path-following position error and the required magnitude of input velocities to the robot. Perspectives concern the extension to the case of general nonlinear systems being transverse feedback linearizable in continuous time and the consequent application to further case studies.

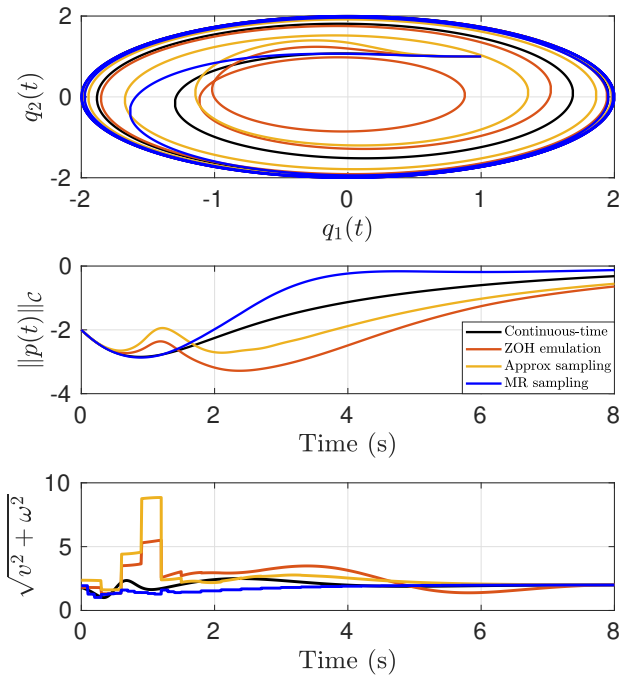

Fig. 3. From top to bottom: position on the plane, path-following error, control effort for $\delta = 0.3s$

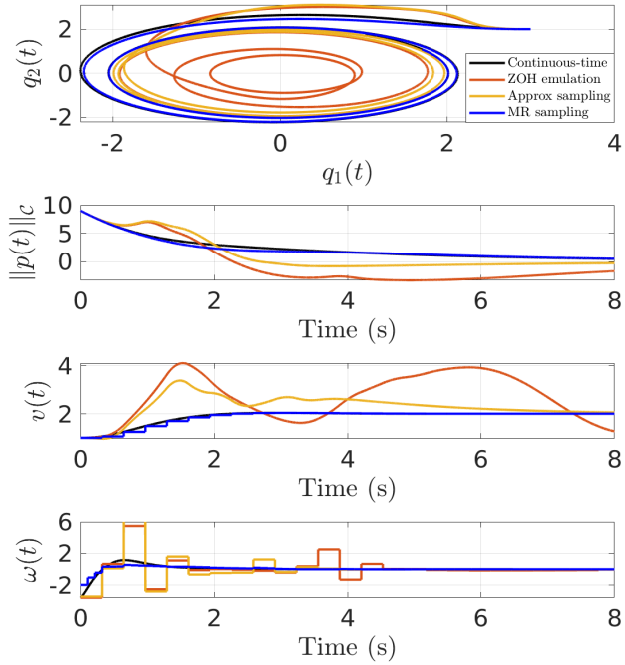

Fig. 4. From top to bottom: position on the plane, path-following error, linear velocity tracking, control effort for $\delta = 0.3235s$

REFERENCES

Aguiar, A.P., Hespanha, J.P., and Kokotović, P.V. (2008). Performance limitations in reference tracking and path following for nonlinear systems. *Automatica*, 44, 598–610.

Akhtar, A., Nielsen, C., and Waslander, S.L. (2015). Path following using dynamic transverse feedback linearization for car-like robots. *IEEE Transactions on Robotics*, 31, 269–279.

Altafini, C. (2002). Following a path of varying curvature as an output regulation problem. *IEEE Transactions on Automatic Control*, 47, 1551–1556.

Aström, K.J., Hagander, P., and Sternby, J. (1984). Zeros of sampled systems. *Automatica*, 20, 31–38.

Banaszuk, A. and Hauser, J. (1995). Feedback linearization of transverse dynamics for periodic orbits. *Systems & Control Letters*, 26, 95–105.

Dagci, O.H., Ogras, U.Y., and Ozguner, U. (2003). Path following controller design using sliding mode control theory. *American Control Conference*, 1, 903–908.

De Luca, A., Oriolo, G., and Vendittelli, M. (2001). Control of wheeled mobile robots: An experimental overview. *Ramsete*, 181–226.

Di Giamberardino, P., Grassini, F., Monaco, S., and Normand-Cyrot, D. (1996). Piecewise continuous control for a car-like robot: implementation and experimental results. *35th IEEE Conference on Decision and Control*, 3, 3564–3569.

Elobaid, M., Monaco, S., and Normand-Cyrot, D. (2020). Approximate transverse feedback linearization under digital control. *IEEE Control Systems Letters*.

Mattioni, M., Monaco, S., and Normand-Cyrot, D. (2017). Immersion and invariance stabilization of strict-feedback dynamics under sampling. *Automatica*, 76, 78–86.

Monaco, S. and Normand-Cyrot, D. (1992). An introduction to motion planning under multirate digital control. *31st IEEE Conference on Decision and Control*, 2, 1780–1785.

Monaco, S., Normand-Cyrot, D., and Stornelli, S. (1986). On the linearizing feedback in nonlinear sampled data control schemes. *25th IEEE Conference on Decision and Control*, 2056–2060.

Monaco, S. and Normand-Cyrot, D. (1997). On nonlinear digital control. In *Nonlinear control*, 127–155. Springer.

Monaco, S. and Normand-Cyrot, D. (1987). Minimum-phase nonlinear discrete-time systems and feedback stabilization. *26th IEEE Conference on Decision and Control*, 26, 979–986.

Nielsen, C. and Maggiore, M. (2004). Maneuver regulation via transverse feedback linearization: Theory and examples. *IFAC symposium on Nonlinear Control systems (NOLCOS)*, 37, 57–64.

Nielsen, C. and Maggiore, M. (2006). Output stabilization and maneuver regulation: A geometric approach. *Systems & Control Letters*, 55, 418–427.

Nielsen, C. and Maggiore, M. (2008). On local transverse feedback linearization. *SIAM Journal on Control and Optimization*, 47, 2227–2250.

Siciliano, B., Sciavicco, L., Villani, L., and Oriolo, G. (2010). *Robotics: modelling, planning and control*. Springer Science & Business Media.

Yi, B., Ortega, R., Manchester, I.R., and Siguerdidjane, H. (2020). Path following of a class of underactuated mechanical systems via immersion and invariance-based orbital stabilization. *International Journal of Robust and Nonlinear Control*, 30, 8521–8544.

Virtual Holonomic Constraints for Euler-Lagrange systems under sampling

Mohamed Elobaid[1,2], Mattia Mattioni[1], Salvatore Monaco[1] and Dorothée Normand-Cyrot[2]

***Abstract*— In this paper, we consider the problem of imposing Virtual Holonomic Constraints to mechanical systems in Euler-Lagrangian form under sampling. An exact solution based on multi-rate sampling of order two over each input channel is described. The results are applied to orbital stabilization of the pendubot with illustrative simulations.**

***Index Terms*— Sampled data control, Feedback linearization, Algebraic/geometric methods.**

I. Introduction

Most control problem rely upon the design of feedback laws asymptotically zeroing a given function of the state as, for instance, orbital or set-point stabilization, motion planning, tracking, path following, to cite a few [1]–[5]. When dealing with mechanical systems, such a function writes $h(q) = 0$, with generalized coordinates q, and is generally referred to as *Virtual Holonomic Constraints* (VHCs, [6]–[9]). Stabilization of VHCs unavoidably requires to asymptotically drive the trajectories of the system onto a sub-manifold associated to the zero-level set of the function. Accordingly, the problem can be recast into a zero-dynamics perspective: setting the function as a dummy output for the dynamics, one must define a feedback making the corresponding zero-dynamics (and the zero-dynamics submanifold) invariant and attractive. With this in mind, it has been proved in [8] that the VHC is stabilizable if and only if the system possesses a well-defined vector relative degree $r = (2, \dots, 2)$ with respect to the associated dummy output function. Accordingly, under suitable hypothesis, the feedback imposing the VHC is the one rendering the corresponding zero-dynamics attractive and invariant (e.g., input-output feedback linearization) while preserving boundedness of the whole system trajectories.

All of this essentially concerns continuous-time systems despite the practical interest to treat mechanical systems under sampling when the control is piecewise constant and the state or output measures are sampled [10]. In this context, it is well known that the relative degree falls to one under single-rate sampling with the rising of an unstable *sampling zero dynamics* making the corresponding sampled-data system non-minimum phase in general [11], [12]. Accordingly, when dealing with stabilization of VHCs, single-rate sampling and, in particular, mere emulation control cannot be employed as the necessary relative degree condition is lost. This motivates the present paper whose contribution stands in providing control strategies ensuring the preservation of VHCs for mechanical systems under sampling. Based on the work in [13], it is shown that VHCs can be imposed under sampling according to a multi-rate device of suitably defined order. The proof is constructive and the feedback is shown to be the solution to a nonlinear implicit equality parameterized by δ, the sampling period, naturally recovering the continuous-time counterpart as $\delta \to 0$. Despite exact forms are hard to be computed in practice, approximate feedback laws computed as approximate solutions to the associated equalities are naturally defined and implemented in practice with notably improved performances with respect to standard emulation controllers [14], [15]. The results are applied to orbital stabilization of the pendubot [8], [16] and based on the VHC associated to the preliminary continuous-time I&I design recently proposed in [17].

The rest of the paper is organized as follows. In Section II, the problem is formally formulated with preliminaries on VHCs for continuous-time mechanical systems and sampled-data dynamics. The main result in Section III with the simulated example of the pendubot in Section IV. Section V concludes the paper with some perspectives.

Notations. $\mathbb{R}$ and $\mathbb{N}$ denote the set of real and natural numbers including 0. For any vector $z \in \mathbb{R}^n$, $\|z\|$ and $z^\top$ define respectively the norm and transpose of z. Given a full rank matrix $B \in \mathbb{R}^{n\times m}$ with $n > m$, $B^\dagger = (B^\top B)^{-1}B^\top$ denotes the pseudoinverse, while $B^\perp$ its orthogonal complement verifying $B^\perp B = 0$. Also, $\ker\{B\}$ denotes the null space of B. Given two matrices of any dimension, $A \otimes B$ denotes the Kronecker product. $\mathbf{1}_n \in \mathbb{R}^n$ is the vector with all unitary entries while 0 denotes the zero matrix of suitable dimensions. $\text{diag}\{a_1, \dots, a_n\} \in \mathbb{R}^{n\times n}$ denotes the diagonal matrix with $a_i \in \mathbb{R}$ the coefficients on the main diagonal for $i = 1, \dots, n$. $x = \text{col}\{a_1, \dots, a_n\} \in \mathbb{R}^{n_1+\dots+n_n}$ denotes the column vector with entries provided by $a_i \in \mathbb{R}^{n_i}$ of suitable dimensions. If $(\mathcal{X}, d)$ is a metric space, $\Gamma \subset \mathcal{X}$ and $x \in \mathcal{X}$, then $\|x\|_\Gamma = \inf_{y\in\Gamma} d(x, y)$ defines the point-to-set distance of x to Γ. I and I_d denote the identity matrix and Identity operator (or function, depending on the context) of suitable dimensions, respectively. Given a twice continuously differentiable function $S(\cdot) : \mathbb{R}^n \to \mathbb{R}$, $\nabla S(\cdot)$ represents its gradient (column) vector while $\nabla^2 S(\cdot)$ is its Hessian matrix. Given a n-dimensional vector field $f(x)$ with $x \in \mathbb{R}^n$,

Supported by *Sapienza Università di Roma* (*Progetti di Ateneo 2018*-Piccoli progetti *RP11816436325B63*).

[1]Dipartimento di Ingegneria Informatica, Automatica e Gestionale *A. Ruberti* (Sapienza University of Rome); Via Ariosto 25, 00185 Rome, Italy { mohamed.elobaid, mattia.mattioni, salvatore.monaco}@uniroma1.it.

[2]Laboratoire de Signaux et Systèmes (L2S, CNRS Université Paris-Saclay); Centrale Supelec 3, Rue Joliot Curie, 91192, Gif-sur-Yvette, France dorothee.normand-cyrot @centralesupelec.fr

$\mathrm{L}_f = \sum_{i=1}^{n} \frac{\partial}{\partial x_i}$ denotes the Lie derivative operator, and recursively, $L_f^i = \mathrm{L}_f \circ \mathrm{L}_f^{i-1}$ with $\mathrm{L}_f^0 = I_d$. For $\delta > 0$, $e^{\delta \mathrm{L}_f} = I_d + \sum_{i>0} \frac{\delta^i}{i!} \mathrm{L}_f^i$ denotes the Lie exponential. Given a smooth function $H : \mathbb{R}^n \to \mathbb{R}$ by the Exchange Theorem $H(e^{\delta \mathrm{L}_f} x) = e^{\delta \mathrm{L}_f} H(x) = H(x) + \sum_{i>0} \frac{\delta^i}{i!} \mathrm{L}_f^i H(x)$. A function $R(x, \delta) = O(\delta^p)$ is said of order δ^p, $p \geq 1$ if whenever it is defined it can be written as $R(x, \delta) = \delta^{p-1} \tilde{R}(x, \delta)$ and there exist a function $\theta \in \mathcal{K}_\infty$ and $\delta^* > 0$ s. t. $\forall \delta \leq \delta^*$, $|\tilde{R}(x, \delta)| \leq \theta(\delta)$.

II. Preliminaries and problem statement

In the sequel, we consider Euler-Lagrange systems of the form

$$D(q)\ddot{q} + C(q, \dot{q})\dot{q} + \nabla P(q) = B(q)u \tag{1}$$

with n-dimensional generalized coordinates $q \in \mathcal{Q}$, $\mathcal{Q} \subset R^n$ the configuration space, input torque $u \in \mathbb{R}^m$ with $m = n - 1$, $D(q) = D^\top(q) \succ 0$ the generalized inertia matrix, $C(q, \dot{q})\dot{q}$ representing the Coriolis and centrifugal forces, $P(q)$ the potential energy function, $B(q)$ of rank $m = n - 1$ and

$$L(q, \dot{q}) = \frac{1}{2} \dot{q}^\top D(q) \dot{q} + P(q)$$

being the Lagrangian verifying

$$\dot{L}(q, \dot{q}) = \dot{q}^\top B^\top(q) u.$$

A. VHCs for EL systems in continuous time

As formalized in [8], a virtual holonomic constraint (VHC) for a mechanical system (1) is a relation of the form $h(q) = 0$ which can be made invariant under feedback. In this sense, the following formal definition is recalled.

Definition 2.1: A virtual holonomic constraint is a relation $h(q) = 0$ where $h : \mathcal{Q} \to \mathbb{R}^m$ is smooth, $\mathrm{rank}(\mathrm{d}h) = m$ for all $q \in h^{-1}(0)$ and the constraint manifold

$$\Gamma = \{(q, \dot{q}) : h(q) = 0,\ \mathrm{d}h(q)\dot{q} = 0\} \tag{2}$$

is controlled invariant. A VHC is stabilizable if there exists a smooth feedback $u(q, \dot{q})$ that asymptotically stabilizes[1] Γ.

In the following, it is assumed that $m = n - 1$ so that the configuration variable can be regrouped, with a slight abuse of notation, as $q = \mathrm{col}\{q_a, q_u\} \in \mathbb{R}^{n-1} \times \mathbb{R}$ so that the VHC can be described in parametric form as

$$q_a = \varphi(q_u), \quad h(q) = q_a - \varphi(q_u)$$

with hence $h^{-1}(0)$ a closed curve. The definition of regular VHC is recalled below as fundamental to characterize asymptotically stabilizable VHS [8][2]

Definition 2.2 ([8]): Consider a smooth relation $h : \mathcal{Q} \to \mathbb{R}^m$ and $\mathrm{rank}(\mathrm{d}h) = m$ for all $q \in h^{-1}(0)$. The relation $h(q) = 0$ is said to be a *regular* VHC of order $m > 0$ for the system (1) if it possesses relative degree $\{2, \ldots, 2\}$ everywhere on the constrained manifold (2); i.e., the matrix

$$U(q) = \mathrm{d}h(q) D^{-1}(q) B(q) \tag{3}$$

has full rank for all $q \in h^{-1}(0)$.

By Definition 2.1, the constraint manifold (2) is the zero-dynamics manifold corresponding to the output $e = h(q)$ so that the reduced dynamics coincides with the zero-dynamics. As a consequence, Γ is asymptotically stabilized via feedback linearization under mild hypotheses on the maps $h(q), \mathrm{d}h(q)\dot{q}$ as recalled in the result below.

Proposition 2.1: Let $h(q) = 0$ be a regular VHC of order $n - 1$ for (1) with constraint manifold Γ in (2). Let

$$H(q, \dot{q}) = \begin{pmatrix} h(q) \\ \mathrm{d}h(q)\dot{q} \end{pmatrix} \tag{4}$$

and assume there exist functions $\alpha_1, \alpha_2 \in \mathcal{K}$ such that

$$\alpha_1(\|(q, \dot{q})\|_\Gamma) \leq \|H(q, \dot{q})\| \leq \alpha_2(\|(q, \dot{q})\|_\Gamma).$$

Then, the input-output linearizing controller

$$\begin{aligned} u(q, \dot{q}) = & U^{-1}(q) \Big(\mathrm{d}h(q) D^{-1}(q) \big(C(q, \dot{q})\dot{q} + \nabla P(q) \big) \\ & - \mathcal{H}(q, \dot{q}) - \kappa_p e - \kappa_d \dot{e} \Big) \end{aligned} \tag{5}$$

with decoupling matrix $U(q)$ as in (3), $h(q) = \mathrm{col}\{h_1(q), \ldots, h_{n-1}(q)\}$, $\mathcal{H}(q, \dot{q}) = \mathrm{col}\{\dot{q}^\top \nabla^2 h_1(q)\dot{q}, \ldots, \dot{q}^\top \nabla^2 h_{n-1}(q)\dot{q}\}$, makes Γ in (2) asymptotically stable for all $\kappa_p, \kappa_d \in \mathbb{R}^{(n-1)\times(n-1)}$ rendering the matrix below Hurwitz

$$A(\kappa_p, \kappa_d) = \begin{pmatrix} 0 & I_{n-1} \\ -\kappa_p & -\kappa_d \end{pmatrix}. \tag{6}$$

B. Problem statement and motivations

From the result recalled in the previous section, imposing VHC generally corresponds to making Γ the zero-dynamics manifold of the dynamics, with a stable zero dynamics. Accordingly, a VHS can be imposed under a continuous-time control if it is regular in the sense of Definition 2.2. However, what does it occur if the control is of sampled-data type, that is a piecewise constant signal based on sampled measures of the configuration variables $q, \dot{q}$? More in detail, denoting by $\delta > 0$ the sampling period, we address the following problem.

VHCs under digital control. Consider the mechanical dynamics (1) and a regular VHC $h(q) = 0$ in the sense of Definition 2.2 with constraint manifold Γ in (2). Let $\delta > 0$ be the sampling period and $q_k := q(k\delta)$, $\dot{q}_k = \dot{q}(k\delta)$ for all $k \geq 0$. Design, if any, a piecewise constant control $u_k = u^\delta(q_k, \dot{q}_k)$, enforcing the VHC $h(q) = 0$, while asymptotically stabilizing the constraint manifold Γ. □

More in detail, setting $u(t) = u_k$ for $t \in [k\delta, (k+1)\delta)$, $x = \mathrm{col}\{q, \dot{q}\}$ and $x_k = x(k\delta)$ for all $k \geq 0$, (1) is described by the so-called sampled-data equivalent model [18]

$$x_{k+1} = F^\delta(x_k, u_k) \tag{7}$$

[1] In the sense of [9, Definition 3]

[2] Necessary and sufficient conditions for the relation $h(q) = 0$ to be a regular VHC are given in [8].

with

$$F^\delta(x,u) = e^{\delta \mathrm{L}_{f(x)+G(x)u}} x = x + \sum_{i>0} \frac{\delta^i}{i!} \mathrm{L}^i_{f(x)+G(x)u} x$$

$$f(x) = \begin{pmatrix} \dot{q} \\ -D^{-1}(q)\big(C(q,\dot{q})\dot{q} + \nabla P(q)\big) \end{pmatrix}$$

$$G(x) = \begin{pmatrix} 0 \\ D^{-1}(q)B(q) \end{pmatrix}.$$

It is convenient to rewrite (7) in block-component-wise as

$$\begin{aligned} q_{k+1} =& F^\delta_q(q_k, \dot{q}_k, u_k) \\ \dot{q}_{k+1} =& F^\delta_{\dot{q}}(q_k, \dot{q}_k, u_k) \end{aligned}$$

with, by definition

$$F^\delta_q(q,\dot{q},u) = q + \int_0^\delta F^s_{\dot{q}}(q,\dot{q},u)\mathrm{d}s.$$

Accordingly, the definition of relative degree for discrete-time systems is recalled here below from [19].

Definition 2.3 (Discrete-time vector relative degree): A discrete-time system

$$\begin{aligned} x_{k+1} =& F(x_k, u_k) \\ y^1_k =& h_1(x_k), \ldots, y^m_k = h_m(x_k) \end{aligned}$$

with $x \in \mathbb{R}^n$, $u \in \mathbb{R}^m$, $y^i \in \mathbb{R}$ for $i = 1, \ldots, m$, is said to possess vector relative degree $r = (r_1, \ldots, r_m) \in \mathbb{R}^m$ at $x^\circ \in \mathbb{R}^n$ if the following holds:

- for all $i = 1, \ldots, m$, $\ell = 1, \ldots, r_i - 1$

  $$\frac{\partial}{\partial u} h_i(F_0^{\ell-1}(F(x,u)) = 0, \quad \frac{\partial}{\partial u} h_i(F_0^{r_i-1}(F(x,u)) \neq 0;$$

- the decoupling matrix

  $$U_d(x,u) = \begin{pmatrix} \frac{\partial}{\partial u} h_1(F_0^{r_1-1}(F(x,u))) \\ \vdots \\ \frac{\partial}{\partial u} h_m(F_0^{r_m-1}(F(x,u))) \end{pmatrix}$$

  is non-singular at $x = x^\circ$, $u = 0$.

It is well-known that under sampling the relative degree is not preserved [12]. As a matter of fact, let us consider the output map $e = h(q)$ with $h(q) = 0$ a regular VHC in the sense of Definition 2.2. By Definition 2.3, one computes for the sampled-data model (7) the discrete-time decoupling matrix

$$\frac{1}{\delta^2} U_d(x,u) = \mathrm{d}h(q) D^{-1}(q) B(q) + O(\delta)$$

that is non-singular in Γ by non-singularity of the continuous-time one in (3). Thus, $h(q)$ is no longer a regular VHC for (7) as it possesses a discrete vector relative degree $(1, \ldots, 1) \in \mathbb{R}^{n-1}$ with respect to the output $e = h(q)$ with a zero-dynamics sub-manifold $\mathcal{Z}^\delta$ of dimension n and corresponding to a generally unstable reduced dynamics (due to the rise of the so-called sampled-data zero dynamics [12]). In addition, $h(q) = 0$ is not a VHC for (7) in the weaker sense of Definition 2.1 as control invariance of Γ is lost under sampling and thus its stabilizability via piecewise constant control. As a particular case, it is naturally deduced that standard emulation of the continuous-time feedback (5) via sampling and hold devices (i.e., setting $u_k = u(q_k, \dot{q}_k)$) fails into imposing $h(q) = 0$.

Remark 2.1: The characterization of the properties and structure of the reduced dynamics (i.e., the scalar dynamics governing (1) over Γ) under sampling is not addressed here. As a matter of fact, such a characterization relies upon sampled-data Lagrangian structures as particular classes of discrete-time Hamiltonian structures as proposed in [20].

III. Main result

The proposed solution, relying upon the results in [13], ensures that regularity of the VHC is preserved under multi-rate sampling of order $(2, \ldots, 2) \in \mathbb{R}^{n-1}$ (i.e., of the same order 2 over each input channel). Namely, we assume the control piecewise constant over the sub-interval of the sampling period of length $\bar{\delta} = \frac{\delta}{2}$; namely, $u^i_k = u(k\delta + (i-1)\bar{\delta}) \in \mathbb{R}^{n-1}$ for $i = 1, 2$ with the multi-rate equivalent model of (1)

$$x_{k+1} = F^{\bar{\delta}}_2(x_k, \underline{u}_k) \tag{8}$$

with $\underline{u} = \mathrm{col}\{u^1, u^2\} \in \mathbb{R}^{2(n-1)}$ and

$$\begin{aligned} F^{\bar{\delta}}_2(x,\underline{u}) =& F^\delta(\cdot, u^2) \circ F^{\bar{\delta}}(x, u^1) \\ =& e^{\delta \mathrm{L}_{f+Gu^1}} \circ e^{\delta \mathrm{L}_{f+Gu^2}} x. \end{aligned}$$

At this point, the following main result can be proved.

Theorem 3.1: Let $h(q) = 0$ be a regular VHC of order $n-1$ for (1) under the hypotheses of Proposition 2.1 and constraint manifold Γ in (2). Then, $h(q) = 0$ is a stabilizable regular VHC of order $n-1$ under multi-rate digital control of order 2; equivalently, it is a regular VHC of order $n-1$ for the sampled-data equivalent model (8).

Proof: For showing the result, one must show that the extended output (4) possesses vector relative degree $(1, 1, \ldots, 1, 1) \in \mathbb{R}^{2(n-1)}$ everywhere on the constraint manifold Γ in (2). By Definition 2.3, one gets that the discrete-time decoupling matrix associated to (8) with the extended output (4) is given by

$$U^\delta_d(q,u) = \Delta \otimes \mathrm{d}h(q) D^{-1}(q) B(q) + O(\delta)$$

with

$$\Delta = \begin{pmatrix} \frac{3}{2} & \frac{1}{2} \\ 1 & 1 \end{pmatrix}.$$

The matrix above is invertible everywhere on Γ because $U(q)$ in (3) is such by assumption and Δ is non singular. ■

In the next result, the sampled-data control law enforcing the VHC $h(q) = 0$ is proved to exist in a constructive way starting from the continuous-time solution.

Proposition 3.1: Let $h(q) = 0$ be a regular VHC of order $n-1$ for (1) under the hypotheses of Proposition 2.1 and constraint manifold Γ in (2). Let (8) be the sampled-data equivalent model of order 2 with extended output $H(x) = H(q, \dot{q})$ in (4). Then, the following holds true.

(i) The implicit equality

$$H(F_2^{\bar\delta}(x,\underline{u})) = A^\delta(\kappa_p,\kappa_d)H(x) \tag{9}$$

with, for $A(\kappa_p,\kappa_d)$ as in (6),

$$A^\delta(\kappa_p,\kappa_d) = e^{\delta A(\kappa_p,\kappa_d)} \tag{10}$$

admits a unique solution $\underline{u} = \underline{u}^{\bar\delta}(x)$ in the form of a series expansion in powers of δ around the continuous-time one in (5); namely, one gets

$$\underline{u}^{\bar\delta}(x) = \mathbf{1}_2 \otimes u(x) + \sum_{\ell>0} \frac{\bar\delta^\ell}{(\ell+1)!}\underline{u}_\ell(x). \tag{11}$$

(ii) The feedback $\underline{u} = \underline{u}^{\bar\delta}(x)$ solution to (9) enforces the VHC $h(q) = 0$ that is, it makes Γ in (2) asymptotically stable.

Proof: The feedback solution to (9) is the one ensuring input-output linearization with respect to the extended mapping $H(x)$. Accordingly, the proof of (i) follows from Theorem 3.1 and by the Implicit Function Theorem along the lines of [13]. As far as (ii) is concerned, by construction of the matrix (6), $A^\delta(\kappa_p,\kappa_d)$ in (10) is asymptotically stable (in the discrete-time sense[3]) and $H(x_k) \to 0$ as $k \to \infty$ ensuring that the trajectories asymptotically converge to Γ so getting the result. ■

Remark 3.1: The constraining feedback is given by the solution of the implicit equality (9) ensuring I/O linearization under sampling with, moreover, output matching of the continuous-time output trajectories under the feedback (5). We underline that such a choice is made to allow, as developed in the next section, comparison with respect to the nominal continuous-time behavior. More general assignments of the output linear dynamics are possible for the closed-loop sampled-data equivalent model. In general, one can compute the feedback so to assign a desired LTI discrete-time equivalent dynamics of the form

$$H(F_2^{\bar\delta}(x,\underline{u})) = (A^\delta + B^\delta F^\delta)H(x)$$

with

$$A_0 = \begin{pmatrix} 0 & 1 \\ 0 & 0 \end{pmatrix}, \quad B_0 = \begin{pmatrix} 0 \\ 1 \end{pmatrix}$$
$$A^\delta = e^{A_0\delta} \otimes I_{n-1}, \quad B_0^\delta = \int_0^\delta e^{A_0 s}\mathrm{d}s B_0$$
$$B^\delta = \begin{pmatrix} A^{\frac{\delta}{2}}B_0^{\frac{\delta}{2}} & B_0^{\frac{\delta}{2}} \end{pmatrix} \otimes I_{n-1}$$

and F^δ any feedback gain ensuring asymptotic stability of the closed loop.

Remark 3.2: The (invariant and attractive) zero-dynamics (i.e., the reduced dynamics over Γ) of the closed-loop sampled-data system under the feedback solution to (9) preserves the same stability and boundedness properties as the continuous-time counterpart, at least in first approximation [12]. Accordingly, nothing can be concluded on the possible preservation of the sampled-data Lagrangian structure.

[3] i.e., all the eigenvalues are in the open unit circle.

Although closed forms to (9) are hard to compute, all terms of the series expansion (5) can be deduced via an iterative and constructive procedure: first, one substitutes (11) into (9) and then equates all terms with the same power of δ; each term $\underline{u}_\ell(x)$ is the solution to a linear equality depending on x and the previous terms $\underline{u}_{\ell-1}(x),\dots,\underline{u}_0(x)$. For the first term, one gets

$$\underline{u}_1(x) = \frac{1}{3}\begin{pmatrix} 1 \\ 5 \end{pmatrix} \otimes \dot u(x), \quad \dot u(x) = \mathrm{L}_{f+Gu(x)}u(x).$$

Accordingly, only controllers computed as truncations of the series expansion (11) at all desired order $\beta \geq 0$ are implementable in practice; namely, the β^{th}-order approximate feedback law is defined by

$$\underline{u}^{\bar\delta}_{[\beta]}(x) = \mathbf{1}_2 \otimes u(x) + \sum_{\ell=1}^{\beta} \frac{\bar\delta^\ell}{(\ell+1)!}\underline{u}_\ell(x) \tag{12}$$

with $\bar\delta = \frac{\delta}{2}$ so recovering for $\beta = 0$ the usual emulation-based control [15]. The stabilizing properties under such feedback laws are guaranteed only in a practical sense with $h(q)$ converging to a ball containing the origin with radius in $O(\delta^{\beta+1})$ [18, Theorem 5.1].

IV. Digital orbital stabilization of the pendubot

Consider the dynamics of a pendulum robot (Pendubot) in Figure 1 in the form (1) with $n = 2$ and [8], [17], [21]

$$D(q) := \begin{pmatrix} d_{uu}(q_u) & d_{ua}(q_u) \\ d_{ua}(q_u) & d_{aa}(q_u) \end{pmatrix}, \quad C(q,\dot q)\dot q = \begin{pmatrix} c_u(q,\dot q) \\ c_a(q,\dot q) \end{pmatrix}\dot q$$
$$\nabla P(q) = \begin{pmatrix} \nabla P_a(q) \\ \nabla P_u(q) \end{pmatrix}$$

where

$$\begin{aligned}
d_{uu}(q_u) =& m_2\ell_{c2}^2 + I_2 \\
d_{ua}(q_u) =& m_2\ell_{c2}^2 + I_2 + m_2\ell_1\ell_{c2}\cos q_u \\
d_{au}(q_u) =& m_2\ell_{c2}^2 + I_2 + m_2\ell_1\ell_{c2}\cos q_u \\
d_{aa}(q_u) =& m_1\ell_{c1}^2 + m_2\ell_1^2 + I_1 + m_2\ell_{c2}^2 + I_2 \\
&+ 2m_2\ell_1\ell_{c2}\cos q_u \\
c_u(q,\dot q)\dot q =& (m_2\ell_1\ell_{c2}\sin q_u)\dot q_a \\
c_a(q,\dot q)\dot q =& (m_2\ell_1\ell_{c2}\sin q_u)\dot q_a - 2(m_2\ell_1\ell_{c2}\sin q_u)\dot q_u \\
\nabla P_a(q) =& m_2\ell_{c2}g_r\sin(q_a+q_u) \\
\nabla P_u(q) =& (m_1\ell_{c1} + m_2\ell_{c2})g_r\sin q_a \\
&+ m_2\ell_{c2}g_r\sin(q_a+q_u)
\end{aligned}$$

$m_i, I_i, \ell_i, \ell_{ci}, g_r$ being the mass, inertia, length and length to center of mass for link $i = 1,2$ and the gravity constant respectively.

Following [8], [17], the design goal stands in the generation of non-trivial stable oscillations of the underactuated link under a sampled-data feedback. This corresponds to stabilizing the regular VHC

$$h(q) = q_a + \kappa q_u \tag{13}$$

with $\kappa \in \mathbb{R}$ [17] and, equivalently, the set

$$\Gamma = \{(q,\dot q) : q_a - \kappa q_u = 0, \dot q_a - \kappa \dot q_u = 0\}. \tag{14}$$

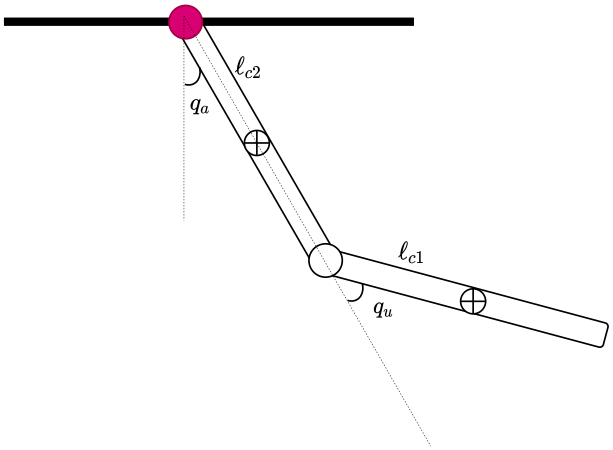

Fig. 1. The pendubot robot

Following Proposition 2.1, the stabilizing continuous-time control is provided by (5) which is specified as

$$\begin{aligned} u =& c_a(q,\dot{q})\dot{q} + \nabla P_a(q) + \gamma_1(q_u)(c_u(q,\dot{q})\dot{q} + \nabla P_u(q) \\ & - \gamma_2(q_u)\Big(\kappa_p h(q) + \kappa_d \dot{h}(q) - c_u(q,\dot{q})\dot{q} + \nabla P_u(q)\Big) \end{aligned}$$

with

$$\begin{aligned} \gamma_1(q_u) =& \frac{d_{au}(q_u)}{d_{uu}(q_u)} \\ \gamma_2(q_u) =& \frac{d_{aa}(q_u)}{(m_2\ell_{c2}^2 + I_2)(d_{aa}(q_u) - \kappa d_{au}(q_u))}. \end{aligned}$$

As far as the sampled-data solution is concerned, following Proposition 3.1 the problem is solved under multi-rate control of order $r = 2$ with $\underline{u}_k = (u_k^1 \;\; u_k^2)^\top$, $u_k^i = u(k\delta + (i-1)\bar{\delta}$, $\bar{\delta} = \frac{\delta}{2}$ and $i = 1, 2$ as in Section III. Applying Proposition 3.1, the feedback takes the form of the series expansion (11) with the first term specified by

$$\begin{aligned} \underline{u}_1(q,\dot{q}) &= \begin{pmatrix} \frac{1}{3} & \frac{5}{3} \end{pmatrix}^\top \dot{u}(q,\dot{q}) \\ \dot{u}(q,\dot{q}) &= \dot{c}_a(q,\dot{q})\dot{q} + c_a(q,\dot{q})\ddot{q} + \nabla^2 P_a(q)\dot{q} \\ &\quad + (\dot{\gamma}_1(q_u) + \dot{\gamma}_2(q_u))c_u(q,\dot{q})\dot{q} \\ &\quad + (\gamma_1(q_u) + \gamma_2(q_u))\dot{c}_u(q,\dot{q})\dot{q} \\ &\quad + (\gamma_1(q_u) + \gamma_2(q_u))c_u(q,\dot{q})\ddot{q} \\ &\quad + (\gamma_1(q_u) - \gamma_2(q_u))\nabla^2 P_u(q)\dot{q} \\ &\quad + (\dot{\gamma}_1(q_u) - \dot{\gamma}_2(q_u))\nabla P_u(q) \\ &\quad - (\gamma_1(q_u) - \gamma_2(q_u))\Big(\kappa_p \dot{h}(q) + \kappa_d \ddot{h}(q)\Big) \\ &\quad - (\dot{\gamma}_1(q_u) - \dot{\gamma}_2(q_u))\Big(\kappa_p h(q) + \kappa_d \dot{h}(q)\Big) \end{aligned}$$

We are now in position to compare the stabilization properties of the obtained sampled-data feedback, approximated at the first order, against that of emulation, i.e. when considering the 0^{th}order approximation in (12).

Simulations

To validate the approach proposed, simulations of the controlled pendubot are performed with the parameters reported in the table below.

m_1 $[kg]$	0.2	m_2 $[kg]$	0.052
I_1 $[kgm^2]$	3.38×10^{-1}	I_2 $[kgm^2]$	1.17×10^{-1}
ℓ_1 $[m]$	0.2	ℓ_2 $[m]$	0.28
ℓ_{c1} $[m]$	0.13	ℓ_{c2} $[m]$	0.15

In all cases, we fix the parameter $\kappa = -1$ in (13) so comparing similar situations to those reported in [17]. Additionally, the stabilizing continuous-time gains in (5) are fixed at $\kappa_p = 1$, $\kappa_d = \sqrt{3}$. In Figure 2 we show the performance of the (1^{st} order approximate) sampled-data multi-rate stabilizing controller for two different sets of initial conditions when compared to the ideal continuous-time solution. The dashed lines corresponds to the multi-rate solution while the continuous line is the ideal continuous-time solution. Both are compared staring from the configuration $q_0 = (\frac{\pi}{6} \;\; \frac{\pi}{1.5})^\top$ with zero velocities, as well as $q_0 = (\frac{\pi}{3} \;\; \frac{\pi}{1.5})^\top$ with zero velocities. The sampled-data control follows closely the ideal continuous-time behaviour even for larger sampling period $\delta = 0.3$.

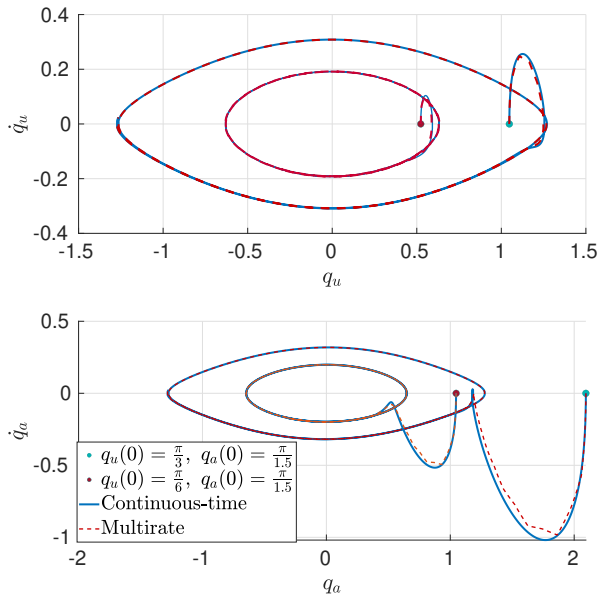

Fig. 2. Sampled-data stabilization for different initial conditions and $\delta = 0.5$ under multi-rate approximate control of order $\beta = 1$.

Figures 3 and 4 highlight the significant benefits obtained from the additive terms introduced by the proposed approximate sampled-data control when compared to standard emulation for increasing values of δ. Also, it is worth to underline that the control effort required by the multi-rate approximate control is comparable with respect to the continuous-time one and much better than emulation. Further simulations have been perormed also considering different control objectives as, for instance, swing-up stabilization[4].

[4]More animated cases at `https://youtu.be/YqGJnm1oNo0`

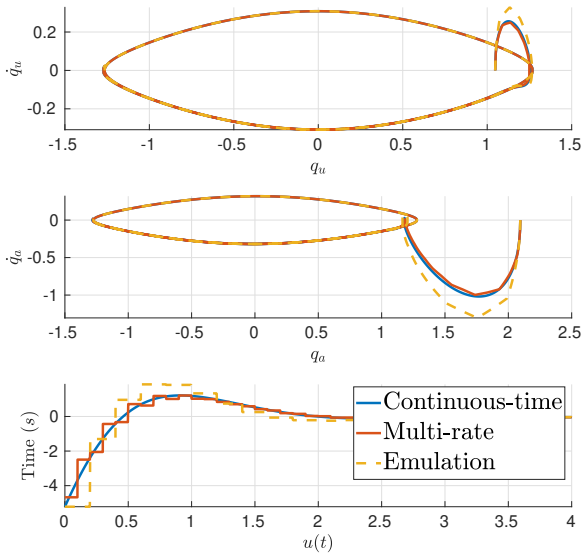

Fig. 3. Simulations for the pendubot when $\delta = 0.2$ seconds

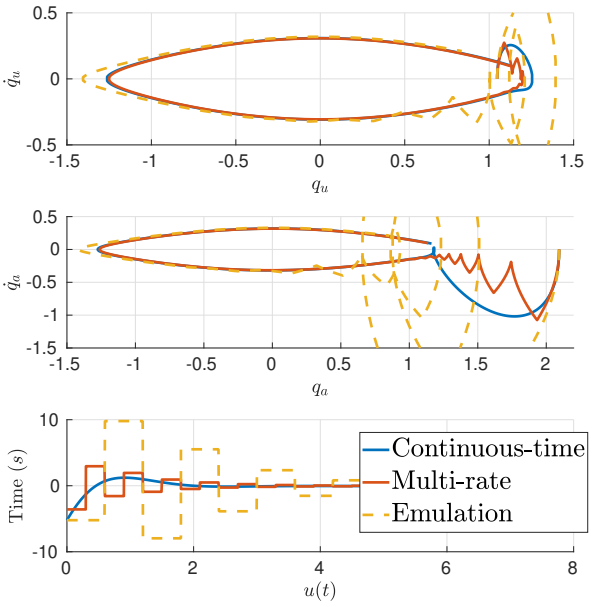

Fig. 4. Simulations for the pendubot when $\delta = 0.6$ seconds

V. Conclusions and Perspectives

In this paper, it is shown that multi-rate sampling allows to impose VHCs to mechanical systems in Euler-Lagrangian form. In particular, the order of the multi-rate must be equal to two over each input channel in order to guarantee invariance of the corresponding surface. Future perspectives concern the problem of preserving the Euler-Lagrangian structure of the residual dynamics (the associated zero-dynamics) possibly exploiting redundant multi-rate control. Also, the application of those methods to deal with control of multi-agent autonomous systems is under investigation [22].

Acknowledgment

Mohamed Elobaid wishes to thank *Université Franco-Italienne/Università Italo-Francese* for supporting his mobility within the PhD programme through *Vinci 2019*.

References

[1] A. Isidori, *Nonlinear Control Systems*. Springer-Verlag, 1995.
[2] P. Kokotović and M. Arcak, "Constructive nonlinear control: a historical perspective," *Automatica*, vol. 37, no. 5, pp. 637–662, 2001.
[3] A. Astolfi and R. Ortega, "Immersion and invariance: a new tool for stabilization and adaptive control of nonlinear systems," *IEEE Transactions on Automatic Control*, vol. 48, no. 4, pp. 590–606, 2003.
[4] E. R. Westervelt, J. W. Grizzle, and D. E. Koditschek, "Hybrid zero dynamics of planar biped walkers," *IEEE transactions on automatic control*, vol. 48, no. 1, pp. 42–56, 2003.
[5] A. van der Schaft and D. Jeltsema, "Port-Hamiltonian systems theory: An introductory overview," *Foundations and Trends® in Systems and Control*, vol. 1, no. 2-3, pp. 173–378, 2014.
[6] C. Canudas-de Wit, "On the concept of virtual constraints as a tool for walking robot control and balancing," *Annual Reviews in Control*, vol. 28, no. 2, pp. 157–166, 2004.
[7] A. Shiriaev, A. Robertsson, J. Perram, and A. Sandberg, "Periodic motion planning for virtually constrained euler–lagrange systems," *Systems & Control Letters*, vol. 55, no. 11, pp. 900–907, 2006.
[8] M. Maggiore and L. Consolini, "Virtual holonomic constraints for euler–lagrange systems," *IEEE Transactions on Automatic Control*, vol. 58, no. 4, pp. 1001–1008, 2012.
[9] A. Mohammadi, M. Maggiore, and L. Consolini, "Dynamic virtual holonomic constraints for stabilization of closed orbits in underactuated mechanical systems," *Automatica*, vol. 94, pp. 112–124, 2018.
[10] S. Monaco and D. Normand-Cyrot, "Advanced tools for nonlinear sampled-data systems' analysis and control," *European journal of control*, vol. 13, no. 2-3, pp. 221–241, 2007.
[11] K. Åström, P. Hagander, and J. Sternby, "Zeros of sampled systems," *Automatica*, vol. 20, no. 1, pp. 31 – 38, 1984.
[12] S. Monaco and D. Normand-Cyrot, "Zero dynamics of sampled nonlinear systems," *Systems & Control Letters*, vol. 11, no. 3, pp. 229–234, 1988.
[13] ——, "Multirate sampling and zero dynamics: from linear to nonlinear," in *Nonlinear synthesis*. Springer, 1991, pp. 200–213.
[14] D. S. Laila, D. Nešić, and A. R. Teel, "Open-and closed-loop dissipation inequalities under sampling and controller emulation," *European Journal of Control*, vol. 8, no. 2, pp. 109–125, 2002.
[15] D. Nešic and R. Postoyan, "Nonlinear sampled-data systems," *Encyclopedia of Systems and Control*, pp. 876–882, 2015.
[16] L. Freidovich, A. Robertsson, A. Shiriaev, and R. Johansson, "Periodic motions of the pendubot via virtual holonomic constraints: Theory and experiments," *Automatica*, vol. 44, no. 3, pp. 785–791, 2008.
[17] J. G. Romero and B. Yi, "Orbital stabilization of underactuated mechanical systems without euler-lagrange structure after of a collocated pre-feedback," *arXiv preprint arXiv:2109.06724*, 2021.
[18] M. Mattioni, S. Monaco, and D. Normand-Cyrot, "Immersion and invariance stabilization of strict-feedback dynamics under sampling," *Automatica*, vol. 76, pp. 78 – 86, 2017.
[19] S. Monaco and D. Normand-Cyrot, "The immersion under feedback of a multidimensional discrete-time non-linear system into a linear system," *International Journal of Control*, vol. 38, no. 1, pp. 245–261, 1983.
[20] A. Moreschini, M. Mattioni, S. Monaco, and D. Normand-Cyrot, "Discrete port-controlled hamiltonian dynamics and average passivation," in *58th IEEE Conference on Decision and Control (CDC)*, 2019, pp. 1430–1435.
[21] M. Spong and D. Block, "The pendubot: a mechatronic system for control research and education," in *Proceedings of 1995 34th IEEE Conference on Decision and Control*, vol. 1, 1995, pp. 555–556 vol.1.
[22] M. Mattioni and S. Monaco, "Cluster partitioning of heterogeneous multi-agent systems," *Automatica*, vol. 138, p. 110136, 2022.

General conclusions and open perspectives

In this work obstructions caused by the instability of the internal dynamics under stabilizing controllers that (partially) cancel the zero dynamics were investigated and solutions proposed. These solutions were developed to ensure stable inversion starting from the continuous-time setting and moving to treating two classes of inversion-based controllers in a digital context.

From the continuous-time perspective, and motivated by the fact that non-minimum phase zero dynamics implies instability of the closed loop under inversion control, a procedure for mitigating this issue is proposed. In particular, for a class of non-minimum phase Multi-Input Multi-Output systems, stable inversion can be guaranteed by ensuring that cancellation only affects the minimum phase component of the zero dynamics. This was done working over the linear tangent model associated with the system and using factorization tools over its corresponding Smith McMillan form. In this sense, the procedure proposed in this work naturally extends previous results for Single-Input Single-Output systems in the same direction. This is further used to solve problems of stabilization and disturbance decoupling with stability in continuous-time. Additionally, this work provides a preliminary and rough claim on the possibility of achieving the same factorization procedure working over the corresponding generalized normal form. The appeal of this is that, by not working over the linear tangent model, the procedure specified will hold everywhere where the coordinates change bringing the system the generalized normal form is defined. This claim was tested on the bench-marking example of a four-tanks process with promising results.

On the digital control side, this work proposed solutions ensuring stable inversion under both model predictive control and digital transverse feedback linearization. For systems under model predictive control with a quadratic cost function penalizing the control and output tracking error, we start by stressing how the optimal solution is of the inversion type when the penalty on the control is small and no state constraints are present. This fact, coupled with the use of sampled-data models which are typically non-minimum phase as prediction models in the model predictive control problem formulation, leads naturally to the use of multi-rate sampled models to mitigate the effects of unstable sampling zero dynamics in the cheap control setting. When used as prediction models in the problem formulation, internal stability of the closed loop is ensured when the penalty on the control is small and the prediction and control horizons coincide. Lacking in robustness and working in open-loop over the smaller sampling sub-intervals, a better solution is then sought and proposed in this thesis. This second solution uses a (possibly simplified under an assumed feedback) multi-rate model of the plant to modify the reference signals coming to the model predictive controller. It is then shown that, under the assumption of cheap control, this solution guarantees internal stability without the need for terminal stabilizing ingredients as done in the literature. Additionally, it improves on the robustness issues faced by the previous solution. Several cases studies were carried out both comparing the proposed solution as well as investigating situations not satisfying the strict assumptions of no state constraints and cheap control.

Starting from systems admitting a continuous-time solution to the (local) transverse feedback linearization problem, sampled-data based methodologies preserving the ideal continuous-time solution under sample and hold devices are proposed. These proposed methodologies being: (1) an approximate single-rate sampled-data solution working by redesigning the continuous-time functions specifying the controlled invariant set to be stabilized, and (2) an exact multi-rate sampled-data solution keeping the functions specifying the controlled invariant set intact and modifying the feedback law. This later solution additionally has the property of providing state feedback laws when only dynamic feedback laws are available in continuous-time. Both sampled-data mythologies are then used to solve interesting control problems in path following for non-holonomic systems and periodic orbit stabilization for underactuated mechanical systems.

The author in no way claims that this work is complete, and accordingly, a wide range of perspectives and open questions still remain. In the following we highlight a few;

- **Stabilization via partial cancellation of the zero dynamics**: the main remaining questions regarding this approach is the generalization to other classes of nonlinear systems, as well as under sampling. In this sense, the factorization of the Smith McMillan form associated with the linear tangent model, may not be the best approach to provide theoretical guarantees in the general setting. The use of generalized normal forms, and the proof of the claim made in Section 1.3 is still open.

- **Model Predictive Control - MPC**: as mentioned previously, one can use simplified models on both the MPC prediction level as well as the MR planner level. If that is the case, one can in principle obtain the "optimal" MPC feedback, by solving a much simpler optimization problem. Indeed, an interesting question would be to ask, if one can provide "general guarantees" on when such simplification can work. An example of that would be the following: consider a feedback linearizable system, and suppose $\gamma_c(x, v)$ is the feedback transformation rendering the system linear. Are there conditions on such $\gamma_c(x, v)$ which, when satisfied, allows one to utilize linear prediction model for the MPC with some performance and stability guarantees?. If such conditions are obtained, one can greatly reduce the complexity of nonlinear MPC problems, allowing for real time implementation while meeting certain performance indices.

  Moreover, concerning the case where strict state constraints are present, the use of *Extended Command Governor- ECG* Bemporad et al. (2010), coupled with the multi-rate planner is natural. This can be a solution providing admissible references that ensure constraints satisfaction to the MPC controlled closed loop system. This point in particular is very useful when dealing with special case of convex box state constraints since the command governor reduces to a least square projection on the maximal output admissible set Gilbert and Tan (1991). Additionally, if it is possible, this implementation will inherit all the benefits of extended command governors (e.g. larger max domain of attraction, convergence guarantees ..etc).

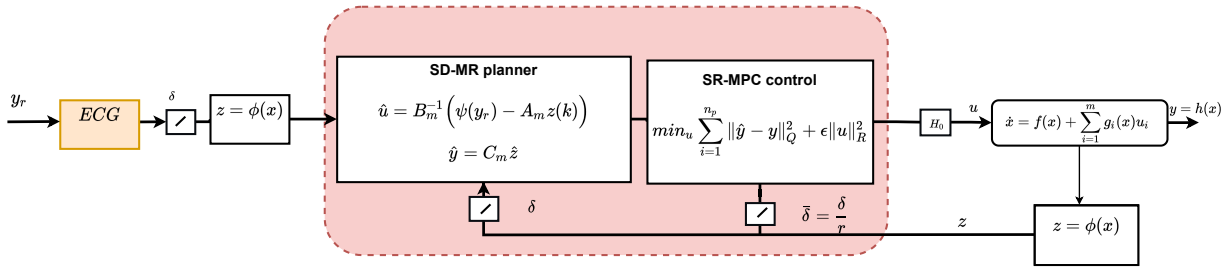

Figure 8.10: A multi-rate sampled-data planner in the state constrained case

- **Transverse Feedback Linearization - TFL**: relevant questions of nested-set stabilization using LTFL techniques in a digital context are being studied. This will allow for the concurrent satisfaction of multiple control requirements modelled as nested sets, while mitigating the known issues arising due to the implementation of partial inversion-like controllers digitally. Applications such as coordinated path following and synchornoization Panteley (2015), together with obstacles avoidance are a direct consequence those investigations.

In any case, research on the wider topic of sampled-data systems is constantly evolving thanks to new challenges that go far beyond the issues addressed in this manuscript. Those challenges arise from both practical and theoretical problems which deserve particular attention. As demonstrated by the example of path following for the car-like robot, sampled-data methodologies can even be used to work around the need for dynamic feedback.

Bibliography

A. Akhtar, C. Nielsen, and S. L. Waslander. Path following using dynamic transverse feedback linearization for car-like robots. *IEEE Transactions on Robotics*, 31:269–279, 2015.

F. Allgöwer and A. Zheng. *Nonlinear model predictive control*, volume 26. Birkhäuser, 2012.

B. D. Anderson and J. B. Moore. *Optimal control: linear quadratic methods*. Courier Corporation, 2007.

E. Aranda-Bricaire, Ü. Kotta, and C. Moog. Linearization of discrete-time systems. *SIAM Journal on Control and Optimization*, 34(6):1999–2023, 1996.

A. Arapostathis, B. Jakubczyk, H.-G. Lee, S. Marcus, and E. Sontag. The effect of sampling on linear equivalence and feedback linearization. *Systems & control letters*, 13(5):373–381, 1989.

A. Astolfi and R. Ortega. Immersion and invariance: A new tool for stabilization and adaptive control of nonlinear systems. *IEEE Transactions on Automatic control*, 48(4):590–606, 2003.

A. Astolfi, D. Karagiannis, and R. Ortega. *Nonlinear and adaptive control with applications*, volume 187. Springer, 2008.

K. J. Åström, P. Hagander, and J. Sternby. Zeros of sampled systems. *Automatica*, 20(1):31–38, 1984.

A. Banaszuk and J. Hauser. Feedback linearization of transverse dynamics for periodic orbits. *Systems & Control Letters*, 26:95–105, 1995.

M. Bando and A. Ichikawa. Formation flying along halo orbit of circular-restricted three-body problem. *Journal of Guidance, Control, and Dynamics*, 38(1):123–129, 2015.

J. Barbot, S. Monaco, D. Normand-Cyrot, and N. Pantalos. Some comments about linearization under sampling. In *[1992] Proceedings of the 31st IEEE Conference on Decision and Control*, pages 2392–2397. IEEE, 1992.

J.-P. Barbot, S. Monaco, and D. Normand-Cyrot. A sampled normal form for feedback linearization. *Mathematics of Control, Signals and Systems*, 9(2):162–188, 1996.

J. Barrow-Green. *Poincaré and the three body problem*, chapter 2,3. Number No. 11. American Mathematical Soc., New York, 1997.

G. Basile and G. Marro. Controlled and conditioned invariant subspaces in linear system theory. *Journal of Optimization Theory and Applications*, 3(5):306–315, 1969.

G. Basile and G. Marro. *Controlled and conditioned invariants in linear system theory*. Prentice Hall Englewood Cliffs, NJ, 1992.

S. Battilotti. A sufficient condition for nonlinear noninteracting control with stability via dynamic state-feedback. In *29th IEEE Conference on Decision and Control*, pages 1276–1281. IEEE, 1990.

A. Bemporad, M. Heemels, and M. Johansson. *Networked Control Systems*. Lecture Notes in Control and Information Sciences. Springer, 2010. ISBN 9780857290328. URL `http://books.google.ro/books?id=cAlKi5J8RicC`.

L. Biagiotti and C. Melchiorri. Trajectory generation via fir filters: A procedure for time-optimization under kinematic and frequency constraints. *Control Engineering Practice*, 87:43–58, 2019.

M. Bobskill and M. Lupisella. The role of cislunar space in future global exploration. In *AIAA Global Space Exploration Conference, Washington, DC*, 2012.

H. W. Bode et al. Network analysis and feedback amplifier design. 1945.

F. Borrelli, A. Bemporad, and M. Morari. *Predictive control for linear and hybrid systems*. Cambridge University Press, 2017.

P. Boucher and D. Dumur. *La commande prédictive*, volume 8. Editions Technip, 1996.

J. V. Breakwell, A. A. Kamel, and M. J. Ratner. Station-keeping for a translunar communication station. *Celestial Mechanics*, 10(3):357–373, 1974. doi: 10.1007/BF01586864.

P. Brunovskỳ. A classification of linear controllable systems. *Kybernetika*, 6(3):173–188, 1970.

C. I. Byrnes and A. Isidori. A frequency domain philosophy for nonlinear systems, with applications to stabilization and to adaptive control. In *The 23rd IEEE Conference on Decision and Control*, pages 1569–1573. IEEE, 1984.

C. Califano, S. Monaco, and D. Normand-Cyrot. On the problem of feedback linearization. *Systems & control letters*, 36(1):61–67, 1999.

E. F. Camacho and C. B. Alba. *Model predictive control*. Springer science & business media, 2013.

S. Carletta, M. Pontani, and P. Teofilatto. Dynamics of three-dimensional capture orbits from libration region analysis. *Acta Astronautica*, 165:331–343, 2019. doi: 10.1016/j.actaastro.2019.09.019.

L. R. Celsi, R. Bonghi, S. Monaco, and D. Normand-Cyrot. Sampled-data stabilization around the l_2 translunar libration point. In *3rd IAA Conference on University Satellite Missions and CubeSat Workshop and International Workshop on LEAN Satellite Standardization*, 2015.

C. Chen and L. Shaw. On receding horizon feedback control. *Automatica*, 18(3):349–352, 1982.

D. W. Clarke, C. Mohtadi, and P. Tuffs. Generalized predictive control—part i. the basic algorithm. *Automatica*, 23(2):137–148, 1987.

J. Descusse and C. Moog. Decoupling with dynamic compensation for strong invertible affine nonlinear systems. *International Journal of Control*, 42(6):1387–1398, 1985.

P. Di Giamberardino and S. Monaco. On halo orbits spacecraft stabilization. *Acta Astronautica*, 38(12):903–925, 1996. doi: 10.1016/S0094-5765(96)00082-3.

P. Di Giamberardino, D. M, Monaco, and D. Normand-Cyrot. Exact steering and stabilization of a pvtol aircraft. In *Proceedings of 1994 33rd IEEE Conference on Decision and Control*, volume 4, pages 3844–3849. IEEE, 1994.

P. Di Giamberardino, F. Grassini, S. Monaco, and D. Normand-Cyrot. Piecewise continuous control for a car-like robot: implementation and experimental results. In *Proceedings of 35th IEEE Conference on Decision and Control*, volume 3, pages 3564–3569. IEEE, 1996a.

P. Di Giamberardino, S. Monaco, and D. Normand-Cyrot. Digital control through finite feedback discretizability. In *Proceedings of IEEE International Conference on Robotics and Automation*, volume 4, pages 3141–3146. IEEE, 1996b.

M. Diehl, H. G. Bock, J. P. Schlöder, R. Findeisen, Z. Nagy, and F. Allgöwer. Real-time optimization and nonlinear model predictive control of processes governed by differential-algebraic equations. *Journal of Process Control*, 12(4):577–585, 2002. doi: 10.1016/S0959-1524(01)00023-3.

E. J. Doedel, V. A. Romanov, R. C. Paffenroth, H. B. Keller, D. J. Dichmann, J. Galán-Vioque, and A. Vanderbauwhede. Elemental periodic orbits associated with the libration points in the circular restricted 3-body problem. *International Journal of Bifurcation and Chaos*, 17(08):2625–2677, 2007. doi: 10.1142/S0218127407018671.

A. Doosthoseini and C. Nielsen. Coordinated path following for unicycles: A nested invariant sets approach. *Automatica*, 60:17–29, 2015a.

A. Doosthoseini and C. Nielsen. Local nested transverse feedback linearization. *Mathematics of Control, Signals, and Systems*, 27(4):493–522, 2015b.

M. Elobaid, M. Mattioni, S. Monaco, and D. Normand-Cyrot. On unconstrained mpc through multirate sampling. *IFAC-PapersOnLine*, 52(16):388–393, 2019.

M. Elobaid, M. Mattioni, S. Monaco, and D. Normand-Cyrot. On stable right-inversion of non-minimum-phase systems. In *2020 59th IEEE Conference on Decision and Control (CDC)*, pages 5153–5158. IEEE, 2020a.

M. Elobaid, M. Mattioni, S. Monaco, and D. Normand-Cyrot. Sampled-data tracking under model predictive control and multi-rate planning. In *IFAC 2020 World Congress*, 2020b. doi: 10.1016/j.ifacol.2020.12.2043.

M. Elobaid, S. Monaco, and D. Normand-Cyrot. Approximate transverse feedback linearization under digital control. *IEEE Control Systems Letters*, 2020c.

M. Elobaid, M. Mattioni, S. Monaco, and D. Normand-Cyrot. Digital path-following for a car-like robot. In *Control Conference Africa (CCA)*, 2021.

R. W. Farquhar. *The control and use of libration-point satellites*, volume 346. National Aeronautics and Space Administration, 1970.

R. W. Farquhar. *The utilization of halo orbits in advanced lunar operations*, volume 6365. National Aeronautics and Space Administration, 1971.

M. Fliess and D. Normand-Cyrot. A lie-theoretic approach to nonlinear discrete-time controllability via ritt's formal differential groups. *Systems & Control Letters*, 1(3):179–183, 1981.

D. Folta and F. Vaughn. *A Survey of Earth-Moon Libration Orbits: Stationkeeping Strategies and Intra-Orbit Transfers*. Number 4741 in AIAA/AAS Astrodynamics Specialist Conference and Exhibit. AIAA, 2004. doi: 10.2514/6.2004-4741.

D. C. Folta, T. A. Pavlak, A. F. Haapala, K. C. Howell, and M. A. Woodard. Earth–moon libration point orbit stationkeeping: theory, modeling, and operations. *Acta Astronautica*, 94(1):421–433, 2014. doi: 10.1016/j.actaastro.2013.01.022.

B. A. Francis and W. M. Wonham. The internal model principle of control theory. *Automatica*, 12 (5):457–465, 1976. doi: 10.1016/0005-1098(76)90006-6.

G. Franklin, J. Powell, and M. Workman. *Digital control of dynamic systems*. Addison-Wesley world student series. Addison-Wesley, 1998. ISBN 9780201820546.

M. Ghanes, J. De Leon, and J.-P. Barbot. Observer design for nonlinear systems under unknown time-varying delays. *IEEE Transactions on Automatic Control*, 58(6):1529–1534, 2012.

E. G. Gilbert and K. T. Tan. Linear systems with state and control constraints: The theory and application of maximal output admissible sets. *IEEE Transactions on Automatic control*, 36(9): 1008–1020, 1991. doi: 10.1109/9.83532.

R. Goedel, R. G. Sanfelice, and A. R. Teel. Hybrid dynamical systems: modeling stability, and robustness, 2012.

G. Gómez, J. Llibre, R. Martínez, and C. Simó. *Dynamics and mission design near libration points*, volume 1, chapter 5. World Scientific Singapore, 2001. doi: 10.1142/4402.

G. Grimm, M. J. Messina, S. E. Tuna, and A. R. Teel. Examples when model predictive control is non-robust. *Automatica*, 40:1729–1738, 10 2004.

G. Grimm, M. J. Messina, S. E. Tuna, and A. R. Teel. Nominally robust model predictive control with state constraints. *IEEE Transactions on Automatic Control*, 52(10):1856–1870, 2007.

J. Grizzle and M. Shor. Sampling, infinite zeros and decoupling of linear systems. 1988.

L. Grüne and J. Pannek. Nonlinear model predictive control. In *Nonlinear Model Predictive Control, Communications and Control Engineering series*, pages 45–69. Springer-Cham, 2017. doi: 10.1007/978-3-319-46024-6_3.

L. Grüne, K. Worthmann, and D. Nešić. Continuous-time controller redesign for digital implementation: a trajectory based approach. *Automatica*, 44(1):225 – 232, 2008.

P. Gurfil and D. Meltzer. Semi-analytical method for calculating the elliptic restricted three-body problem monodromy matrix. *Journal of guidance, control, and dynamics*, 30(1):266–271, 2007. doi: 10.2514/1.22871.

B. Harvey. *China in Space, The Great Leap Forward*, chapter 9, pages 443–496. Springer, 2 edition, 2019.

Y. Hayakawa, S. Hosoe, and M. Ito. On the limiting zeros of sampled multivariable systems. *Systems & Control Letters*, 2(5):292–300, 1983.

R. Hermann and A. Krener. Nonlinear controllability and observability. *IEEE Transactions on automatic control*, 22(5):728–740, 1977.

L. Hetel, C. Fiter, H. Omran, A. Seuret, E. Fridman, J.-P. Richard, and S. I. Niculescu. Recent developments on the stability of systems with aperiodic sampling: An overview. *Automatica*, 76: 309–335, 2017.

G. Hicks and W. Ray. Approximation methods for optimal control synthesis. *The Canadian Journal of Chemical Engineering*, 49(4):522–528, 1971.

M. Hilairet, M. Ghanes, O. Béthoux, V. Tanasa, J.-P. Barbot, and D. Normand-Cyrot. A passivity-based controller for coordination of converters in a fuel cell system. *Control engineering practice*, 21(8):1097–1109, 2013.

R. Hirschorn. Invertibility of multivariable nonlinear control systems. *IEEE Transactions on Automatic Control*, 24(6):855–865, 1979.

R. M. Hirschorn. (a,b)-invariant distributions and disturbance decoupling of nonlinear systems. *SIAM Journal on Control and Optimization*, 19(1):1–19, 1981.

A. Hladio, C. Nielsen, and D. Wang. Path following for a class of mechanical systems. *IEEE Transactions on Control Systems Technology*, 21(6):2380–2390, 2012.

B. Houska, H. J. Ferreau, and M. Diehl. Acado toolkit—an open-source framework for automatic control and dynamic optimization. *Optimal Control Applications and Methods*, 32(3):298–312, 2011. doi: 10.1002/oca.939.

K. C. Howell and H. J. Pernicka. Station-keeping method for libration point trajectories. *Journal of Guidance, Control, and Dynamics*, 16(1):151–159, 1993. doi: 10.2514/3.11440.

A. Isidori. *Lectures in feedback design for multivariable systems*, volume 3. Springer.

A. Isidori. *Nonlinear Control Systems*. Springer-Verlag, 1995.

A. Isidori and C. I. Byrnes. Output regulation of nonlinear systems. *IEEE transactions on Automatic Control*, 35(2):131–140, 1990.

A. Isidori and J. W. Grizzle. Fixed modes and nonlinear noninteracting control with stability. *IEEE transactions on automatic control*, 33(10):907–914, 1988.

A. Isidori, A. Krener, C. Gori-Giorgi, and S. Monaco. Nonlinear decoupling via feedback: a differential geometric approach. *IEEE transactions on automatic control*, 26(2):331–345, 1981.

K. H. Johansson and J. L. R. Nunes. A multivariable laboratory process with an adjustable zero. In *Proceedings of the 1998 American Control Conference. ACC (IEEE Cat. No. 98CH36207)*, volume 4, pages 2045–2049. IEEE, 1998.

P. Kabamba. Control of linear systems using generalized sampled-data hold functions. *IEEE transactions on Automatic Control*, 32(9):772–783, 1987.

T. Kailath. *Linear systems*, volume 156. Prentice-Hall Englewood Cliffs, NJ, 1980.

U. Kalabic, A. Weiss, S. Di Cairano, and I. Kolmanovsky. Station-keeping and momentum-management on halo orbits around l2: Linear-quadratic feedback and model predictive control approaches. In *Proc. AAS Space Flight Mechanics Meeting*, pages 15–307, 2015.

J. Kavaja, A. Minari, and A. Piazzi. Stable input-output inversion for nondecoupable nonminimum-phase linear systems. In *2018 European Control Conference (ECC)*, pages 2855–2860. IEEE, 2018.

S. Keerthi and E. G. Gilbert. Optimal infinite-horizon feedback laws for a general class of constrained discrete-time systems: Stability and moving-horizon approximations. *Journal of optimization theory and applications*, 57(2):265–293, 1988.

D. E. Kirk. *Optimal control theory: an introduction*. Courier Corporation, 2004.

A. J. Krener. On the equivalence of control systems and the linearization of nonlinear systems. *SIAM Journal on Control*, 11(4):670–676, 1973.

D. Limón, I. Alvarado, T. Alamo, and E. F. Camacho. Mpc for tracking piecewise constant references for constrained linear systems. *Automatica*, 44(9):2382–2387, 2008.

D. Limon, T. Alamo, D. M. Raimondo, D. M. De La Peña, J. M. Bravo, A. Ferramosca, and E. F. Camacho. Input-to-state stability: a unifying framework for robust model predictive control. In *Nonlinear model predictive control*, pages 1–26. Springer, 2009.

G. Marro. *Teoria dei sistemi e del controllo*. Zanichelli, 1990.

MATLAB. *version 9.8 (R2020a)*. The MathWorks Inc., Natick, Massachusetts, 2020.

M. Mattioni. *Stabilization of cascaded nonlinear systems under sampling and delays*. PhD thesis, Università degli Studi di Roma La Sapienza, 2018.

M. Mattioni, M. Hassan, S. Monaco, and D. Normand-Cyrot. On partially minimum phase systems and nonlinear sampled-data control. In *Decision and Control (CDC), 2017 IEEE 56th Annual Conference on*, pages 6101–6106. IEEE, 2017a.

M. Mattioni, S. Monaco, and D. Normand-Cyrot. Immersion and invariance stabilization of strict-feedback dynamics under sampling. *Automatica*, 76:78–86, 2017b.

M. Mattioni, M. Hassan, S. Monaco, and D. Normand-Cyrot. On partially minimum-phase systems and disturbance decoupling with stability. *Nonlinear Dynamics*, 97(1):583–598, 2019.

D. Q. Mayne, J. B. Rawlings, C. V. Rao, and P. O. Scokaert. Constrained model predictive control: Stability and optimality. *Automatica*, 36(6):789–814, 2000a.

D. Q. Mayne, J. B. Rawlings, C. V. Rao, and P. O. Scokaert. Constrained model predictive control: Stability and optimality. *Automatica*, 36(6):789–814, 2000b. doi: 10.1016/S0005-1098(99)00214-9.

F. Mazenc, M. Malisoff, and T. N. Dinh. Robustness of nonlinear systems with respect to delay and sampling of the controls. *Automatica*, 49(6):1925–1931, 2013.

H. Michalska and D. Q. Mayne. Robust receding horizon control of constrained nonlinear systems. *IEEE transactions on automatic control*, 38(11):1623–1633, 1993.

G. Misra, H. Peng, and X. Bai. Halo orbit station-keeping using nonlinear mpc and polynomial optimization. In *2018 Space Flight Mechanics Meeting*, page 1454, 2018. doi: 10.2514/6.2018-1454.

S. Monaco. *Sistemi Lineari. Elementi di Analisi.* Società Editrice Esculapio, 2020.

S. Monaco and D. Normand-Cyrot. Some remarks on the invertibility of nonlinear discrete-time systems. In *1983 American Control Conference*, pages 324–328. IEEE, 1983a.

S. Monaco and D. Normand-Cyrot. The immersion under feedback of a multidimensional discrete-time non-linear system into a linear system. *International Journal of Control*, 38(1):245–261, 1983b.

S. Monaco and D. Normand-Cyrot. On the sampling of a linear analytic control system. In *1985 24th IEEE Conference on Decision and Control*, pages 1457–1462. IEEE, 1985.

S. Monaco and D. Normand-Cyrot. Minimum-phase nonlinear discrete-time systems and feedback stabilization. *26th IEEE Conference on Decision and Control*, 26:979–986, 1987.

S. Monaco and D. Normand-Cyrot. Zero dynamics of sampled nonlinear systems. *Systems & Control Letters*, 11(3):229–234, 1988.

S. Monaco and D. Normand-Cyrot. An introduction to motion planning under multirate digital control. *31st IEEE Conference on Decision and Control*, 2:1780–1785, 1992.

S. Monaco and D. Normand-Cyrot. A unified representation for nonlinear discrete-time and sampled dynamics. In *Journal of Mathematic, System, Estimation and Control*. Citeseer, 1995.

S. Monaco and D. Normand-Cyrot. On nonlinear digital control. In *Nonlinear systems*, pages 127–155. Springer, 1997.

S. Monaco and D. Normand-Cyrot. Issues on nonlinear digital control. *European Journal of Control*, 7(2-3):160–177, 2001.

S. Monaco and D. Normand-Cyrot. On the differential/difference representation of sampled dynamics. In *Proceedings of the 44th IEEE Conference on Decision and Control*, pages 6597–6602. IEEE, 2005.

S. Monaco, D. Normand-Cyrot, and S. Stornelli. On the linearizing feedback in nonlinear sampled data control schemes. In *Proc. 25th IEEE-CDC, Athens*, pages 2056–2060, 1986a.

S. Monaco, D. Normand-Cyrot, and S. Stornelli. On the linearizing feedback in nonlinear sampled data control schemes. In *1986 25th IEEE Conference on Decision and Control*, pages 2056–2060. IEEE, 1986b.

A. Moreschini, M. Mattioni, S. Monaco, and D. Normand-Cyrot. Stabilization of discrete port-hamiltonian dynamics via interconnection and damping assignment. *IEEE Control Systems Letters*, 5(1):103–108, 2020.

R. M. Murray and S. S. Sastry. Steering nonholonomic systems in chained form. 1991.

D. Nešić, A. R. Teel, and P. V. Kokotović. Sufficient conditions for stabilization of sampled-data nonlinear systems via discrete-time approximations. *Systems & Control Letters*, 38(4-5):259–270, 1999.

D. Nesic, A. R. Teel, and D. Carnevale. Explicit computation of the sampling period in emulation of controllers for nonlinear sampled-data systems. *IEEE transactions on Automatic Control*, 54 (3):619–624, 2009.

C. Nielsen and M. Maggiore. Output stabilization and maneuver regulation: A geometric approach. *Systems & control letters*, 55(5):418–427, 2006.

C. Nielsen and M. Maggiore. On local transverse feedback linearization. *SIAM Journal on Control and Optimization*, 47(5):2227–2250, 2008. doi: 10.1137/070682125.

C. Nielsen, C. Fulford, and M. Maggiore. Path following using transverse feedback linearization: Application to a maglev positioning system. *Automatica*, 46(3):585–590, 2010.

D. Normand-Cyrot. *Théorie et pratique des systèmes non linéaires en temps discret.* PhD thesis, 1983.

R. Ortega, A. Van Der Schaft, F. Castanos, and A. Astolfi. Control by interconnection and standard passivity-based control of port-hamiltonian systems. *IEEE Transactions on Automatic Control*, 53(11):2527–2542, 2008.

E. Panteley. *A stability-theory perspective to synchronisation of heterogeneous networks.* PhD thesis, Université Paris-Sud, 2015.

B. Picasso, D. Desiderio, and R. Scattolini. Robustness analysis of nominal model predictive control for nonlinear discrete-time systems. *IFAC Proceedings Volumes*, 43(14):214 – 219, 2010. ISSN 1474-6670. 8th IFAC Symposium on Nonlinear Control Systems.

H. Poincaré. *Les méthodes nouvelles de la mécanique céleste: Méthodes de MM. Newcomb, Glydén, Lindstedt et Bohlin*, volume 2, chapter 1. Gauthier-Villars it fils, 1893.

S. Prajna, A. Papachristodoulou, and P. A. Parrilo. Introducing sostools: A general purpose sum of squares programming solver. In *Proceedings of the 41st IEEE Conference on Decision and Control, 2002.*, volume 1, pages 741–746, 2002. doi: 10.1109/CDC.2002.1184594.

D. Pucci, T. Hamel, P. Morin, and C. Samson. Nonlinear control of pvtol vehicles subjected to drag and lift. In *2011 50th IEEE Conference on Decision and Control and European Control Conference*, pages 6177–6183. IEEE, 2011.

D. Pucci, F. Romano, and F. Nori. Collocated adaptive control of underactuated mechanical systems. *IEEE Transactions on Robotics*, 31(6):1527–1536, 2015.

M. Putinar. Positive polynomials on compact semi-algebraic sets. *Indiana University Mathematics Journal*, 42(3):969–984, 1993. doi: 10.1016/S0764-4442(99)80251-1.

Y. Qi and A. de Ruiter. Station-keeping strategy for real translunar libration point orbits using continuous thrust. *Aerospace Science and Technology*, 94:105376, 2019. doi: 10.1016/j.ast.2019.105376.

L. Qiu and E. J. Davison. Performance limitations of non-minimum phase systems in the servomechanism problem. *Automatica*, 29(2):337–349, 1993.

T. Raff, C. Ebenbauer, R. Findeisen, and F. Allgöwer. Nonlinear model predictive control and sum of squares techniques. In *Fast Motions in Biomechanics and Robotics*, pages 325–344. Springer, 2006. doi: 10.1007/978-3-540-36119-0_15.

J. R. Ragazzini and G. F. Franklin. *Sampled-data control systems*. McGraw-Hill, 1958.

A. Rahmani, M.-A. Jalali, and S. Pourtakdoust. Optimal approach to halo orbit control. In *AIAA Guidance, Navigation, and Control Conference and Exhibit*, number 5748, Austin, Texas, 2003. doi: 10.2514/6.2003-5748.

D. L. Richardson. Analytic construction of periodic orbits about the collinear points. *Celestial mechanics*, 22(3):241–253, 1980. doi: 10.1007/BF01229511.

J. G. Romero and B. Yi. Orbital stabilization of underactuated mechanical systems without euler-lagrange structure after of a collocated pre-feedback. *arXiv preprint arXiv:2109.06724*, 2021.

H. Rosenbrock. Transformation of linear constant system equations. In *Proceedings of the Institution of Electrical Engineers*, volume 114, pages 541–544. IET, 1967.

S. Sastry. *Nonlinear Systems - Analysis,Stability and Control,, 1999*. Springer-Verlag, New York, 1999.

P. Seibert. On stability relative to a set and to the whole space. In *5th Int. Conf. on Nonlinear Oscillations (Izdat. Inst. Mat. Akad. Nauk. USSR, 1970)*, volume 2, pages 448–457, 1969.

R. Sepulchre, M. Jankovic, and P. V. Kokotovic. *Constructive nonlinear control*. Springer Science & Business Media, 2012.

M. M. Seron, J. H. Braslavsky, P. V. Kokotovic, and D. Q. Mayne. Feedback limitations in nonlinear systems: From bode integrals to cheap control. *IEEE Transactions on Automatic Control*, 44(4): 829–833, 1999.

A. S. Shiriaev. The notion of v-detectability and stabilization of invariant sets of nonlinear systems. *Systems & Control Letters*, 39(5):327–338, 2000.

M. Shirobokov, S. Trofimov, and M. Ovchinnikov. Survey of station-keeping techniques for libration point orbits. *Journal of Guidance, Control, and Dynamics*, 40(5):1085–1105, 2017. doi: 10.2514/1.G001850.

B. Siciliano, L. Sciavicco, L. Villani, and G. Oriolo. *Robotics: modelling, planning and control*. Springer Science & Business Media, 2010.

L. Silverman. Inversion of multivariable linear systems. *IEEE Transactions on automatic control*, 14(3):270–276, 1969.

C. Simó, G. Gómez, J. Llibre, R. Martinez, and J. Rodriguez. On the optimal station keeping control of halo orbits. *Acta Astronautica*, 15(6-7):391–397, 1987. doi: 10.1016/0094-5765(87)90175-5.

S. Singh. A modified algorithm for invertibility in nonlinear systems. *IEEE Transactions on Automatic Control*, 26(2):595–598, 1981.

S. Skogestad and I. Postlethwaite. *Multivariable feedback control: analysis and design*, volume 2. Citeseer, 2007.

E. Sontag. Realization theory of discrete-time nonlinear systems: Part i-the bounded case. *IEEE Transactions on Circuits and Systems*, 26(5):342–356, 1979.

E. D. Sontag. Feedback stabilization of nonlinear systems. *Robust control of linear systems and nonlinear control*, pages 61–81, 1990.

M. Spong and D. Block. The pendubot: a mechatronic system for control research and education. In *Proceedings of 1995 34th IEEE Conference on Decision and Control*, volume 1, pages 555–556 vol.1, 1995. doi: 10.1109/CDC.1995.478951.

M. Sznaier and M. J. Damborg. Heuristically enhanced feedback control of constrained discrete-time linear systems. *Automatica*, 26(3):521–532, 1990.

A. Teel and L. Praly. Tools for semiglobal stabilization by partial state and output feedback. *SIAM Journal on Control and Optimization*, 33(5):1443–1488, 1995.

Y. Ulybyshev. Long-term station keeping of space station in lunar halo orbits. *Journal of Guidance, Control, and Dynamics*, 38(6):1063–1070, 2015. doi: 10.2514/1.G000242.

W. M. Wonham and A. S. Morse. Decoupling and pole assignment in linear multivariable systems: a geometric approach. *SIAM Journal on Control*, 8(1):1–18, 1970.

M. Woodard, D. Folta, and D. Woodfork. Artemis: the first mission to the lunar libration orbits. In *21st International Symposium on Space Flight Dynamics*, Toulouse, France, 2009. ISSFD.

W. Wu, Y. Tang, L. Zhang, and D. Qiao. Design of communication relay mission for supporting lunar-farside soft landing. *Science China Information Sciences*, 61(4):1–14, 2018. doi: 10.1007/s11432-017-9202-1.

J. I. Yuz and G. C. Goodwin. On sampled-data models for nonlinear systems. *IEEE transactions on automatic control*, 50(10):1477–1489, 2005a.

J. I. Yuz and G. C. Goodwin. On sampled-data models for nonlinear systems. *IEEE Transactions on Automatic Control*, 50(10):1477–1489, 2005b.

H. Zhang and S. Li. Station-keeping of libration point orbits by means of projecting to the manifolds. *Acta Astronautica*, 163:38–44, 2019. doi: 10.1016/j.actaastro.2018.12.002.

E. M. Zimovan-Spreen, K. C. Howell, and D. C. Davis. Near rectilinear halo orbits and nearby higher-period dynamical structures: orbital stability and resonance properties. *Celestial Mechanics and Dynamical Astronomy*, 132(5):1–25, 2020.